Modelling the Impact of Climate Change on the Wildebeest of the Serengeti-Mara Ecosystem



Josephine Mahony

Wolfson College

University of Oxford

A thesis submitted for the degree of

Doctor of Philosophy

Hilary Term 2020

Abstract

Migratory wildebeest are a key component of the Serengeti-Mara ecosystem. Their population dynamics and movement patterns depend on, and contribute to, a complex set of interactions between the soils, wildlife, vegetation, fire, topography, geology, and precipitation patterns. Yet climate change is projected to alter precipitation patterns across the globe. This thesis set out to explore how future mean precipitation patterns may change over the SME, and how this may impact the migratory wildebeest.

The first paper of the thesis quantified the past mean climatological state of the regional precipitation, and identified the key atmospheric processes governing its spatial and temporal distribution. Precipitation over the SME was heterogeneous; different parts of the region were found to have distinct annual cycles, peak precipitation months, dry season precipitation totals and time of peak daily precipitation. These were found to be controlled by interactions between the complex rift topography, mid-tropospheric large-scale easterlies (at approximately 700 hPa), and lower tropospheric lake breeze westerlies from Lake Victoria (present between the surface and 800 hPa).

The second paper assessed the suitability of mechanistic ecological model for use in ecological climate change impact studies, by driving the model with a spectrum of novel precipitation conditions. The study found that modelled wildebeest population size was most sensitive to changes in annual precipitation, dry season precipitation, and precipitation over the south-east of the SME. As long as the annual cycle was present, simulated movement only ceased when all environmental gradients were removed, suggesting climate change would unlikely to stop the migration (although increased rainfall could weaken the environmental gradients that drive it).

The third paper evaluated the performance of a convection-permitting climate model over the SME, examined the projected future changes to the regional climate, and modelled the impact of the future changes on the SME wildebeest. The climate model captured the zonal component of the precipitation gradient across the ecosystem and the annual cycle of precipitation, although unrealistically high totals were simulated in wet season months. Overly strong lake breeze winds were suggested as a causal mechanism for a dry annual bias over Lake Victoria's shoreline, and abnormally high precipitation totals over the rift highlands. Future mean precipitation was projected to increase over the SME in every month except August. Analysis of mid-tropospheric winds suggested this was due to anomalous southerlies over the Lake Victoria basin. The projected increase in future precipitation resulted in an increase in the modelled wildebeest population size. This suggests that climate change may cause a mean state that is favourable to the SME wildebeest, although changes to interspecific competition or interannual variability of precipitation could undermine these favourable mean conditions.

Acknowledgments

Thanks must first go to my supervisors: Tim, Ellen and Richard. Tim you have been the most bubbly, funny, supportive boss I have ever had. Thank you for having my back over the past four and a half years, helping me over every hurdle, giving excellent advice, fostering a generous lab group, and buying so, so many rounds. Ellen, thank you for the tea, the code, the plants, the politics and for helping me out when I really needed it. You have been a rock and a friend, and I will never forget it. Richard, thank you for encouraging me before I even arrived in Oxford and for helping me to do this amazing project. Your passion for a subject that is so important to many of the most vulnerable people and places in this world is admirable.

I also need to thank the NERC DTP. It was a gamble letting students write their own projects, and this thesis is the direct result of the risk I was allowed to take. The DTP also created an environment that encouraged friendships between the 28 of us that met in a manor house in 2015. Amongst them, I would especially like to thank Sam and Gen. Sam, thanks for the tasty food, days of coding lessons, and being lovely. Gen, thanks for the R help, the adventures, and being an excellent friend.

Thanks to the people who make Isis Canoe Club so special, especially Adam, Kerstin and Andy. My PhD and the river will be forever entwined in my mind, and those wonderful evenings on the water were the best way to recharge after a long day of coding.

Suzie, Claude, and Rob, thank you for helping me to see the Serengeti and making it such a fun experience. Being able to see this wonderful place was an actual dream, and your conversations helped me to understand this incredible place on an even deeper level.

For the other great adventure I had during my PhD, I need to thank the Aldabrans. Technically everyone named here delayed this PhD getting finished, but if there was ever a reason to suspend, it is to pick up plastic for 5 weeks in 40 degree heat. Thank you April, Kalsey, Jeremy, Martyna, Becca, Craig, Thomas, Ivan, Sheena, Sam, Ash, Jude, Lindsay, J-Bo, Ronny-Ronny, Jake, Jessica, Marvin, Jilani, Jean-Ives, Edward, and everyone else involved in ACUP for the adventure of a lifetime. I came away with an understanding of what we could lose to climate change that is hard to appreciate from reading journal articles alone.

I have been lucky to have so many wonderful housemates during my time in Oxford, as well as friends who have opened their homes to me when I needed a place to stay. Thank you Martin, Erik, Jack, Natalie, Ash, Cael, George and Jienchi for making me laugh and giving me a friendly place to sleep while I have worked on this project. I would also like to say an extra thank you to the people who gave me a place to stay when I really needed it. Ross, Sophie, Leejiah and Martyna, thanks so much, it meant more than you know.

I have been blessed with incredible lab groups whilst in Oxford. Sebastian, Neil, Rachel, James, Amy, Boi, Ellen, Karsten, Thomas, Lisa, Callum, Ian, Neven, David, Ruksana and Tommy, thank you for making the climate lab such a lovely place to work, and for the help, excellent brunches and discussions. Special thanks to Emma, Boi and Karsten, for making my evenings so fun.

The Coulson lab group have been more friends than colleagues since the day I joined. Thanks Lara, Emily, Leejiah, Erik, Marc, Jeremy, Rocio, Claudio, Rosemarie, Shelly, Aura, Xuefei, Susanna, Ollie, Emma, Gioele, Tom, Willem, Jin, Marie, Gwen, Anya, Alex, Holly, Sharon, Ben, Ash, James and Gen. You made coming to work an absolute joy.

Thanks to my family for always having my back and being brilliant. I am continually amazed by how lucky I am to come from such an impressive, loving lot. I will forever think of a wedding when I remember handing in my PhD. Thank you Steve, Carol, Niketa, Nathan and Naomi, for an amazing day full of love.

Michael, thank you for always being there. You're the best. I don't know how to say it better than that.

Finally, Mum and Dad, this PhD would not have been finished without you. Thank you so much for the house moves, the meals, the money, the hugs, the greenhouse, the tea, the love, the encouragement, for sitting with me, and supporting me no matter what. I do not know what I did to deserve you, but your love and support has allowed me to finish something that has become incredibly important to me. Thank you.

Table of Contents

ABSTRACT ..... **I**

ACKNOWLEDGMENTS ..... **III**

TABLE OF CONTENTS ..... **V**

LIST OF FIGURES ..... **XII**

LIST OF TABLES ..... **XX**

LIST OF ACRONYMS ..... **XXI**

CHAPTER 1. INTRODUCTION **1**

1.1 MOTIVATION 1

1.2 RATIONALE 3

1.3 DEFINITION OF SCALE 5

1.4 THE SERENGETI-MARA ECOSYSTEM 7

1.4.1 Topography and Lakes *7*

1.4.2 Nutrient Distribution *10*

1.4.3 Vegetation Distribution and Dynamics *12*

1.4.3.1 Vegetation distribution across SME 12

1.4.3.2 Controls on Vegetation 13

Rainfall 13

Soil Properties 14

Fire 15

Herbivores 16

Termites 17

Vegetation Interactions 18

1.4.4 Wildebeest Migration *19*

1.4.4.1 Movement Patterns 19

1.4.4.2 Population Dynamics 20

1.4.5 Ecosystem Dynamics *21*

1.4.6 Potential Impacts of Climate Change on Wildebeest *23*

1.4.7 Modelling the Migratory Wildebeest *26*

1.5 CLIMATE OF EASTERN AFRICA 27
1.5.1 Observed Climate of East Africa *27*
1.5.1.1 Large-Scale Precipitation Patterns and Drivers 28
1.5.1.2 Mesoscale Precipitation Patterns and Drivers 29
1.5.1.3 Patterns and Drivers of Precipitation over the Serengeti-Mara Ecosystem 30
1.5.1.4 Past Precipitation Trends 32
1.5.2 Simulated Climate of East Africa *34*
1.5.2.1 Climate Models 34
1.5.2.2 Model Selection 36
Statistical Downscaling vs Dynamic Downscaling 36
Resolution 37
1.5.2.3 CP4-Africa 37
1.5.2.4 Projected Future Precipitation Trends 39
1.6 INTEGRATING CLIMATE SCIENCE AND ECOLOGY 40
1.7 THESIS AIMS 42
1.8 NOTES ON THE FORMAT OF THE THESIS 42
1.8.1 Authorship declaration *44*
CHAPTER 2. THE CHARACTERISTICS AND DRIVERS OF CLIMATOLOGICAL PRECIPITATION OVER THE SERENGETI REGION IN EAST AFRICA 45
2.1 INTRODUCTION 46
2.2 DATA AND METHODS 49
2.2.1 Datasets *49*
2.2.1.1 Precipitation Data 49
2.2.1.2 Wind and specific humidity 49
2.2.1.3 Topography 50
2.2.2 Methods *50*
2.2.2.1 Cluster analysis 50
2.2.2.2 Atmospheric and Topographic Cross-sections 51
2.3 RESULTS 52
2.3.1 Annual and Monthly Precipitation over the Wider Serengeti Domain *52*
2.3.1.1 Annual Precipitation 52

2.3.1.2 Monthly Precipitation 53
2.3.1.3 Variation in Annual Cycles 55
2.3.1.4 Cluster Analysis 56
South-west 58
East 58
North-west 59
North-east 59
Central 59
2.3.2 Seasonal and Diurnal Wind over East Africa 60
2.3.2.1 Monthly Wind Patterns 60
2.3.2.2 Monthly and Diurnal Wind, Convergence and Moisture Patterns 62
2.3.3 Diurnal Precipitation and Wind over the Wider Serengeti Domain 66
2.3.3.1 Diurnal Precipitation and Surface Wind Patterns 66
2.3.3.2 Monthly Afternoon Vertical Wind Profiles 70
2.4 DISCUSSION 72
2.4.1 Evaluation of Precipitation Data 72
2.4.2 Large-scale Circulation Patterns 73
2.4.3 Topography 74
2.4.4 Lake Breeze Winds 75
2.4.5 Afternoon Storm Development 76
2.4.6 Key Differences between Annual Cycles of Precipitation 79
2.4.7 Rainfall Gradient over the Serengeti National Park 81
2.5 CONCLUSIONS 83
CHAPTER 3. MODELLING WILDEBEEST MOVEMENT AND POPULATION DYNAMICS IN THE FACE OF ENVIRONMENTAL CHANGE 84
3.1 INTRODUCTION 85
3.2 METHODS 87
3.2.1 Model 87
3.2.1.1 Environmental input layers 88
Precipitation 88
Nitrogen 90

Habitat type 90
3.2.2 Experiments *91*
3.2.2.1 Experiment 1: Removal of Interannual Variability 93
3.2.2.2 Experiment 2: Annual Precipitation Elasticity Analysis 94
3.2.2.3 Experiment 3: Removal of Environmental Gradients 95
3.2.2.4 Experiment 4: Monthly Precipitation Elasticity Analysis 96
3.2.2.5 Experiment 5: Monthly Precipitation Sensitivity Analysis 97
3.2.2.6 Experiment 6: Spectrum of Past Precipitation Conditions 97
3.3 RESULTS 98
3.3.1 Removal of Interannual Variability *98*
3.3.2 Annual Precipitation Elasticity Analysis *99*
3.3.3 Removal of Environmental Gradients *100*
3.3.4 Monthly Precipitation Elasticity Analysis *102*
3.3.5 Monthly Precipitation Sensitivity Analysis *103*
3.3.6 Spectrum of Past Precipitation Conditions *104*
3.4 DISCUSSION 106
3.4.1 Removal of Interannual Variability *106*
3.4.2 Response of Movement Patterns to Removal of Environmental Gradients *107*
3.4.3 Interactions between Precipitation and Tree Cover *108*
3.4.4 Precipitation Characteristics of an Individual Year *110*
3.4.4.1 Annual Precipitation Totals 110
3.4.4.2 Monthly Precipitation Totals 111
Dry Season Months 111
Wet Season Months 112
All Months 113
3.4.4.3 Spatial Distribution of Rainfall 114
3.4.5 Model Limitations and Potential Improvements *115*
3.5 CONCLUSIONS 117
CHAPTER 4. MODELLING THE IMPACT OF FUTURE CHANGES TO MEAN PRECIPITATION ON THE SURVIVAL RATES OF THE SERENGETI-MARA WILDEBEEST 119
4.1 INTRODUCTION 120

4.2 METHODS 123
4.2.1 Savannah Dynamics Model 123
4.2.1.1 Model Adjustments 125
4.2.1.2 Displaying Savannah Dynamics Model Output 126
4.2.2 Climate Datasets 126
4.2.2.1 CHIRPS v2.0 127
4.2.2.2 ERA5 127
4.2.2.3 CP4-Africa Hindcast and Future Projection 127
4.3 RESULTS 129
4.3.1 Observed and Modelled Atmospheric Conditions 129
4.3.1.1 Annual Cycle of Precipitation 129
4.3.1.2 Annual Precipitation 131
4.3.1.3 Past Monthly Wind and Precipitation 133
4.3.1.4 Future Monthly Wind and Precipitation 134
4.3.2 Wildebeest Response to Precipitation Regimes 135
4.3.2.1 Model Runs 135
4.3.2.2 Impact of Spatiotemporal Distribution of Precipitation 137
4.3.2.3 Population Dynamics 139
4.4 DISCUSSION 142
4.4.1 Evaluation of CP4 Hindcast Climate Model 143
4.4.2 Future Precipitation Changes over the SME 144
4.4.3 Wildebeest Response to Precipitation Changes 148
4.5 CONCLUSIONS 152
CHAPTER 5. CONCLUSIONS 154
5.1 SUMMARY OF KEY FINDINGS 155
5.1.1 The Characteristics and Drivers of Climatological Precipitation over the Serengeti Region in East Africa. 155
5.1.2 Modelling Wildebeest Movement and Population Dynamics in the Face of Environmental Change. 156
5.1.3 Modelling the Impact of Future Changes to Mean Precipitation on the Survival Rates of the Serengeti-Mara Wildebeest 157

5.2 LIMITATIONS 158
5.2.1 The Characteristics and Drivers of Climatological Precipitation over the Serengeti Region in East Africa. *158*
5.2.2 Modelling Wildebeest Movement and Population Dynamics in the Face of Environmental Change. *159*
5.2.3 Modelling the Impact of Future Changes to Mean Precipitation on the Survival Rates of the Serengeti-Mara Wildebeest *160*
5.3 FUTURE AVENUES OF RESEARCH 162
5.3.1 The Characteristics and Drivers of Climatological Precipitation over the Serengeti Region in East Africa. *162*
5.3.2 Modelling Wildebeest Movement and Population Dynamics in the Face of Environmental Change. *163*
5.3.3 Modelling the Impact of Future Changes to Mean Precipitation on the Survival Rates of the Serengeti-Mara Wildebeest *167*
5.4 THE UNIQUE CLIMATIC CONDITIONS OF THE SERENGETI-MARA ECOSYSTEM 168
5.5 FULFILMENT OF GOAL AND AIMS 171
5.6 CONTRIBUTION TO KNOWLEDGE 175
REFERENCES 180
APPENDIX A. THE MIGRATION, MOVEMENT AND GRASS DYNAMICS EQUATIONS OF THE SAVANNAH DYNAMICS MODEL 216
A1. MODEL DESCRIPTION 216
A2. MODEL TERMS 217
A3. GRASS DYNAMICS 219
A3.1 Rainfall and Grass growth rate ($\boldsymbol{rmax}$) *220*
A3.2 Grass carrying capacity ($\boldsymbol{KG}$) *221*
A3.3 Grass proportion ($\boldsymbol{g}$) *and tree canopy cover* ($\boldsymbol{T}$) *221*
A3.4 Intake of green grass ($\boldsymbol{IG}$) *and dry grass* ($\boldsymbol{ID}$) *221*
A4. RESOURCE AVAILABILITY 222
A5. WILDEBEEST MOVEMENT DYNAMICS 222

A5.1 Emigration *223*

A5.2 Immigration *223*

A5.3 Change in wildebeest density ΔWij *224*

A6. WILDEBEEST POPULATION DYNAMICS 225

A7. REFERENCES 226

APPENDIX B. CLUSTER ANALYSIS 227

B1. TRMM CLUSTER ANALYSIS 227

B2. CHIRPS CLUSTER ANALYSIS 228

B3. REFERENCES 230

List of Figures

Main Thesis

FIGURE 1.1: APPROACH TO USE OF MODELS IN THIS THESIS. REPRESENTATION OF KEY PROCESSES SHAPES MODEL SELECTION, ASSESSMENT OF MODEL PERFORMANCE HIGHLIGHTS KEY UNCERTAINTIES BEFORE MODEL IS USED TO MAKE PREDICTIONS 5

FIGURE 1.2: TOPOGRAPHY OF THE EAST AFRICAN RIFT SYSTEM. (A) MAP OF TECTONIC PROCESSES OCCURRING WITHIN AND BETWEEN THE AFRICAN AND ARABIAN PLATES (REPRODUCED FROM ENCYCLOPAEDIA BRITANNICA (NO DATE)). (B) TOPOGRAPHIC ELEVATION OVER THE SERENGETI NATIONAL PARK AND WIDER SURROUNDING AREA. IN PANEL (B), COLOUR REPRESENTS 2 MINUTE RESOLUTION TOPOGRAPHIC ELEVATION DATA FROM THE GLOBAL 30 ARC-SECOND ELEVATION DATASET (GESCH ET AL., 1999), EXCEPT FOR WATER BODIES THAT ARE MASKED BY LIGHT BLUE (LAKES) AND DARK BLUE (OCEAN). COUNTRY BOUNDARIES AND LAKE/COASTLINE BOUNDARIES ARE SHOWN BY THIN BLACK LINES, WHILE THE BOUNDARIES OF THE SERENGETI NATIONAL PARK HAVE A THICK BLACK LINE. 8

FIGURE 1.3: TOPOGRAPHY OF THE REGION SURROUNDING THE SERENGETI NATIONAL PARK. THE BOUNDARIES OF PROTECTED AREAS AND LAKES ARE INDICATED BY THICK AND THIN SOLID BLACK LINES RESPECTIVELY. THE DASHED BLACK LINE SHOWS THE BORDER BETWEEN KENYA (NORTH) AND TANZANIA (SOUTH). COLOUR DISPLAYS 2 MINUTE RESOLUTION TOPOGRAPHIC ELEVATION DATA FROM THE GLOBAL 30 ARC-SECOND ELEVATION DATASET (GESCH ET AL., 1999), AND LAKES ARE MASKED WITH LIGHT BLUE. GREY LINES DEMARCATE TOPOGRAPHIC CONTOURS WITH 500 M INTERVALS. PROTECTED AREAS AND NATURAL FEATURES ARE LABELLED WITH NORMAL AND ITALIC TEXT RESPECTIVELY. ACRONYMS "GR", "WMA" AND "(N)" REFER TO "GAME RESERVE", "WILDLIFE MANAGEMENT AREA", AND "NORTH", RESPECTIVELY. THE PROTECTED AREA SHAPEFILES WERE SOURCED FROM PROTECTED PLANET (KENYA WILDLIFE SERVICE, NO DATE; TANZANIAN NATIONAL PARKS, NO DATE). THE SHAPEFILE FOR THE CENTRAL PORTION OF THE MASWA GAME RESERVE HAS NOT BEEN MADE AVAILABLE BY THE TANZANIA NATIONAL PARKS ON THIS PLATFORM, AND IS THEREFORE MISSING FROM THIS FIGURE. 9

FIGURE 1.4: AIMS AND STRUCTURE OF THESIS. COLOURS REFER TO THE PAPER IN WHICH EACH AIM IS ADDRESSED. 43

FIGURE 2.1: MAP OF THE OROGRAPHY AND KEY LANDMARKS OF THE SERENGETI NATIONAL PARK AND SURROUNDING AREA. THE AREA SHOWN IN THIS FIGURE IS TERMED THE "WIDER SERENGETI DOMAIN" IN THIS

STUDY. COLOUR AND CONTOUR LINES DENOTE ELEVATION (USING GTOPO30 TOPOGRAPHY DATA), WITH THE EXCEPTION OF LAKES WHICH ARE MASKED WITH BLUE. THE DASHED LINE SHOWS THE PATH OF ATMOSPHERIC CROSS-SECTIONS ANALYSED IN SECTION 2.3.3.2. 48

FIGURE 2.2: CLIMATOLOGICAL MEAN ANNUAL PRECIPITATION IN THE SERENGETI AND SURROUNDING REGION. CALCULATED FROM (A) CHIRPS DATA (1987-2016); AND (B) TRMM DATA (1998-2014). LAKES ARE OUTLINED WITH THIN BLACK LINES, WHILE A THICK BLACK LINE SHOWS THE OUTLINE OF THE SERENGETI NATIONAL PARK. GREY CONTOURS ILLUSTRATE REGIONAL TOPOGRAPHY (GTOPO30 DATA). 52

FIGURE 2.3: MONTHLY CLIMATOLOGICAL MEAN PRECIPITATION ACROSS THE WIDER SERENGETI DOMAIN. MONTHLY RAINFALL CLIMATOLOGIES CALCULATED FROM CHIRPS DATASET (1987-2016) FOR EACH MONTH, STARTING WITH JANUARY (A) AND FINISHING WITH DECEMBER (L). GTOPO30 TOPOGRAPHY DATA OVERLAID. 54

FIGURE 2.4: ANNUAL CYCLE OF PRECIPITATION OVER THE WIDER SERENGETI DOMAIN (1-4 S, 33-37 E). THE SOLID BLACK LINE SHOWS THE ANNUAL CYCLE AVERAGED ACROSS ALL OF THE CHIRPS GRID CELLS, WHILE THE DASHED BLACK LINE SHOWS THE AVERAGE OF THE TRMM DATA. ORANGE LINES SHOW THE CLIMATOLOGICAL ANNUAL CYCLES OF INDIVIDUAL CHIRPS GRID CELLS, AND BLUE LINES REPRESENT ANNUAL CYCLES OVER INDIVIDUAL TRMM GRID CELLS. DATA (CHIRPS 1987-2016, AND TRMM 1998-2014). 55

FIGURE 2.5: SPATIAL DISTRIBUTION OF CHANGE IN PRECIPITATION SIGNAL BETWEEN CONSECUTIVE WET SEASON CORE MONTHS. CLIMATOLOGICAL RAINFALL DECREASED (YELLOW) OR INCREASED (GREEN) BETWEEN ONE MONTH AND THE NEXT IS SHOWN, THEREFORE COLOUR CORRESPONDS TO WET SEASON PEAK RAINFALL MONTH. RAINFALL CHANGE SIGNALS DISPLAYED FOR (A) NOVEMBER –DECEMBER, AND (B) MARCH – APRIL. DATA: CHIRPS (1987-2016). 56

FIGURE 2.6: CLUSTER ANALYSIS OF NORMALISED CLIMATOLOGICAL ANNUAL CYCLES. FOR EACH SPATIAL DATAPOINT/LOCATION, THE ANNUAL CYCLE OF PRECIPITATION WAS CLUSTERED USING HIERARCHICAL CLUSTER ANALYSIS (WARD'S CRITERION). THE SPATIAL DISTRIBUTION OF THE RESULTING CLUSTERS IS SHOWN FOR THE (A) TRMM (1998-2014); AND (C) CHIRPS (1987-2016) PRECIPITATION DATASETS. THE ANNUAL CYCLES FOR THE IDENTIFIED CLUSTERS ARE SHOWN FOR (B) TRMM; AND (D) CHIRPS. ERRORBARS INDICATE THE 95 % CONFIDENCE INTERVALS FOR CLUSTER MONTHLY MEANS, CALCULATED WITH A NON-PARAMTERIC BOOTSTRAP RESAMPLING PROCEDURE BASED ON 10000 SAMPLES. 58

FIGURE 2.7: CLIMATOLOGICAL PRECIPITATION AND 750 HPA WIND PATTERNS DURING THE EAST AFRICAN WET SEASONS. PRECIPITATION (CHIRPS, 1987-2016) AND WIND (ERA5, 1986-2017) CLIMATOLOGIES SHOWN FOR (A) MARCH; (B) OCTOBER; (C) APRIL; (D) NOVEMBER; (E) MAY; AND (F) DECEMBER. WIND VECTORS WERE REGRIDDED TO A RESOLUTION OF 0.75° FOR EASE OF VIEWING. GTOPO30 TOPOGRAPHY DATA OVERLAID. .. 61

FIGURE 2.8: CLIMATOLOGICAL PRECIPITATION AND 750 HPA WIND PATTERNS DURING THE EAST AFRICAN DRY SEASONS. PRECIPITATION (CHIRPS, 1987-2016) AND WIND (ERA5, 1986-2017) CLIMATOLOGIES SHOWN FOR (A) JANUARY-FEBRUARY; AND (B) JUNE-SEPTEMBER. WINDS REGRIDDED TO 0.75 ° RESOLUTION. GTOPO30 TOPOGRAPHY DATA OVERLAID. 62

FIGURE 2.9: MEAN ANNUAL SURFACE WIND (VECTORS) AND DIVERGENCE (SHADING) OVER EAST AFRICAN FOR (A) EARLY MORNING (06:00 EAT) AND (B) EARLY EVENING (18:00 EAT). AREAS WITH DIVERGING WINDS ARE SHOWN IN BLUE, AND AREAS WITH CONVERGING WINDS ARE SHOWN IN RED. WIND VECTORS WERE REGRIDDED TO A 0.5° RESOLUTION FOR EASE OF VIEWING, WHILE DIVERGENCE VALUES ARE DISPLAYED AT THE NATIVE RESOLUTION OF 0.25°. DATA: ERA5 (1987-2016). GTOPO30 TOPOGRAPHY DATA OVERLAID. 63

FIGURE 2.10: MEAN SURFACE WIND (VECTORS) AND DIVERGENCE (SHADED) AT 18:00 EAT IN (A) FEBRUARY, (B) APRIL, (C) AUGUST, AND (D) NOVEMBER. WIND VECTORS WERE REGRIDDED TO A RESOLUTION OF 0.5° FOR EASE OF VIEWING, WHILE DIVERGENCE VALUES ARE DISPLAYED AT THE NATIVE RESOLUTION OF 0.25°. DATA: ERA5 (1987-2016). GTOPO30 TOPOGRAPHY DATA OVERLAID. 64

FIGURE 2.11: MEAN MONTHLY EARLY EVENING (18:00 EAT) SURFACE WIND PATTERNS (VECTORS) AND 825 HPA SPECIFIC HUMIDITY (SHADING) FROM ERA5 DATA (1987-2016). SPECIFIC HUMIDITY VALUES AT LEVELS BELOW SURFACE PRESSURE ARE MASKED WITH LIGHT GREY. GTOPO30 TOPOGRAPHY DATA OVERLAID. 65

FIGURE 2.12: TIME OF MAXIMUM ANNUAL PRECIPITATION. ANALYSIS BASED ON PRECIPITATION CLIMATOLOGIES THAT WERE CALCULATED FOR EACH 3-HOURLY TIMESTEP OF THE TRMM DATASET (1998-2014). GTOPO30 TOPOGRAPHY DATA OVERLAID. 66

FIGURE 2.13: MONTHLY TIME OF MAXIMUM PRECIPITATION AND 15:00 (EAT) SURFACE WIND PATTERNS. PLOTS (A)-(L) REPRESENT JANUARY-DECEMBER RESPECTIVELY. PRECIPITATION CLIMATOLOGIES WERE CALCULATED FOR EACH 3-HOURLY TIMESTEP USING TRMM DATA (1998-2014), AND WIND CLIMATOLOGIES WERE CALCULATED USING SURFACE WIND VECTORS FROM THE ERA5 DATASET (1987-2016). GTOPO30 TOPOGRAPHY DATA OVERLAID. 68

FIGURE 2.14: MEAN AFTERNOON PRECIPITATION AND SURFACE WIND PATTERNS DURING A WET AND DRY SEASON MONTH. MEAN HOURLY RAINFALL AND WIND VECTORS WERE CALCULATED DURING MARCH FOR (A) 15:00

(13:30-16:30 precipitation), (b) 18:00 (16:30-19:30 precipitation), and (c) 21:00 (19:30-22:30 precipitation), and in August for (d) 15:00 (13:30-16:30 precipitation), (e) 18:00 (16:30-19:30 precipitation), and (f) 21:00 (19:30-22:30 precipitation). Times in East Africa Time. Data: TRMM (1998-2014) and ERA5 (1987-2016). Gtopo30 topography data overlaid. 69

Figure 2.15: Topographic and afternoon atmospheric cross-sections over the Serengeti during a wet and dry month of the year. The cross-sections run in a diagonal line from 1°S, 33°E in the north-west (NW) to 4°S, 36°E in the south-east (SE) (path shown in Figure 2.1). Individual panels show atmospheric conditions in March at (a) 15:00 EAT, (b) 18:00 EAT, (c) 21:00 EAT, and August at (d) 15:00 EAT, (e) 18:00 EAT, and (f) 21:00 EAT. Panels (g) and (h) are identical and depict the topography along the transect line (Gtopo30 data). In panels (a)-(f) colour illustrates ascending (red) and descending (blue) motion. Values below the surface pressure are masked with black. The x-components of the vectors show the magnitude of winds tangential to the transect line (m/s). The diagonal nature of the transect means that vectors with a positive (negative) x-component represent the north-westerly (south-easterly) component of the winds. The y-components show vertical velocity (Pa/s). The vertical component of the vectors is scaled by -10 for ease of viewing. The tenfold multiplication of the vectors allows the vertical motion to be more easily visible, while the negative multiplication allows areas with ascending motion to have upward-pointing arrows. Data: ERA5 (1987-2016). 71

Figure 3.1: Environmental input layers used to drive SD model. (A) Unaltered climatological annual precipitation; (B) spatially averaged annual precipitation; (C) unaltered plant nitrogen concentration; (D) spatially averaged plant nitrogen concentration; (E) unaltered habitat classification map; and spatially homogenous habitat maps entirely composed of (F) grassland (0 % tree canopy coverage) or (F) savannah (36 % tree canopy coverage). 90

Figure 3.2: Modelled wildebeest population size driven by stochastic and non-stochastic rainfall conditions. The ensemble mean of unaltered model runs (labelled Unaltered Model Run) was calculated from 100 runs with the original model setup (random annual rainfall conditions and fire frequency). The remaining model runs were single runs, using a set fire frequency of 0.5, and driven repeatedly by the same rainfall conditions. These rainfall consisted of either the mean rainfall climatology (calculated from 1961 to 1990; labelled "Rainfall

CLIMATOLOGY"), OR THE MEAN RAINFALL CLIMATOLOGY ALTERED BY ± 5-20 % (LABELLED "CLIMATOLOGY +/- N %"). 99

FIGURE 3.3: IMPACT OF THE REMOVAL OF ENVIRONMENTAL GRADIENTS ON MODELLED WILDEBEEST (A) POPULATION SIZE AND (B)-(E) MOVEMENT PATTERNS. ENVIRONMENTAL GRADIENTS WERE REMOVED FROM THE MODEL BY SPATIALLY AVERAGING NITROGEN AND PRECIPITATION AROSS THE WHOLE REGION, WHILE HABITAT TYPE WAS CHANGED TO EITHER 100 % SAVANNAH OR 100 % GRASSLAND. (A) POPULATION SIZE RESPONSE TO REMOVING 8 COMBINATIONS ENVIRONMENTAL GRADIENTS (MODEL RUNS 0-5,10 AND 11). THE IMPACT ON MOVEMENT PATTERNS IS SHOWN BY THE COEFFICIENT OF VARIATION, FOR RUNS WITH (B) 0; (C) 1; (D) 2; AND (E) 3 ENVIRONMENTAL GRADIENTS REMOVED. THE ENVIRONMENTAL LAYERS THAT WERE SPATIALLY HOMOGENISED IN THE MODEL RUNS WERE (B) NONE (RUN 0); (C) RAINFALL (RUN 1); (D) RAINFALL AND NITROGEN (RUN 5); AND (E) RAINFALL, NITROGEN AND HABITAT TYPE (CLASSIFIED AS 100 % SAVANNAH) (RUN 10). 101

FIGURE 3.4: RESPONSE OF MODELLED WILDEBEEST TO ALTERED MONTHLY PRECIPITATION TOTALS. IN THE ELASTICITY ANALYSIS, INDIVIDUAL MONTHS OF THE MEAN RAINFALL CLIMATOLOGY WERE ALTERED BY ± 5-20 %, AND THE PREDICTED WILDEBEEST POPULATION SIZE IS SHOWN IN RELATION MEAN ECOSYSTEM-WIDE ANNUAL RAINFALL. IN THE SENSITIVITY ANALYSES, THE ENVIRONMENTAL LAYERS DRIVING THE MODEL (HABITAT TYPE, NITROGEN CONCENTRATION AND PRECIPITATION) WERE SPATIALLY HOMOGENISED. INDIVIDUAL MONTHS OF THE MEAN RAINFALL CLIMATOLOGY WERE THEN ALTERED BY ± 0.5-20 MM MONTH^{-1} CELL^{-1}. THE HABITAT LAYERS USED IN THE SENSITIVITY ANALYSES WERE CLASSIFIED AS ENTIRELY SAVANNAH (36 % TREE COVER), OR GRASSLAND (0 % TREE COVER). NOTE THAT Y-AXIS TOTALS DIFFER BETWEEN PANELS. 103

FIGURE 3.5: THE RELATIONSHIP BETWEEN PREDICTED WILDEBEEST STABLE POPULATION EQUILIBRIUM SIZE AND PRECIPITATION (AVERAGED ACROSS TWO TEMPORAL AND SPATIAL SCALES). EACH OF THE 47 MODEL RUNS WAS DRIVEN USING THE RAINFALL CONDITIONS RECORDED IN A SINGLE YEAR (1960-2006), AND UNALTERED NITROGEN AND HABITAT CLASSIFICATION LAYERS. ECOSYSTEM-WIDE RAINFALL WAS CALCULATED ACROSS THE WHOLE REGION INCLUDED IN THE SD MODEL, WHILE SOUTH-EASTERN RAINFALL WAS CALCULATED ACROSS THE AREA CLASSIFIED AS GRASSLAND. NOTE THAT X-AXIS RANGES DIFFER BETWEEN PANELS. 105

FIGURE 4.1: OBSERVED AND MODELLED MEAN ANNUAL CYCLES OVER THE SERENGETI-MARA ECOSYSTEM (TOP) AND ITS SOUTH-EASTERN SECTION (BOTTOM). DASHED LINES REPRESENT MEAN ANNUAL PRECIPITATION. OBSERVED DATA: CHIRPS V2.0 (1997-2006). MODELLED DATA: CP4-AFRICA HINDCAST (1997-2006) AND

future projection (10 years c. 2100). Colour represents precipitation dataset, with red, green and blue representing the CHIRPS, CP4-Africa hindcast and CP4-Africa future projection datasets respectively. 130

Figure 4.2: Annual precipitation climatologies in mm/year and the differences between them. Climatological annual precipitation over the Serengeti-Mara ecosystem in (a) observed (CHIRPS, 1997-2006), (b) climate model hindcast (CP4-Africa, 1997-2006) and (c) climate model future projection (CP4-Africa, 10 year period circa. 2100) datasets. (d) Differences between mean hindcast and observations over the Lake Victoria basin. (e) Projected changes to mean annual precipitation over the Lake Victoria basin, calculated by subtracting the CP4-Africa model hindcast from the future projection. In panels (a)-(c) precipitation datasets were linearly interpolated to match the 10 km grid size of the SD model, while in panel (d) CHIRPS values were linearly interpolated to match the CP4-Africa grid size and allow comparison between the datasets. Colourbars vary between panels to allow the spatial distribution of precipitation to be clearly displayed. 132

Figure 4.3: Mean monthly precipitation in mm/month and late afternoon 800 hPa wind vectors during March and August. Observed conditions in (a) March and (b) August were calculated from the CHIRPS v2.0 (precipitation, 1997-2006) and ERA5 (winds, 800 hPa, 18:00 EAT, 1997-2006) datasets. Modelled conditions were calculated from the CP4-Africa hindcast dataset (monthly precipitation, monthly 800 hPa winds at 18:00 EAT, 1997-2006). Observed and modelled precipitation have different colour-bar scales to allow the spatial distribution of precipitation to be clearly displayed. 134

Figure 4.4: Projected future changes to mean monthly precipitation in mm/month and 700 hPa evening (21:00 EAT) wind vectors in (a) March and (b) August. Future changes were calculated by subtracting the mean monthly wind and precipitation values in the CP4-Africa hindcast (1997-2006) from those in the CP4-Africa future projection (10 year period c. 2100)..... 135

Figure 4.5: Modelled response of wildebeest population to observed past, modelled past, and modelled future mean precipitation conditions. The Savannah Dynamics model was driven with mean monthly precipitation climatologies from 3 datasets: CHIRPS v2.0 (observed precipitation, 1997-2006); CP4-Africa hindcast (modelled precipitation, 1997-2006); and the CP4-Africa future projection (modelled precipitation, 10-year period c. 2100). Colour represents

THE PRECIPITATION DATASET USED TO DRIVE THE SD MODEL, WITH RED, GREEN AND BLUE REPRESENTING THE CHIRPS, CP4-AFRICA HINDCAST AND CP4-AFRICA FUTURE PROJECTION DATASETS RESPECTIVELY. 136

FIGURE 4.6: RELATIONSHIPS BETWEEN WILDEBEEST EQUILIBRIUM POPULATION SIZE AND SEASONAL/SPATIAL CHARACTERISTICS OF PRECIPITATION. PRECIPITATION IS SPATIALLY AVERAGED OVER THE WHOLE OF THE SME OR JUST THE SOUTH-EAST. PRECIPITATION IS TEMPORALLY SUMMED OVER EITHER THE WHOLE YEAR, OR JUST THE DRY SEASON MONTHS OF JUNE TO OCTOBER. X-AXIS RANGES VARY BETWEEN PANELS DUE TO THE DIFFERENCES IN THE EXAMINED PRECIPITATION RANGES. COLOUR REPRESENTS THE PRECIPITATION DATASET USED TO DRIVE THE SD MODEL, WITH RED, GREEN AND BLUE REPRESENTING THE CHIRPS, CP4-AFRICA HINDCAST AND CP4-AFRICA FUTURE PROJECTION DATASETS RESPECTIVELY. 138

FIGURE 4.7: MEAN DAILY (A) NORMALISED POPULATION SIZE AND (B) DEATH RATE OVER THE ANNUAL CYCLE. WILDEBEEST POPULATION DYNAMICS IN MODEL RUNS DRIVEN BY OBSERVED, MODELLED PAST, AND MODELLED FUTURE MEAN PRECIPITATION CONDITIONS. DAY 0 REPRESENTS THE 1ST OF NOVEMBER AND NEW MONTHS ARE MARKED BY DASHED BLUE LINES. THE ORANGE DASHED LINE REPRESENTS THE DAY FIRES OCCUR. COLOUR REPRESENTS THE PRECIPITATION DATASET USED TO DRIVE THE SD MODEL, WITH RED, GREEN AND BLUE REPRESENTING THE CHIRPS, CP4-AFRICA HINDCAST AND CP4-AFRICA FUTURE PROJECTION DATASETS RESPECTIVELY. 140

Appendices

FIGURE A-1: MAP OF THE SERENGETI-MARA ECOSYSTEM AND SPATIAL EXTENT OF THE SAVANNAH DYNAMICS MODEL. THE BOUNDARIES OF THE SERENGETI NATIONAL PARK AND MARA RESERVE ARE OUTLINED IN BLACK. THE GREEN GRID CELLS SHOW THE AREA USED IN THE SD MODEL (EACH GRID CELL IS 10 KM X 10 KM). 217

FIGURE B-1: CLUSTER ANALYSIS OF TRMM CLIMATOLOGICAL ANNUAL CYCLES (1998-2014) DISPLAYED AS (A) A CLUSTER DENDOGRAM, AND (B)-(C) EUCLIDEAN DISTANCE BETWEEN CLUSTERS VS. AGGLOMERATION STEP. DIFFERENT SCALES ARE SHOWN IN (B) AND (C) TO BETTER ILLUSTRATE THE STEP CHANGES IN FINAL STAGES OF THE CLUSTERING ALGORITHM. THE DENDROGRAM SHOWS THE ORDER IN WHICH THE OBSERVATIONS (ANNUAL CYCLES AT INDIVIDUAL LOCATIONS) WERE CLUSTERED TOGETHER. THE EUCLIDEAN DISTANCE AT WHICH THE CLUSTERING OCCURRED DEPENDED ON THE SIMILARITY BETWEEN THE TWO CLUSTERS BEING JOINED. 228

FIGURE B-2: CLUSTER ANALYSIS OF CHIRPS CLIMATOLOGICAL ANNUAL CYCLES (1987-2016) DISPLAYED AS (A) A CLUSTER DENDOGRAM, AND (B)-(C) EUCLIDEAN DISTANCE BETWEEN CLUSTERS VS. AGGLOMERATION STEP.

DIFFERENT SCALES ARE SHOWN IN (B) AND (C) TO BETTER ILLUSTRATE THE STEP CHANGES IN FINAL STAGES OF THE CLUSTERING ALGORITHM. THE DENDROGRAM SHOWS THE ORDER IN WHICH THE OBSERVATIONS (ANNUAL CYCLES AT INDIVIDUAL LOCATIONS) WERE CLUSTERED TOGETHER. THE EUCLIDEAN DISTANCE AT WHICH THE CLUSTERING OCCURRED DEPENDED ON THE SIMILARITY BETWEEN THE TWO CLUSTERS BEING JOINED. 229

List of Tables

Main Thesis

TABLE 2.1: SUMMARY OF THE KEY CHARACTERISTICS OF ANNUAL PRECIPITATION CYCLES IN DIFFERENT PARTS OF THE WIDER SERENGETI DOMAIN. THE ~ SYMBOL REPRESENTS DISAGREEMENT BETWEEN CLUSTERS IN DIFFERENT DATASETS. 60

TABLE 3.1: RESEARCH OBJECTIVES AND NAMES OF THE EXPERIMENTS CARRIED OUT IN THIS STUDY 91

TABLE 3.2: COMBINATIONS OF SPATIALLY HOMOGENOUS ENVIRONMENTAL LAYERS USED TO DRIVE SD MODEL. 96

List of Acronyms

ARC-Lake *Along-Track Scanning Radiometer (ATSR) Reprocessing for Climate: Lake Surface Water Temperature and Ice Cover*

CHIRPS *Climate Hazards Group InfraRed Precipitation with Station dataset*

CoV *Coefficient of variation*

CP4-Africa *Pan-African Convection-Permitting Regional Climate Simulation with the Met Office Unified Model*

ENSO *El Niño Southern Oscillation*

ERA *European Centre for Medium-Range Weather Forecasts Re-Analysis*

GCM *General circulation model*

HadGem2 *Hadley Global Environment model 2*

IPCC *Intergovernmental Panel on Climate Change*

MGR *Maswa Game Reserve*

RCM *Regional climate model*

SD *Savannah Dynamics*

SME *Serengeti-Mara ecosystem*

SOI *Southern Oscillation Index*

SST *Sea surface temperature*

TRMM *Tropical Rainfall Measuring Mission*

UM	*Unified Model*
WMO	*World Meteorological Organisation*

Chapter 1. Introduction

1.1 Motivation

The Serengeti-Mara ecosystem (SME) is home to the world's largest and most species-rich extant ungulate migration (Harris *et al.*, 2009), and includes 1.3 million blue wildebeest *(Connochaetes taurinus)* (Hopcraft *et al.*, 2015; G. Hopcraft 2020, personal communication, 11th August). Every year the wildebeest migrate around the 30,000 km^2 of the SME in a quest for fresh grazing, driven by the presence of opposing nutritional and precipitation gradients across the ecosystem (Holdo *et al.*, 2009b). In wet months the herds spend time on the nutrient rich south-eastern grassland plains, while the driest months are spent in the wooded highlands of the Mara that receive year-round precipitation (Sinclair *et al.*, 2008).

The sheer abundance of the wildebeest make them a cornerstone of the SME. Through direct and indirect mechanisms, they affect the fauna, vegetation dynamics, nutrient cycling and fire regime of the ecosystem (McNaughton *et al.*, 1997; Packer *et al.*, 2005; Sinclair *et al.*, 2008; Eby *et al.*, 2015). The dominant role the wildebeest play in shaping the ecosystem dynamics, means that the SME can be classified as a "grazing ecosystem", one where the ecological processes are significantly regulated by a prominent herbivore-based food web (McNaughton, 1985; Frank *et al.*, 1998).

As recently as the 19th century, large swathes of the terrestrial surface of the planet were covered by natural grasslands (Smith, 2020), which likely had similar ecosystem dynamics (Frank *et al.*, 1998) and supported millions of large migratory herbivores (Harris *et al.*, 2009). Now, due to modern human activity, grazing ecosystems are restricted to a few isolated locations (Frank *et al.*, 1998). Across the globe the population sizes of migratory terrestrial mammals, and the distances they travel, have been decreasing for decades (Wilcove and

Wikelski, 2008; Tucker *et al.*, 2018). In 2009 the SME was one of only three locations in the world in which the remaining populations of large mammalian migrants were not in decline (Harris *et al.*, 2009). The continuing disappearance of our grazing ecosystems is a great loss. As well as the inherent value of these unique natural systems, grazing ecosystems are highly productive, biodiverse habitats, which support large animal biomasses and hold large reservoirs of carbon (McNaughton, 1985; Fryxell, 1995; Smith, 2014; Sinclair *et al.*, 2015a). Therefore when large herbivore migrations collapse, the carbon storage capacity, biodiversity, and biomass supported by the area are typically negatively affected as well (Dobson *et al.*, 2010; Holdo *et al.*, 2011b; Smith, 2014).

The continued loss of migratory ungulates and grazing ecosystems makes the protection of those that remain an important endeavour. The SME has been conserved by extensive efforts by the Tanzanian and Kenyan governments (Thirgood et al., 2004), a particularly impressive feat when the GDPs of these nations are considered (World Bank, no date). The Serengeti National Park is also relatively unique in its original purpose to protect the entire range of a migratory species (Sinclair *et al.*, 2015a). This means 90% of the wildebeest migration takes place within the core protected areas of a network of national parks (Thirgood *et al.*, 2004), allowing a population of 1.2-1.4 million migratory individuals to remain at a stable level for decades (Harris *et al.*, 2009; Hopcraft *et al.*, 2015; G. Hopcraft 2020, personal communication, 11th August).

There are still a number of local threats to the Serengeti wildebeest and the SME (Dobson *et al.*, 2010; Veldhuis *et al.*, 2019). Yet the size of the protected area, the consideration that went into its establishment, and the level of protection afforded to animals that reside within its boundaries, mean that the migratory wildebeest of the SME have a better chance of success than many other migratory species around the world (Bolger *et al.*, 2008).

The region may now be affected by a global phenomenon to which Tanzania and Kenya have contributed little. In recent decades East Africa has experienced a greater frequency of extreme precipitation events (both droughts and floods) (Niang *et al.*, 2014; Nicholson, 2016b), as well as a reduction in rainfall during March to May (Rowell *et al.*, 2015; Wainwright *et al.*, 2019). While research is ongoing to establish whether these changes are linked to anthropogenic climate change or natural variability, in the coming centuries climate model projections show high confidence that anthropogenic climate change will alter precipitation patterns across the globe (Collins et al., 2013; Kirtman et al., 2013).

We know that the Serengeti wildebeest migration is driven by specific rainfall patterns, and that inter-annual fluctuations in precipitation strongly affect the wildebeest's population size and movement patterns (Mduma *et al.*, 1999; Fryxell *et al.*, 2015). This therefore leads to the central question of this thesis: how might climate change affect the migratory wildebeest of the Serengeti?

1.2 Rationale

Limited work has been carried out investigating how the population of migratory wildebeest in the SME will be affected by climate change. It is surprising that more work hasn't been done on this topic, as ecologists have been warning that the migratory wildebeest and SME may be at risk from climate change for decades (McNaughton, 1994; Owen-Smith and Ogutu, 2013). Previous work has established the dependence of the migratory wildebeest on specific precipitation patterns (Holdo *et al.*, 2009b), and recorded their response to past rainfall fluctuations (Mduma et al., 1999; Fryxell et al., 2015). However, to date only one study has examined the impact of altered future rainfall on the Serengeti-Mara wildebeest (Holdo *et al.*, 2010). Holdo *et al.* (2010) used a combined socioeconomic and ecological model to investigate potential futures with altered rainfall patterns and poaching activities. Wet and dry future

climate scenarios were generated by the authors, by identifying past decades with above and below average rainfall respectively, and then used to drive the model. This work provided valuable information about how the wildebeest may respond to future changes in mean annual rainfall. However, the study did not use rainfall projections generated by climate models. This is potentially an issue, as the precipitation conditions projected by many climate models are different to those that have been observed in the past (Niang *et al.*, 2014; Dosio *et al.*, 2019; Kendon *et al.*, 2019).

The lack of studies in this area may be due to the high level of uncertainty involved in mathematically simulating complex systems. There are a multitude of ways to model the impact of environmental disturbance, and experiments would ideally be carried out in a controlled environment. Yet for large, complex systems, such as the global climate system or long-distance mass migrations, it is not possible to carry out controlled experiments in the real world. In these situations, it is necessary to either infer future change based on past observed relationships, or to use these relationships (and the underlying laws/theory of the relevant discipline) to develop mechanistic mathematical models that represent the system. Given the novelty of current and future atmospheric concentrations of CO_2 (Cubasch *et al.*, 2013), the use of mathematical simulations of the climate, and ecosystem response, are arguably the best tools to understand and prepare for future change.

When taking this approach, it is important to carefully consider model uncertainty. Any model simulating a complex system has to make assumptions and rely on parameterisations that introduce uncertainty (Baker *et al.*, 2017). The more complex a system, the more assumptions are required, and thus a greater degree of uncertainty is an inherent feature of complex models. In addition, even without assumptions and parameterisation, the model may not simulate the target subject well, therefore model performance has to be appraised.

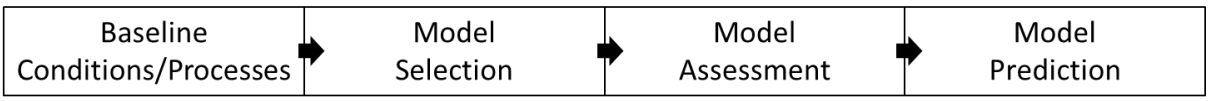

Figure 1.1: Approach to use of models in this thesis. Representation of key processes shapes model selection, assessment of model performance highlights key uncertainties before model is used to make predictions

In this thesis the following approach is used to reduce the uncertainty of both the ecological and climate models which are used: (1) consider the key processes controlling the relevant natural systems; (2) identify models which have the potential to simulate these processes; (3) critically assess the performance of those models; and (4) use the models to explore the impact of future change (Figure 1.1).

To address the first two stages of this approach, Sections 1.4 and 1.5 summarise the relevant baseline knowledge of the ecological and atmospheric systems in the SME, as well as the scientific community's current ability to model them. Section 1.3 discusses how spatial and temporal scales are defined in the fields of climate science, ecology, and this thesis.

1.3 Definition of Scale

This thesis is an interdisciplinary piece of work in the fields of climate science and ecology. One of the key differences between these fields is the classification of scale. In climate science, atmospheric phenomena are typically broken up into three categories: microscale, mesoscale, and macroscale/large-scale. While there is overlap between these terms depending on the specific phenomenon of interest, large-scale atmospheric processes typically have an average diameter > 1000 km and a temporal scale of several days to months, mesoscale phenomena have an average diameter of approximately 1-1000 km and a temporal scale of several hours to a couple of days, and microscale phenomena have an average diameter from 2 km to < 1 m and a temporal scale of seconds to minutes (Coleman and Law, 2015; Pielke *et al.*, 2020). When large-scale and mesoscale atmospheric processes are discussed in this thesis, it is according to these definitions. When "relatively small" distances or atmospheric processes are

referred to in Chapter 2, these terms should be interpreted as small in comparison to the large-scale atmospheric processes present in the region. Small storms refer to those that are not possible to be represented by convection-permitting atmospheric models with a 4 km horizontal spatial resolution (such as the CP4-Africa model). Finally, large water bodies are defined as those that are able to affect the local climate.

By contrast, in the ecological literature, the definition of large-, meso- and small-scale processes typically depend on the ecological system, and/or research question, of interest (Schneider, 2001; Torney *et al.*, 2018). For example, Barnes *et al.* (1998) and Delcourt and Delcourt (1988) describe spatiotemporal scales relevant to forest ecology. They define micro-time scales as < 500 years and micro-spatial scales as 1 m to 1 km diameter, meso-temporal scales as 500 to 10 000 years and meso-spatial scales as 1 km to 100 km diameter (phenomena occurring over meso-spatial and meso-temporal scales are stated to relate to landscape ecology), macro-temporal scales as 10 000 to 1 million years and macro-spatial scales as 100 km to 1 000 km diameter, and phenomena occurring on larger scales as mega-scale. As these spatial scales are deemed important for the study of the spatial distribution of vegetation patterns and landscape features, it could be argued that this would be a relevant set of scales to use when studying the Serengeti-Mara ecosystem. (Especially as the wildebeest migration is driven by environmental conditions and processes that operate across a wide-range of temporal and spatial scales, including geological time.) Yet by contrast, when Torney *et al.* (2018) discuss the range of scales that can be used to measure the movement of the Serengeti wildebeest, they describe “fine scale” measurements as occurring across metres and over seconds to minutes, while large-scale dynamics occur over months to years across the spatial extent of the whole Serengeti-Mara ecosystem. They specifically state that there is no “right” scale in ecological questions; only the scale that best answers the question of interest.

Therefore, the range of spatiotemporal ecological scales used in this thesis could be defined according to the data used within it. This thesis heavily focuses on the representation of the Serengeti-Mara ecosystem in the existing Savannah Dynamics mathematical model. Multiple ecological processes are represented in the model, many of which are updated on daily timescales, and the study is interested in the impact of rainfall conditions changing over decadal and centurial timescales, over a grid of 307 10 x 10 km grid cells. However, classifying the range of spatiotemporal dimensions of ecological processes based on their representation in a model (rather than measurements taken by the author, or underlying ecological theory tailored to the specific research questions of this thesis) is not necessarily an ideal scientific approach.

Overall, due to variation in the literature related to the definition of small and large-scale ecological phenomena, and the wide range of temporal and spatial scales relevant to key processes in the Serengeti-Mara ecosystem (in reality and within the SD model), this thesis avoids classifying ecological processes as large, meso-, or small-scale. Instead the spatial and temporal dimensions of relevant ecological phenomena are explicitly stated as numerical values. An exception is made when ecological effects are described as occurring on a "landscape-scale", which should be interpreted as impacting the whole Serengeti-Mara ecosystem.

1.4 The Serengeti-Mara Ecosystem

1.4.1 Topography and Lakes

The SME is situated in East Africa, and the physical environment of this part of the world is dominated by the East African Rift Valley; a rift system that runs from the Red Sea to Malawi. At approximately 3 °N, in the region of Lake Turkana (formerly known as Lake Rudolf), the rift splits into an eastern and western branch (

Figure 1.2a). These branches mark the boundaries of the Lake Victoria basin, with Lake Victoria situated in the centre. The lake covers 68,000 km^2 but is only 80 m deep (Scoon, 2018).

The Serengeti National Park is situated in northern Tanzania and protects a large proportion of the SME.

Figure 1.2b shows that the park lies between the eastern branch of the East African Rift Valley and Lake Victoria. It is also positioned to the south of an area of high ground called the Kenya Highlands, which has many peaks exceeding 3000 m.

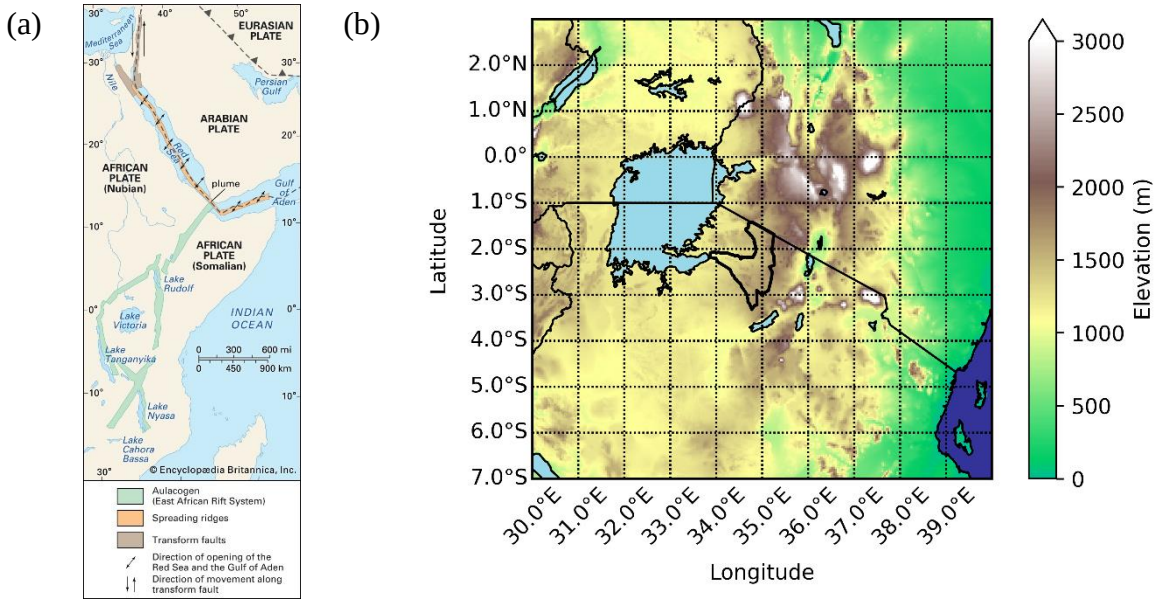

Figure 1.2: Topography of the East African Rift System. (a) Map of tectonic processes occurring within and between the African and Arabian Plates (reproduced from Encyclopaedia Britannica (no date)). (b) Topographic elevation over the Serengeti National Park and wider surrounding area. In panel (b), colour represents 2 minute resolution topographic elevation data from the Global 30 Arc-Second Elevation dataset (Gesch et al., 1999), except for water bodies that are masked by light blue (lakes) and dark blue (ocean). Country boundaries and lake/coastline boundaries are shown by thin black lines, while the boundaries of the Serengeti National Park have a thick black line.

As the name suggests, the East African Rift Valley is a lowland flanked by highlands, and the rift itself can clearly be seen in the vicinity of Lake Natron in Figure 1.3. The Serengeti National Park sits in the shadow of the rift highlands, which include the Loita hills to the north-east, and the Ngorongoro highlands and Ngorongoro Crater to the south-east. Within the Serengeti National Park, elevation decreases from east to west; elevations of approximately 1850 m are

present near the Ngorongoro Highlands, whilst elevations are less than 1000 m in the westernmost part of the park.

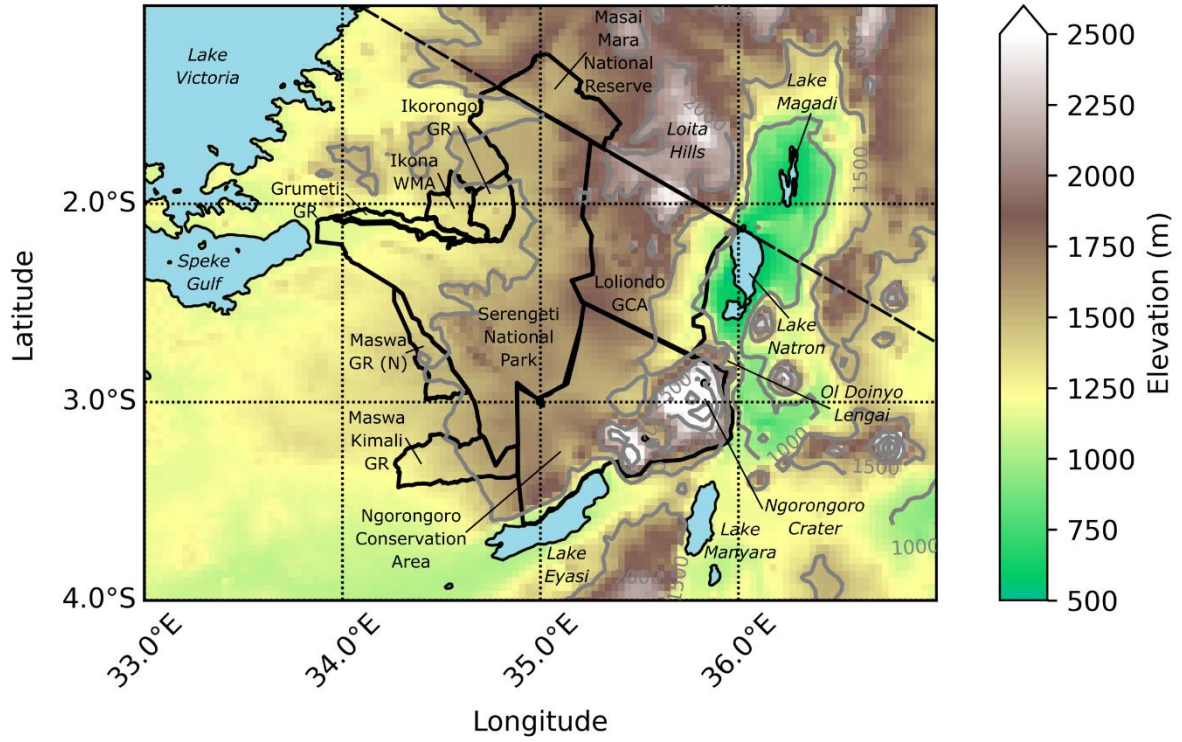

Figure 1.3: Topography of the region surrounding the Serengeti National Park. The boundaries of protected areas and lakes are indicated by thick and thin solid black lines respectively. The dashed black line shows the border between Kenya (north) and Tanzania (south). Colour displays 2 minute resolution topographic elevation data from the Global 30 Arc-Second Elevation dataset (Gesch et al., 1999), and lakes are masked with light blue. Grey lines demarcate topographic contours with 500 m intervals. Protected areas and natural features are labelled with normal and italic text respectively. Acronyms "GR", "WMA" and "(N)" refer to "Game Reserve", "Wildlife Management Area", and "North", respectively. The protected area shapefiles were sourced from Protected Planet (Kenya Wildlife Service, no date; Tanzanian National Parks, no date). The shapefile for the central portion of the Maswa Game Reserve has not been made available by the Tanzania National Parks on this platform, and is therefore missing from this figure.

While the Serengeti National Park protects a large central part of the SME, it does not protect all of it. The SME extends over a network of protected areas (in both Kenya and Tanzania) that serve a vital role (Thirgood *et al.*, 2004). At certain times of year, the wildebeest migration passes through the varied terrain of areas within: Masai Mara National Reserve, Maswa Game Reserve, Grumeti Game Reserve, Ikona Wildlife Management Area, Ikorongo Game Reserve, Loliondo Game Controlled Area, and Ngorongoro Conservation Area (Figure 1.3). Many of these protected areas are crucial to the survival of the migratory wildebeest. For example, the Masai Mara National Reserve provides a dry season refuge for the wildebeest (Maddock,

1979), the Maswa Game Reserve provides a refuge in the south during dry periods of the wet season (Sinclair *et al.*, 2008), and the Ngorongoro Conservation Area contains a sizable portion of the Serengeti plains that the wildebeest preferentially graze during the wet season (Maddock, 1979).

Finally, a feature of crucial importance to the SME lies between the Ngorongoro highlands and Lake Natron. Ol Doinyo Lengai, which means "The Mountain of God" in Masai, sits at 2°45′52″ S, 35°54′58″ E and is the most persistently active volcano in the region (Scoon, 2018).

1.4.2 Nutrient Distribution

Soil properties vary considerable across the SME, with variation in salinity, alkalinity, depth, texture, pH, water holding capacity, organic matter content, microbial biomass and nutrient concentrations (Anderson *et al.*, 2008; Olff and Hopcraft, 2008; Metzger *et al.*, 2015). This is as a result of complex geological, climatic and biotic processes that have occurred over the Serengeti on a spectrum of timescales.

The broad scale variation in soil fertility is strongly determined by the geology of the region. The rocks which underlie the SME are amongst the oldest in the world. Much of the ecosystem sits above exposed Archaen (2.5-4 Ga) and Neoproterozoic (541-1000 Ma) geological formations (Scoon, 2018). However, the surface geology of the west and south-east of the ecosystem is relatively recent. Holocene (< 11.7 ka) era sediments are present in the west due to large rivers that flow across the Serengeti plains towards Lake Victoria, including the Grumeti, Mara, Mbalageti and Orangi rivers. Alluvial deposits are found along the river beds and banks, and on the low-lying plains adjacent to the Speke Gulf of Lake Victoria where the rivers meet the lake (Scoon, 2018). By contrast, the plains in the south-east of the SME are covered by a thin layer of semi-consolidated calcareous ash deposits from Holocene eruptions of the Ol Doinyo Lengai volcano (Dawson, 2008). This layer sits atop old volcanic deposits

from eruptions that occurred over the past 4.3 – 4.5 Ma (Peters *et al.*, 2008). Ol Doinyo Lengai is the only volcano that is currently active in this area, but it is surrounded by 9 other inactive/extinct volcanoes (approximately situated between Lake Natron and Lake Eyasi). When these volcanoes erupted, prevailing winds blew the ash eastward. Therefore eruptions from multiple volcanoes (during their respective periods of activity) have periodically added ash to the area that is now the SME plains over millions of years (Peters *et al.*, 2008). To this day Ol Doinyo Lengai continues to erupt every 15-20 years (Scoon, 2018), and provides periodic new ash deposits over the plains of the SME. In addition, in the far south-east rainfall has caused calcium carbonate salts from the ash to be precipitated out and be redeposited at approximately 1 m below the surface as a shallow impermeable layer of hard pan (caliche) (Sinclair, 1979c; Sinclair *et al.*, 2008). This hard pan layer sits between the ash layer and old rocks, raising the level of the water table and preventing tree root penetration (Sinclair, 1979c; Scoon, 2018).

The age of the underlying rocks largely determines the nutritional content of the soil. In old rocks, exposure to millennia of precipitation has removed the majority of soluble minerals. So while these rocks can be rich in chemically stable (and thus economically valuable) minerals such as gold (Scoon, 2018), their age means that the nutritional value of the soils overlying them is low. Conversely, nutrient concentrations in the soils overlying young rocks are much higher. Overall this means that there is a broad scale soil fertility gradient across the Serengeti, with high nutrient concentrations in the south-east (close to the volcanoes) and low nutrients in the north-west.

Superimposed upon this pattern, there is also a great deal of fine scale variability in soil nutrient distribution. This is due to both physical processes (such as local topography, riverine deposits and fire disturbance) and biotic processes (such as termite activity and vegetation growth) (Eby *et al.*, 2015; Metzger *et al.*, 2015).

Most elements of key nutritional importance to wildebeest are found in significantly high concentrations in plants that grow in the young soils (McNaughton, 1990). However, grass nutritional composition is determined by multiple factors, including fire frequency, climate, plant community composition and abundance, herbivory, and soil properties (Anderson *et al.*, 2007, 2010, 2018).

These complex interactions result in different plant nutrient gradients across the landscape; e.g. nitrogen concentrations in grasses in the south and south-east are 4 x higher than the north-west of the ecosystem, whilst in parts of the south and west of the SME grass sodium concentrations are > 100 x greater than in the north (Holdo *et al.*, 2009b).

Vegetation nutrients act as a proxy to soil nutrient concentrations, but are not a direct measurement, e.g. the high sodium concentrations in the south and west rely also on the presence of sodium accumulating grasses (McNaughton, 1990; Anderson *et al.*, 2007). However, they serve as direct indicators of nutrients available to the migratory wildebeest, and when all nutrients key for wildebeest survival are considered, the picture that emerges is one of a nutritional gradient across the SME: low values in the north; high values in the south-east; and high values of some, but not all, key nutrients in the west.

1.4.3 Vegetation Distribution and Dynamics

The underlying soils have a strong impact on the vegetation of the SME, however the structure and productivity of the vegetation is affected by a complex set of interactions between biotic and abiotic processes.

1.4.3.1 Vegetation distribution across SME

The SME is typically described as savannah, however the vegetation composition varies dramatically across the ecosystem. The SME is home to sand dunes, swamps, grasslands,

scrubland, and woodlands (with a spectrum of ground and canopy cover) (Anderson and Talbot, 1965; Reed et al., 2009; Kimaro et al., 2019). The vegetation can broadly be divided into grassland in the south-east, and Acacia-Commiphora woodlands in the central and northern SME (Norton-Griffiths et al., 1975; Munishi, 2018). Small areas of closed canopy riverine forest are found in the northern and western SME (Turkington *et al.*, 2015), and in the far north-west broadleaved *Terminalia-Combretum* woodlands are present (Herlocker, 1976; Sinclair *et al.*, 2007). However, it should be noted that there is a great deal of fine-scale variability, and this overview does not represent the diversity of vegetation species and communities across the SME (including 200 species of grass (Williams *et al.*, 2016)), nor the numerous detailed classifications of vegetation zones present in the literature (Anderson and Talbot, 1965; Norton-Griffiths *et al.*, 1975; Herlocker, 1976; Sinclair, 1979c; McNaughton, 1983; Reed *et al.*, 2009; Kija *et al.*, 2020).

1.4.3.2 Controls on Vegetation

This distribution of vegetation is controlled by a combination of soil properties, precipitation conditions and disturbance patterns.

Rainfall

A gradient in annual precipitation is present across the SME, with the north-west of the Serengeti National Park receiving 3 times more rainfall than the south-east (approximately 1100 mm/year and 400 mm/year are received in the north-west and south-east respectively) (Norton-Griffiths *et al.*, 1975). In addition, the south-east only receives precipitation during the wet season from November to May and, whilst in the north-west rainfall occurs year round (Norton-Griffiths *et al.*, 1975).

This spectrum of rainfall conditions impact plant growth across the ecosystem in a multitude of ways. Annual rainfall totals affect tree-grass dynamics, as in African savannas the upper bound of maximum woody cover is capped in areas that receive < 650 mm/year (allowing grasses and trees to coexist) (Sankaran *et al.*, 2005). In addition, the calcite hard pan layer that prevents tree growth in the south-east is likely only able to form due to the low precipitation totals in that area (Sinclair *et al.*, 2008). High rainfall totals can erode and leach soluble elements from soils (Schlesinger and Bernhardt, 2013), and soil characteristics strongly determine the plant communities that can grow upon them. Rainfall has been found to control the productivity of grass in the SME; when grazing is excluded, annual grass biomass is linearly related to annual rainfall totals (McNaughton, 1985). The temporal availability of rainfall also affects the length of the grass growing season; growing seasons are as short as 76 days in the south-east, but are essentially continuous in the north-west (McNaughton, 1985).

Soil Properties

Soils provide the substrate for vegetation and are therefore a key determinant of the vegetative communities that can exist in different locations across the SME (Anderson and Talbot, 1965; Sinclair, 1979c; McNaughton, 1985; Holdo *et al.*, 2020). As stated in Section 1.4.2, soil properties are affected on a large scale by the underlying geology (Anderson *et al.*, 2008) and on smaller scales by topography (McNaughton, 1985), fire (Eby *et al.*, 2015), and biotic interactions (Holdo *et al.*, 2007; de Visser *et al.*, 2015).

Plant productivity is broadly affected by the nutrient availability and water holding capacity of soils, which are greater in the south-east and south-west compared to the north-west of the ecosystem (Metzger *et al.*, 2015).

Yet individual species are adapted to specific ranges in soil conditions (e.g. depth, pH, organic matter content, moisture content, and macro- and micro-nutrient availability) (Gregory and

Nortcliff, 2013). As variation in these conditions affects the germination, survival, growth rate and competitive advantage of individual plant species, the varied soils of the SME are one of the key reasons for the diversity of plants present across the ecosystem (Anderson *et al.*, 2008).

Fire

Fire is a major disturbance feature in savannah ecosystems, and approximately 20-50 % of the SME burns annually (Probert *et al.*, 2019). However the spatial distribution, frequency and intensity of fires are not spread equally across the ecosystem. Savannah fires are fuelled by grass biomass growth during the wet season followed by favourable burning conditions in the dry season (Norton-Griffiths, 1979; Holdo *et al.*, 2009a). The amount of fuel (grass biomass) available in a given year is determined by seasonal rainfall patterns (totals and timing), and later in the year, by herbivory and decomposition (Stronach and McNaughton, 1989; Higgins *et al.*, 2000; Sinclair *et al.*, 2007; Holdo *et al.*, 2009a). The strong rainfall gradient across the SME therefore provides a wide variety of fire regimes. Much of the south-eastern grasslands rarely burn as they receives low rainfall totals and therefore has limited fuel for fires, whereas in the rest of the ecosystem burns regularly (Norton-Griffiths, 1979; Anderson *et al.*, 2008).

Fire affects vegetation in the SME in multiple ways. It is one of the main factors preventing the "wet savannahs" (areas receiving > 650 mm/year in rainfall) which make up the majority of the central and northern SME (area with > 650 mm/year) from reverting to closed woodland (Sankaran *et al.*, 2005). This is because there is a negative relationship between fire and tree abundance in savannah ecosystems and the SME. Moderate to heavy burning can kill tree seedlings and stunt the growth of immature plants, therefore limiting tree recruitment (Norton-Griffiths, 1979; Holdo *et al.*, 2009a; Staver *et al.*, 2011).

Fire affects grass by causing a decrease in litter and standing dead material and altering plant species composition (Eby *et al.*, 2015). McNaughton (1983) observed a slight increase in SME

grass production in the first growing season post-fire. In addition, plant regrowth after fire has increased nutrient, water and protein contents (Eby *et al.*, 2015), which is attractive to grazers and can therefore alter grazing patterns (Archibald and Bond, 2004).

Finally, fire affects biodiversity in savannah ecosystems. It is associated with increased plant species diversity in the SME (Belsky, 1992), and pyrodiversity positively impacts bird and mammal biodiversity in wet savannahs across Africa (Beale *et al.*, 2018). However, fire is also contributing to a decline in the rare riverine forests in the SME (Turkington *et al.*, 2015).

Herbivores

Grazers

Grazers have a profound impact on the vegetation of the SME. One of the most important effects that they have on an ecosystem level is through compensatory vegetation production, where grazing stimulates new vegetation growth, therefore increasing the net productivity (McNaughton, 1985). While overgrazing can reduce productivity and damage soils (Angerer *et al.*, 2016), the grazers of the SME naturally adjust their movements and density according to the productivity of the vegetation (McNaughton, 1985; Holdo *et al.*, 2009b). This leads to positive consumer-resource interactions at the most productive sites (such as the grassland plains of the SME). Highly productive areas attract more grazers (McNaughton, 1984), which in turn stimulates increased production, through mechanisms such as reduced light competition (Järemo *et al.*, 1996), selection for grazing tolerant species (McNaughton, 1984), prevention of leaf senescence (McNaughton, 1976), and input of nutrients through dung and urine (McNaughton *et al.*, 1997).

Grazers also alter vegetation dynamics through other mechanisms such as seed dispersal (Anderson *et al.*, 2014), trampling of tree seedlings (Dublin *et al.*, 1990), and (in the case of large megafauna) altering the geomorphology of the ecosystem (McCarthy *et al.*, 1998).

The large population size of the wildebeest in the SME means that their grazing and behaviour has a large impact on the vegetation (Dublin, 1995; Hopcraft *et al.*, 2015). The wildebeest are obligate grazers, with the majority of their diet made up of graminoid species (herbaceous plants with a grass-like morphology) (Gagnon and Chew, 2000), and they are strongly impacted by both the quantity (Mduma *et al.*, 1999) and nutritional quality (Murray, 1995) of grasses available to them across the ecosystem. However, grazers as a whole have a diverse array of effects, and the impact of an individual species will depend on its body size, dietary requirements, spatial range, population size/density, and evolutionary history (Milchunas *et al.*, 1988; Olff and Ritchie, 1998; Hopcraft *et al.*, 2012, 2015).

Browsers

Browsers affect tree cover (Holdo *et al.*, 2009a), community composition (Rugemalila *et al.*, 2016), regeneration rates (Pellew, 1983; Belsky, 1984), and mortality (Morrison *et al.*, 2016) in the SME. Of all the browsing mammals in the SME, elephants have the largest impact on the vegetation. They can damage and kill mature trees by uprooting them and stripping their bark (Morrison *et al.*, 2016). They also selectively consume tree seedlings and therefore reduce recruitment (Dublin, 1995). These actions can alter both tree community composition (Rugemalila *et al.*, 2016) and total tree cover (Dublin, 1995; Holdo *et al.*, 2009a; Morrison *et al.*, 2016).

Termites

Termites also play an important role in the ecosystem dynamics of the SME, and impact the vegetation in multiple ways. Termites act as herbivores as well as decomposers, feeding on a wide range of living, dead, and decaying plant material (Traniello and Leuthold, 2000; de Visser *et al.*, 2015). They also decompose animal dung (Freymann *et al.*, 2008) and remains (Freymann *et al.*, 2007). Termites therefore play an important role in savannah nutrient cycling

(Bignell and Eggleton, 2000; de Visser *et al.*, 2015). Termites also actively change the structure of the landscape by building physical mounds (which provide habitat for multiple other species (de Visser *et al.*, 2008; Metzger *et al.*, 2015)) , and altering the soil properties (Holt and Lepage, 2000; Jouquet *et al.*, 2002). These physical changes to the environment affect vegetation distribution above and around termite mounds and contribute to fine scale spatial heterogeneity of vegetation in the SME (Anderson *et al.*, 2008; Metzger *et al.*, 2015).

Vegetation Interactions

Finally the vegetation itself plays a dominant role in controlling the structure and composition of SME vegetation. Plants compete for water, light and nutrients. This results in interspecific and intraspecific competition for resources in herbaceous and woody communities (Scholes and Archer, 1997; Metzger *et al.*, 2015). Individual plants can impact local nutrient cycling (Scholes and Archer, 1997), microbial processes (Hamilton and Frank, 2001), disturbance patterns (McNaughton, 1984; Holdo *et al.*, 2009a; Griffith *et al.*, 2017), and microclimate (Belsky *et al.*, 1989), which affect the survival and recruitment of other plant species (Belsky, 1992; Anderson *et al.*, 2008; Rugemalila *et al.*, 2020)

A set of relationships that are of fundamental importance to the SME wildebeest, and the ecosystem as a whole, are those between grasses and trees. Savannahs are defined by the co-existence of both grasses and trees (Scholes and Archer, 1997), and the interactions between them are of crucial importance to the ecosystem dynamics (Holdo *et al.*, 2009a).

Due to competition for resources, trees and grass can have negative impacts on each other. Woody encroachment into grassland areas often results in decreased grass production, due to factors such as rainfall interception, shading, water competition, litter accumulation, and root competition (Scholes and Archer, 1997; Anderson *et al.*, 2008). Meanwhile grasses can have direct negative effects on tree seedling survival rates (Morrison *et al.*, 2019) and the growth

rate of trees in a range of size classes (Riginos, 2009). They can also cause indirect negative effects by acting as fuel for fires that kill tree seedlings and young trees (Higgins *et al.*, 2000; Anderson *et al.*, 2008).

However there is also evidence of facilitative tree-grass interactions. Trees can reduce water stress and increase nutrient availability (through tree litter and animal droppings) for understory vegetation (Weltzin and Coughenour, 1990; Belsky, 1994). Recent empirical work in the SME found evidence of positive associations between grass biomass and tree cover, suggesting either facilitative effects, or that environmental conditions are favouring both tree and grass growth (Holdo *et al.*, 2020).

The relative importance of positive and negative interactions can also change through time. Fire (caused by dry grass build up) causes high mortality rates for young trees, but tree seedlings that germinate after fires can have faster growth rates due to reduced water competition (February *et al.*, 2013). Ludwig *et al.* (2001) found canopy shade had a positive effect on grass productivity during the dry season by limiting water loss, but a negative effect during the wet season by limiting light availability.

1.4.4 Wildebeest Migration

1.4.4.1 Movement Patterns

The famous annual migration of the Serengeti wildebeest is shaped by the nutritional, vegetative, geological and precipitation gradients which run across the SME (Holdo *et al.*, 2009b). The exact timing of migration and the specific locations in which the herds are found vary from year to year depending on rainfall conditions (Maddock, 1979; McNaughton, 1990; Fryxell *et al.*, 2015). However, the migration typically consists of a triangular route around the ecosystem.

At the end of the dry season (October) the migratory herds are in the Masai Mara National Reserve, a dry season refuge which receives rainfall throughout the year. When the rains arrive in November, the herds start to move south and arrive on the south-eastern plains in December (Maddock, 1979). This area has the highest nutritional forage, and the lowest risk of predation as it is difficult for predators to hide in the short grass (Packer *et al.*, 2005). The females calve on the plains in synchrony from mid-February to early March (Hopcraft *et al.*, 2015). This means access to the optimal conditions of the plains coincides with late pregnancy, calving and lactation, the period of highest energy expenditure and nutritional requirement for the reproductive females (Murray, 1995; Rysava *et al.*, 2016), and the period of highest vulnerability for new-born calves (Hopcraft *et al.*, 2005).

At the end of the wet season (May) both drinking water and fresh grazing begin to run out on the plains (Strauch, 2013). The herds are therefore compelled to leave, and they travel towards the west of the ecosystem (Maddock, 1979). Here there are higher annual precipitation totals than in the south-east, rivers provide fresh water, and grasses over alluvial sediments have higher nutrient concentrations than those in the north. In August the herds finally return to the wet, nutrient-poor, wooded savannahs of the Mara highlands, where the grass remains sufficiently abundant, and they remain here until the end of the dry season (Maddock, 1979).

1.4.4.2 Population Dynamics

The constant movement of the migratory wildebeest allows them to maximise their access to the best available resources throughout the year. However, this migratory strategy has a number of additional benefits, which allow the population size to be much higher than if they were always resident in one location (Fryxell *et al.*, 1988). Through sheer numbers the migratory wildebeest are able to locally swamp predators (Sinclair, 2003) whilst simultaneously increasing their ability to detect them (Robinson and Merrill, 2013). Their grazing makes the

grasslands more productive by generating compensatory vegetation production (McNaughton, 1979), especially as their constant movement allows the grass in individual locations adequate recovery time (Fryxell, 1995). This has resulted in a fluctuating but stable equilibrium size of 1.2 million wildebeest since the late 1970s (Hopcraft *et al.*, 2015), although recent surveys found the migratory population was between 1.3 and 1.4 million (G. Hopcraft 2020, personal communication, 11th August). As the migratory wildebeest are not limited by predation, they are instead limited by food availability. And as a typical wet season generates enough grass to sustain the entire population, they are regulated by dry season food availability, which is determined by dry season rainfall (Mduma *et al.*, 1999).

1.4.5 Ecosystem Dynamics

The success and resulting abundance of the migratory wildebeest has resulted in them having a large influence on the SME (Hopcraft *et al.*, 2015). They impact directly on other species through mechanisms such as competition (Sinclair, 1979a) and being predated (Packer *et al.*, 2005). Yet their significance extends beyond these direct interactions, and their indirect effects occur on a landscape scale. They impact the productivity and composition of the grass species across the SME through the intensity of their grazing (McNaughton, 1985; Sinclair *et al.*, 2008). The migratory wildebeest strongly affect the nutrient cycling of the whole ecosystem, as the arrival of over 1 million herbivores represents a dramatic local nutrient pulse; their movements import nutrients from across the ecosystem, depositing them as dung and carcasses (Dobson *et al.*, 2010; Subalusky *et al.*, 2017).

They also play a fundamental role in controlling the state of the SME. Extensive monitoring and research in the SME over multiple decades has meant the ecological consequences of changes to wildebeest population size have been documented. The wildebeest population size changed dramatically during the 20th century as a result of the elimination of rinderpest.

Rinderpest is a virus that affects large ruminants and pigs, and often results in significant mortality in these species (Barrett and Rossiter, 1999). In 1887 it was introduced to the African continent, and spread from Ethiopia to Cape Town in under a decade (Pankhurst, 1966; Sinclair *et al.*, 2008). The epizootic decimated cattle populations, and the devastating human impact is explained in publications such as Pankhurst (1966) and Morens *et al.*, (2011).

The disease also had dramatic ecological consequences, as it resulted in high mortality rates in species such as buffalo, greater kudu and wildebeest (Barrett and Rossiter, 1999). The virus remained endemic in the SME wildebeest population until the 1960s and caused a high mortality rates in juveniles (Talbot and Talbot, 1963). Rinderpest was eliminated from the Serengeti-Mara wildebeest population in the early 1960s, due to cattle vaccination campaigns in the surrounding area (Dobson, 1995). This led to a six fold increase in the wildebeest population between 1963 and 1977 (Sinclair, 1995). This increase was large enough to alter the amount of grass being consumed within the ecosystem, and resulted in a reduction in dry season grass biomass (Sinclair *et al.*, 2008). Dry grass provides fuel for fires, so this altered the ecosystem's fire regime and led to a decline in the amount of area burned annually in the Serengeti (Eby *et al.*, 2015). In turn, this led to an increased survival rate of tree seedlings that had previously been unable to escape from fire, and resulted in an increase in woody vegetation in the savannah portion of the Serengeti National Park (Sinclair *et al.*, 2008; Anderson *et al.*, 2015).

Grass productivity typically declines when in competition for resources with trees (Scholes and Archer, 1997). Therefore the dynamics that played out in the ecosystem illustrated a negative feedback cycle between grazer abundance and vegetation structure in savannahs. Increased grazing leads to reduced fires; fire reduction leads to increased tree recruitment; increased tree cover leads to decreased grass production; and decreased grass production limits grazer population size (Holdo *et al.*, 2009a).

However, the increase in woody cover did not occur across the whole ecosystem; while woody tree cover increased in the Serengeti, it decreased across the border in the Mara Reserve in Kenya (Dublin, 1995). This was found to be due to differences in the elephant population size on the Tanzanian and Kenyan sides of the border. Severe elephant poaching took place in the Serengeti during the 1980s (leading to an 80 % population decline), whereas little poaching occurred in the Mara Reserve (where the population increased) (Sinclair *et al.*, 2008). Ivory poaching ceased after 1988 due to the international ban on ivory trading, and the elephant population in the Serengeti subsequently increased (Sinclair *et al.*, 2008; Morrison *et al.*, 2016). However, the contrasting elephant population densities in the Mara and Serengeti during the 1980s had a dramatic impact on the state of the ecosystem. Elephants in the Mara damaged existing woodland, consumed seedlings, and thus prevented tree recruitment from taking place (Dublin, 1995). This maintained the Mara in a grassland state, despite the reduction in fires brought about by increased wildebeest grazing (Dublin, 1995; Sinclair *et al.*, 2007). This research illustrated that the SME can exist in multiple natural states, and that herbivores play a crucial role in the ecosystem's dynamics. Therefore, when considering the impact of rainfall changes on the SME wildebeest it is necessary to consider the ecosystem as a whole, as the wildebeest are a key, dynamic component of a complex, interactive system.

1.4.6 Potential Impacts of Climate Change on Wildebeest

The dynamic biotic and abiotic interactions present in the SME mean that there are a spectrum of ways in which climate change could impact the SME wildebeest.

Rainfall is usually considered the key limiting climatic factor of plant growth (and thus herbivores) in savannah ecosystems (Owen-Smith and Ogutu, 2013). Within the SME, monthly and annual rainfall totals in the SME are positively associated with wildebeest survival. This is largely due to the role of rainfall in controlling grass productivity. Higher annual totals

support higher grass production (McNaughton, 1985), and above average dry season rainfall (and thus food availability) lowers wildebeest mortality (Mduma *et al.*, 1999). Droughts have a particularly severe effect on wildebeest survival; approximately 3000 wildebeest died every day during the peak month of the 1993 drought (Mduma *et al.*, 1999). The distribution of rainfall also affects the wildebeest; calf mortality increases if rains are more widely spaced during the wet season (Hopcraft *et al.*, 2015). Therefore changes to the mean state and variability of rainfall conditions will likely impact SME grass production, and thus the wildebeest.

Altered rainfall totals could also change soil conditions (Schlesinger and Bernhardt, 2013), fire occurrence and intensity (Dublin, 1995; Holdo *et al.*, 2009a; Beale *et al.*, 2018), and tree-grass dynamics (Holdo *et al.*, 2009a, 2020). Changes to these crucial components of the SME would likely impact grass productivity and/or nutritional content, and would therefore affect the wildebeest.

The wildebeest and SME could also be affected by changes outside of the ecosystem. Rainfall changes, or climate change induced changes to human activity, in the catchment area for the Mara River may affect river flow (Gereta *et al.*, 2009; Mwangi *et al.*, 2016). Low water levels during droughts could lead to high levels of wildebeest mortality (Gereta *et al.*, 2009). Whereas high river discharge rates affect the occurrence of wildebeest mass drowning events during river crossings (Subalusky *et al.*, 2017).

While rainfall is known to play a crucial role in wildebeest survival, behaviour and savannah ecosystem dynamics, changes to other climatic variables could also affect the wildebeest and SME. Increased levels of CO_2 availability in the atmosphere can increase plant productivity and may favour the establishment of woody plants in the SME (Ritchie, 2008). Temperature changes can affect wildebeest behaviour and physiology. Wildebeest are adapted to be able to

survive hot arid conditions (Curtin *et al.*, 2018). However they are more vulnerable to high temperatures than smaller antelope (Shrestha *et al.*, 2014), and have to alter their behaviour to avoid heat stress (Selebatso *et al.*, 2017). As a species that is limited by food availability (Mduma *et al.*, 1999), and has to travel long distances to access food (Hopcraft *et al.*, 2015), a reduction in the amount of time they are able to be active during the day may impact their survival. In addition, many prey species have limits on their ability to use behaviour to avoid heat stress, due to the competing risks of heat stress during the day and predation at night (Veldhuis *et al.*, 2020). As maximum and minimum temperatures are projected to increase in East Africa (Niang *et al.*, 2014), these changes could impact the SME wildebeest.

Finally, changes to multiple climatic variables could also interact to impact the wildebeest and SME. In the 1990s and early 2000s, increased temperatures in combination with rainfall declines caused habitat desiccation in the Masai Mara National Reserve, which led to high ungulate mortality rates (Ogutu *et al.*, 2008a). In addition, Fryxell *et al.* (2015) found that both wildebeest and lion recruitment were positively correlated with the Southern Oscillation Index (SOI). The SOI is a proxy for the El Niño Southern Oscillation, and affects both temperature and seasonal rainfall in the SME (high SOI values are associated with temperatures and dry season rainfall that were above average, and below average wet season rainfall).

This thesis chooses to focus on the impact of changing rainfall totals, due to its strong role in determining wildebeest survival (Mduma *et al.*, 1999) and movement patterns (Holdo *et al.*, 2009b) in the SME. However, it should be recognised that by solely focusing on the effects of changes to a single climatic variable, it is not possible to explore the full story of how climate change may impact the wildebeest and SME.

1.4.7 Modelling the Migratory Wildebeest

This thesis aims to model the impact of changing future rainfall on the wildebeest of the Serengeti. A common method used to investigate the impact of climate change on an individual species is to use a correlative approach, such as climate envelope modelling (Scholes *et al.*, 2014). However, these approaches typically struggle to model migratory species (Robinson *et al.*, 2009), as correlative models can assume a species is able to tolerate the climatic conditions in parts of their range in which they can actually only persist temporarily (Sinclair *et al.*, 2010).

In addition, the wildebeest's key role in the ecosystem dynamics means that any environmental change which affects their movement, or population size, will alter the environment of the SME. These environmental changes would then in turn affect the wildebeest, and these feedbacks would continue until a new equilibrium was reached. Correlative models by definition do not account for such ecosystem dynamics and feedback loops (Sinclair *et al.*, 2010).

Considering these limitations, a mechanistic model is a preferable approach to modelling the impact of climatic change on the migratory Serengeti wildebeest. An ideal model should be able to represent: the key ecosystem dynamics of relevance to the wildebeest; the diverse changes to rainfall patterns which may occur across their migratory range; and their ability to alter their movement patterns to respond to environmental change.

A model that meets these criteria is the Savannah Dynamics (SD) model developed by Holdo *et al.* (2009) (fully described in Appendix A). The SD model has already been used to investigate the impact of climate change on the Serengeti wildebeest by using combinations of past rainfall conditions (Holdo *et al.*, 2010). However, it is not yet known how the model would perform if it were driven by precipitation conditions that differ from those recorded between 1960 and 2006.

The SD model is arguably the best candidate to investigate the impact of future rainfall change on the wildebeest of the SME. However, it would first be necessary to test the model's response to a spectrum of altered precipitation conditions before being driven by climate model data. This would allow the dynamic causes of the modelled wildebeest's response to novel precipitation conditions to be identified, and allow the plausibility of the model's response to be understood.

1.5 Climate of Eastern Africa

The SME is situated within East Africa and is subject to the large-scale climatic drivers that shape the region. Therefore, to understand the precipitation patterns over the SME, knowledge of the observed precipitation patterns and drivers over both the SME and wider region are required. In addition, as this study aims to investigate the impacts of future changes to rainfall, it is necessary to examine the ability of climate models to simulate past and future precipitation conditions over East Africa. Key literature related to the observed and simulated climate of East Africa are summarised in Sections 1.4.1 and 1.4.2 respectively.

1.5.1 Observed Climate of East Africa

In climate literature East Africa is often described as including the countries of Sudan, South Sudan, Ethiopia, Eritrea, Djibouti, Somalia, Kenya, Uganda, Rwanda, Burundi and Tanzania (Nicholson, 2017). Precipitation patterns across this region are varied and complex. Annual totals and seasonality vary dramatically across relatively small distances, and are controlled by interactions between large-scale climatic drivers, mesoscale circulations and complex topography.

1.5.1.1 Large-Scale Precipitation Patterns and Drivers

East Africa sits between two of the largest monsoon systems in the world; the West African monsoon, and the Indian Ocean monsoon (Camberlin, 2018). The topography of the East African Rift Valley separates East Africa from the West African monsoon system. This prevents moisture from the Congo basin and West Africa from reaching the region. It also means East Africa is dominated by the seasonally reversing Indian Ocean monsoon winds (Camberlin, 2018). The shape of the rift topography channels these winds, and predominantly reduces their penetration into the African continent and accelerates their passage parallel to its coastlines (although gaps in the topography, the largest being the Turkana Channel, also funnel winds westward (Nicholson, 2016a)). The resulting large-scale climatological wind patterns over East Africa always have an easterly component, and a seasonally reversing meridional component.

The timing of the wet seasons in East Africa coincide with the migration of the tropical rainfall belt across the equator. The tropical rainfall belt is an area of low pressure and high rainfall, driven by seasonal changes to the latitudinal position of maximum solar radiation (Nicholson, 2018). The majority of equatorial East Africa is classified as having two wet seasons, from March to May and October to December, termed the long rains and short rains respectively. Northern East Africa receives a single wet season from June to September, while southern parts of the region have a single wet season from December to February (Nicholson, 2017).

From April until October, the winds have a southerly component, as they flow from the southern hemisphere toward the Indian and East Asian monsoon systems. In November the wind directions switch and develop a northerly component, which remains until March (Funk *et al.*, 2016).

The topographic barrier to Congo basin moisture, and the dominance of alongshore rather than onshore winds, provide a partial explanation for East Africa's anomalously dry conditions; the region receives much less rainfall than other locations at tropical latitudes (Yang *et al.*, 2015). The other contributing factor is that, for most of the year, equatorial East Africa is situated below the descending limb of a zonal circulation cell over the Indian Ocean (Nicholson, 2017). The combination of this upper level descent, and the advection of air with low moist static energy from the winter hemisphere (by large-scale easterly winds with strong meridional components), results in a convectively stable atmosphere which suppresses moist convection for much of the year (Yang *et al.*, 2015). However, during the long rains and short rains wet seasons, the weak meridional component to the large-scale easterly winds, and the increase in off-coast sea surface temperatures in the Indian Ocean, lead to a less stable atmosphere, which allows moist convection to take place (Yang *et al.*, 2015). The highest levels of rainfall and specific humidity over East Africa occur in April, when sea surface temperatures are highest in the western Indian Ocean (Yang *et al.*, 2015).

1.5.1.2 Mesoscale Precipitation Patterns and Drivers

Large-scale climate drivers can explain the timing of the wet seasons in East Africa (Yang *et al.*, 2015). However, the spatial heterogeneity in annual rainfall totals and seasonality observed over East Africa are due to the dominant influence of mesoscale atmospheric processes (Camberlin, 2018). Of particular importance to the Lake Victoria basin are the effects of the rift topography and lake circulations.

The topography of the East African Rift Valley is known to strongly affect East African precipitation (Camberlin, 2018), and interactions between these topographic features and rainfall generating systems can be numerous and complex (Houze, 2012). Rainfall totals vary dramatically on opposing mountain sides (Oettli and Camberlin, 2005; Camberlin *et al.*, 2014),

with orographic uplift generating precipitation on the windward mountain slopes, and rain shadows on the leeward mountain side. Anabatic and katabatic winds are also generated in many of the mountainous regions of East Africa, and the resulting convergence over high ground often triggers afternoon storms (Anyah *et al.*, 2006; Vizy and Cook, 2019).

Local lake circulations are generated by surface temperature differences between these large water bodies and the surrounding land. At night the lake is warmer than the surrounding land, so "land breeze" winds flow towards it, resulting in convergence and night-time thunderstorms over East Africa's lakes (Camberlin *et al.*, 2018). During the day, the land becomes warmer than the lakes, so diverging "lake breeze" winds flow away from the lakes toward the surrounding land. These mesoscale circulations result in unique precipitation conditions over and around East Africa's lakes (Camberlin *et al.*, 2018).

In addition, topographic- and lake-induced mesoscale atmospheric processes are known to interact over the eastern Lake Victoria basin. Over Lake Victoria, the night-time land breeze combine with the katabatic winds from the neighbouring highlands, and generate thunderstorms of such intensity that they sadly claim the lives of thousands of fishermen every year (International Federation of Red Cross and Red Crescent Societies, 2014). During the day, these wind patterns switch and diverging winds are generated over the lake and then amplified by anabatic winds over the Kenya Highlands (Davies *et al.*, 1985; Finney *et al.*, 2019). These interactions generate afternoon storms over the Kenya Highlands, resulting in year-round precipitation in this area (Anyah *et al.*, 2006).

1.5.1.3 Patterns and Drivers of Precipitation over the Serengeti-Mara Ecosystem

The key features of SME precipitation conditions were briefly described in Section 1.4.3; an annual precipitation gradient across the ecosystem, year-round precipitation in the north-west, and a single double peaked wet season lasting from November to May. This information was

outlined by Norton-Griffiths et al. (1975) who carried out a comprehensive investigation into the precipitation conditions over the Serengeti National Park. They also reported that annual cycles varied significantly across the national park, and that the orientation of the rainfall gradient was not static, but instead changed on a monthly basis. Norton-Griffiths *et al.* (1975) proposed that the high rainfall totals and year-round precipitation in the north-west were due to winds from Lake Victoria creating a migratory lake convergence zone. Subsequent work has confirmed this mechanism over the Kenya Highlands to the north of the SME, and that anabatic and katabatic winds amplify this process (Anyah *et al.*, 2006). Norton-Griffiths *et al.* (1975) also noted the low precipitation conditions in the south-east of the National Park were due to the presence of a rain shadow from the rift highlands. They also speculated that this rain shadow eliminated the April precipitation peak in the east of the park.

The study by Norton-Griffiths *et al.* (1975) provides a solid foundation of knowledge about precipitation conditions in the Serengeti National Park. However, questions remain about the distribution of precipitation across the SME, and the drivers of these spatial patterns. The April rainfall peak observed across East Africa is caused by large scale climatic processes (Yang *et al.*, 2015), so it is unclear how a local rain shadow could remove this large-scale feature. In addition, the description of a single wet season over most of the SME is at odds with the description of the climate of East Africa. January and February are dry periods across most of equatorial East Africa (Yang *et al.*, 2015), yet in the south-eastern SME (the driest portion of the ecosystem), precipitation totals are so high that it is a key grazing period for the migratory wildebeest (Pennycuick, 1975; Maddock, 1979). Logically, these patterns must be due to the influence of mesoscale processes, but as yet no study has identified the precise mechanisms causing these conditions. It is challenging to understand the drivers of interannual variability in a region, or the ability of climate models to accurately simulate an area, without a comprehensive knowledge of the mean state conditions. In addition, the study by Norton-

Griffiths *et al.* (1975) was carried out using limited data by current standards. High resolution satellite datasets (CHIRPS v2.0, Funk *et al.* (2014); TRMM, Huffman *et al.* (2007); TAMSAT, Tarnavsky *et al.* (2014)) and reanalysis datasets (ERA5, Hersbach *et al.* (2020); ERA-Interim, Dee *et al.* (2011)) with greater spatial coverage are now available and allow the examination of precipitation and wind patterns in the SME and surrounding area on hourly to decadal timescales. Therefore, using these datasets to gain a better understanding of the characteristics and drivers of the mean state of precipitation over the SME is a key focus of this thesis.

1.5.1.4 Past Precipitation Trends

Natural climatic oscillations mean that past regional rainfall conditions were dramatically different to the present. Verschuren, Laird and Cumming (2000) used sediment from Lake Naivasha in Kenya to reconstruct precipitation variability over the past 1100 years. They found that the climate of the region has at times been very different from the regime today. A much drier climate was present during the Medieval Warm Period (~ AD 1000 - 1270). The climate was much wetter during Little Ice Age (~ AD 1270 – 1850), although this was interrupted by three prolonged droughts, more severe than any recorded in the 20th century (AD 1380-1420, 1560-1620 and 1760-1840). Additionally it was found that dry periods were correlated with phases of high solar radiation. This shows that the climate of the region has changed dramatically in the past due to natural variability.

Analysis of lake sediments only allows rainfall to be reconstructed on decadal time scales, whereas in more recent years, direct measurements have been recorded. This allows us to distinguish between trends in the long rains during March-May (MAM) and the short rains during October-December (OND). Over recent decades, a decline in precipitation over East Africa has been observed during the long rains (Rowell *et al.*, 2015). This was found to be caused by warmer sea surface temperatures off the coast of Madagascar delaying the northward

movement of the tropical rainfall belt in the southern hemisphere, and warmer sea surface temperatures in the Arabian Sea in combination with decreased surface pressure over Arabia accelerating its passage in the northern hemisphere (Wainwright *et al.*, 2019). Therefore this rainfall decline was due to later onsets and earlier cessations of the long rains, rather than a change in rainfall intensity.

In addition, since the 1980s, the short rains have exhibited large year to year variability (Rowell *et al.*, 2015). East Africa has also suffered from an increase in hydrometeorological disasters (from 3 per year in 1980s, up to 10 per year between 2000-2006) and floods (1 per year in the 1980s, 7 per year in 2000-2006) (Shongwe *et al.*, 2011).

Within the Lake Victoria basin, the presence of past trends depended on location. Kizza *et al.* (2009) analysed seasonal and annual trends in precipitation records collected from 20 rain gauge stations surrounding Lake Victoria between the early 20th century and mid-2000s. Out of 400 "cases" (referring to the combination of station, temporal period, and season/annual metric analysed) they found that 17 % had significant trends, and 67 % of significant trends were positive. At the Musoma station (by the eastern shores of Lake Victoria) an overall positive trend was recorded, and between 1971 and 2006 this manifested as increased rainfall between January and June, and decreased rainfall between July and December.

Analysis of past changes in rainfall over the Serengeti-Mara ecosystem have also shown mixed results. Rain gauge data averaged across the Serengeti, showed an increase in annual and wet season (November-May) rainfall over the first half of the century, and a decrease in the second half (Ritchie, 2008). Dry season rainfall (June-October) increased throughout the twentieth century (Ritchie, 2008). In the Mara reserve long-term dry season rainfall (1965–2003) was largely below average from 1980s to 2003 (Ogutu *et al.*, 2008b). Rising temperatures and declining rainfall were also recorded throughout the 1990s and early 2000s, with unprecedented

prolonged and strong ENSO episodes, led to progressive habitat desiccation and a reduction in vegetation production in the ecosystem (Ogutu *et al.*, 2008a). At the Mugumu rain gauge, situated just outside of the Serengeti, no trend in annual rainfall was found between the 1960s and late 2000's, there was a positive trend in rainfall between March and May after 1971 (Kizza *et al.*, 2009). Within the Serengeti-Mara ecosystem, over the past 15 years a small central area of the park has had a significant increase in annual rainfall, while the rest of the region has had no significant change (Veldhuis *et al.*, 2019).

The lack of coherence in regional trends is likely due to the complexity of the local climate and the importance of mesoscale atmospheric processes involved in generating regional precipitation.

1.5.2 Simulated Climate of East Africa

It is clear that both large scale and mesoscale processes shape the fundamental climate of the SME and East Africa. The representation of both synoptic and mesoscale process is therefore important to consider when selecting climate models to represent this area. Here, Section 1.5.2.1 gives an overview of climate model structures, Section 1.5.2.2 outlines key decisions involved in climate model selection to reduce uncertainty, and Section 1.5.2.3 describes the climate model used in this thesis.

1.5.2.1 Climate Models

Numerical climate models (referred to as climate models in this thesis) are the prime route to future climate projections, and are mathematical models based on the fundamental laws of physics, chemistry and fluid motion. However the term describes a range of model types of varying complexity. The type of model data most commonly used in climate change impact

studies are General Circulation Models (GCMs). GCMs represent the atmosphere and/or ocean as a multidimensional grid. Equations describing the relevant atmospheric processes which can be resolved are computed in each cell, while processes that are too small to be resolved are parameterised (Le Treut *et al.*, 2007). Inevitably, climate models contain uncertainty due to issues such as stochastic processes in the climate system, and assumptions related to model structure and parameterisation (Collins *et al.*, 2013).

Due to the computational processing power required to run GCMs, spatial resolution is typically low. The majority of the recent generation of GCMs have a resolution of > 1 degree of latitude (approximately 111 km at the equator; covering 12321 km^2) (European Network for Earth System Modelling, no date). This leads to a mismatch between the spatial resolutions of GCM datasets and the majority of ecological datasets, processes and questions (for example, the whole Serengeti National Park covers just over 14 000 km^2).

Downscaling is a way to address this spatial mismatch (Evans, 2011; Platts *et al.*, 2015). There are two approaches to downscaling. The first is dynamic downscaling, where a higher resolution Regional Climate Model (RCM) is driven by a GCM. The RCM covers a smaller spatial area, and uses data from the GCM as boundary conditions. The second is statistical downscaling, which uses statistical relationships between current/historical large scale atmospheric processes and local conditions to derive future conditions.

Both approaches generate data of higher spatial resolution, yet they come with their own sets of uncertainties. RCMs contain errors due to model structural and parametric uncertainty (Flato *et al.*, 2013). Statistically downscaled models assume that the statistical relationships between large scale and local features remain stable over time; an assumption that has not been fully validated (Baker *et al.*, 2017). In addition, both statistically and dynamically downscaled models contain uncertainty derived from the driving GCM (Flato *et al.*, 2013).

1.5.2.2 Model Selection

Uncertainty is an inherent part of modelling, but the degree of uncertainty in climate model projections varies depending on the region and climatic variable of interest. Over much of East Africa, most climate models agree that rainfall intensities and annual totals will increase in the future (Niang *et al.*, 2014). However, there is disagreement between models whether there will be an increase or decrease in future annual rainfall, and many other rainfall metrics over the Lake Victoria basin (Dosio *et al.*, 2019). Studies investigating the impact of rainfall changes in this region must therefore account for this disagreement.

One possible approach is to analyse data from as many climate models as possible, and report the spread of results. However, Baker *et al.* (2017) provide a framework for the use of climate model data in ecological studies, and recommend against this method. They argue that this risks including future projections from models that poorly represent the regional climate or the climatic variable of interest. Instead they recommend selecting models that best represent climatic variables of most ecological importance. This requires consideration of factors such as the most suitable downscaling method, and model resolution.

Statistical Downscaling vs Dynamic Downscaling

Both large-scale and mesoscale atmospheric processes are of great importance to determining the distribution of precipitation over East Africa, as described in Section 1.5.1. Since it is unknown whether past relationships between large- and mesoscale atmospheric processes will remain stable in the future, this study chose not to use statistically downscaled data, and instead used dynamically downscaled data to better capture future changes to the atmospheric dynamics.

Resolution

Convective rainfall is responsible for the majority of precipitation over Africa (Geerts and Dejene, 2005). It is therefore preferable to use RCM output from models that can simulate this type of rainfall. The atmospheric process responsible for convective precipitation are relatively small, and "convection-permitting models" require a spatial resolution of approximately 4 km or less (Prein *et al.*, 2015). These models are also known to be of particular benefit for simulating precipitation over mountainous regions such as the East African Rift Valley (Prein *et al.*, 2015). The high computational and financial costs of running such high resolution simulations mean that few convection-permitting climate model runs have been carried out over East Africa. However, recently a convection-permitting model run called CP4-Africa has been performed over the whole African continent (Stratton *et al.*, 2018), the results of which are used for this study.

1.5.2.3 CP4-Africa

The newly available CP4-Africa model is the first convection permitting model to be run across the whole African continent (Stratton *et al.*, 2018). The model has a horizontal grid spacing of 4.5 km at the equator, 80 vertical levels up to 38.5 km, and represents lakes by modelling them as inland sea grid cells (Stratton *et al.*, 2018). It was hypothesised that the increased resolution would improve the model's ability to simulate precipitation patterns over Africa, especially in regions with complex topography and maritime or lake influences. This has been confirmed over the eastern Lake Victoria basin, where the SME is situated (Finney *et al.*, 2019). The CP4 model was able to accurately capture the annual cycle of precipitation; when compared to a lower resolution RCM (25 km grid spacing), CP4 had improved representation of storms over the Kenya Highlands, and the diurnal cycle of rainfall (Finney *et al.*, 2019). In addition, the pan-African domain of the CP4 model allowed local changes to water budgets (that arose from

improved representation of convection) to be incorporated into large scale moisture fluxes across the continent (Finney *et al.*, 2019). This demonstrates the benefit of running high resolution models over large spatial domains.

It is also worth noting the limitations of the CP4 model. The hindcast and forecast model runs only span 10 years (Stratton *et al.*, 2018); whereas to create a climatological mean it is preferable to use 30 years of data (WMO, 2017). The model contains seasonal biases, including a wet bias over the Lake Victoria basin during March to May (Finney *et al.*, 2019). The future climate model run is driven by only one GCM (HadGEM2-ES), so biases in this model will affect the CP4 results. Finally, the model has only been run using an RCP 8.5 scenario (Stratton *et al.*, 2018), so only simulates changes that would occur under high warming conditions. Despite these limitations, it was decided that the ability of the model to represent atmospheric processes of crucial importance to the SME justifies its use in this study.

Only two previous studies have reported on CP4-Africa future projected changes to precipitation patterns over the eastern Lake Victoria basin. Kendon *et al.* (2019) reported that, during the long rains, there was a projected increase in: total rainfall; intensity of rainfall; intensity of wet extremes; and frequency of wet extremes. However, there was also an overall decrease in the frequency of rainfall events. Finney *et al.* (2020) found similar changes to projected annual rainfall, except changes to annual rainfall frequency were insignificant.

We can therefore expect the CP4-Africa future climate projection to have increased annual and long rains precipitation totals. Nonetheless, it is unclear how the model represents precipitation in individual months in both the hindcast and forecast runs. Therefore, examination of how past and future SME rainfall is simulated in the CP4-Africa model runs is a focus of this thesis, and a novel use of this exciting new dataset.

1.5.2.4 Projected Future Precipitation Trends

The majority of future GCM and RCM projections show a wetter future over East Africa with more intense wet seasons and less severe droughts during both the long and short rains, and a greater increase in mean precipitation during the short rains compared to the long rains (Shongwe *et al.*, 2011; Niang *et al.*, 2014; Ongoma *et al.*, 2018; Dosio *et al.*, 2019; Kendon *et al.*, 2019). However there is disagreement between model projections, as well as discrepancies between hindcast simulations and observed past climate (Rowell *et al.*, 2015; Rowell and Chadwick, 2018; Endris *et al.*, 2019). An area that has recently received a great deal of research has been the discrepancy between the projections for increased long rains precipitation, and an observed decline in March-May rainfall over this East Africa in recent decades. Coupled GCM hindcasts have largely been unable to simulate this decrease in precipitation, and this problem has been labelled the "East Africa Climate Paradox" (Rowell *et al.*, 2015). This has called into question the reliability of future projections for this region during the long rains.

The fact that AMIP models were more consistently able to simulate the drying trend suggested the drying trend was partially due to changes in SST patterns that the coupled models were unable to consistently capture (Hoell *et al.*, 2017). Recent work by Wainwright *et al.* (2019) showed that the decline in long rains rainfall that has occurred since 1998 was due to changes in surface temperatures both north and south of East Africa, which altered the pressure differentials between the tropics and sub-tropics and thus affected the speed of the passage of the tropical rainfall belt. The partial recovery of long rains rainfall totals since 2009 was due to cooling SSTs south of Madagascar (preventing a delayed long rains onset) and a weaker contrast in SST temperatures between the northern and southern Arabian Sea (reducing the early cessation of long rains rainfall). In addition, they found that future CMIP5 projections (under RCP8.5) showed a shift to earlier onset and cessation dates for long rains rainfall, but

no change in length of the wet season. Therefore projected future rainfall increases were due to greater rainfall intensity, rather than increased wet season length.

This issue highlights the need to be cautious when interpreting future projections over spatial areas, and temporal periods, where there is disagreement between model projections (such as the projected increase in long rains precipitation over East Africa). It also illustrates the value of identifying the atmospheric processes that control regional rainfall, so it is possible to investigate how well they are represented within individual climate model simulations, and thus identify why there may be uncertainty in projected regional trends. In areas where mesoscale atmospheric dynamics play a large role in determining local precipitation patterns, the role and representation of mesoscale processes are arguably as important as large-scale processes over the wider region. In the Lake Victoria basin there is a greater degree of uncertainty in the sign of future rainfall trends than in other parts of East Africa, likely due to the strong impact of mesoscale atmospheric dynamics in this area (Dosio *et al.*, 2019). Therefore this thesis chooses to examine the representation of mesoscale atmospheric processes in a high-resolution regional climate model, which has the capability to simulate dynamics of key importance to the region. When the results are discussed, findings that are in agreement with other model runs over East Africa are highlighted. However, the analysis must be interpreted in its wider context; as the output from a single RCM run, driven by a single GCM under one Representation Concentration Pathway, over an area that has a high degree of inter-model uncertainty over future rainfall changes.

1.6 Integrating Climate Science and Ecology

Studies into the ecological impacts of climate change typically have three approaches: inference from analogous past situations, manipulative experimentation, or mathematical modelling (Scholes et al., 2014). As stated in Section 1.2, this thesis chooses to take a

mechanistic modelling approach. Interrogating a mechanistic ecological model to ascertain the reliability of the model is common within the research literature (Benton and Grant, 1999; McKenzie *et al.*, 2019). Recognising uncertainty in the ability of climate models to represent climatic variables (that are used to drive ecological impact models) is also standard practice in ecological impact studies (Beaumont *et al.*, 2008; Baker *et al.*, 2017). It is also common for climate scientists to interrogate the extent and potential causes of uncertainty in climate models; evaluating both their ability to simulate specific climatic variables, and the atmospheric processes that generate them (Randall *et al.*, 2007; Flato *et al.*, 2013).

However, it is rare for ecological impact studies to consider the potential causes of uncertainty in the climate model projections used to drive ecological impact studies. Therefore this thesis sought to take a novel approach to modelling the potential ecological impacts of climate change by: identifying the atmospheric processes of key importance to a migratory species; evaluating how well a single climate model can represent those processes; identifying the climatic conditions to which a mechanistic ecological model are most (and least) sensitive; and using this information when interpreting the output of a mechanistic ecological model driven by past and future simulations of the local climate.

This is a wider approach than is usually taken in ecological impact studies. Given the extra work this entailed, the thesis had to narrow its focus with regards to the climatic variable used in this study. Therefore the thesis focused solely on mean rainfall and did not investigate interannual variability. The main reason mean rainfall was chosen was the previous lack of knowledge about the atmospheric drivers of rainfall over the SME. It was considered too complex to investigate the potential atmospheric drivers of climatic variability, without first understanding what controlled the mean state. However, mean precipitation conditions are also of key importance to the ecological dynamics of the SME. The mean conditions have shaped the soils, vegetation communities, and the distribution, abundance and behaviour of animals in

the SME. Therefore knowledge of how these conditions may change is an important component of studying how climatic changes may impact the wildebeest and SME, even if it is not the whole story. In addition, the findings of this thesis lay the foundation for future research into the causes and impacts of rainfall variability in this region.

1.7 Thesis Aims

The overarching goal of this thesis is to understand how climate change may alter mean precipitation patterns over the SME and thus impact the migratory wildebeest.

Based on gaps in the literature identified above, the following aims were established:

1. Quantify mean climatological precipitation patterns over the SME.
2. Identify the key atmospheric processes generating precipitation over the SME.
3. Identify the spatial and temporal precipitation patterns over the SME to which the wildebeest in the SD model are most sensitive.
4. Assess the plausibility of the SD model response to novel precipitation conditions.
5. Evaluate the ability of the CP4-Africa climate model to represent climatological mean precipitation over the SME.
6. Investigate how climate change may alter future mean precipitation patterns over the SME
7. Model the wildebeest response to projected future changes in mean climatological precipitation.

1.8 Notes on the format of the thesis

This study is presented as a thesis by publication, with Chapters 2-4 taking the form of research articles which have been submitted to peer reviewed journals. Each paper fulfils key aims of the thesis, and forms part of a framework shown in Figure 1.4.

In this framework, for both the atmospheric and the ecological system: (1) the key processes were defined; (2) models were selected based on their inclusion of these processes; (3) model performance was assessed; and finally (4) the models were used to answer the main question of this thesis; the impact of future changes to mean rainfall conditions on the migratory wildebeest of the SME.

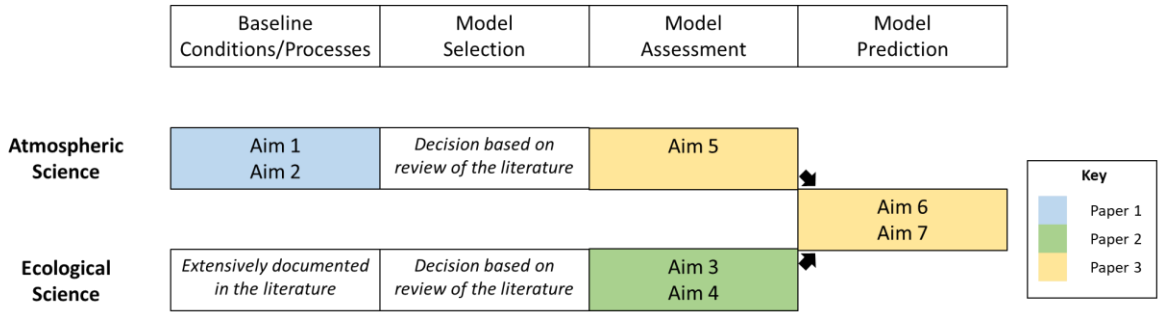

Figure 1.4: Aims and structure of thesis. Colours refer to the paper in which each aim is addressed.

Paper 1 focuses on aims 1 and 2, and investigates the climatological mean rainfall and atmospheric processes over the SME. Paper 2 addresses aims 3 and 4, driving the SD model with a spectrum of altered spatial and temporal precipitation patterns and discussing the plausibility of the SD model's response. The 3rd and final paper evaluates the performance of CP4-Africa climate model over the SME, examines the projected changes to future mean precipitation, and models the response of the migratory Serengeti wildebeest to these precipitation conditions (aims 5, 6 and 7).

The papers included in the thesis are listed below.

- Mahony, J., Dyer, E. and Washington, R. *The Characteristics and Drivers of Climatological Precipitation over the Serengeti Region in East Africa.* Submitted to The International Journal of Climatology (April 2020)

- Mahony, J. and Coulson, T. *Modelling Wildebeest Movement and Population Dynamics in the Face of Environmental Change*. Submitted to The American Naturalist (March 2020)
- Mahony, J., Dyer, E., Washington, R., and Coulson, T. *Modelling the Impact of Future Climate Change on the Population Size of the Serengeti-Mara Wildebeest.* Submitted to Journal of Biogeography (April 2020)

1.8.1 Authorship declaration

I conducted all of the analysis and writing for the papers included in this thesis. I discussed the methods, results and structure of the papers with my supervisors, and they provided comments on manuscript drafts. The areas to which each supervisor contributed depended on their area of expertise. Ellen Dyer and Richard Washington advised on the climate science included in Papers 1 and 3, while Tim Coulson gave advice on the ecological content of Papers 2 and 3.

Chapter 2. The Characteristics and Drivers of Climatological Precipitation over the Serengeti Region in East Africa

The unique precipitation patterns over the Serengeti National Park in East Africa form the foundation of an internationally important ecosystem. Improving understanding of present precipitation conditions, through quantifying their spatial and temporal distribution and identifying the associated atmospheric processes, is an important basis for understanding past and future change to regional precipitation. Precipitation and reanalysis datasets (CHIRPS v2.0, TRMM 3B42, ERA5, ERA-Interim) are used to quantify the regional climatic conditions on annual, monthly and hourly timescales. Hierarchical cluster analysis identified regions with distinct annual cycles of precipitation.

Seasonality in the wider Serengeti domain is broadly controlled by the biannual passage of the tropical rainfall belt. Cluster analysis identified 5 sub-regions with distinct annual cycles, with differing rainfall totals during January-February and June-September, wet season peak rainfall months, and rainfall peak symmetry. The orientation of a rainfall gradient across the Serengeti National Park changes seasonally, influenced by the meridional component of tropical easterlies. Interactions between tropical easterlies and complex topography generate high rainfall totals on windward slopes, and rain shadows in their lees. Convection is generated at the wind convergence zone between tropical easterlies and Lake Victoria lake breeze winds. The spatial progression of diurnal rainfall follows the direction of the prevailing easterlies. From October to March an early afternoon rainfall peak is present between the mean wind convergence line and the rift valley topography. We suggest this is either due to variability in the position of the lake front, or small storms generated by localised solar heating.

Our findings improve understanding of the complex atmospheric processes over the Serengeti. This provides a foundation for future work exploring past and future rainfall changes over this ecologically important area.

2.1 Introduction

Precipitation is a primary driver of one of the world's most iconic ecological phenomena; the annual migration of 1.3 million wildebeest around the Serengeti-Mara ecosystem (Holdo *et al.*, 2009b; G. Hopcraft 2020, personal communication, 11th August). A rainfall gradient stretches across the ecosystem with the north-west receiving three times more annual rainfall than the south-east (Norton-Griffiths *et al.*, 1975), and the continued presence of precipitation in the north-west from June to October provides a refuge for the migratory herds (Thirgood *et al.*, 2004).

These complex spatial rainfall patterns are typical of East Africa, an area renowned for having markedly heterogeneous precipitation patterns (Nicholson, 1996). Across the wider region, annual totals and seasonality often change dramatically over tens of kilometres (Nicholson, 2017), as the large scale atmospheric circulation interacts with complex topography, local lake circulations, and maritime influences (Camberlin, 2018). This climatic complexity supports an impressive array of ecosystems and human occupations (Niang *et al.*, 2014), and could account for the conflicting rainfall trends recorded in the region (Ogutu *et al.*, 2008b; Ritchie, 2008; Kizza *et al.*, 2009; Veldhuis *et al.*, 2019). Unfortunately it is also a key reason for a lack of certainty about how climate change will affect future precipitation in areas such as the Lake Victoria basin (Dosio *et al.*, 2019). Simulations with high resolution models are required to simulate mesoscale atmospheric processes, and have been rare due to high computational and financial costs. A new generation of high resolution regional climate model projections are now becoming available (Thiery *et al.*, 2016; Kendon *et al.*, 2019), and it is likely that these

will improve precipitation projections over East Africa, including the Serengeti. However, to be able to evaluate the capacity of these climate models to simulate a region's future, we first require a detailed understanding of that region's past.

Despite the complexity of rainfall over the Serengeti-Mara ecosystem, and the recognition of its importance to the ecological community (Mduma *et al.*, 1999; Fryxell *et al.*, 2015; Veldhuis *et al.*, 2019), limited work has focused on the region's mean climate. To date, the most thorough investigation into the regional rainfall was carried out by Norton-Griffiths et al., (1975). The authors quantified the rainfall gradient across the ecosystem, and noted that the orientation of this gradient altered throughout the year. They attributed these precipitation patterns to a rain shadow in the south-east, dry season wind convergence over Uganda and western Kenya (illustrated by Findlater (1971)), and a low-level lake convergence zone which migrated between Lake Victoria and the western Kenyan highlands over the diurnal cycle (described by Fraedrich (1972)).

For decades, the work carried out by Norton-Griffiths et al. (1975) has provided a valuable foundation for understanding the ecosystem's unique climate, but this was carried out using limited data by current standards. More recent satellite datasets with high spatial and temporal coverage and resolution, can allow us to examine the region's climatological precipitation patterns in greater detail. Reanalysis circulation data provides the opportunity to test the mechanisms suggested by Norton-Griffiths *et al.* (1975), and better understand the dynamics of this region.

Here we use these datasets to: (1) quantify the spatial and temporal distribution of annual and monthly rainfall totals, and identify regions with distinct annual cycles with cluster analysis; (2) examine regional wind, precipitation, and moisture patterns over East Africa, and identify rainfall-generating atmospheric processes relevant to the Serengeti, and (3) map the timing of

peak rainfall over the Serengeti, and examine local wind patterns at key points in the diurnal cycle. We focus the majority of our analysis on the area between 1-4 °S, 33-37 °E (Figure 2.1), which we define as the wider Serengeti domain. However, when focusing on larger swathes of East Africa, we investigate the region between 3 °N – 9.75 °S, 30 °E – 42 °E, which includes Lake Victoria, the southern Lake Victoria basin, the western Indian Ocean, and the eastern branch of the East African Rift Valley. Overall, we aim to quantify the spatial distribution of rainfall over the Serengeti on annual, monthly and hourly timescales, and identify the atmospheric processes generating the unique rainfall patterns observed over this important ecosystem.

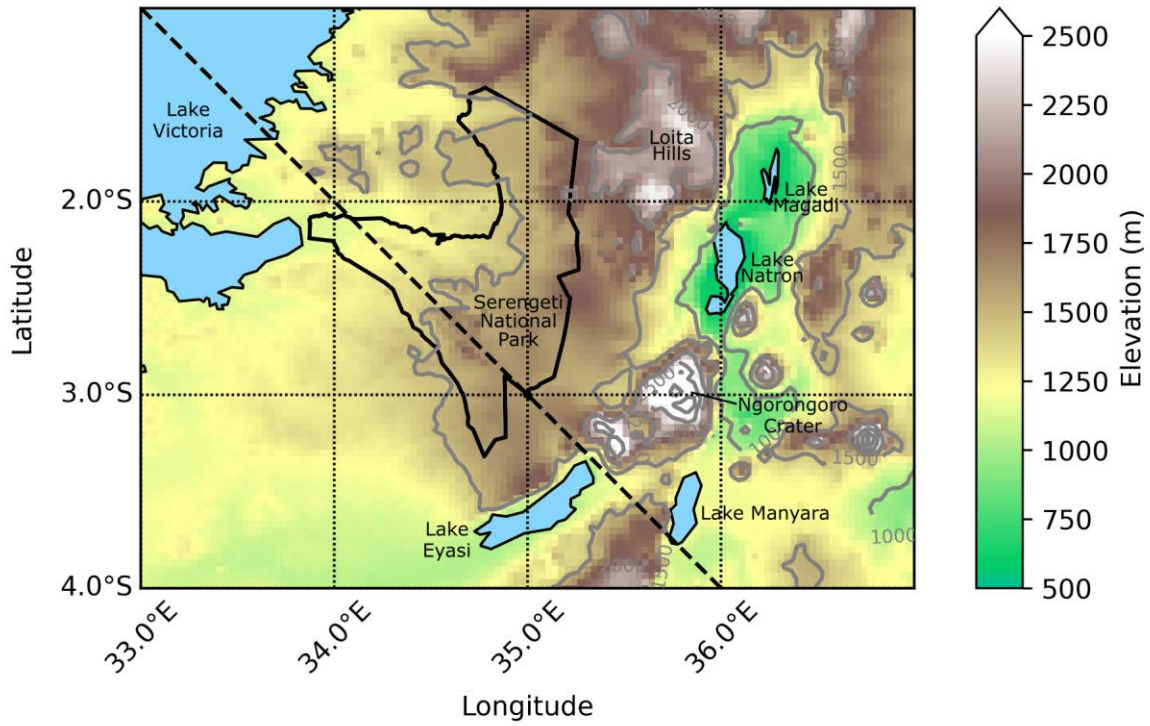

Figure 2.1: Map of the orography and key landmarks of the Serengeti National Park and surrounding area. The area shown in this figure is termed the "wider Serengeti domain" in this study. Colour and contour lines denote elevation (using Gtopo30 topography data), with the exception of lakes which are masked with blue. The dashed line shows the path of atmospheric cross-sections analysed in section 2.3.3.2.

2.2 Data and Methods

2.2.1 Datasets

Precipitation, reanalysis and topography datasets were used to explore the atmospheric conditions over the Serengeti and East Africa. When data is shown for different points in the diurnal cycle, this study uses East Africa Time (EAT), which is three hours ahead of Coordinated Universal Time (UTC).

2.2.1.1 Precipitation Data

The satellite products CHIRPS v2.0 and TRMM 3B42 were used in this study. The Climate Hazards Group InfraRed Precipitation with Stations dataset (CHIRPS v2.0) was chosen due it's high spatial resolution, large temporal range and proven performance over East Africa (Dinku *et al.*, 2018). It provides daily precipitation estimates at 0.05° resolution between 1981 and 2017, based on blended station and satellite data (Funk *et al.*, 2014). Tropical Rainfall Measuring Mission (TRMM) data is available at 0.25° resolution, between 1998 and 2014 (Huffman *et al.*, 2007). The TRMM 3B42 dataset was chosen for the availability of 3-hourly measurements. Climatological averages were calculated for CHIRPS from 1987-2016, and TRMM from 1998-2014. It should be noted that the TRMM and CHIRPS datasets are not independent, as both incorporate local gauge readings for calibration, and CHIRPS also includes data from TRMM 3B42 to calibrate global cold cloud duration rainfall estimates (Funk *et al.*, 2014).

2.2.1.2 Wind and specific humidity

ERA5 reanalysis wind and specific humidity data was used to examine the regional atmospheric dynamics. This dataset was chosen for its high temporal and spatial resolution, as

it provides hourly global data on a 0.25° x 0.25° grid (Hersbach *et al.*, 2020). Our study included monthly and hourly climatological averages of ERA5 horizontal wind, vertical velocity, and specific humidity, using data from 1987-2016. 825 hPa specific humidity data was used in section 3.2.2 as surface values were not available for this variable (Copernicus Climate Change Service (C3S), 2019).

2.2.1.3 Topography

A 2-minute resolution version of the Global 30 Arc-Second Elevation (GTOPO30) dataset was used to display topography (Gesch *et al.*, 1999). The 2-minute (or 0.333°) resolution was chosen as it is similar to that of the CHIRPS dataset (0.05°), which is the highest resolution atmospheric dataset used in this study.

2.2.2 Methods

2.2.2.1 Cluster analysis

We used cluster analysis to identify areas with similar annual cycles of precipitation. The annual cycle of each station/grid cell was normalised prior to the cluster analysis, to ensure all monthly values fell between 0 and 1, using the formula:

$$\frac{x_i - x_{min}}{x_{max} - x_{min}}$$

x_i = individual monthly climatological totals

x_{max} = wettest monthly total

x_{min} = driest monthly total

Normalising the data meant that the clustering algorithm detected differences between annual cycle structure, rather than annual rainfall totals, allowing us to focus on the analysing the annual cycle.

We calculated the Euclidean distances between the normalised mean annual cycles in every grid cell. We then used this data to perform agglomerative hierarchical cluster analysis using Ward's minimum variance method (Ward, 1963). Using this method, initially every grid cell was defined as an individual cluster. Clusters were then iteratively joined until only 1 cluster remained. At each step, the two clusters that were joined were those that minimised the total sum of the error sums of squares of each individual cluster. Hierarchical cluster analysis was chosen as we did not have pre-existing knowledge of the number of clusters that would best represent regional rainfall (Wilks, 2011). Ward's minimum variance method was chosen as it is known to perform well in climatological studies (Gong and Richman, 1995; Unal *et al.*, 2003; Dezfuli, 2011). We carried out the analysis with the dist(method = "euclidean") and hclust(method = "ward.D2") functions from the "stats" package (version 3.6.1) in R (R Core Team, 2019). This analysis was performed separately on CHIRPS and TRMM.

The number of clusters used in each dataset were chosen based on the size of the step changes in Euclidean distance between different numbers of clusters, and the spatial coherence of those clusters. Further details can be found in Appendix B.

2.2.2.2 Atmospheric and Topographic Cross-sections

Diagonal cross-sections of the atmosphere and topography were generated between 1°S, 33°E and 4°S, 36°E (Figure 2.1) using the MetPy library (May *et al.*, 2020). Transects were generated using the cross_section() function, and horizontal wind vectors tangential to the transect line were calculated using the tangential_component() function. The transect line was chosen as it included both Lake Victoria and a south-eastern part of the Serengeti National Park: an area of crucial ecological importance where the wildebeest calve in February/March (Hopcraft *et al.*, 2015).

2.3 Results

2.3.1 Annual and Monthly Precipitation over the Wider Serengeti Domain

In the first section of our study, we mapped the spatial and temporal distribution of rainfall over the wider Serengeti domain on annual and monthly timescales.

2.3.1.1 Annual Precipitation

We aimed to identify the key spatial patterns of regional precipitation, beginning with the climatological annual mean, and assess the stability of these patterns across two datasets (CHIRPS v2.0, and TRMM 3B42). Figure 2.2 shows that in both datasets, there was a south-east to north-west rainfall gradient across the Serengeti National Park. Areas north-west of the park received approximately 1500 mm year^{-1}, three times the 500 mm year^{-1} recorded over the south-eastern parts of the park. In both datasets there were high rainfall totals over the mountains south-east of the Serengeti National Park (1200-1500 mm year^{-1}), and wetter rainfall conditions (> 750 mm year^{-1}) in the west of the wider Serengeti domain. Rainfall generally increased with proximity to Lake Victoria, and over Lake Manyara and Lake Eyasi in the south-east.

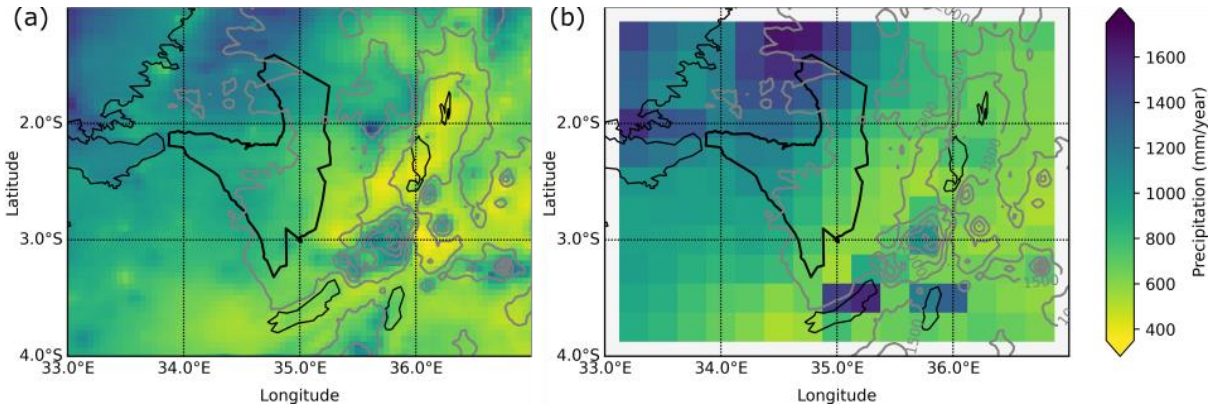

Figure 2.2: Climatological mean annual precipitation in the Serengeti and surrounding region. Calculated from (a) CHIRPS data (1987-2016); and (b) TRMM data (1998-2014). Lakes are outlined with thin black lines, while a thick black line shows the outline of the Serengeti National Park. Grey contours illustrate regional topography (Gtopo30 data).

However, there were also differences between the datasets in the spatial distribution and range of precipitation totals. The CHIRPS dataset had lower regional maximum and minimum values than TRMM, with a difference of approximately 150 mm $year^{-1}$ recorded between the minimum CHIRPS and TRMM values. Compared to CHIRPS, the TRMM dataset also recorded higher rainfall totals over the Kenya highlands, Lake Eyasi and Lake Manyara. The TRMM dataset also had a comparatively low spatial resolution, less distinction between rainfall totals on opposing mountain sides, and less spatial heterogeneity in the driest area in the south-east of the Serengeti National Park. The two climatological averages cover different time periods (1987-2016 for CHIRPS; 1998-2014 for TRMM), which partially explains these discrepancies. However similar patterns remained when TRMM and CHIRPS were compared over the same time period (1998-2014; results not shown). TRMM still recorded higher values over the majority of the wider Serengeti domain, including higher totals over Lake Manyara, Lake Eyasi and east of Lake Victoria, and lower totals over certain south-facing mountain slopes as well as a small region south-east of the Serengeti National Park.

2.3.1.2 Monthly Precipitation

We next examined the evolution of the spatial distribution of monthly precipitation patterns through the annual cycle (Figure 2.3). We focused solely on the CHIRPS due to its higher spatial resolution (compared to TRMM). Precipitation was recorded across the majority of the wider Serengeti domain from November to April, with elevated rainfall totals over high ground and Lake Victoria. From June to September, rainfall was limited to Lake Victoria, Ngorongoro Crater, and the highlands north of the Serengeti National Park. May and October saw high precipitation totals on mountain slopes and along the shores of Lake Victoria, and minimal

rainfall in other parts of the region. The wettest and driest months were April and July respectively.

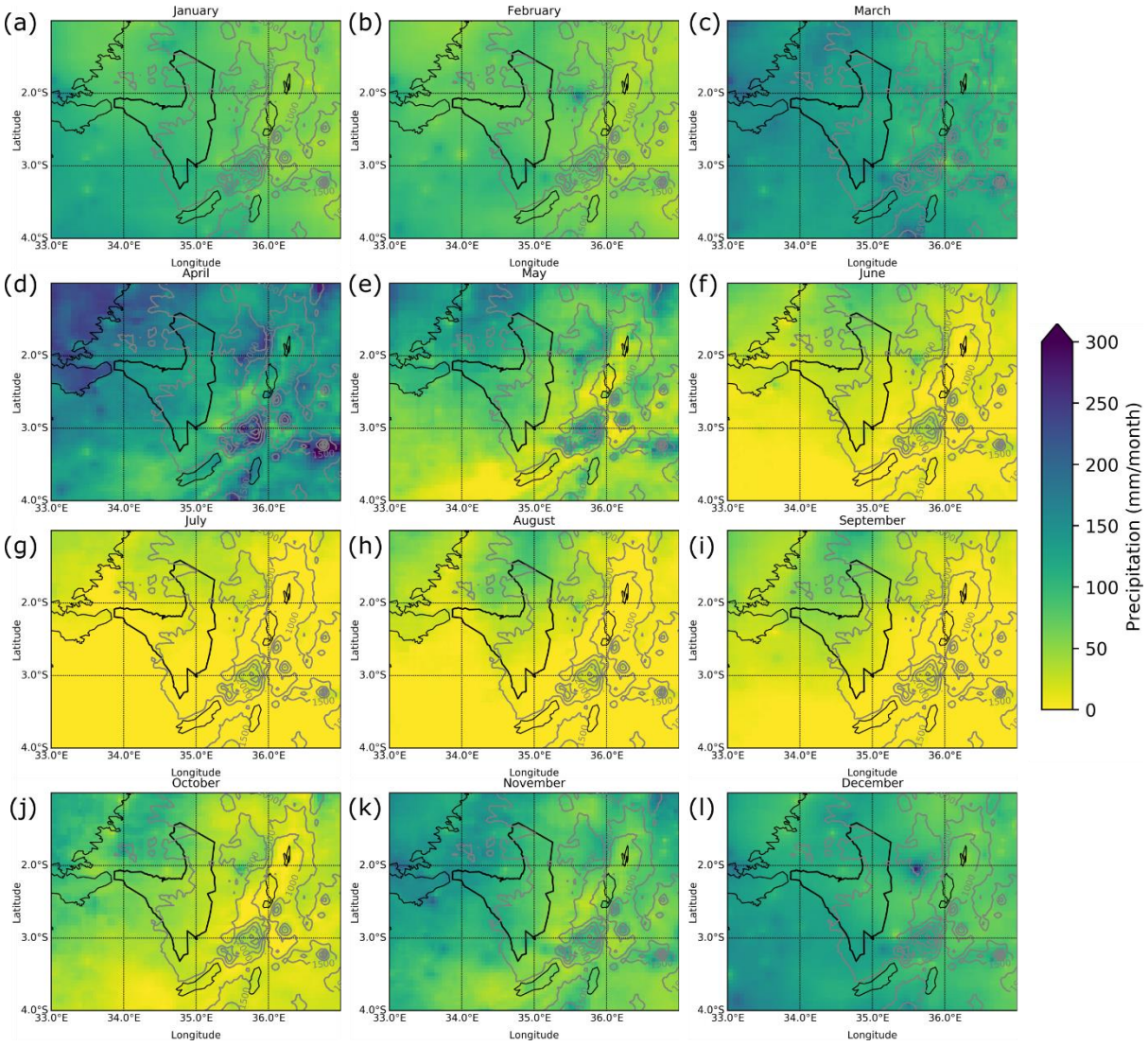

Figure 2.3: Monthly climatological mean precipitation across the wider Serengeti domain. Monthly rainfall climatologies calculated from CHIRPS dataset (1987-2016) for each month, starting with January (a) and finishing with December (l). Gtopo30 topography data overlaid.

The rainfall gradient identified in the annual climatology was present throughout the year, however its orientation altered through time. From March to May, and October to November, the north-west received greater rainfall than the south-east. From June to September, the north received more rainfall than the south, and from December to February the south-west received greater precipitation than the north-east. Another notable seasonal feature was the

exceptionally high rainfall totals on the eastern and southern slopes of the south-eastern mountains in April and May.

2.3.1.3 Variation in Annual Cycles

The monthly changes to the spatial distribution of rainfall suggested that the annual cycles would be distinctly different across the region. We therefore examine the diversity of annual cycles present in the wider Serengeti domain (Figure 2.4). The black lines show the mean precipitation across the whole region, and the means of both datasets reveal a dry season from June to October, and a wet season from November to May. This wet season had two rainfall peaks, one in November/December, a larger one in March/April, and a reduced amount of rainfall in the interceding January-February period. When comparing the mean annual cycles of TRMM and CHIRPS values, the monthly totals were similar, which was unexpected given the higher regional maximum and minimum annual values recorded in TRMM (Figure 2.2). This suggests that in the TRMM dataset there were a greater number of comparatively dry grid cells to compensate for the higher maximum and minimum precipitation values.

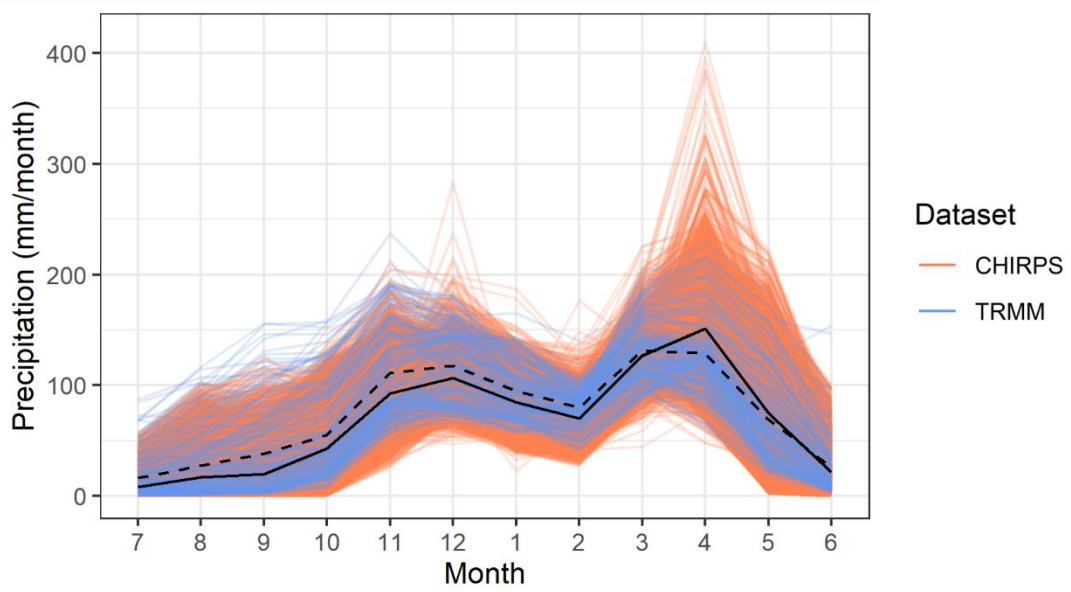

Figure 2.4: Annual cycle of precipitation over the wider Serengeti domain (1-4 S, 33-37 E). The solid black line shows the annual cycle averaged across all of the CHIRPS grid cells, while the dashed black line shows the average of the TRMM data.

Orange lines show the climatological annual cycles of individual CHIRPS grid cells, and blue lines represent annual cycles over individual TRMM grid cells. Data (CHIRPS 1987-2016, and TRMM 1998-2014).

Examining the annual cycles of individual grid cells (coloured lines) in Figure 2.4, there was a large range in the magnitude of the recorded precipitation totals. The CHIRPS dataset had the largest range in precipitation values, but also a greater number of data points. There was also variability in peak rainfall months, with different localities having peaks in November or December, and March or April.

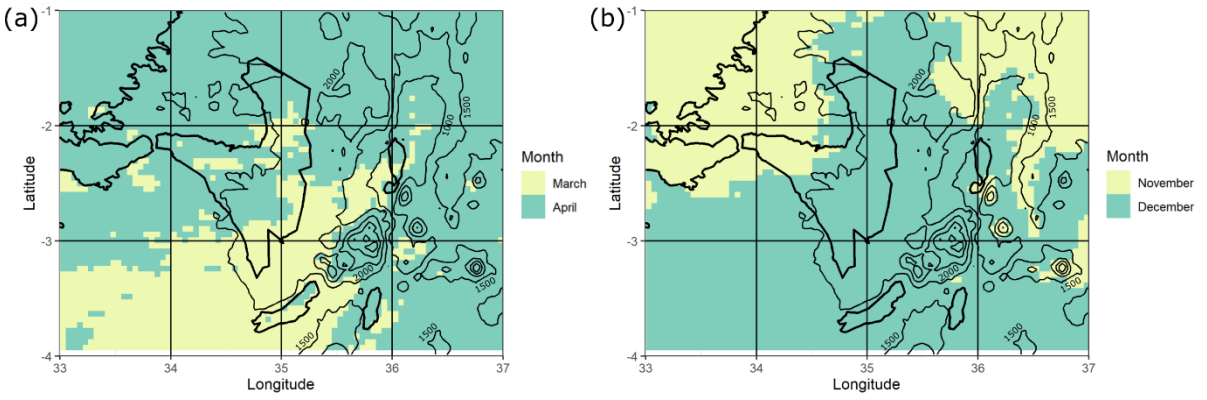

Figure 2.5: Spatial distribution of change in precipitation signal between consecutive wet season core months. Climatological rainfall decreased (yellow) or increased (green) between one month and the next is shown, therefore colour corresponds to wet season peak rainfall month. Rainfall change signals displayed for (a) November –December, and (b) March – April. Data: CHIRPS (1987-2016).

Figure 2.5 shows that there are clear patterns to the spatial distribution of peak rainfall months, which appear partially linked to the local topography. Southern areas which were to the west of the East African Rift mountains typically had a March instead of an April rainfall peak (Figure 2.5a). Later in the year, the majority of the Serengeti National Park had a December peak, while there was a November peak in areas close to Lake Victoria and in northern areas east of the East African Rift mountains (Figure 2.5b).

2.3.1.4 Cluster Analysis

We performed cluster analysis on the annual cycles represented in each of the precipitation datasets, to identify areas with similar annual precipitation cycles. The number of clusters were chosen based on the Euclidean distance between different steps of the clustering algorithm. In

both CHIRPS and TRMM, a large step change was present between 1 and 2 clusters, showing that there was a strong difference between these two sets of annual cycles. However, we were interested in further spatial differentiation of the region, so we therefore looked for the distinctions between higher numbers of clusters. In the CHIRPS and gauge dataset, there was a large step change between 3 and 4 clusters, suggesting that there was a strong distinction between the 4 clusters. In the TRMM dataset there were strong step changes in Euclidean distance between 2-3 clusters, and 4-5 clusters. As we were aiming looking to spatially differentiate the region, we chose to investigate 5 clusters in the TRMM dataset, and 4 clusters in the CHIRPS datasets. While there were discrepancies between the datasets, in each case areas with distinct annual cycles were identified in the north-west, south-west, east and centre of the region (Figure 2.6). An additional cluster was identified in the north-east in the TRMM dataset (Figure 2.6a). The mean normalised annual cycles of each cluster are shown in Figure 2.6b and d. The key differences that emerged between the annual cycles of each cluster were; dry season precipitation, wet season peak months, the ratio between wet season and January-February rainfall totals, and the symmetry of the rainfall peaks (Table 2.1).

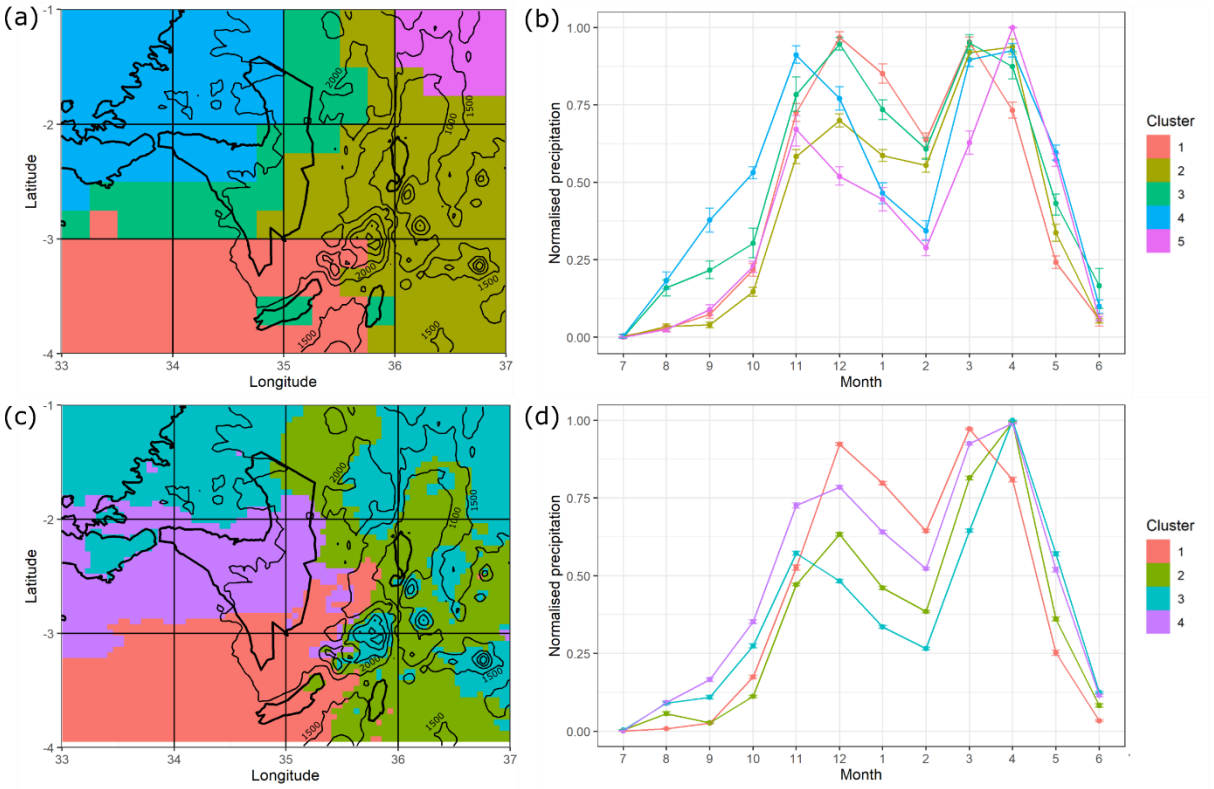

Figure 2.6: Cluster analysis of normalised climatological annual cycles. For each spatial datapoint/location, the annual cycle of precipitation was clustered using hierarchical cluster analysis (Ward's criterion). The spatial distribution of the resulting clusters is shown for the (a) TRMM (1998-2014); and (c) CHIRPS (1987-2016) precipitation datasets. The annual cycles for the identified clusters are shown for (b) TRMM; and (d) CHIRPS. Errorbars indicate the 95 % confidence intervals for cluster monthly means, calculated with a non-paramteric bootstrap resampling procedure based on 10000 samples.

South-west

The annual cycles in the south-west (cluster 1 in the TRMM and CHIRPS datasets) consistently had a symmetrical profile, with peaks in December and March. The ratios between peak months and January/February totals were low, and the annual cycle had an appearance closer to a single than a double wet season. The proportion of annual rainfall occurring in the dry season was low.

East

In the east (cluster 2 in the TRMM and CHIRPS datasets), December and April were peak rainfall months. There was an asymmetry between these rainfall peaks, with much higher totals

in April, and only slightly more rainfall in November compared to January and February. In this region, a low proportion of annual precipitation fell during the dry season.

North-west

Cluster 4 in the TRMM data covered an area over the north-west, while cluster 3 in the CHIRPS dataset included the north-east of the region, and an area on the shores of Lake Victoria. Both had rainfall peaks in November and April, and proportionally high dry season rainfall totals. However, the symmetry between the rainfall peaks, and ratios between peak rainfall months and January-February totals, differed between datasets.

North-east

The annual cycle of TRMM's cluster 5 in the north-east, was similar to its cluster 4 in the north-west. It had November and April peaks, and relatively high rainfall totals in these months compared to January and February. The main difference was that the proportion of rain falling in the dry season was much smaller in the north-east compared to the north-west, and the April peak was higher than the November peak.

Central

While a central cluster was present in both datasets, the spatial extent and structure of the mean annual cycles differed. This may be an artefact of the analysis, or alternatively suggests that local annual cycles changed rapidly over short distances in this area. The L-shaped central TRMM cluster (cluster 3) had wet season peak months in December and March and a high proportion of rainfall in the dry season. There was a moderate difference between Jan-Feb totals and the peak month totals. The central CHIRPS cluster (cluster 4) extended from 2-3 °S and 33-35 °E. It had asymmetric December and April peaks, high levels of dry season rainfall, and a moderate ratio between January-February totals and wet season rainfall peaks.

Table 2.1: Summary of the key characteristics of annual precipitation cycles in different parts of the wider Serengeti domain. The ~ symbol represents disagreement between clusters in different datasets.

Cluster	Proportional January - February Precipitation	Proportional June - October Precipitation	Wet Season Peaks		Rainfall Peak Symmetry
			Nov/Dec	Mar/Apr	
South-west	High	Low	Dec	Mar	Symmetric
East	Low	Low	Dec	Apr	Asymmetric
North-west	~	High	Nov	Apr	~
North-east	Low	Low	Nov	Apr	Asymmetric
Central	High	~	Dec	~	~

2.3.2 Seasonal and Diurnal Wind over East Africa

The next stage of our study explored the atmospheric mechanisms that could be causing the spatial distribution of regional rainfall, and the distinct annual cycles identified by the cluster analysis.

2.3.2.1 Monthly Wind Patterns

Figure 2.7 and Figure 2.8 show the climatological 750 hPa winds over East Africa, which help explain the main structure of the Serengeti's seasonality. Easterlies were present throughout the year and had a seasonally changing meridional component. Although there were greater rainfall totals over Lake Victoria and much of the topography in the Lake Victoria basin, the wettest periods in the Serengeti were similar to the rest of East Africa, in that they coincide with the migration of the tropical rainfall belt over the equator. The meridional wind direction switched from northerly in March (Figure 2.7a) to southerly in May (Figure 2.7c), and from southerly in October (Figure 2.7d) to northerly in December (Figure 2.7f).

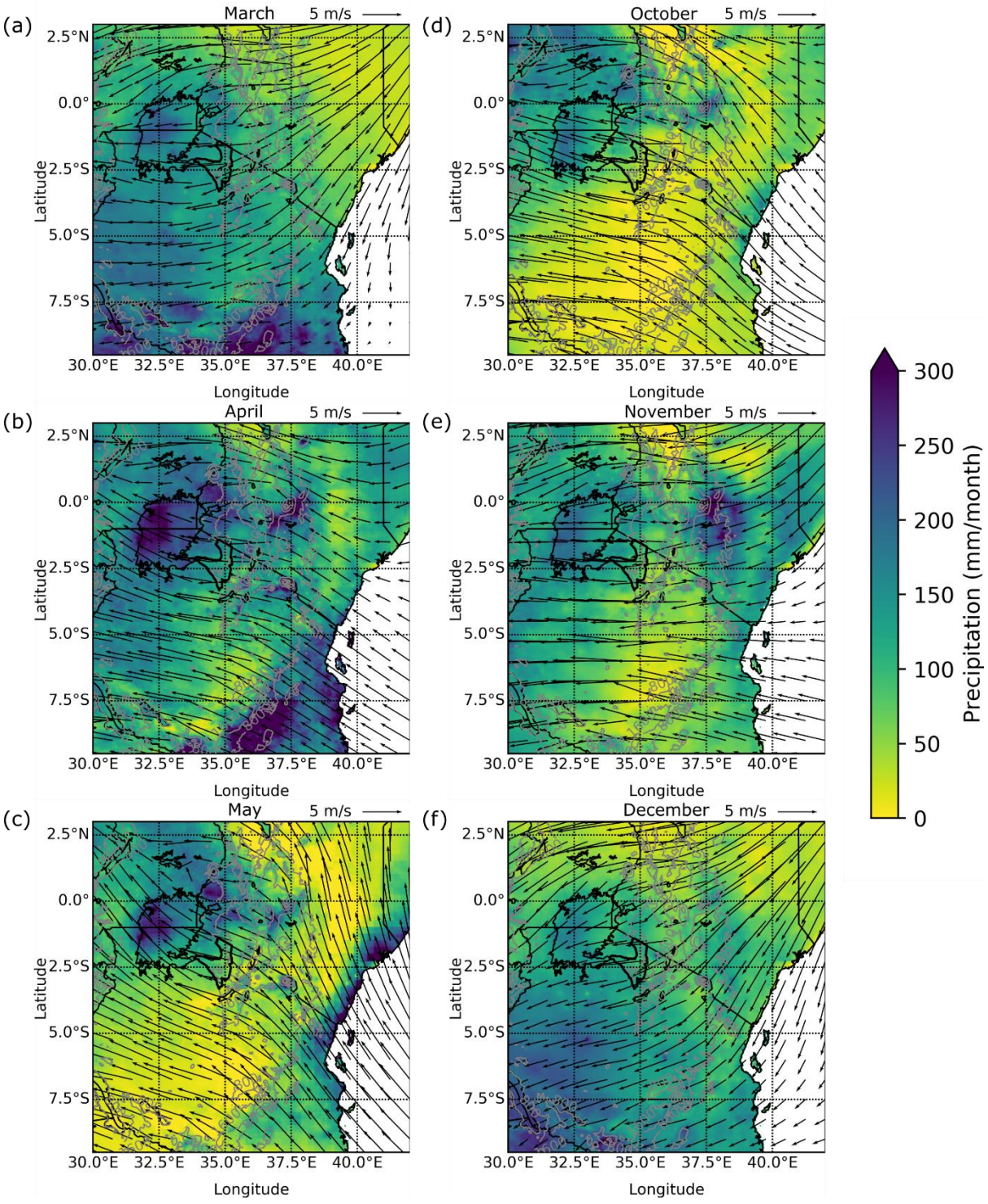

Figure 2.7: Climatological precipitation and 750 hPa wind patterns during the East African wet seasons. Precipitation (CHIRPS, 1987-2016) and wind (ERA5, 1986-2017) climatologies shown for (a) March; (b) October; (c) April; (d) November; (e) May; and (f) December. Wind vectors were regridded to a resolution of 0.75° for ease of viewing. Gtopo30 topography data overlaid.

However, the rainfall patterns over the Serengeti and surrounding region differ from much of East Africa during the "dry" seasons. These dry seasons occurred when the tropical rainfall belt was furthest from the equator (Figure 2.8). However, comparatively high precipitation

totals remained over the Serengeti and around Lake Victoria during these months, even though there was minimal precipitation further east.

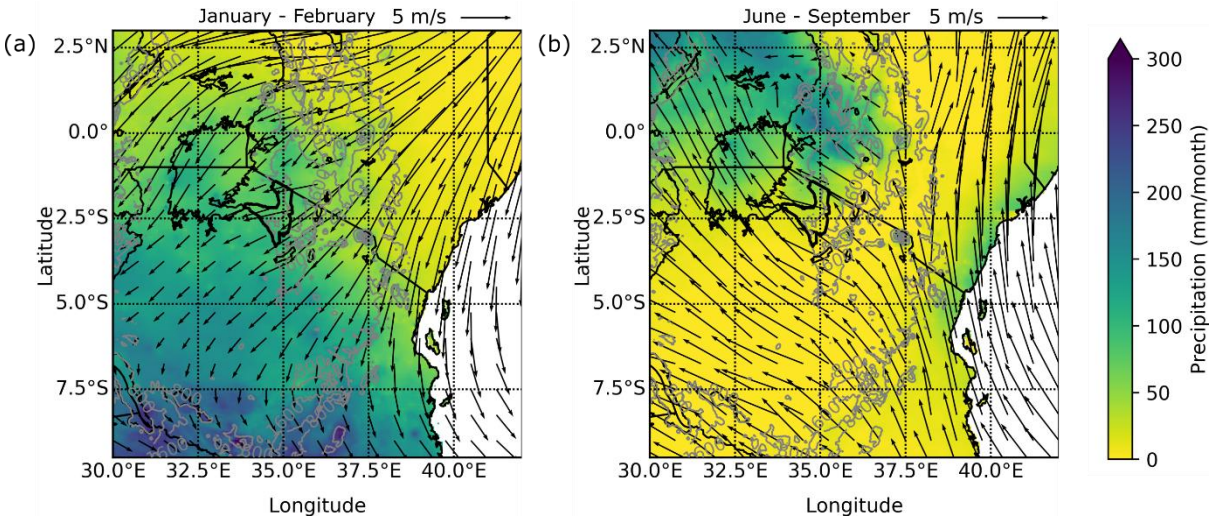

Figure 2.8: Climatological precipitation and 750 hPa wind patterns during the East African dry seasons. Precipitation (CHIRPS, 1987-2016) and wind (ERA5, 1986-2017) climatologies shown for (a) January-February; and (b) June-September. Winds regridded to 0.75 ° resolution. Gtopo30 topography data overlaid.

The additional moisture provided by Lake Victoria appeared to be the reason for the increased rainfall during this time. However, to investigate how the moisture was carried eastwards, against the prevailing easterlies, we examined winds at a lower atmospheric level.

2.3.2.2 Monthly and Diurnal Wind, Convergence and Moisture Patterns

Figure 2.9 shows surface wind patterns were strongly influenced by topographic features, the East African coastline, and land-lake breezes. The winds diverged (blue) and converged (red) over the largest lakes at 06:00 and 18:00 respectively, while the topography of the East African rift both channelled and blocked the tropical easterlies from the Indian Ocean. Figure 2.9b shows that at 18:00 convergence occurred over the Serengeti National Park, and regions where diverging lake breeze winds from Lake Victoria met tropical easterlies or topographic boundaries. Complex patterns occurred over the East African rift highlands, with strong convergence over the highest topography and divergence in the valleys.

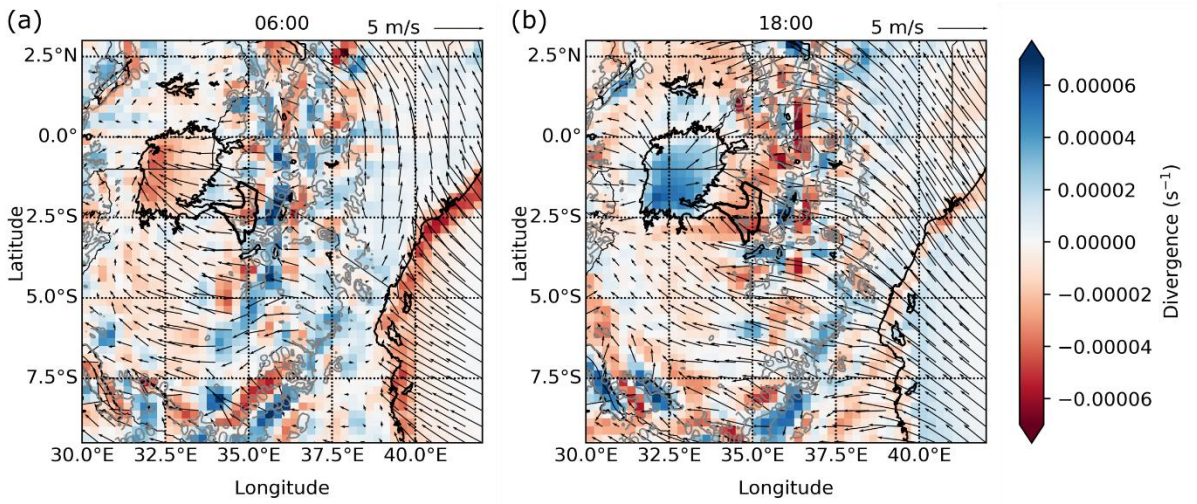

Figure 2.9: Mean annual surface wind (vectors) and divergence (shading) over East African for (a) early morning (06:00 EAT) and (b) early evening (18:00 EAT). Areas with diverging winds are shown in blue, and areas with converging winds are shown in red. Wind vectors were regridded to a 0.5° resolution for ease of viewing, while divergence values are displayed at the native resolution of 0.25°. Data: ERA5 (1987-2016). Gtopo30 topography data overlaid.

Analysis of the wind and divergence patterns on a monthly timescale, showed that these convergence patterns changed throughout the year depending on the meridional component of the tropical easterly winds, yet the Serengeti National Park remained one of the locations in East Africa where surface wind convergence was always present in the afternoon (Figure 2.10). In addition, divergence often extended by up to 2° latitude to the north (Figure 2.10b, c) and south (Figure 2.10a, d) of the lake, depending on the meridional component of the tropical easterlies.

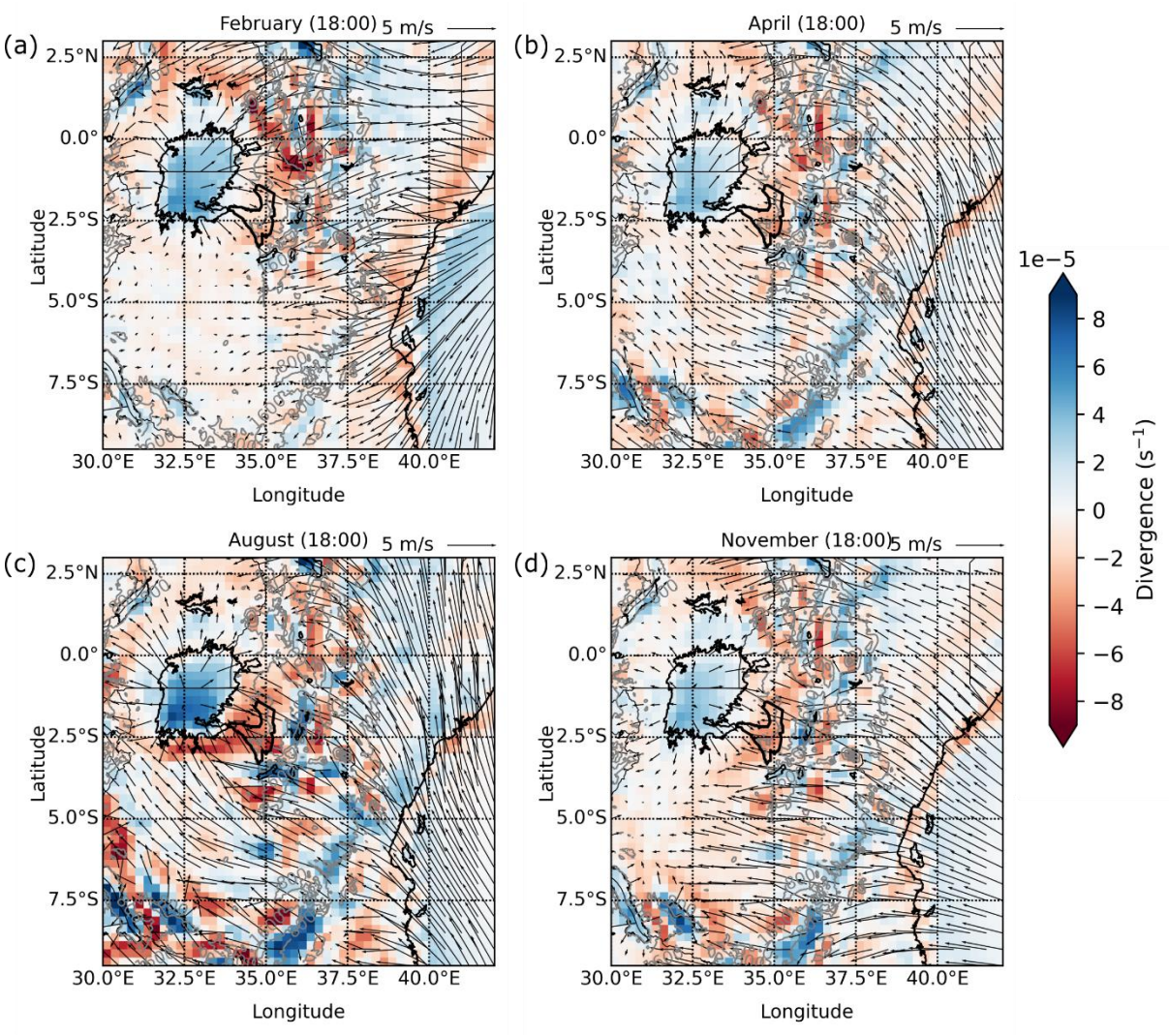

Figure 2.10: Mean surface wind (vectors) and divergence (shaded) at 18:00 EAT in (a) February, (b) April, (c) August, and (d) November. Wind vectors were regridded to a resolution of 0.5° for ease of viewing, while divergence values are displayed at the native resolution of 0.25°. Data: ERA5 (1987-2016). Gtopo30 topography data overlaid.

These wind and convergence patterns also played a large part in the distribution of moisture from Lake Victoria, as shown in Figure 2.11. Relatively high levels of specific humidity were present across the whole of East Africa during the months of November to May. In other months, the rift topography acted as a barrier to moisture being transported westward from the Indian Ocean, illustrating the rain shadow generated by these highlands. Within the Lake Victoria basin, increased moisture levels were associated with diverging lake breeze winds from Lake Victoria.

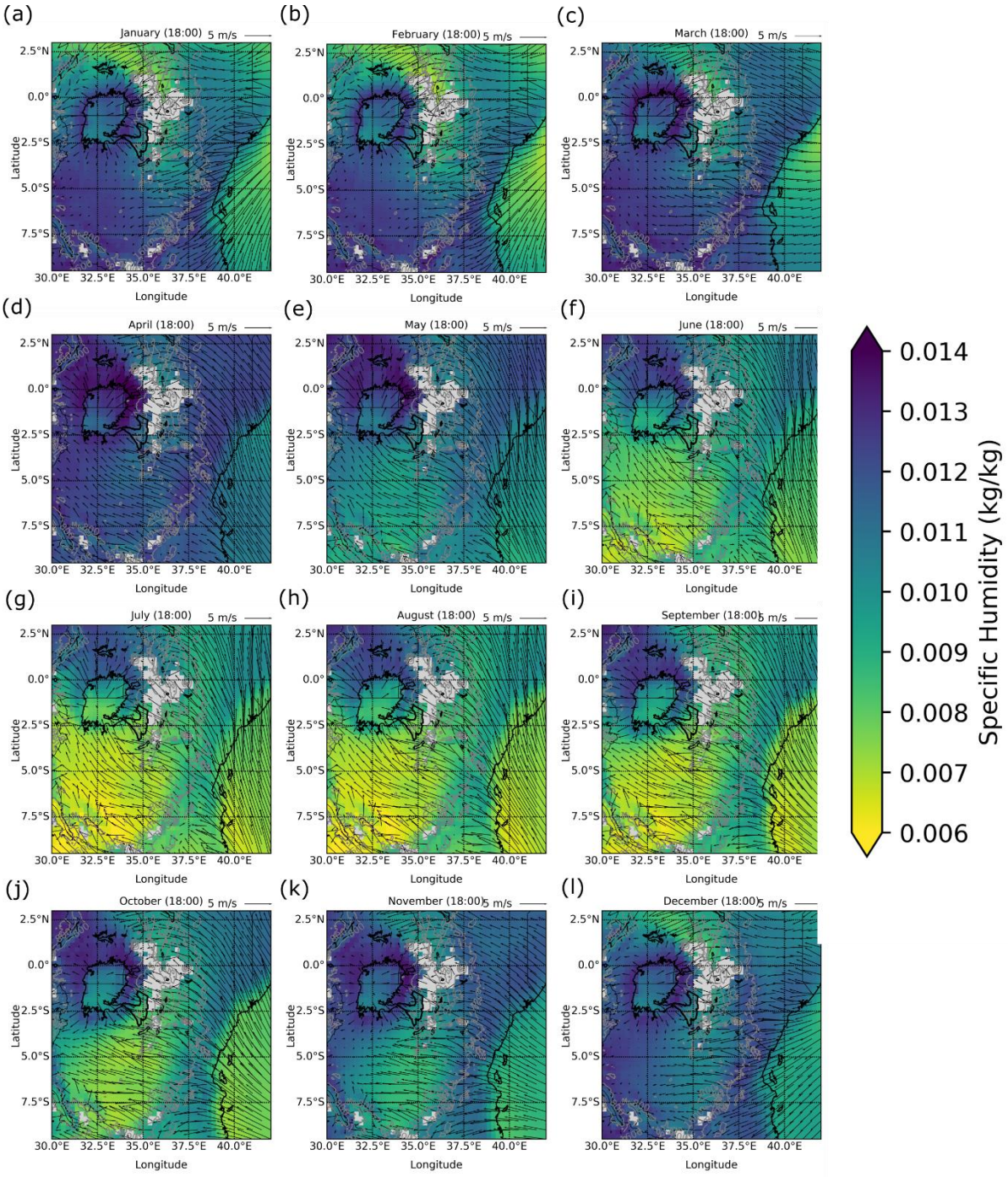

Figure 2.11: Mean monthly early evening (18:00 EAT) surface wind patterns (vectors) and 825 hPa specific humidity (shading) from ERA5 data (1987-2016). Specific humidity values at levels below surface pressure are masked with light grey. Gtopo30 topography data overlaid.

2.3.3 Diurnal Precipitation and Wind over the Wider Serengeti Domain

The previous results (section 2.3.2) showed an association between rainfall and afternoon surface wind patterns, and illustrated the importance of the diurnally changing lower level winds to moisture availability within the Lake Victoria basin. Therefore, the final stage of our study investigated the evolution of rainfall and wind patterns over the wider Serengeti domain on an hourly timescale.

2.3.3.1 Diurnal Precipitation and Surface Wind Patterns

Figure 2.12 shows that the time of peak annual rainfall differed across the wider Serengeti domain. Maximum rainfall occurred between 03:00-09:00 over Lake Victoria, around Lake Manyara and to the east of Ngorongoro Crater. The majority of the rest of the region had a late afternoon/early evening rainfall maximum (18:00, light brown), including half of the Serengeti National Park. However, along the eastern edge of the Serengeti National Park, maximum rainfall occurred in the early afternoon (15:00, off-white).

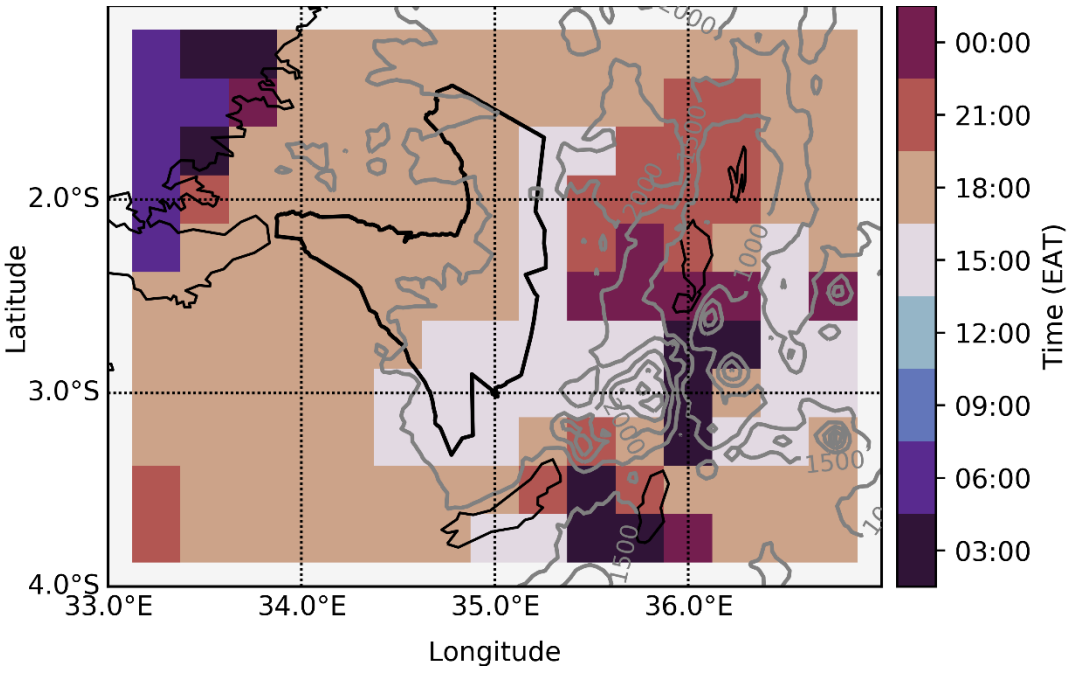

Figure 2.12: Time of maximum annual precipitation. Analysis based on precipitation climatologies that were calculated for each 3-hourly timestep of the TRMM dataset (1998-2014). Gtopo30 topography data overlaid.

This early afternoon rainfall peak appeared to be where a rain shadow from the mountains would be expected. In addition, when peak rainfall time in individual months (Figure 2.13) was inspected, the early afternoon rainfall peak was not present through the whole year, and instead appeared to be correlated with the southerly extent of the diverging lake breeze winds. From October to March, the lake westerlies extended to below 4 °S, and there was a striking match between the wind convergence line and the boundary between the areas receiving early and late afternoon rainfall peaks. This relationship appeared to partially break down in April, May and September, which were also months when the diverging lake breeze winds did not reach below 3 °S. From June to August, when the surface level lake winds did not reach any part of the Serengeti National Park below 2 °S, early afternoon rainfall peaks were absent from most of the wider Serengeti domain.

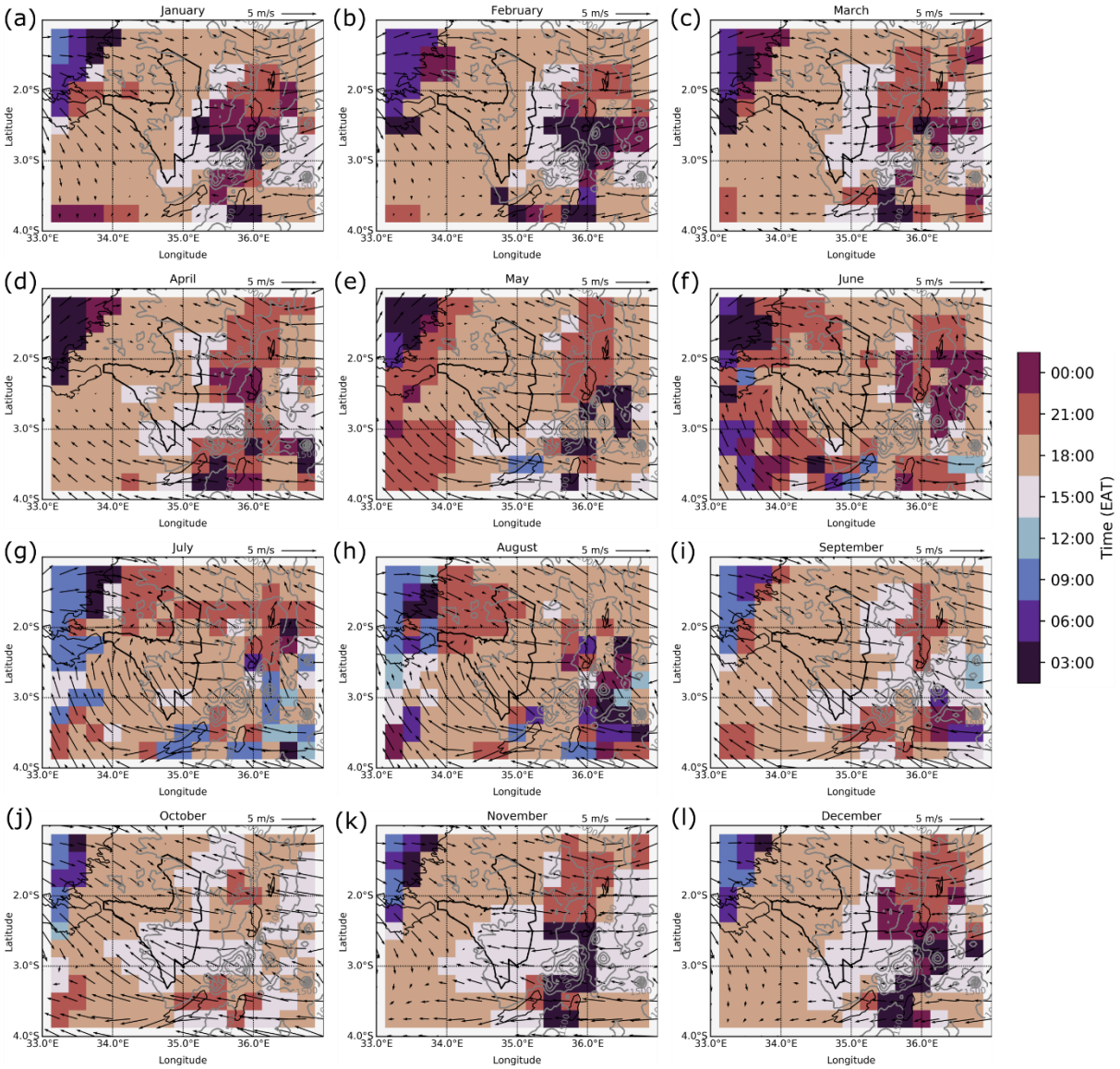

Figure 2.13: Monthly time of maximum precipitation and 15:00 (EAT) surface wind patterns. Plots (a)-(l) represent January-December respectively. Precipitation climatologies were calculated for each 3-hourly timestep using TRMM data (1998-2014), and wind climatologies were calculated using surface wind vectors from the ERA5 dataset (1987-2016). Gtopo30 topography data overlaid.

To better understand the role of the lake breeze westerlies in generating rainfall at different points in the annual and diurnal cycle, we inspected the afternoon climatological rainfall and wind patterns in a wet and dry season month (Figure 2.14).

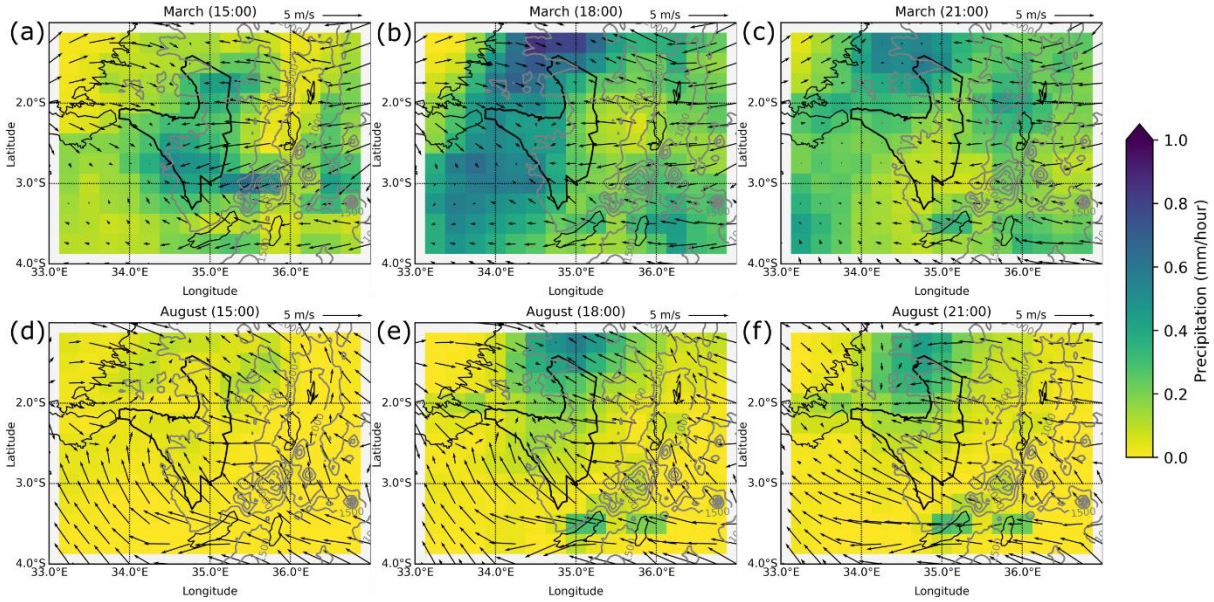

Figure 2.14: Mean afternoon precipitation and surface wind patterns during a wet and dry season month. Mean hourly rainfall and wind vectors were calculated during March for (a) 15:00 (13:30-16:30 precipitation), (b) 18:00 (16:30-19:30 precipitation), and (c) 21:00 (19:30-22:30 precipitation), and in August for (d) 15:00 (13:30-16:30 precipitation), (e) 18:00 (16:30-19:30 precipitation), and (f) 21:00 (19:30-22:30 precipitation). Times in East Africa Time. Data: TRMM (1998-2014) and ERA5 (1987-2016). Gtopo30 topography data overlaid.

In both wet season and dry season months, rainfall over the Serengeti National Park was more widespread at 15:00 (Figure 2.14a, d) than at 18:00 (Figure 2.14b, e), and 15:00 rainfall did not concentrate in areas where the winds were converging. By 18:00 the lake breeze winds penetrated further west and rainfall totals increased, but the spatial distribution of rainfall shifted to the west of the converging winds (Figure 2.14b, e). This pattern remained at 21:00, although the wind convergence line and areas of highest rainfall moved westward towards the lake (Figure 2.14c, f).

When comparing 15:00 rainfall in the two seasons, in March the rainfall was widely spread across the Serengeti National Park, including in the "rain shadow" the East African rift topography. Whereas in August, limited rainfall occurred across the region during this time period. At 18:00 and 21:00, similar rainfall totals were recorded in the north-west of the wider Serengeti domain in March and August, so the main differences were in the spatial extent of rainfall, with minimal totals recorded in August away from the northern highlands and southern lakes.

2.3.3.2 Monthly Afternoon Vertical Wind Profiles

To further understand the temporal evolution of rainfall-generating atmospheric conditions, we examined the vertical structure of the atmosphere over a diagonal transect between 1°S, 33°E and 4°S, 36°E (path shown in Figure 2.1). Figure 2.15 shows afternoon/evening vertical atmospheric cross-sections during March (Figure 2.15a, c, e) and August (Figure 2.15b, d, f), and the topography of the transect line (Figure 2.15g, h). Distinct differences were present between March and April, both above and below 600 hPa.

Above 600 hPa there was near-ubiquitous descending motion in August, with weak south-easterly winds and the presence of winds with a north-westerly component between 500-650 hPa (Figure 2.15b, d and e). March had stronger south-easterly winds (compared to August) but more variable patterns of vertical motion. At 15:00 descending motion was present north-west to the lake shoreline (33.7°E) and south-east of 35.7°E, with ascending motion present in between (Figure 2.15a). This region of ascending motion (which extended from the surface to 400 hPa) coincided with the areas receiving rainfall in Figure 2.14a. By 18:00 descending motion was present over the lake and stretched diagonally from the lake shoreline at the surface (33.7°E) to approximately 35.2°E at 400 hPa (Figure 2.15c). By 21:00 ascending motion had returned to the majority of the troposphere above 600 hPa (Figure 2.15e).

Below 600 hPa there was a clear lake circulation cell in the north-west, strong ascending motion over the centre, and topographic effects in the south-east. South-easterly winds were stronger in August than March. The lake circulation cell occurred over Lake Victoria and the adjoining land, with air descending and ascending in the north-western and south-eastern portions respectively. The position and size of the cell changed depending on month and time of day. Between 15:00 and 18:00 the centre of the lake cell moved inland, then retreated back towards the lake by 21:00. The height of the circulation cell also decreased to below 700 hPa by 21:00.

The centre of the circulation cell reached further inland in March (33.8°E, 34.0°E and 34.0°E at 15:00, 18:00 and 21:00 respectively) than in August (33.6°E, 33.7°E and 33.5°E at 15:00, 18:00 and 21:00 respectively), and the orientation of the cell was steeper in August.

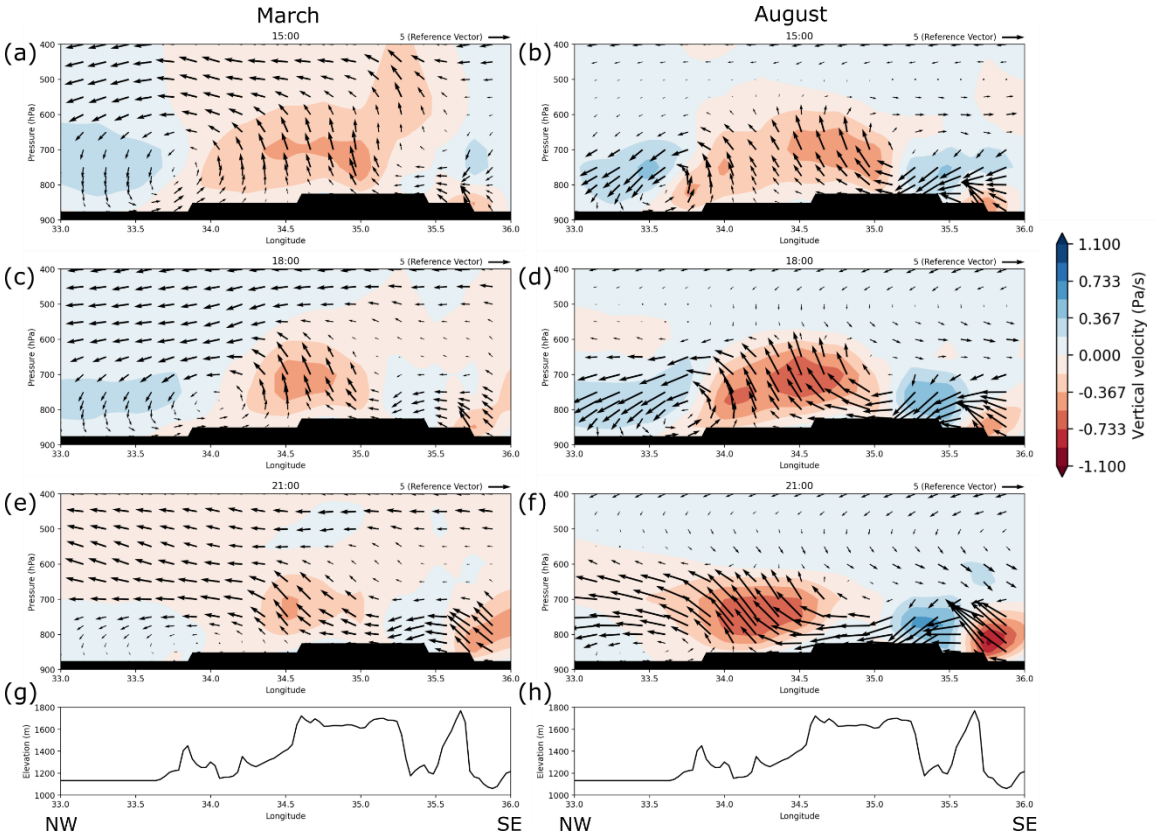

Figure 2.15: Topographic and afternoon atmospheric cross-sections over the Serengeti during a wet and dry month of the year. The cross-sections run in a diagonal line from 1°S, 33°E in the north-west (NW) to 4°S, 36°E in the south-east (SE) (path shown in Figure 2.1). Individual panels show atmospheric conditions in March at (a) 15:00 EAT, (b) 18:00 EAT, (c) 21:00 EAT, and August at (d) 15:00 EAT, (e) 18:00 EAT, and (f) 21:00 EAT. Panels (g) and (h) are identical and depict the topography along the transect line (Gtopo30 data). In panels (a)-(f) colour illustrates ascending (red) and descending (blue) motion. Values below the surface pressure are masked with black. The x-components of the vectors show the magnitude of winds tangential to the transect line (m/s). The diagonal nature of the transect means that vectors with a positive (negative) x-component represent the north-westerly (south-easterly) component of the winds. The y-components show vertical velocity (Pa/s). The vertical component of the vectors is scaled by -10 for ease of viewing. The tenfold multiplication of the vectors allows the vertical motion to be more easily visible, while the negative multiplication allows areas with ascending motion to have upward-pointing arrows. Data: ERA5 (1987-2016).

A peak of ascending motion was always present at approximately 700-800 hPa over 34.5°E, a position just north-west of an increase in the topography of approximately 260 m over 7 km. At 15:00 this peak was predominantly present between 34.4°E and 35.1°E, which is slightly north-west of a topographic plateau (34.6°E-35.2°E). This region of ascending motion moved towards the north-west/lake at 18:00, and again at 21:00. This was despite the surface lake

breeze winds reaching further inland at 18:00 than 15:00. Additionally the magnitude of peak ascending motion increased between 15:00 and 21:00 in August, and decreased in March.

Finally there were topographic effects present below 700 hPa in the south-east. Ascending motion was present north-west of 35.2°E and south-east of 35.7°E, approximately corresponding to the escarpments next to Lake Eyasi and Lake Manyara respectively. Descending motion was present between these regions of ascent. This matched a gap in the rift topography between Lake Eyasi and Lake Manyara (Figure 2.1, Figure 2.15g), making it likely that the descending motion was due to zonal winds being funnelled through this channel.

2.4 Discussion

The complex precipitation patterns over the Serengeti National Park are an integral part of the internationally important Serengeti-Mara ecosystem. Our results suggest that these diverse precipitation conditions are caused by interactions between tropical easterlies, land-lake breezes generated by Lake Victoria, and regional topography. Here we consider the performance of the precipitation data used in our study and the roles of the above three key features in controlling regional precipitation. We then discuss their combined effect on the spatial distribution of rainfall, local storm development, and seasonality over the Serengeti.

2.4.1 Evaluation of Precipitation Data

If we compare our results to monthly rain gauge measurements reported by Norton-Griffiths *et al.* (1975), we see that both TRMM and CHIRPS captured the rainfall gradient and spectrum of annual cycles previously reported over the Serengeti National Park. The magnitude of the CHIRPS measurements closely matched those reported by Norton-Griffiths *et al.* (1975), whereas TRMM values were higher across the majority of the national park, particularly east of Lake Victoria. These high totals may be partially due to the shorter time period used to

calculate the TRMM climatology (1998-2014), as it contained two exceptionally wet years over the northern Serengeti (1998 and 2001) (Ogutu *et al.*, 2008a). However, TRMM also differed from CHIRPS readings taken from 1998-2014, with patterns similar to those found by Haile *et al.* (2013); TRMM 3B42 overestimated totals over lake surfaces and underestimated totals over mountaintops. Overall, this suggests both TRMM and CHIRPS provide accurate representations of the spatial and temporal patterns of monthly precipitation over the wider Serengeti domain, but the absolute precipitation totals in TRMM should be interpreted with caution.

2.4.2 Large-scale Circulation Patterns

Examination of the annual cycles across the wider Serengeti domain showed that all locations had (1) a drier period from June to September/October, (2) a double peaked wet period from October/November to May, and (3) rainfall peaks in November/December and March/April. These results were not unexpected, since it is well documented that the wettest periods in East Africa occur between March to May and October to December during the biannual passage of the tropical rainfall belt (Nicholson, 2018). In these months the tropical easterly winds are weak and have a low meridional component, while Indian Ocean sea surface temperatures (SSTs) are high, and this results in an unstable atmosphere (Yang *et al.*, 2015). Conversely, low SSTs and strong cross-equatorial tropical easterly winds during the dry seasons of January-February and June-September, result in a stable atmosphere which suppresses moist convection (Yang *et al.*, 2015). Our results confirm the major determinants of seasonality in the Serengeti are the tropical rainfall belt, and the large-scale circulation patterns that dominate East African climate. Future changes to large-scale regional circulation would therefore likely impact Serengeti rainfall.

2.4.3 Topography

Despite overarching similarities amongst annual cycles over the wider Serengeti domain, there were also distinct differences, many of which were associated with the rift topography. Our results show that high rainfall totals were recorded on mountain slopes facing tropical easterlies, and low rainfall totals were recorded in their lees. Different slopes received this topographic rainfall throughout the year depending on the orientation of the tropical easterlies. Particularly high precipitation totals were recorded on slopes that faced the tropical easterlies in April, which is the wettest month of the year across much of East Africa (Yang *et al.*, 2015). These findings were expected, as the generation of topographic rainfall through orographic uplift on windward slopes, and the presence of rain shadows in their lees, is a well-known phenomenon (Houze, 2012). The impact of topographic rainfall is also well documented in East Africa: the rain shadow generated by the rift valley is a recognised regional feature (Camberlin, 2018); exposure is known to be one of the key determinants of annual rainfall totals over the rift highlands (Oettli and Camberlin, 2005); and Norton-Griffiths *et al.* (1975) highlighted the rain shadow caused by Ngorongoro Crater highlands as a key cause of low rainfall totals in the south-eastern Serengeti.

However, our results suggest that the topography has additional effects over the Serengeti that have not previously been discussed. At 15:00 a region of ascending motion was present over a topographic plateau in the south-eastern Serengeti National Park. This region of ascending air moved towards the north-west between 15:00 and 18:00, despite the surface winds from the lake penetrating further inland. The mid-afternoon ascent over, and evening movement away from, the highest topography suggests this pattern may be generated by diurnal heating. The diurnal heating of mountain peaks is known to play an important role in triggering orographic

precipitation (Houze, 2012), and anabatic-katabatic flows are well documented in the highlands of East Africa (Anyah *et al.*, 2006; Nicholson, 2016a).

In addition, a region of descending motion is present in the gap in the topography between Lake Manyara and Lake Eyasi, showing the impact of the topography on channelling local winds. This descending motion would likely suppress rainfall over this region. There is also ascending motion over the Serengeti plateau to the north-west of this gap, however it is unclear whether this ascent is related to winds being channelled through the gap, or simply due to prevailing tropospheric south-easterlies.

Overall, the impact of topographic flows on precipitation generation and suppression over the wider Serengeti domain should be considered.

2.4.4 Lake Breeze Winds

Our results showed high rainfall totals over Lake Victoria and the surrounding areas. They also showed diverging daytime lake breeze winds associated with high moisture levels in the lower troposphere. In the eastern Lake Victoria basin, a wind convergence line was present between the westerly lake breeze winds and the tropical easterlies. This wind convergence line always passed through the Kenya highlands and the north of the Serengeti National Park; these regions received high annual rainfall totals. The impact of the convergence of lake westerlies over the Kenya Highlands is well documented (Fraedrich, 1972; Okeyo, 1986; Anyah *et al.*, 2006), with moisture-rich lake breeze winds known to combine with anabatic winds to generate thermally-triggered afternoon storms over the high ground. These storms drift westward over the afternoon and evening, and become reinvigorated once over Lake Victoria by the reversal of the lake breeze, and addition of katabatic winds overnight (Anyah *et al.*, 2006; Finney *et al.*, 2019). Over the Serengeti National Park, Norton-Griffiths *et al.* (1975) correctly suggested that

storms generated by the lake front were the reason that the north-west received heavier and less variable rainfall than the rest of the park throughout the year.

However, less attention has been paid to the seasonal impact of lake westerlies to the south of the Kenya highlands. Our results show that a convection cell between the lake breeze winds and tropical easterlies was always present over part of the Serengeti National Park. During months when the tropical easterlies have a northerly or neutral meridional component, the lake breeze winds extended further south into the Lake Victoria basin and Serengeti National Park. Logically, the ascending branch of these convection cells would provide favourable conditions for triggering convective storms, similar to those seen over the Kenya highlands. Thus, these results suggest that the lake plays a role in determining precipitation over a larger proportion of the Serengeti than was suggested by Norton-Griffiths *et al.* (1975), who described its influence as being restricted to the north-west of the ecosystem.

2.4.5 Afternoon Storm Development

Given the importance of the topography and Lake Victoria, and the magnitude of the changes to mountain-top heating and lake breeze strength over the diurnal cycle, it is unsurprising that we observe a diversity of peak rainfall times over the wider Serengeti domain. Our results show that peak rainfall always occurred during the day over the Serengeti National Park, and in the dry season it occurred in the late afternoon/early evening (18:00). However, during many of the wettest months of the year, the eastern Serengeti National Park had an early afternoon rainfall peak (15:00). This early afternoon peak typically occurred between the surface wind convergence line and the rift topography, suggesting the influence of both features.

Camberlin *et al.* (2018) found that early afternoon (15:00) rainfall maximums are a common feature around lakes in East Africa, caused by their diverging lake breeze winds. Therefore the late afternoon (18:00) rainfall maximums found on the east coast of Lake Victoria are

regionally anomalous. This late afternoon peak may be caused by the greater strength of the Lake Victoria westerlies, or positive feedbacks between anabatic winds and the lake breeze, resulting in an increased intensity and duration of the storms. However, this does not explain the early afternoon maximum we found to the east of the mean position of the lake breeze winds. A potential explanation may be variability in the position of the lake front. Our study has focused on the mean atmospheric conditions over the wider Serengeti domain, but the position of the lake front in fact varies from day to day (Woodhams *et al.*, 2019). Rainfall in the south-eastern part of the Serengeti National Park may only occur on the rare occasions when the lake front penetrates this far south-east. Given the distance from the lake, the storm may then be blown west by mid-tropospheric (> 750 hPa) easterly winds by late-afternoon, resulting in an early afternoon rainfall peak in the east and a later afternoon rainfall peak in the west.

An alternative explanation for the different peak precipitation times observed over the Serengeti National Park could be cloud formation over the high topography in the east resulting in light rainfall. Our results show a region of lower tropospheric ascending motion was present at 15:00 over the high plateau (34.5-35°E) in the eastern Serengeti in both March and August. By 18:00 the magnitude of peak ascent had strengthened in August, but weakened in March. If the ascending motion over the south-eastern Serengeti high ground is controlled by land surface temperatures, the formation of rain clouds in March may lower the surface temperature, which would then reduce ascending motion in the lower troposphere and could prevent small storms from growing. It's known that over the East African mountains, maximum surface temperatures can occur early in the day due to the formation of afternoon clouds, which block further solar heating (Duane *et al.*, 2008; Camberlin, 2018). In addition, over the African continent, early afternoon rainfall is often associated with weak shallow storms, whilst late afternoon rainfall is associated with deep storms and heavy rainfall (Geerts and Dejene, 2005).

Therefore it's possible that during wetter months, when higher levels of atmospheric moisture are present (compared to the dry season), rainfall in the two halves of the national park are generated in separate ways. Cloud formation over the high topography in the east may generate light topographic storms with an early rainfall peak, while larger storms in the west caused by the converging lake westerlies and tropical easterlies result in a late afternoon peak. However, this scenario would not explain why the early afternoon rainfall peak is largely absent in April, as this is the month with the highest specific humidity values across the wider Serengeti domain, and would therefore provide favourable conditions for the formation of topographic storm clouds.

Understanding the processes generating precipitation over the eastern Serengeti would also help us understand what may cause the rains to fail over the south-eastern Serengeti plains. Rain failure over the plains during December-April causes the wildebeest to travel into the neighbouring Maswa Game Reserve (MGR) (Sinclair *et al.*, 2015a), which is situated to the south-west of the Serengeti National Park. Extended periods in woodlands have negative impact on calf survival (Hopcraft *et al.*, 2005, 2015), nevertheless this area acts as an important refuge for the migratory herds. Our cluster analysis shows the MGR's annual cycle has a similar structure to the parts of the Serengeti National Park at the same latitude. This would suggest monthly rainfall in the MGR is determined by similar atmospheric processes to those generating rainfall over the southern and central Serengeti. If rainfall over the southern Serengeti and the MGR is caused by the same atmospheric processes, it would suggest the reason for the wildebeest using the MGR as a refuge during dry periods from December-April, may be due to increased moisture related to the region's deeper soils or downstream hydrology, rather than differences in rainfall patterns.

However, the spatial distribution of mean afternoon precipitation during March, shows that the southern Serengeti receives its highest rainfall totals at 15:00, while the MGR to the south-west

receives its highest rainfall at 18:00. If the rainfall is generated by different processes in the two regions, e.g.by small topographic storms over the Serengeti, and rainfall slightly further west over the MGR is generated by winds from Lake Victoria (or moisture brought from the Indian Ocean by winds channelled through the gap in the topography between Lake Manyara and Lake Eyasi), the wildebeest may be leaving the plains when the small local topographic storms fail, and moving to the MGR which is still receiving rainfall from alternative atmospheric processes.

It is not possible to fully understand the mechanisms generating storms while solely focusing on mean precipitation conditions. Instead, further research would need to examine local wind and precipitation patterns on daily timescales, focusing on afternoons when rainfall occurred in the south-eastern Serengeti and/or MGR. Ideally this would use a combination of ground-based observations and remotely sensed datasets.

2.4.6 Key Differences between Annual Cycles of Precipitation

Despite limits to our understanding of rainfall-generating processes in the south-east, we propose that interactions between tropical easterlies, topography and lake breeze westerlies can still explain key differences in the structure of annual cycles of precipitation. Cluster analysis identified these key differences as precipitation during January-February and June-September, the symmetry between rainfall peaks, and wet season peak months.

We suggest that rainfall totals during months that are dry across much of East Africa (January to February and June to October) depend on the presence of westerlies from Lake Victoria. This results in relatively high totals in the northwest during June to October, and the south-west during January and February.

Similarly, the relative symmetry between rainfall peaks depends on the availability of moisture from Lake Victoria. Regions that do not receive westerlies from Lake Victoria have less

symmetric annual cycles, similar to the rest of East Africa (Yang *et al.*, 2015). This asymmetry is amplified over topographic features with slopes facing the prevailing tropical easterlies during April.

The position of the tropical rainfall belt is the first order control on the distribution of peak rainfall months. However, the rift topography and lake breeze winds slightly augment the spatial distribution of November and December rainfall peaks. During November, monthly rainfall totals are higher to the west of the wind convergence line (compared to the east) due to storms generated at the lake front. Whereas in the north-east, the November peak is due to the orographic rainfall generated by the tropical easterlies meeting the rift topography. A rain shadow generated by the tropical easterlies hitting the rift topography also contributes to the December rainfall peak present in the lee of these highlands.

Similarly, the first order control on the spatial distribution of the March and April rainfall peaks is the northward progression of the tropical rainfall belt. However, in the south there is a clear difference in peak rainfall month between areas east and west of the rift topography. Norton-Griffiths *et al.* (1975) suggested that the lack of an April rainfall peak in the south-eastern Serengeti National Park was due to a rain shadow blocking the moisture from the Indian Ocean. However, our results show that high moisture levels and afternoon convergence are still present in the south-eastern Serengeti National Park during April, suggesting that lack of moisture is not the main reason for this decreased rainfall. We propose instead that the March rainfall peak is due to the Lake Victoria westerlies penetrating further south and enhancing rainfall in the southern Serengeti National Park during March. In April, the increased southerly component of the tropical easterly winds prevents moisture from Lake Victoria reaching this area. Simultaneously, exceptionally high rainfall totals are produced by orographic uplift on the south-facing rift topography during April. The combination of these features, results in a March rainfall peak in the southern Lake Victoria basin, and an April rainfall peak in the northern

basin, and along the rift topography. However, further analysis of the atmospheric conditions present over the southern wider Serengeti domain on wet days in March and April would be necessary to prove this hypothesis.

2.4.7 Rainfall Gradient over the Serengeti National Park

Overall, our results suggest that the rainfall gradient across the Serengeti is generated by interactions between tropical easterlies, lake breeze westerlies, and the rift topography. This is similar to the combination of factors suggested by Norton-Griffiths *et al.* (1975), who surmised that low rainfall totals were present in the south-east due to the rift's rain shadow, and high rainfall totals were generated in the north-west by the lake breeze winds, whilst the orientation of the rainfall gradient depended on the position of the tropical rainfall belt. Yet our analysis of hourly precipitation and reanalysis data (information not available in the 1970s) has demonstrated that the roles of these mesoscale features are more complex than originally suggested by Norton-Griffiths *et al.* (1975).

First, our results confirm the theory put forward by Norton-Griffiths *et al.* (1975), that the lake breeze is responsible for providing year-round rainfall in the north-west of the Serengeti National Park. Yet our results also show the importance of the lake westerlies to other parts of the park, as the seasonal presence of lake breeze westerlies in the southern Serengeti provide an important boost to local moisture and rainfall from October to March. Second, our results agree with Norton-Griffiths *et al.* (1975) that the topography generates a rain shadow in the eastern Serengeti National Park, blocking Indian Ocean moisture from reaching this area. However, we observed that the rift topography also traps moisture from Lake Victoria, encourages ascending atmospheric motion, and affects the position of the storm-generating lake breeze front. Third, Norton-Griffiths *et al.* (1975) identified that the seasonally changing gradient across the Serengeti is dependent on the position of the tropical rainfall belt. Our

results suggest that this is likely due to afternoon storms forming at the seasonally changing convergence line of lake breeze westerlies and tropical easterlies. These storms are then blown in the direction of the easterly winds, which also change direction on a seasonal basis.

2.5 Conclusions

Wildlife in the Serengeti National Park depends on rainfall. To understand past rainfall conditions, and predict future changes, it is essential to quantify the region's mean precipitation patterns, and identify the causal atmospheric processes. We found that the local rainfall is determined by interactions between Indian Ocean tropical easterlies, Lake Victoria daytime westerlies and the complex topography of the East African rift valley. The relative importance of the three key features depended on location, time of year, and time of day. The passage of the tropical rainfall belt is the first order determinant of seasonality, generating a dry season and double peaked wet season across the whole region. The topography augments lower tropospheric vertical motion through orographic channelling and solar heating of high ground, while orographic uplift generates topographic precipitation and rain shadows. Lake Victoria affects local rainfall through the seasonal provision of moist westerlies. Storms are likely generated at the lake front where these daytime westerlies meet the tropical easterlies, then are blown in the direction of the tropical easterlies, generating a seasonally changing rainfall gradient across the Serengeti National Park. Further research focusing on daily changes to the position of this wind convergence zone would likely improve our understanding of rainfall-generation over the south-eastern plains of the Serengeti. Overall, this study provides an updated understanding of the Serengeti's climate. In addition, by highlighting the importance of the topography and lake breeze winds, we show that research aiming to understand past or future changes to rainfall in this ecologically significant area, must consider the dominant roles of these key mesoscale features.

Chapter 3. Modelling Wildebeest Movement and Population Dynamics in the Face of Environmental Change

The wildebeest of the Serengeti Mara ecosystem are dependent on regional rainfall patterns that will likely be affected by climate change. To better understand how well we can model the impacts of changing rainfall, we manipulated the environmental input data of a model of wildebeest population dynamics and movement. The key results were: (1) Removal of interannual precipitation variability increased the population size, as the periodic occurrence of years with poor rainfall conditions (which lead to high mortality rates) cap population size. (2) Changing the spatial distribution of rainfall over the Serengeti did not stop the simulated migration, which could only be broken by removing all environmental gradients within the park. (3) Increased tree cover reduced population size by decreasing the amount of grass available; this in turn decreased wildebeest resilience to reduced dry season rainfall. (4) The precipitation conditions within an individual year to which the simulated wildebeest were most sensitive were annual rainfall, dry season rainfall, and rainfall over the south-east of the ecosystem. The final finding allowed us to classify rainfall conditions as beneficial or detrimental to modelled wildebeest survival. Key weaknesses within the model were identified, including the inability of the relationship between rainfall and grass growth to saturate. However, we concluded that the majority of the modelled wildebeest's responses to altered environmental conditions were plausible, suggesting that the model could be a useful tool for exploring the impact of climate change projections on the Serengeti wildebeest population.

3.1 Introduction

The Serengeti-Mara ecosystem (SME) is home to 1.3 million migratory blue wildebeest (*Connochaetes taurinus*) (G. Hopcraft 2020, personal communication, 11th August). Every year the herds travel around the ecosystem in a roughly triangular shape, calving in the south-eastern plains between January and March, swinging north-west into the Western Corridor in May-June, before reaching the northern highlands of the Mara between July and September (Hopcraft *et al.,* 2015). This dramatic ecological event is partially due the unique physical conditions of the SME. Countervailing nutritional and precipitation gradients across the ecosystem drive the wildebeest to migrate to the ephemeral, nutrient-rich grassland plains of the south-east during the wet season, and return to the wet, nutrient-poor, wooded savannah highlands of the north during the dry season (Holdo *et al.,* 2009b). The migratory strategy allows the population to escape limitation by predation (Sinclair, 2003). They are instead limited by food availability, which is in turn limited by dry season precipitation totals (Mduma *et al.,* 1999). Climate models suggest that rainfall in East Africa will change over the coming decades (Shongwe *et al.,* 2011; Niang *et al.,* 2014; Dosio *et al.,* 2019). It is therefore important to investigate the potential consequences of these changes for the wildebeest. Yet we first have to understand our ability to model the wildebeest's response to changing environmental conditions.

Attempts to model the changing rainfall in the SME must account for the spatial complexity of the regional rainfall patterns, which are often driven by relatively small atmospheric processes (Camberlin, 2018; Woodhams *et al.,* 2019). Past rainfall changes have not been uniform across the SME (Veldhuis *et al.,* 2019), and future changes may be similarly spatially heterogeneous. It can also be challenging to model the impacts of a changing climate on species which travel through regions with different climatic conditions on an annual basis (Robinson *et al.,* 2009).

It is not enough to simply measure the average change across the ecosystem, as the wildebeest spend only a fraction of their time each year in individual parts of the ecosystem, thus would likely be unaffected by precipitation changes in the rest of the year. Nor is it necessarily as simple as observing the typical movement patterns of the wildebeest, and extrapolating the impact of predicted precipitation changes along their standard route. Tropical ungulate migration is usually an adaptation to irregular rainfall (Owen-Smith and Ogutu, 2013). Therefore, any model attempting to assess the wildebeest's response to altered rainfall, must account for their capacity to adapt their movement patterns to compensate for environmental change.

An ideal model would be able to incorporate information about the spatial and temporal distributions of future rainfall, and the ability of the wildebeest to alter their movement patterns in response to these changes, while still being constrained by key biotic and abiotic conditions. With this criteria, we chose to investigate the Savannah Dynamics (SD) model (Holdo *et al.*, 2009b). The spatially explicit model is driven by multiple environmental layers including realistic monthly rainfall maps, incorporates fire, vegetation and herbivore dynamics, and allows the simulated wildebeest to move responsively around the ecosystem.

The model has already provided insight into how wildebeest may respond to wetter or drier futures, by driving the model with combinations of past years with above and below average annual rainfall respectively (Holdo *et al.*, 2010). However, we are interested in the suitability of driving the model with rainfall patterns that are distinctly different to what has been observed in the past, as this is what may be generated by climate models.

This study therefore aims to understand how and why the wildebeest simulated in the SD model respond to a spectrum of spatial and temporal rainfall conditions. We aim to classify how wildebeest population size will respond if driven by rainfall conditions with specific

characteristics, and consider the plausibility of these responses. Through this we aim to identify the strengths and weaknesses of the SD model if used in rainfall-focused climate change studies, and explore the impact of hypothetical changes to the rainfall conditions on the wildebeest of the Serengeti-Mara ecosystem.

In this study, section 3.2 contains a description of the SD model and an outline our experiments. Results are presented in Section 3.3, and address our aim to understand how and why modelled wildebeest respond to a spectrum of spatiotemporal rainfall conditions. In section 3.4 we discuss our key findings, including our proposed classification of how the modelled wildebeest population size responds to key spatiotemporal rainfall characteristics. We also consider the plausibility of the SD model's response by comparing our results to the literature. Through this we identify some of the models strengths and weaknesses, and reflect on how the wildebeest of the Serengeti-Mara ecosystem may respond to changing rainfall conditions in reality. Conclusions are summarised in section 3.5.

3.2 Methods

3.2.1 Model

The Savannah Dynamics (SD) model is an established model (Holdo *et al.*, 2009b) that simulates vegetation, fire, and herbivore dynamics. The SME is represented as a grid with 307 cells, each 10 km x 10 km (Figure A-1). The model has a lattice structure, with each variable represented as a layer on the grid. Environmental data are included in the model as realistic GIS layers, with nitrogen concentration, tree canopy cover and precipitation totals used as input layers. Nitrogen concentration and tree canopy cover are introduced as static variables at the beginning of a model run, and new static precipitation layers are called annually. Vegetation growth and decay is dependent on precipitation totals, fire, and grass consumption levels.

Rainfall conditions also control grass growth, grass decay, and the length of the growing season. The protein content of that vegetation depends on the soil nutrient concentrations. Wildebeest are able to move adaptively through the landscape in response to changes in resource availability, with their mortality rates tied to the quantity and quality of the available food. The SD model is described in detail in Holdo et al. (2009*a*) and Holdo et al. (2009*b*), and the key model equations are also summarised in Appendix A.

The original model code from Holdo et al. (2011) was written in Borland C, whereas the model runs in this experiment were carried out in C++ using CLion 2017.3.4. Therefore a small number of functions were translated from Borland C to C++. Figures were plotted using ggplot2 (Wickham, 2016) in R (R Core Team, 2019).

3.2.1.1 Environmental input layers

In the majority of the experiments carried out in this study, we alter the environmental layers used to drive the SD model. The motivation behind these alterations are explained in section 3.2.2.

Precipitation

The static rainfall input layers are made up of 12 sub-units corresponding to the months of the year, starting in November and finishing in the following October. We use the same rainfall layers as Holdo et al. (2009*b*). These were interpolated from rain gauge measurements taken between 1960 and 2006 (from 127 gauges spread over the SME) to make 47 rainfall layers. In many of the experiments, we use a rainfall climatology (Figure 3.1a), calculated by taking the mean monthly rainfall in each grid cell, using the precipitation recorded between 1961 and 1990. We also use a spatially averaged climatology (Figure 3.1b), where the climatological

rainfall for each month was spatially averaged, to create twelve spatially homogenous monthly maps of the Serengeti.

When elasticity analyses were performed, either the whole climatology, or individual months of the climatology, were altered by ± 5-20 %, by multiplying every cell in the precipitation matrix by 1 ± 0.05-0.2. When sensitivity analyses were performed, either the whole spatially averaged climatology, or just individual months of the spatially averaged climatology, had 0.5-20 mm month^{-1} added or subtracted to each grid cell.

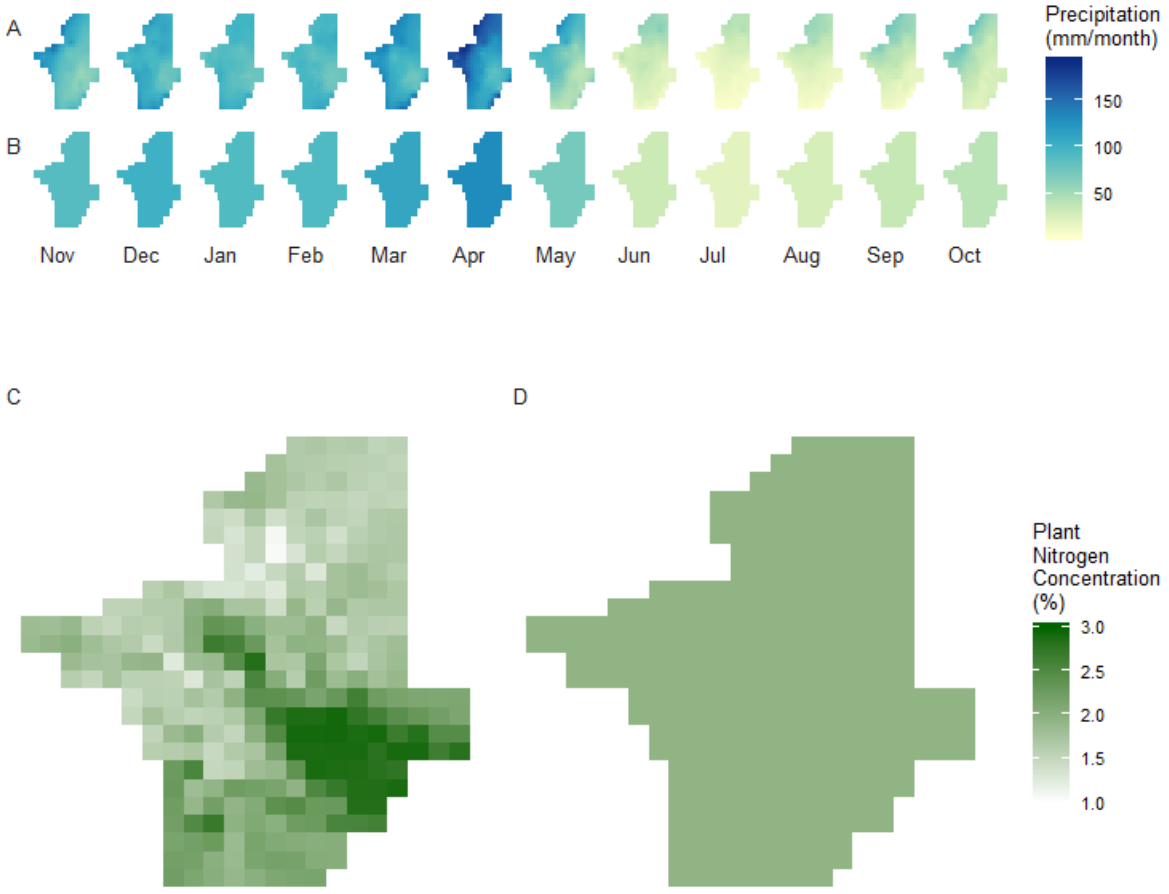

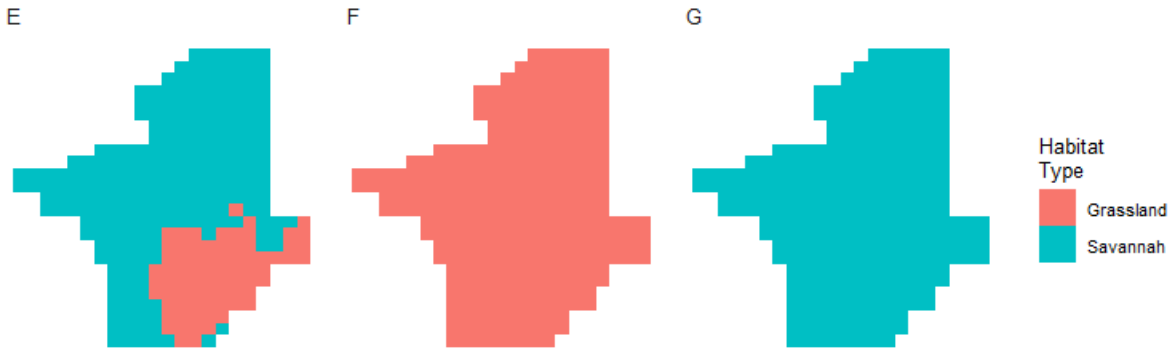

Figure 3.1: Environmental input layers used to drive SD model. (A) Unaltered climatological annual precipitation; (B) spatially averaged annual precipitation; (C) unaltered plant nitrogen concentration; (D) spatially averaged plant nitrogen concentration; (E) unaltered habitat classification map; and spatially homogenous habitat maps entirely composed of (F) grassland (0 % tree canopy coverage) or (F) savannah (36 % tree canopy coverage).

Nitrogen

Two different nitrogen layers were used in the model: unaltered and spatially averaged. The unaltered layer is the same one used in the original SD model (Holdo *et al.*, 2009b), derived from observations of plant nitrogen concentrations across the Serengeti (Figure 3.1c). The spatially averaged layer has identical values in each cell, calculated from the mean of all nitrogen concentrations in the unaltered nitrogen layer (Figure 3.1d).

Habitat type

In the SD model, two types of habitat are classified in the Serengeti region: grassland in the southeast and savannah throughout the rest of the region (Figure 3.1e). The habitat classification acts as a proxy tree canopy cover, with savannah cells contain 36 % tree canopy coverage, while in grassland cells there is 0 % tree canopy coverage. In certain model runs it was necessary to remove all of the environmental gradients from the region. As habitat is coded as a binary variable in the model, habitat maps composed entirely of grassland (Figure 3.1f) and savannah (Figure 3.1g) were used.

3.2.2 Experiments

We used the SD model to carry out six experiments. These were performed to meet the following research aims: (1) understand how and why the wildebeest simulated in the SD model respond to a spectrum of spatial and temporal rainfall conditions, and (2) classify how wildebeest population size will respond if driven by rainfall conditions with specific characteristics. The research objectives of each experiment are summarised in Table 3.1 below, and the reasoning behind each experiment is explained fully in the individual sub-sections below.

Table 3.1: Research objectives and names of the experiments carried out in this study

Experiment	Experiment Name	Research Objective
1	Removal of interannual variability	Test the impact of removing interannual rainfall variability on wildebeest population size.
2	Annual Precipitation Elasticity Analysis	Test the impact of changing annual precipitation totals (while maintaining the same annual cycle and spatial distribution) on wildebeest population size.
3	Removal of Environmental Gradients	Test the relative impacts of changing the spatial distribution of rainfall and other environmental layers driving the model (without altering the total rainfall received by the ecosystem) on wildebeest movement patterns and population size.
		Test the impact of increasing and decreasing tree cover on wildebeest population size.
4	Monthly Precipitation Elasticity Analysis	Test the impact of changing rainfall in individual months (while minimising the change to the spatial precipitation patterns) on wildebeest population size.
5	Monthly Precipitation Sensitivity Analysis	Test the impact of changing absolute rainfall totals in individual months on wildebeest population size.
6	Spectrum of Past Precipitation Conditions	Test the impact of a spectrum of spatiotemporal rainfall conditions (that have previously been observed over the Serengeti Mara ecosystem) on wildebeest population size.

It should be noted that although our experiments state an interest in the impact of changing environmental conditions on wildebeest population size, the set-up of the model runs mean that none of the experiments carried out in this study can provide realistic numerical predictions for

exact population size. Instead we seek to understand how various environmental conditions may be harmful or beneficial to the migratory wildebeest population, and how the dynamic processes within the SD model generate those changes. We are therefore using changes to the stable equilibrium population size of the simulated wildebeest as a proxy for how beneficial or harmful various environmental conditions may be, but not as a prediction of absolute population totals.

Similarly when we state an interest in the impact of changing environmental conditions on wildebeest movement patterns, this should be interpreted as an investigation into the representation of movement dynamics within the model, rather than a prediction of actual movement patterns.

Five of the experiments involved altering monthly precipitation totals by 0-20 % or 0-20 mm/month. These ranges were mainly chosen as they are comparable to future climate model projections under a high warming scenario. A recent review of precipitation projections over the African continent by Dosio *et al.* (2019) analysed 5 regional climate models (RCMs), driven by 23 general circulation models (GCMs) which were forced by the Representation Concentration Pathway 8.5. Over the area south-east of Lake Victoria (where the Serengeti National Park is situated) the projected RCM ensemble median showed a combination of projected increases, decreases, and uncertainty in mean seasonal rainfall change (although projected increases were most common). The largest projected changes to mean seasonal rainfall were in September to November and March to May. During March-May (the wettest season of the year), both regional and general circulation model ensemble medians suggested an increase in mean seasonal rainfall of between 0 and 0.5 mm/day, (although in some parts of the region the signal was uncertain). A change of 0.5 mm/day corresponds to 15-16.5 mm/month (depending whether a 30 or 31 day month is considered), totals that are approximately 10 % and 22 % of the respective 30-year mean April and May rainfall totals

averaged over the wider Serengeti domain (Chapter 2). Therefore it is sensible for us to look at both positive and negative changes to rainfall, and investigating a range of changes to rainfall between 0-20 % of current totals is consistent with potential changes suggested by climate models.

Similarly, changes of 15 mm/month are comparable to the range of totals examined in the sensitivity analysis in experiment 5 (±0-20 mm/month). However, in this experiment, the values were also capped by past dry season rainfall totals; mean past July rainfall spatially averaged across just the Serengeti-Mara ecosystem was 20 mm/month. As we wished to add and remove consistent rainfall amounts each month, 20 mm/month was the maximum amount we could subtract.

3.2.2.1 Experiment 1: Removal of Interannual Variability

Our study aimed to identify how the spatial and temporal precipitation conditions of an individual rainfall year impacted the simulated wildebeest's population size and movement patterns. For each model run, we allowed the SD model to run for multiple years to allow the population size to equilibrate. We also deemed it necessary to use the same rainfall conditions every year, to prevent the model from responding to a variety of rainfall conditions rather than just the ones we were testing. By using the same rainfall conditions each year, we removed the majority of environmental stochasticity from the model. As this stochastic element had been removed from the model, we decided to create a completely deterministic model by also removing the stochasticity from fire occurrence (the only other random variable in the model). This allowed us to test the impact of very slight changes to rainfall on the simulated wildebeest, and know that the resulting changes were entirely due to altered rainfall conditions (instead of stochastic processes within the model). (It should be noted that when we describe

environmental stochasticity in this paper, this terminology refers to the way the SD model represents environmental variability, even though this does not necessarily reflect reality.)

Evidently, the removal of environmental variation from an ecological model is not realistic. We deemed this acceptable as our key aim was to identify the relative (rather than absolute) impacts of different spatiotemporal rainfall conditions. Nonetheless we still needed to know how the removal of environmental stochasticity would affect the modelled wildebeest, both to recognise the magnitude of the impact of removing this element from the model, and to act as a baseline against which other model runs (without environmental stochasticity) could be compared. Therefore, in Experiment 1 we aimed to compare the ensemble mean of runs that included environmental stochasticity to a single deterministic model run driven by static, mean precipitation and fire conditions. First, the SD model was run 100 times with its original set up, which included stochastic fire frequency and randomly selected rainfall years, and from this the ensemble mean was calculated. Second, we removed all stochasticity from the model, by performing a single run with a constant fire frequency (50 %, instead of random values ranging from 0-100 %), and using the mean rainfall climatology to drive the model every year.

The remaining model runs in experiments 2-6 were deterministic single model runs, driven by constant rainfall conditions (the same rainfall file was called each year) and constant fire frequency (50 %).

3.2.2.2 Experiment 2: Annual Precipitation Elasticity Analysis

In Experiment 2 we aimed to test how wildebeest population size would be affected by changing annual rainfall totals. To do this, we carried out an elasticity analysis, as this allowed us to alter annual totals while maintaining the same annual cycle and spatial distribution of rainfall. We created six altered rainfall climatologies, by changing the rainfall totals in every

cell, in every month, by ± 5 %, ± 10 % and ± 20 %. The SD model was driven by these six altered rainfall climatologies.

3.2.2.3 Experiment 3: Removal of Environmental Gradients

In Experiment 3 we intended to test the impact of changing the spatial distribution of rainfall on wildebeest movement and population size. This was a complex task, as there are 307 grid cells within the SD model grid. In addition, in the SD model, rainfall impacts the vegetation dynamics of the Serengeti-Mara ecosystem, and thus the wildebeest, through interactions between rainfall totals (controlling the amount of grass that can grow), plant nitrogen concentrations (controlling the nutritional quality of the grass), and habitat classification (controlling the amount of space available for grass). Therefore any change to the spatial distribution of rainfall, would affect the interactions between these three environmental layers, each of which have spatial patterns of their own.

The complexity of the spatial patterns of these environmental layers, and the interactions between them, meant we decided the simplest way to examine the impact of altering the spatial distribution of rainfall was to examine the impact of spatially homogenising the three environmental layers. This would allow us to test:

1) The impact of changing the spatial distribution of rainfall (without altering the total rainfall received by the ecosystem) on wildebeest movement and population size.

2) The relative impact of altering the spatial distribution of the three environmental layers within the model on wildebeest population size.

3) The impact of removing environmental gradients on wildebeest movement patterns.

4) The impact of altering the tree canopy coverage within the ecosystem (as the binary savannah and grassland habitat layers contain different proportions of trees) on wildebeest population size.

To achieve this, we spatially homogenised the three key environmental layers in the model: precipitation, nitrogen concentration and habitat type (as shown in Figure 3.1). We then drove the model with eleven different combinations of the unaltered and spatially homogenous layers (Table 3.2).

Table 3.2: Combinations of spatially homogenous environmental layers used to drive SD model.

Number of spatially averaged features	Model run	Spatially Homogenous Features			
		Rainfall	Nitrogen	Habitat	
				Savannah	Grassland
0	0				
1	1	■			
	2		■		
	3			■	
	4				■
2	5	■	■		
	6	■		■	
	7	■			■
	8		■	■	
	9		■		■
3	10	■	■	■	
	11	■	■		■

This also laid the groundwork for the temporal sensitivity analysis of rainfall carried out in Experiment 5.

3.2.2.4 Experiment 4: Monthly Precipitation Elasticity Analysis

In Experiment 4 we intended to test the impact of changing the temporal distribution of rainfall on wildebeest population size, and chose to do this by performing a monthly elasticity analysis. The rainfall conditions used to drive the SD model are composed of 12 monthly rainfall maps, so the smallest temporal change we could investigate was the impact of changes to monthly rainfall totals. An elasticity analysis also allowed us to test the impact of changing rainfall in individual months on wildebeest population size, whilst minimising the change to the spatial distribution of precipitation. We created 72 altered versions of the rainfall climatology, where

the precipitation values of individual months were changed by ± 5 %, ± 10 % and ± 20 %. We then performed 72 model runs, with each one driven by one of the altered versions of the rainfall climatology.

3.2.2.5 Experiment 5: Monthly Precipitation Sensitivity Analysis

Experiment 5 had a similar aim to Experiment 4, as it also aimed to test the impact of changing the temporal distribution of rainfall on wildebeest population size. However, in this experiment we wished to examine the impact of changing rainfall totals by equal amounts in each cell and month of the year (a sensitivity analysis). To be able to subtract precipitation values that were significant compared to annual rainfall totals, from the driest parts of the ecosystem in the driest months of the year, it was necessary to use spatially averaged rainfall conditions. As the spatial characteristics of the rainfall were unrealistic, we also chose to use spatially averaged nitrogen and homogenous habitat layers, to eliminate potential interactions that could be caused by the discrepancy between the spatial patterns of the spatially averaged rainfall and the other environmental layers.

For every month, each grid cell in the spatially-averaged rainfall climatology was altered by ± 0.5, ± 1.0, ± 5.0, ± 10.0, ± 15.0 and ± 20.0 mm month^{-1} (72 altered rainfall climatologies). We then carried out 144 model runs, with each altered rainfall climatology used to drive the SD model in combination with the spatially averaged nitrogen, and one of the homogenous habitat layers (savannah or grassland).

3.2.2.6 Experiment 6: Spectrum of Past Precipitation Conditions

Experiment 6 aimed to test the impact of a spectrum of rainfall conditions (which have previously been observed over the SME) on wildebeest population size. The previous experiments were designed to identify the impact of changes to specific spatial and temporal

rainfall characteristics, but the rainfall used to drive the SD model was always a variant of the rainfall climatology. This experiment aimed to test if the relationships identified in the previous experiments held across a range of spatiotemporal rainfall conditions. Therefore SD model was driven by the same "rainfall year" each year, with 47 model runs corresponding to the 47 years between 1960 and 2006. The nitrogen and habitat layers were unaltered.

3.3 Results

3.3.1 Removal of Interannual Variability

Our first area of interest was the consequence of removing environmental stochasticity (Experiment 1). Figure 3.2 shows that the ensemble mean of 100 unaltered model runs (which acts as a control in Experiment 1) had a fluctuating, yet stable population size of approximately 1.2 million wildebeest. We then removed environmental stochasticity from the model, by driving the model with identical fire frequency (50 %) and rainfall conditions (climatological rainfall) each year. The removal of environmental stochasticity was beneficial to the modelled wildebeest, evidenced by the increase in population size from 1.2 million in the ensemble mean, to 2 million in the single model run driven by the mean rainfall climatology. Repeat runs of the model driven by constant rainfall and fire conditions gave identical results (not shown), demonstrating that all stochasticity had been successfully removed from the model. In an additional experiment (not shown) we drove the model 100 times with variable fire frequency and constant climatological rainfall, and found only a 3 % difference in final wildebeest population size between this ensemble mean and a single model run with a constant fire frequency. This illustrates that the increase in population size was due to the constant rainfall conditions, as opposed to the constant fire conditions.

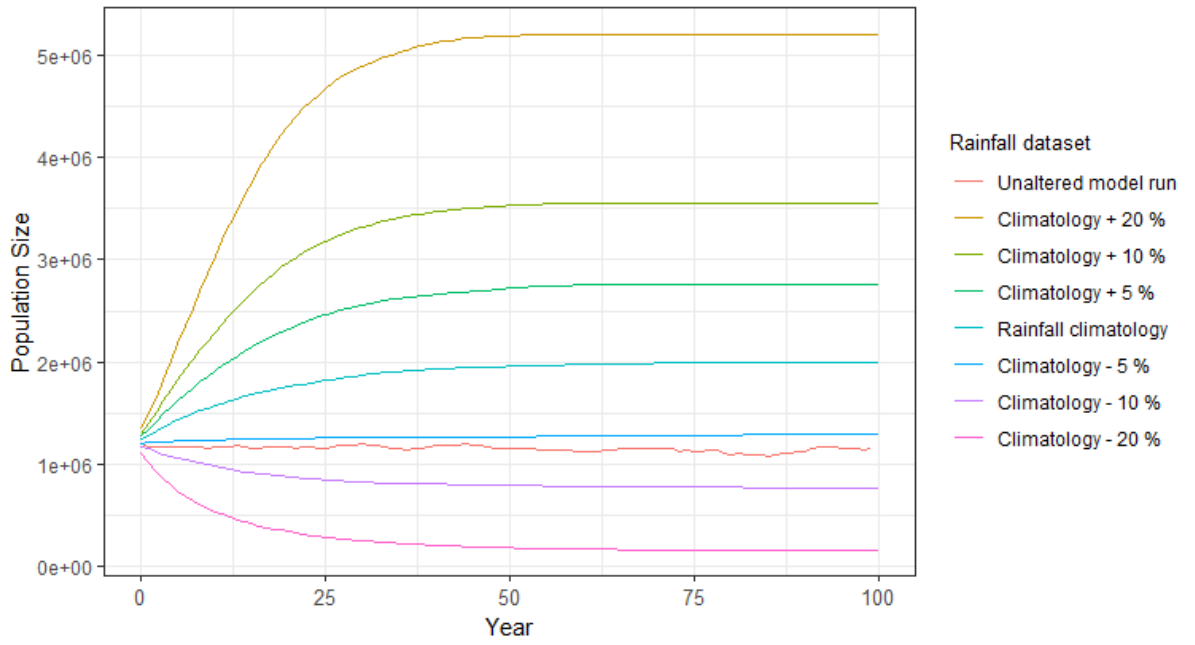

Figure 3.2: Modelled wildebeest population size driven by stochastic and non-stochastic rainfall conditions. The ensemble mean of unaltered model runs (labelled Unaltered Model Run) was calculated from 100 runs with the original model setup (random annual rainfall conditions and fire frequency). The remaining model runs were single runs, using a set fire frequency of 0.5, and driven repeatedly by the same rainfall conditions. These rainfall consisted of either the mean rainfall climatology (calculated from 1961 to 1990; labelled "Rainfall climatology"), or the mean rainfall climatology altered by ± 5-20 % (labelled "Climatology +/- n %").

3.3.2 Annual Precipitation Elasticity Analysis

We then investigated the impact of altering annual rainfall totals, without altering the spatial and temporal distribution of precipitation, by changing the annual rainfall climatology by ± 5-20 % (Experiment 2). The results in Figure 3.2 show that when the model is driven by constant environmental conditions, the population size gradually increased/decreased before reaching a new stable equilibrium within approximately 75 years. Amongst the model runs driven by altered rainfall climatologies, a clear positive relationship is present between annual precipitation and wildebeest population size. This relationship is non-linear, with a 20 % reduction in annual rainfall leading to a simulated final population size of approximately 160 000, while a rainfall increase of 20 % resulted in a final wildebeest population size of approximately 5.201 million individuals. These respective totals were approximately 1.846

million lower, and 3.195 million greater, than the 2.006 million wildebeest simulated as a response to the unaltered mean rainfall climatology.

3.3.3 Removal of Environmental Gradients

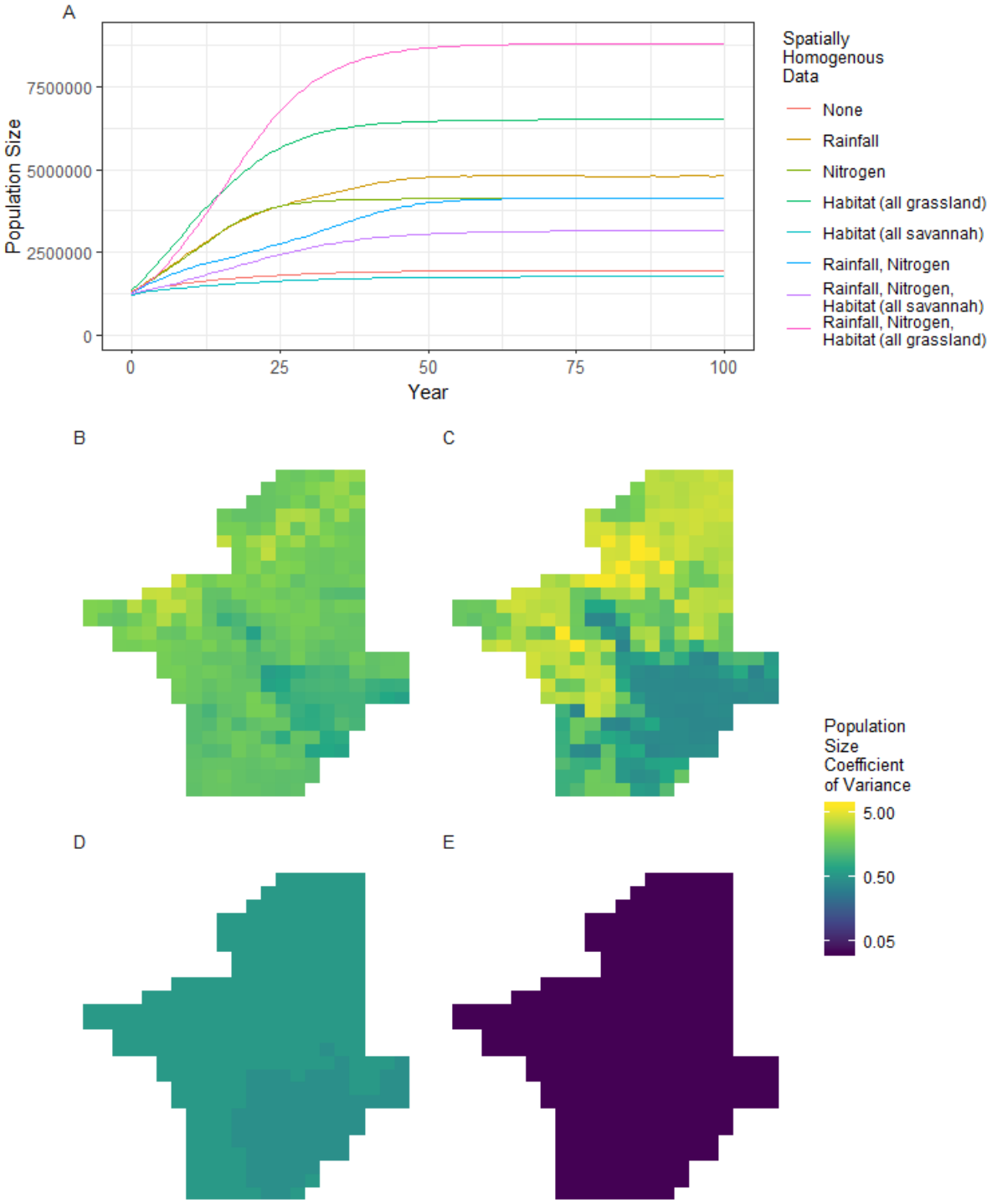

Figure 3.3: Impact of the removal of environmental gradients on modelled wildebeest (A) population size and (B)-(E) movement patterns. Environmental gradients were removed from the model by spatially averaging nitrogen and precipitation aross the whole region, while habitat type was changed to either 100 % savannah or 100 % grassland. (A) Population size response to removing 8 combinations environmental gradients (model runs 0-5,10 and 11). The impact on movement patterns is shown by the coefficient of variation, for runs with (B) 0; (C) 1; (D) 2; and (E) 3 environmental gradients removed. The environmental layers that were spatially homogenised in the model runs were (B) none (run 0); (C) rainfall (run 1); (D) rainfall and nitrogen (run 5); and (E) rainfall, nitrogen and habitat type (classified as 100 % savannah) (run 10).

We next chose to examine the effect of changing the spatial distribution of the rainfall, without altering rainfall totals, as well as the impact of these altered spatial rainfall patterns on the interactions between precipitation and other environmental variables. In Experiment 3, we spatially homogenised precipitation, nitrogen concentration and habitat type, and drove the model with different combinations of these spatially homogenous variables.

The results in Figure 3.3a show that the modelled population size is sensitive to altering the spatial distribution of all three environmental variables. Spatially averaging precipitation and nitrogen (separately) increased the final wildebeest population sizes to 4.9 million and 4 million respectively. However, spatially homogenising the habitat variables had the greatest range of results. When the entire ecosystem was classified as grassland and savannah, the modelled wildebeest population increased to 6.3 million, and decreased to 1.1 million, respectively. However, creating ecosystems with homogenous habitats required us to alter the amount of tree cover across the ecosystem. So the magnitude of these changes are likely due to the change in total tree cover, instead of solely the altered spatial distribution of habitat classification. All models driven by combinations of spatially homogenous features resulted in an increase in wildebeest population size, ranging from 3.1 million to 8.75 million. Overall this shows that an unaltered version of the model would be most sensitive to changes in precipitation over grid cells with high nutrient concentrations and low tree cover. It also shows that the population size of the modelled wildebeest is constrained by the mismatched spatial distribution of the environmental resources in the original model setup.

However, it is the mismatch between precipitation and nutrient concentrations that drives the migration of the wildebeest. We were therefore curious what impact removing the

countervailing environmental gradients would have on the modelled wildebeest movement patterns. Figure 3.3b-e shows the coefficient of variation (CoV) of four of the spatially averaged model runs, representing examples of movement within the model when 0-3 of the environmental variables were spatially homogenous. As the environmental spatial gradients were removed, the CoV changed from high across the whole ecosystem (illustrating variation in the amount of wildebeest in a cell throughout the year, due to their simulated seasonal movement), to lower CoV values in the south-east than the north-west (as many more simulated wildebeest remained in the south-east), until the removal of all three spatial gradients caused movement to cease (illustrated by uniformly low CoV across the whole ecosystem).

3.3.4 Monthly Precipitation Elasticity Analysis

We next wanted to test how the model responded to changes in rainfall during different months of the year, without altering the spatial distribution of rainfall. In Experiment 4, we carried out 72 model runs driven by climatological rainfall, with the rainfall totals of individual months of the mean rainfall climatology altered by ± 5-20 %. An unaltered climatological run is also displayed for reference. The elasticity analysis in Figure 3.4 shows that the positive relationship between annual rainfall and wildebeest population size is maintained, independent of the month in which the change in rainfall occurs. However, there is a clear distinction in the gradients of the lines in wet season months (November to May) and dry season months (June-October). Wildebeest numbers were most sensitive to changes in the precipitation totals of dry season months, even though the changes to total annual rainfall were smaller than in wet season months.

These results make it clear that the temporal distribution of rainfall does have an effect, even if the spatial patterns of rainfall remain the same.

3.3.5 Monthly Precipitation Sensitivity Analysis

We were next interested in altering rainfall in individual months by equal absolute amounts (rather than by percentage amounts). To do so, we drove the model with three spatially homogenous environmental variables (precipitation, nitrogen and habitat). This allowed us to subtract equal rainfall amounts from all cells (including cells in the south-east during the dry season), and avoid unintended interactions with other environmental features. In

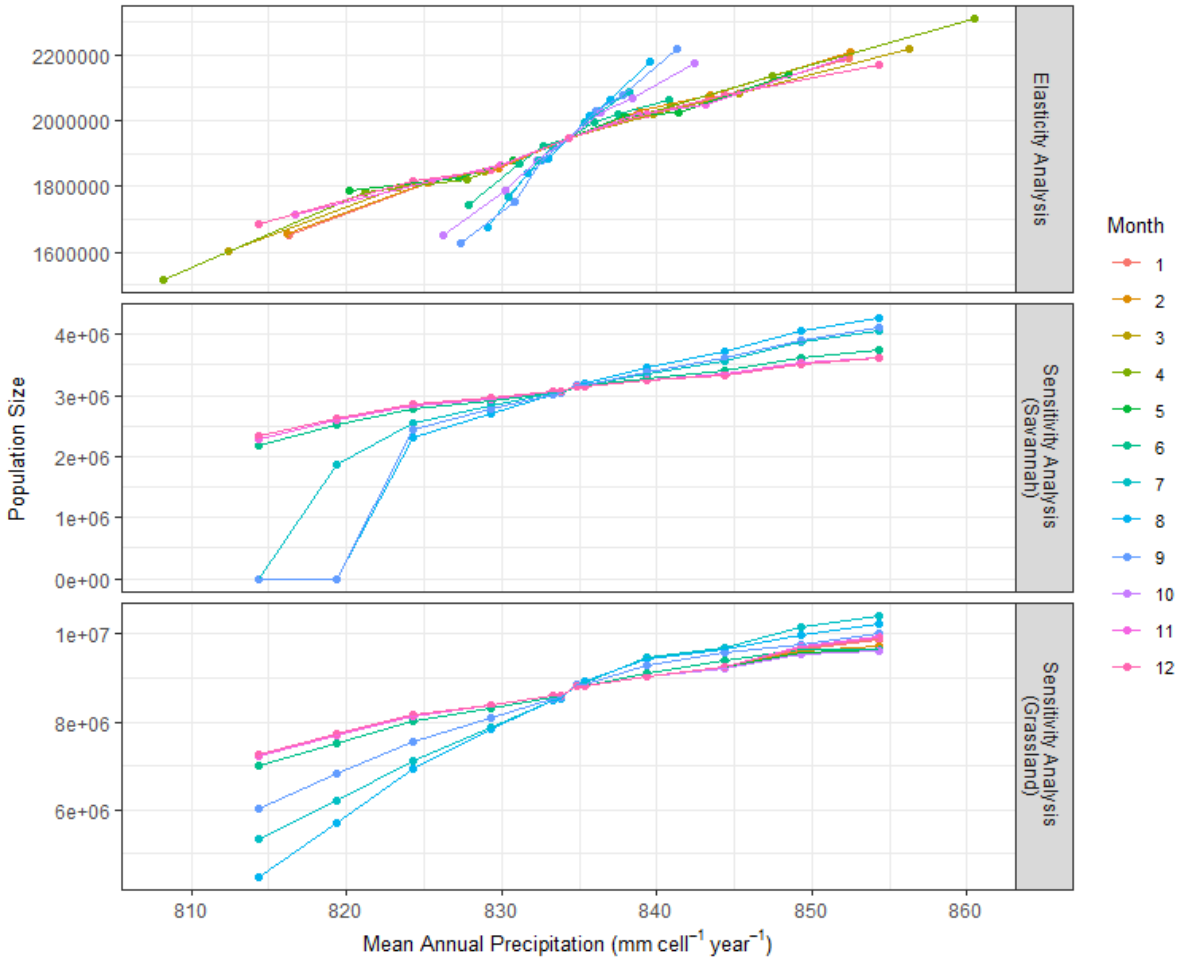

Figure 3.4: Response of modelled wildebeest to altered monthly precipitation totals. In the elasticity analysis, individual months of the mean rainfall climatology were altered by ± 5-20 %, and the predicted wildebeest population size is shown in relation mean ecosystem-wide annual rainfall. In the sensitivity analyses, the environmental layers driving the model (habitat type, nitrogen concentration and precipitation) were spatially homogenised. Individual months of the mean rainfall climatology were then altered by ± 0.5-20 mm month^{-1} cell^{-1}. The habitat layers used in the sensitivity analyses were classified as entirely savannah (36 % tree cover), or grassland (0 % tree cover). Note that y-axis totals differ between panels.

Experiment 5, we performed 144 model runs, with the spatially averaged rainfall totals of individual months altered by ± 0.5-20 mm month^{-1} cell^{-1}.

The sensitivity analyses in Figure 3.4 show that the positive relationship between annual rainfall and population size was still present in the spatially homogenous model runs. This relationship was asymmetric during the dry season, with the modelled wildebeest more sensitive to decreased precipitation. Under both habitat scenarios, the modelled population size had near identical responses to changing rainfall amounts from October to April, but stronger, unique responses to changes in the individual months of June to September (especially August). The results were similar to those of the elasticity analysis, with the exception of the months of October and May.

The negative effect of increased tree cover is also apparent from the lower population sizes, and increased sensitivity to fluctuations in dry season rainfall, in the savannah model run. When the whole ecosystem was classified as savannah, the highest simulated population size was just over 4 million, and a reduction of 15-20 mm month^{-1} in July, August and September rainfall caused the population to crash to zero. Whereas in the grassland scenario, the population didn't crash, and the simulated population sizes ranged from approximately 4.5 – 11.25 million.

3.3.6 Spectrum of Past Precipitation Conditions

The results of all the previous experiments suggest a strong model sensitivity to changes in annual rainfall, dry season rainfall, and rainfall over the south-eastern portion of the ecosystem (which has no tree cover and high nutrient concentrations). To check the stability of these relationships under a spectrum of rainfall conditions, we carried out 47 model runs, in each case driving the model with rainfall observed in an individual year between 1960 and 2006 (Experiment 6).

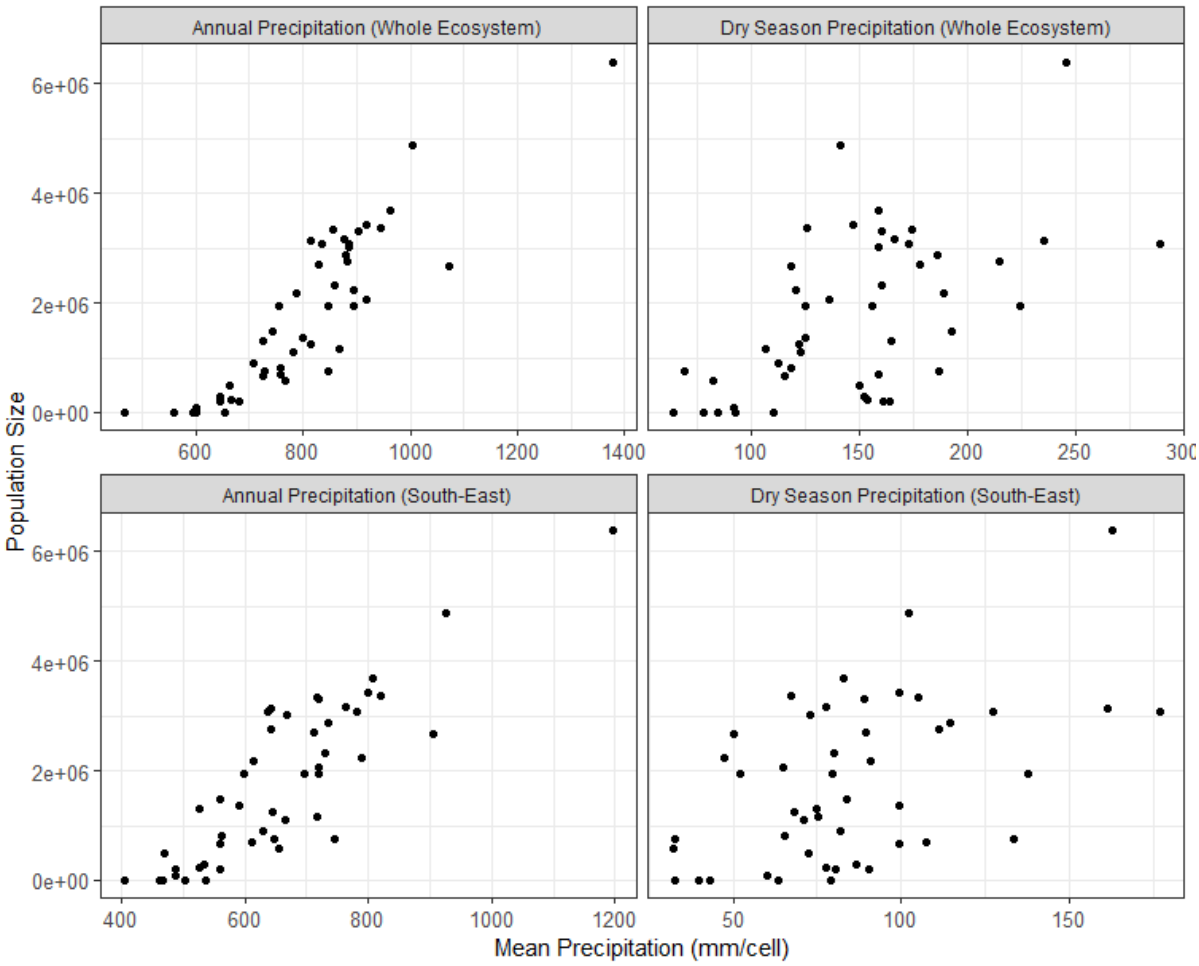

Figure 3.5: The relationship between predicted wildebeest stable population equilibrium size and precipitation (averaged across two temporal and spatial scales). Each of the 47 model runs was driven using the rainfall conditions recorded in a single year (1960-2006), and unaltered nitrogen and habitat classification layers. Ecosystem-wide rainfall was calculated across the whole region included in the SD model, while south-eastern rainfall was calculated across the area classified as grassland. Note that x-axis ranges differ between panels.

Figure 3.5 shows a positive relationship between all of the metrics and final wildebeest population size. However there is less variability in the relationship between annual rainfall and wildebeest population size, than dry season rainfall and modelled wildebeest population size. This likely reflects the fact that the variables are inter-related, as south-eastern rainfall contributes to ecosystem-wide rainfall, and dry season rainfall contributes to annual rainfall. In addition, dry season rainfall encompasses 5 months, so fluctuations in individual months could have an effect on the model, but not show up as a strong signal in the dry season sum.

Overall, we found that: (1) removing interannual precipitation variability increased the population size of modelled wildebeest. (2) The simulation of migration only stopped when

rainfall, habitat and nutrient gradients were removed. (3) Increased tree cover reduced population size, and decreased resilience to below average dry season rainfall totals. (4) The precipitation changes to which the model were most sensitive were annual rainfall, dry season rainfall, rainfall over regions with high nutrient concentrations, and rainfall over regions with low woodland cover.

3.4 Discussion

We were interested in the SD model's response to being driven by alternative rainfall regimes. To test this, we also had to examine the interactions between rainfall and other environmental conditions. Here we discuss the plausibility of our key findings, and whether they suggest that the SD model is a suitable tool to investigate the impact of future environmental change in the Serengeti.

3.4.1 Removal of Interannual Variability

Our first finding was that removing interannual variability in precipitation led to an increase in population size. It is commonly accepted in population modelling that reduced variability in resource availability, leads to an increase in population size (Lewontin and Cohen, 1969; Lande *et al.*, 2003). It was therefore an expected model response, and suggests the model has potential for examining the effect of altered precipitation variability. This is an important area of study, as climate models predict future changes to interannual precipitation variability across Africa (Niang *et al.*, 2014). However, we'd first recommend further assessment of the accuracy of the model's response to changing rainfall variability.

3.4.2 Response of Movement Patterns to Removal of Environmental Gradients

Our second key finding was that the model only ceased to generate movement across the ecosystem when all environmental gradients were removed. This shows that all three environmental layers within the model (tree cover, nitrogen and precipitation) contribute to successfully simulating the migration. It also suggests that as long as the basic structure of a wet and dry season is present, a feat achieved by the majority of coupled climate models (Dunning *et al.*, 2016), no rainfall scenario would stop the SD model simulating migration. In reality, the environmental gradients driving the migration are unlikely to disappear. The nutritional gradient is a result of volcanic activity that has been present for an estimated 370 000 years (Scoon, 2018). The gradient in tree canopy cover is partially due to the geology; a shallow hardpan layer in the south-east prevents tree roots from establishing (Sinclair, 1979c; Scoon, 2018) (although this environmental gradient is much more dynamic, as wildebeest grazing and elephant damage strongly impact tree recruitment (Holdo *et al.*, 2009a; Morrison *et al.*, 2016)). Meanwhile, the gradient in annual rainfall is caused by local topography and relative proximity to Lake Victoria (Norton-Griffiths *et al.*, 1975). This rainfall gradient would be unlikely to disappear unless Lake Victoria dried up completely, a scenario that has not occurred since the late Pleistocene Ice Ages (Scoon, 2018), and is not contemplated by current climate model projections (Vanderkelen *et al.*, 2018).

However, while these gradients are unlikely to disappear, they may weaken under elevated rainfall conditions. Ecosystem-wide increases to rainfall totals could alter soil properties (especially in the south-east); reducing their fertility through increased leaching, and potentially removing the calcite hard pan layer present in the south-eastern plains (Schlesinger and Bernhardt, 2013). This would allow woody encroachment further south-east. Higher

rainfall totals would also allow tree growth in areas previously limited by low rainfall totals (Sankaran *et al.*, 2005). An increase in woody plant cover could lead to a decline in grass productivity (Scholes and Archer, 1997), and thus wildebeest population size.

Nevertheless, the migration did still occur in the 1960s when the population size was much lower than it is today (Sinclair *et al.*, 2008). If the migration did not cease due to the population collapse caused by rinderpest, there is no reason to suspect that a decline in population size due to increased tree cover would cause the migration to cease. The migration is driven by opposing nutritional and precipitation gradients that stretch across the ecosystem (Holdo *et al.*, 2009b), and it can be argued that the drivers of the migration are likely to continue to exist (unless high rainfall totals cause catastrophic losses to soil fertility in the south-east). In addition, wildebeest move adaptively to respond to the favourability of conditions (Owen-Smith and Ogutu, 2013). Thus, as long as multiple aspects of the environment remain spatially heterogeneous, the wildebeest will continue to move (even if they don't migrate).

Overall, this means that the fact movement will always be simulated in the model (no matter what rainfall conditions are used to drive it) supports the argument that it is a useful tool for examining the impact of future rainfall changes on the wildebeest population. However, if tree recruitment dynamics (which are currently available in another version of the SD model (Holdo *et al.*, 2009a)) and soil dynamics (which not represented in any version of the SD model) were incorporated into the SD model, this would arguably improve the model's capacity to investigate the impact of future climate change on the SME and its wildebeest.

3.4.3 Interactions between Precipitation and Tree Cover

Our third key finding was that higher tree cover reduced the modelled wildebeest population size, and decreased their resilience to reductions in dry season rainfall totals. The model's negative relationship between tree cover and wildebeest population size reflects reality. A

negative relationship between grazer population size and woodland cover is a key feature of savannah dynamics (Eby et al., 2015). For wildebeest specifically, there is a greater threat from ambush predators in woodlands (Hopcraft et al., 2005), and graminoid species make up the majority of their diet (> 85 %) (Gagnon and Chew, 2000; Codron et al., 2009). However, the extreme sensitivity of the model to increased tree cover in combination with decreased dry season rainfall, was unexpected. It is difficult to assess the plausibility of this scenario, as a complete crash of the wildebeest population has never been observed (Mduma et al., 1999; Hopcraft et al., 2015). Similarly, the modelled ecosystem that caused the simulated population crash (one without the south-eastern grasslands), has also never been observed, due to the unique geology of the south-eastern SME preventing tree growth (Sinclair, 1979c). The spatially homogenous nutrient concentrations and precipitation in this model run were unrealistic, and the crash may be a synergistic effect of driving the model with multiple unrealistic environmental layers. It is therefore tempting to assume that this scenario is implausible and can be ignored. However, even if the south-east remains treeless, a net increase in tree cover across the ecosystem is possible. An increase in woody plant cover was observed in the Serengeti and Mara woodlands in the 1980s, largely due to the increase in wildebeest population size (Dublin *et al.*, 1990; Packer *et al.*, 2005). In addition, woodland cover has increased in savannahs across Africa (Venter et al., 2018). Regional changes in herbivory, fire, and direct anthropogenic disturbance have had the strongest local impacts, but the overall increase in woody plant cover has been exacerbated by warmer, wetter climates (Venter et al., 2018). As many climate model projections show East Africa becoming warmer and wetter (Dosio et al., 2019), but with reduced dry season rainfall (Patricola and Cook, 2011), it is essential to consider both the direct effect of altered rainfall, and the indirect effect of altered vegetation composition. Given the extreme population crashes shown in our results, we are uncertain about the suitability of using the SD model to simulate the impact of altered tree

canopy cover in conjunction with altered precipitation. However we wish to highlight this as an important area of future research.

3.4.4 Precipitation Characteristics of an Individual Year

Our fourth key finding outlined the rainfall conditions within an individual year, to which modelled wildebeest population size was most sensitive as: annual rainfall, dry season rainfall, and south-eastern rainfall. These metrics could be used to evaluate future rainfall conditions used to drive the SD model, and better interpret the model output. Here we discuss the plausibility of the model's response to these conditions.

3.4.4.1 Annual Precipitation Totals

The strong modelled relationship between annual rainfall and population size is logical, given wildebeest are limited by grass availability (Mduma *et al.*, 1999), and grass growth is limited by annual rainfall (McNaughton, 1985). Despite this, very few studies have investigated the impact of annual rainfall on African ungulate population dynamics. Instead studies typically examine the impact of wet and dry season rainfall separately (Sinclair, 1979b; Mduma *et al.*, 1999; Packer *et al.*, 2005). However, exceptions include Owen-Smith *et al.* (2005), Ogutu *et al.* (2008) and Ogutu *et al.* (2010). These studies typically found stronger relationships between monthly or seasonal (compared to annual) rainfall and ungulate population dynamics, and none included research into wildebeest. The lack of research into the relationship between wildebeest and annual rainfall suggests that the SD model may be oversensitive to the effects of annual rainfall.

Within the model, the strong relationship between annual rainfall and wildebeest population size is due to multiple equations describing: (1) positive sigmoidal and linear relationships between annual precipitation and grass growth, and (2) positive relationships between grass

growth and wildebeest survival. The grass growth equations were based on observations in the Serengeti, with annual rainfall totals between approximately 380 and 1000 mm $year^{-1}$ (3-year means) (McNaughton, 1985). However, there is no mechanism within the model to allow the linear relationships between annual rainfall and grass growth to saturate once outside of these bounds. Therefore, if climate model projections were used to drive the SD model, and those projections had annual rainfall totals that were much higher than the climatological average, this would result in potentially unrealistically large amounts of grass growth, and thus predict an unrealistically high wildebeest population size.

3.4.4.2 Monthly Precipitation Totals

Dry Season Months

On a monthly timescale, our study found that the modelled wildebeest were most sensitive to changes in precipitation during dry season months, a finding supported by the literature (Sinclair, 1979b; Mduma *et al.*, 1999; Packer *et al.*, 2005). In addition, Mduma et al. (1999) concluded that dry season rainfall was the most important extrinsic factor limiting total wildebeest population size. This contrasts with our results, which show a stronger relationship between annual rainfall and population size, compared to dry season rainfall and population size. This suggests that the model's response may be oversensitive to annual rainfall, and/or under-sensitive to dry season rainfall. However, this may also be due to different definitions of dry season rainfall, as Mduma et al. (1999) examined July-October rainfall averaged over the northern Serengeti, while our study examined June-October rainfall averaged across either the whole ecosystem or the south-east.

The modelled population size was most sensitive to precipitation changes in the individual months of June-October when environmental gradients were present, and June-September when environmental gradients were removed. This difference demonstrates that within the

model, the presence of opposing environmental pressures (nutrients, tree cover and rainfall) in October limits the spatial range of the wildebeest, and increases local density and mortality. The sensitivity of modelled population size to altered rainfall in the middle of the dry season (e.g. July), slightly contrasts with research that found the highest monthly mortality rates were at the end of the dry season in September-November (Mduma *et al.*, 1999). However, these high mortality rates were the result of multiple consecutive months of reduced rainfall. This is not a direct comparison to altering the rainfall in individual months, as we did in our study.

Nevertheless, it is important to consider whether the model is able to simulate multi-month droughts, as these have the highest impact on wildebeest survival. The model's strong sensitivity to altered rainfall in individual dry season months, suggests it would generate high mortality rates if driven by climate model projections that included multiple consecutive dry season months. However, the SD model equations cause the dry season to "end" at the beginning of every November, regardless of the monthly rainfall totals. This means that the model may struggle to capture the cumulative impact of multi-month reduced precipitation, if the drought continued past October into November and December.

Wet Season Months

Compared to dry season months, changes to precipitation totals in wet season months (November-May) resulted in small changes to modelled population size. This is supported by the literature, as a typical wet season receives sufficient rainfall to provide food for the entire wildebeest population (Mduma *et al.*, 1999). In addition, when precipitation totals in individual wet season months were altered, the modelled population size responses were similar. These near identical responses may be less realistic, as in reality, sub-sections of the population are more vulnerable to fluctuations in late wet season rainfall. The Serengeti wildebeest are highly synchronous breeders, and the vast majority of calves are born in February-March (Estes, 2014;

Hopcraft *et al.*, 2015). This means the period of highest nutritional stress for reproductively active females (20-30 % of the adult population) is March-May, coinciding with the period of peak lactation (Kreulen, 1975; Rysava *et al.*, 2016). Similarly, calves make up approximately 25 % of the population (Hopcraft et al. 2015), and are highly vulnerable during their first few months (Mduma *et al.*, 1999).

These altered vulnerabilities are not accounted for in the SD model, as it is unstructured with regards to age and sex, and has a constant birth rate (Pascual *et al.*, 1997; Holdo *et al.*, 2009a). This may not matter, as at a population level, adult survival has been the most important factor determining the rate of wildebeest population change (Mduma *et al.*, 1999), and the majority of adult males and non-pregnant females show the highest levels of nutritional stress during the dry season (Rysava *et al.*, 2016). However, we cannot be certain that this would remain the case under different environmental conditions, and the inclusion of non-uniform impacts of environmental conditions on different demographics can be essential for accurately capturing population dynamics in ungulate populations (Coulson *et al.*, 2001). Therefore, the increased sensitivity of calves and pregnant/lactating females to February-May rainfall should be considered when interpreting SD model outputs.

All Months

For the population as a whole, there are two main temporal periods of vulnerability; the end of the wet season from February-May (calves and mothers), and the dry season/beginning of the wet season from June-October/November (all wildebeest). The SD model correctly identifies the dry season as the period of greatest vulnerability for the whole population. Where it potentially fails is in not recognising the increased impact of altered rainfall in wet season months February-May and November. Therefore, if the SD model were driven with climate

model projections which had altered rainfall totals in these months, the model may underestimate the impact of this change on population survival.

3.4.4.3 Spatial Distribution of Rainfall

Spatially, the modelled wildebeest population size had the greatest sensitivity to altered rainfall over the south-east. In reality, this is the case during the wet season. Rain failure on the southern plains during the wet season is associated with high calf mortality, as the migratory wildebeest have to leave the plains. The inferior nutrient conditions in the north-west of the ecosystem mean that the females cannot sustain lactation (Murray, 1995), and the calves are more vulnerable to predation in wooded areas (Hopcraft *et al.*, 2005) such as the Maswa Game Reserve (which the herds use as a refuge if the rains fail during the wet season) (Sinclair *et al.*, 2015b). Conversely, dry season precipitation in the south can delay or reverse the herd's movement from the south-eastern plains, giving wildebeest prolonged access to nutritional food (Fryxell *et al.*, 2015).

However, there is a limited extent to which increased dry season rainfall in the southeast could translate into an increase in wildebeest population totals. The distance from Lake Victoria means that year-round rainfall is essentially impossible in the south-eastern Serengeti (Norton-Griffiths *et al.*, 1975). As there are no rivers in the southeast, permanent residency is also not possible due to the lack of a stable water source (Strauch, 2013; Hopcraft *et al.*, 2015). Therefore, while it is sensible that the SD model shows increased sensitivity to rainfall over this area, caution should be taken if a large increase in simulated wildebeest resulted from driving the model with rainfall scenarios with dramatically increased precipitation over the south-east during dry season months.

3.4.5 Model Limitations and Potential Improvements

Finally, we wish to highlight areas which we have not assessed, as they are not part of the SD model's structure. These limitations should be considered when interpreting output from this version of SD model. We also suggest avenues of future research, outlining how the SD model could potentially be developed to include these factors.

The SD model is not able to capture sub-monthly changes to rainfall. However, there is strong agreement that the intensity of hourly and daily precipitation will change in the future (Dosio *et al.*, 2019; Kendon *et al.*, 2019). Future changes to daily precipitation may change precipitation-vegetation dynamics (Xu *et al.*, 2015), and/or saturate the linear relationship between daily rainfall and grass growth rate within the SD model. We therefore wish to highlight this as an issue which may affect the ecosystem in the future, and warrants further research.

Representing rainfall as a process updated on a daily basis, instead of inputting monthly values, could be addressed by altering the model code. An amendment to the model code to change the start of the wet season to the first day that rainfall over a certain threshold occurred, rather than the 1st of November, could also allow droughts to be better represented. However, further work should first test whether these changes cause errors within the model, or resulted in unrealistic processes being simulated.

Changes to the relationship between rainfall and grass growth would be harder to code into the model, as the current equations are based on work carried out by McNaughton (1985) in areas that received annual rainfall totals between 300 and 1100 mm/year of annual rainfall. Amending the mathematical relationships between precipitation and grass growth in the model code would be simple. However, further empirical research would need to be carried out to determine the potential impact of higher annual totals, and whether the relationship between

grass growth and daily precipitation totals remained the same if daily totals increased in intensity or became more variable.

Plant nutrient concentrations are not able to change in the model as they are represented as a static layer within the model. However, plant nutrient content is known to change based on many factors, including species community composition, fire, water availability and soil nutrient concentrations (Anderson *et al.*, 2008); factors could be affected by climate change. For example, increased rainfall may cause soil leaching; reducing the fertility of the soils or preventing the formation of caliche (Sinclair *et al.*, 2008; Schlesinger and Bernhardt, 2013) (Schlesinger and Bernhardt, 2013). Further research is needed into how changing rainfall patterns may affect plant nutrient and soil dynamics in the SME; therefore including these dynamics into the model would be a complex task (one that is not necessarily possible based on our current understanding of the quantitative relationships between vegetation-soil-nutrient dynamics). However, if they could be modelled and incorporated into the SD model, it would provide a valuable tool to examine the long-term dynamic changes that may occur due to climate change.

As stated in section 3.4.4.2 the SD model is unstructured and currently represents birth rate as constant. However, this was based on research by Pascual *et al.* (1997) who also investigated age-structured models and found that they fitted wildebeest census data equally well. Therefore, future research could investigate whether the SD model could be made more sensitive to changes in recruitment, and thus potentially more suitable for climate change impact studies, by including demographic age classes, sex, and a synchronous birth rate.

This version of the SD model also relies on grass availability as the sole determinant of wildebeest mortality, but this does not account for the contribution of other factors. Individually, the effects of mass drowning (Subalusky *et al.*, 2017), predation (Sinclair, 2003),

hunting (Rentsch and Packer, 2015), competition with livestock (Veldhuis *et al.*, 2019), and interactions with other herbivores (Sinclair, 1979a), are of less importance to wildebeest population mortality rate than food availability (Mduma *et al.*, 1999). However, in reality they have a significant cumulative effect, and their impact on the wildebeest may change in the future. The SD model has previously been adapted to include the influence of elephants (Holdo *et al.*, 2009a), tree-grass feedbacks (Holdo *et al.*, 2009a), and human activities (Holdo *et al.*, 2010). Therefore, depending on the question that is being asked, uncaptured factors should be considered when interpreting any SD model output driven by future climate model projections, or an altered version of the SD model should be used if appropriate.

Finally, it should be noted that a number of features that are important to wildebeest behaviour and movement patterns (such as memory and social interactions) cannot be included in the SD model, as it does not represent wildebeest as individuals. Therefore, for research explicitly interested in the impact of climate change on wildebeest behaviour and movement, the development of novel agent-based models may be a more suitable option (Tang and Bennett, 2010; DeAngelis and Diaz, 2019).

3.5 Conclusions

We assessed whether the SD model responds in a plausible manner to altered rainfall and environmental conditions. Our results showed that (1) removing interannual precipitation variability increased population size. (2) Cessation of simulated migration only occurred when rainfall, habitat and nutrient gradients were eliminated. (3) Increased tree cover lowered population size, and decreased resilience to lowered dry season rainfall totals. (4) The precipitation changes to which the modelled wildebeest were most sensitive were annual rainfall, dry season rainfall, and rainfall over the south-east (the area with the highest nutrient concentrations and lowest woodland cover). The first finding was in agreement with the

literature, while the ecological relationships behind the second and third relationships were plausible. However, the severity of the population crash observed when the model was driven by reduced dry season rainfall and increased tree cover, meant we were unsure whether the model was suitable for studying the impact of altered rainfall in conjunction with altered tree canopy cover. For the fourth finding, we found that the model may be oversensitive to annual rainfall, and this combined with uncapped linear relationships between annual rainfall and grass growth, means the model may generate unrealistically high numbers of wildebeest if it were driven by exceptionally high annual rainfall totals. The model accurately captured an increased sensitivity to dry season rainfall, but is not be able to capture the increased vulnerability of calves during February to May, and of the whole population to reduced November rainfall at the end of the dry season. The increased sensitivity to rainfall over the south-east is realistic during the wet season, but not necessarily as accurate during the late dry season. Finally the model is unable to capture changes to sub-monthly rainfall, and certain ecological and human risk factors, which may impact the future ecosystem. Overall, the majority of the modelled wildebeest's responses to altered environmental conditions are plausible, and suggests that as long as these caveats are considered, the model could be a useful tool for exploring the impact of climate change on the Serengeti wildebeest population.

Chapter 4. Modelling the Impact of Future Changes to Mean Precipitation on the Survival Rates of the Serengeti-Mara Wildebeest

The migratory wildebeest of the Serengeti-Mara ecosystem (SME) depend on specific precipitation patterns, making them vulnerable to climate change. To explore the impact of changes to mean precipitation on the wildebeest, we evaluated precipitation conditions over the SME in a newly-available convection-permitting climate model (CP4-Africa). We then drove a mechanistic ecological model of wildebeest and savannah dynamics (SD model), with observed, modelled past, and modelled future mean precipitation.

The CP4-Africa hindcast captured the annual cycle and meridional component of a precipitation gradient over the SME, however precipitation totals were too high over highlands to the east of the SME and too low over Lake Victoria's shoreline. March late afternoon lake breeze winds were too strong over the SME, and their convergence over the highlands coincided with anomalously high local precipitation totals. The CP4-Africa model also had a wet annual precipitation bias due to unrealistically high totals simulated from November through April.

Annual precipitation is projected to increase across the SME and Lake Victoria basin by the end of the 21st century. A net increase occurred over the SME in every month except August. A drying signal was observed over the Kenya Highlands during July and August. The wetting and drying signals over the SME in March and August respectively were associated with southerly wind anomalies over the Lake Victoria basin.

The SD model runs found the most beneficial mean precipitation conditions for wildebeest survival and population growth were those in the future climate projection. Through most of

the year, simulated wildebeest death rates were lower in the SD model run driven by the CP4-Africa future projection than in the SD model driven by the CP4-Africa hindcast. The exception was during August, when a projected future decrease in August precipitation led to higher death rates.

The results from this climate model run suggest climate change may lead to a mean precipitation state that would benefit SME wildebeest. However, decreased dry season precipitation to the north may increase competition from livestock and wildlife, and changes to precipitation variability may undermine this beneficial mean state.

4.1 Introduction

The Serengeti-Mara ecosystem (SME) is home to the iconic annual wildebeest migration. Every year 1.3 million individuals travel hundreds of kilometres around a network of protected areas (Thirgood *et al.*, 2004; G. Hopcraft 2020, personal communication, 11th August), shaping an entire ecosystem in their perpetual quest for fresh grazing (Hopcraft *et al.*, 2015). This migration is intricately linked to the local precipitation conditions; partially driving wildebeest movement patterns (Holdo *et al.*, 2009b) and regulating their population size (Mduma *et al.*, 1999). However, climate change is predicted to alter precipitation patterns across the globe (Collins *et al.*, 2013; Kirtman *et al.*, 2013), including over East Africa (Niang *et al.*, 2014). It is therefore important to consider how the wildebeest of the SME may be impacted by future precipitation conditions.

Modelling the impact of climate change on migratory species is a complex task (Robinson *et al.*, 2009). Approaches such as ecological niche modelling are challenging to apply to species that move through climatically distinct regions on a seasonal basis (Sinclair *et al.*, 2010). While the role wildebeest hold as keystone species mean that changes to their numbers and movement patterns impact the SME and generate feedbacks (Sinclair *et al.*, 2008; Eby *et al.*, 2015). A

mechanistic model developed by Holdo et al. (2009b) that is able to represent wildebeest movement and their role in SME dynamics, is therefore a promising tool. Previous work has used this Savannah Dynamics (SD) model to explore the impact of altered precipitation on wildebeest population size (Holdo *et al.*, 2010). However, their study used combinations of wet and dry years previously recorded over the SME rather than climate model output.

This is understandable given the challenges involved in plausibly modelling the climate of the SME. SME precipitation is strongly influenced by relatively small-scale atmospheric processes such as lake breeze winds, orography-induced rain shadows, and anabatic/katabatic flows (Norton-Griffiths *et al.*, 1975; Woodhams *et al.*, 2019). We chose to use a newly available high resolution model that has been run across the whole African continent (CP4-Africa) (Stratton *et al.*, 2018) in this study. Convection-permitting (CP) models (< 5 km grid spacing) have been shown to add value over mountainous regions (Prein *et al.*, 2015), and the CP4-Africa model is able to simulate key mesoscale atmospheric processes over the Lake Victoria basin (Finney *et al.*, 2019).

Even at this high resolution, it is not guaranteed that this model will be able to simulate characteristics such as the precipitation gradient across the SME, which is of crucial importance to the wildebeest (Holdo *et al.*, 2009b) but is a result of a set of complex interactions between mesoscale atmospheric processes (Chapter 2; Norton-Griffiths *et al.*, 1975). It is therefore necessary to evaluate the performance of this model, to determine whether the future projection is suitable for an ecological application. Given the complexity of this task, we chose to focus solely on the impact of changes to mean monthly precipitation and exclude investigation of changes to interannual variability.

In this study, we evaluate the ability of the CP4-Africa climate model to capture precipitation and wind patterns over the SME; examine future changes to regional precipitation and wind

patterns; drive the SD model with observed, modelled past, and modelled future precipitation conditions; and report the modelled response of wildebeest to these precipitation scenarios, as well as its dynamical causes. Through this work, we aim to understand how mean precipitation conditions may change over the SME in the future, the plausibility of these projected changes, and the impact they may have on the migratory wildebeest of the SME.

4.2 Methods

4.2.1 Savannah Dynamics Model

The Savannah Dynamics (SD) Model is an established spatially explicit model which simulates vegetation, fire, and herbivore dynamics in savannah ecosystems, and is driven by spatially realistic precipitation and nitrogen concentration patterns across the ecosystem. It has successfully simulated the annual movement of wildebeest herds around the SME (Holdo *et al.*, 2009b), and was previously used to model the impact of anthropogenic activities on wildebeest population size (Holdo *et al.*, 2010, 2011a). The model represents the SME as a multi-layered grid of 307 cells with a 10 km resolution. Habitat is classified by vegetation type, with grassland (0 % tree cover) in the southeast, and savannah (36 % tree cover) throughout the rest of the region. Vegetation growth and decay is dependent on precipitation totals, fire, and grass consumption levels, while the protein content of the vegetation depends on nitrogen concentrations. Wildebeest are able to move adaptively through the landscape in response to changes in vegetation availability, with their mortality rates tied to the quantity and quality of available food. Calculations governing vegetation and population dynamics occur daily, wildebeest movement is updated weekly, and a new precipitation map is input monthly.

Three key equations determining wildebeest movement and population dynamics are shown below. The amount of grass consumed by wildebeest is dependent on the amount of green and dry grass available in the cell. If there is an abundance of grass available, then the intake value is set to an estimate of the wildebeest's maximum daily voluntary intake of green grass.

Equation 1

$$I_G = min\left(DVI_G, \frac{\alpha_W G}{\beta_W + G + D}\right)$$

I_G = per capita intake of G (kg day^{-1})

DVI_G = 5.4 g ha m^{-2} day^{-1} = wildebeest maximum daily voluntary intake of G

α_W = 10.5 g ha m^{-2} day^{-1} = maximum wildebeest cropping rate

β_w = 9.9 g m^{-2} = biomass at which wildebeest intake is 50 % of maximum

G = Green grass (g m^{-1})

D = Dry grass (g m^{-1})

The resource availability in cells is dependent on the proportion of the cell on which grass can grow, the amount of green grass available for consumption, and the nutrient density of the green grass.

Equation 2

$$Z = gI_G N^q$$

Z = Resource availability

g = Proportion of cell that is occupied by grass versus trees, rocks, bare ground, etc.

I_G = per capita intake of green grass

N = Plant nitrogen content (%)

q = 3.15 = Habitat preference parameter

The change in wildebeest density in a cell is dependent on ratio between birth and death rate, and the movement in and out of the cell. All three components are dependent on the resource availability in an individual cell, while the immigration and emigration is also dependent on the resources in the cells surrounding it.

Equation 3

$$\Delta W = (b_w - m_w e^{-a_w Z})W - \Theta + \Omega$$

b_w = 0.00049 = Wildebeest birth rate

m_w = 0.0032 = Maximum wildebeest mortality rate

a_w = 0.24 = Conversion of food intake to energy for wildebeest

Θ = Emigration of wildebeest to other cells

Ω = Immigration of wildebeest into cell

We outline other key model equations in Appendix A, and a full description of the SD model is in Holdo et al. (2009).

4.2.1.1 Model Adjustments

The model code used in these experiments was recoded from Holdo et al. (2011) into C++. In the default model settings, rainfall conditions are called randomly each year to simulate interannual variability. However, we decided this would be unsuitable for this study for two reasons. First, chapter 3 examined the impact of altered mean precipitation conditions on wildebeest population size, but did not investigate the impact of altered variability of rainfall. Therefore if we included stochasticity of precipitation in this set of model runs, we would not necessarily be able to differentiate between the effects of altered mean conditions and altered interannual variability. Second, the CP4-Africa climate model used in this study is not ideal for the study of projected future changes to interannual variability. Lake Victoria has a strong impact on the local precipitation conditions (Chapter 2), but in the hindcast the lake surface temperatures are represented by a climatology and do not include interannual variability (Stratton *et al.*, 2018). In addition the CP4-Africa future projection was only run for 10 years, and therefore contains less representation of interannual variability than the 30 years typically recommended to calculate a climatological normal (WMO, 2017). Therefore three adjustments were made to eliminate internal stochasticity and highlight the wildebeest response to different mean precipitation climatologies: (1) The model was run for 200 years (instead of 100 years) to allow the population size to stabilise. (2) The probability of fire occurrence was set to a constant rate of 50 %, instead of yearly random values of 0-100 % (this was shown to have a

minimal effect on final wildebeest population size in Chapter 3). (3) Interannual variability of precipitation was removed by using the same precipitation conditions to drive the model every year.

4.2.1.2 Displaying Savannah Dynamics Model Output

The population size and death rate of the simulated wildebeest was recorded on daily time steps for the whole 200 years of each model run. However the data are displayed as annual population size counts (taken on the last day of each year), stable population equilibrium sizes (mean of final 50 years of annual counts), and mean daily population size and death rate (daily averages over the final 50 years of each model run). In section 3.2.3 mean daily population sizes were normalised to allow comparison between model runs, using the equation:

$$\frac{x_i - x_{min}}{x_{max} - x_{min}}$$

x_i = daily population size

Spatially averaged precipitation data is either calculated over the SME (the area covered by all 307 SD model grid cells) or the south-east (75 grid cells within the SD model classified as grassland).

4.2.2 Climate Datasets

We drove the SD model with precipitation data from two sources: CHIRPS data and CP4-Africa climate model output. Wind vectors from the CP4-Africa hindcast were also compared to wind vectors from the ERA5 reanalysis dataset, to evaluate the plausibility of the CP4-Africa atmospheric dynamics, and thus rainfall values.

4.2.2.1 CHIRPS v2.0

The Climate Hazards Group InfraRed Precipitation with Stations dataset (CHIRPS v2.0) provides daily precipitation estimates at 0.05° resolution between 1981 and 2017, based on blended station and satellite data (Funk *et al.*, 2015). It was chosen due it's high spatial resolution and proven performance over East Africa (Dinku *et al.*, 2018). Climatological means were calculated using data from 1997-2006, to match the time period modelled by the CP4-Africa hindcast. When being used to drive the SD model, CHIRPS values were linearly interpolated to fit the SD model's 10 km grid.

4.2.2.2 ERA5

Wind data from the ERA5 reanalysis dataset was chosen due to its high spatial resolution (0.25°) (Copernicus Climate Change Service (C3S), 2017) and use in past work investigating topographically complex regions of East Africa (Chapter 2; Vizy and Cook, 2019). Climatological means were calculated (1997-2006) from monthly horizontal wind vectors (18:00 and 21:00 East Africa Time (EAT), 700 and 800 hPa).

4.2.2.3 CP4-Africa Hindcast and Future Projection

The CP4-Africa model is the Met Office Unified Model run at convection permitting resolution over a pan-African domain (39°N – 45°S, 25°W – 56°E) (Stratton *et al.*, 2018). The horizontal grid spacing is 4.5 km at the equator (0.0405°) with 80 levels up to 38.5 km allowing simulation of deep convection (Stratton *et al.*, 2018). 3-hourly lateral boundary conditions are provided to the regional model (a climate model covering a limited spatial domain) by a 30-year global model run (a climate model run across the whole globe) of the UM Global Atmosphere/Land 7.0 (GA7/GL7) (Walters *et al.*, 2019). The regional hindcast was run for 10 years and 2 months (January 1997 - February 2007) including 2 months of spin-up. The global model hindcast was

run from 1988-2010, driven by daily sea surface temperature (SST) analyses from a 0.25^{o} grid (Reynolds *et al.*, 2007). Only values from 1997-2007 were used to drive the regional model. The future climate simulation was run for a 10 year period around 2100, for the IPCC Representative Concentration Pathway 8.5 (RCP8.5) climate change scenario. RCP8.5 models the potential impacts of climate change under a high emissions scenario. The climatological change in sea surface temperatures was calculated from a coupled climate model (HadGEM2-ES) between 1975-2005 and 2085-2115 RCP8.5 run. This change was added to the daily SST analyses used to drive the hindcast model. Lake surface temperatures in the regional model are represented as inland sea grid cells. In the hindcast, climatological monthly lake surface temperatures are calculated from the ARC-Lake, version 3, dataset (Hook *et al.*, 2012; MacCallum and Merchant, 2012) from 1995-2012. Stratton *et al.* (2018) do not provide a justification for their choice to calculate lake surface temperatures over 1995-2012 instead of 1997-2007 (the time period over which the CP4-Africa model was run). The ARC-Lake v3 dataset spans the years 1995 to 2012 (University of Reading, no date), so the lake surface temperature climatologies were clearly calculated from the maximum number of years possible, instead of the years that corresponded to the CP4-Africa hindcast run. Future lake surface temperatures are calculated from the change in lake surface temperatures between past and future climate model runs, and adding this to the ARC-Lake lake surface temperatures used in the hindcast model run. Full details of the hindcast model run can be found in Stratton *et al.* (2018), and the future model run in Kendon *et al.* (2019).

The CP4-Africa model was chosen for its capacity to simulate mesoscale atmospheric processes and the fact that the hindcast compared well to observations over the eastern Lake Victoria basin (Finney *et al.*, 2019). Climatological means were calculated from the 10 years of data in each model run. To drive the SD model, CP4-Africa output was linearly interpolated to 10 km grid spacing.

4.3 Results

To understand the potential impact of future changes to mean precipitation on the wildebeest of the SME, we examined the modelled regional precipitation patterns and the modelled wildebeest response. Section 4.3.1 contains comparisons between observed, modelled past, and modelled future atmospheric conditions. Section 4.3.2 shows the results of driving the SD model with observed and modelled precipitation, and the ecological model dynamics causing these responses.

4.3.1 Observed and Modelled Atmospheric Conditions

4.3.1.1 Annual Cycle of Precipitation

The annual cycle of precipitation is a key driver of the migration of the wildebeest around the SME. We therefore examined the representation of seasonality in the observed and modelled datasets. Figure 4.1 shows the annual cycle of precipitation averaged across the whole SME (top) and its south-eastern portion (bottom) during the years 1997-2006 (the time period covered by the CP4-Africa hindcast). The CHIRPS observations show the SME had a wet season from November to May with peaks in December and March/April, and a dry season from June to October. The south-east had a long rains peak in March, while the SME average had an April peak. Monthly and annual totals are higher in the SME average compared to the south-east average.

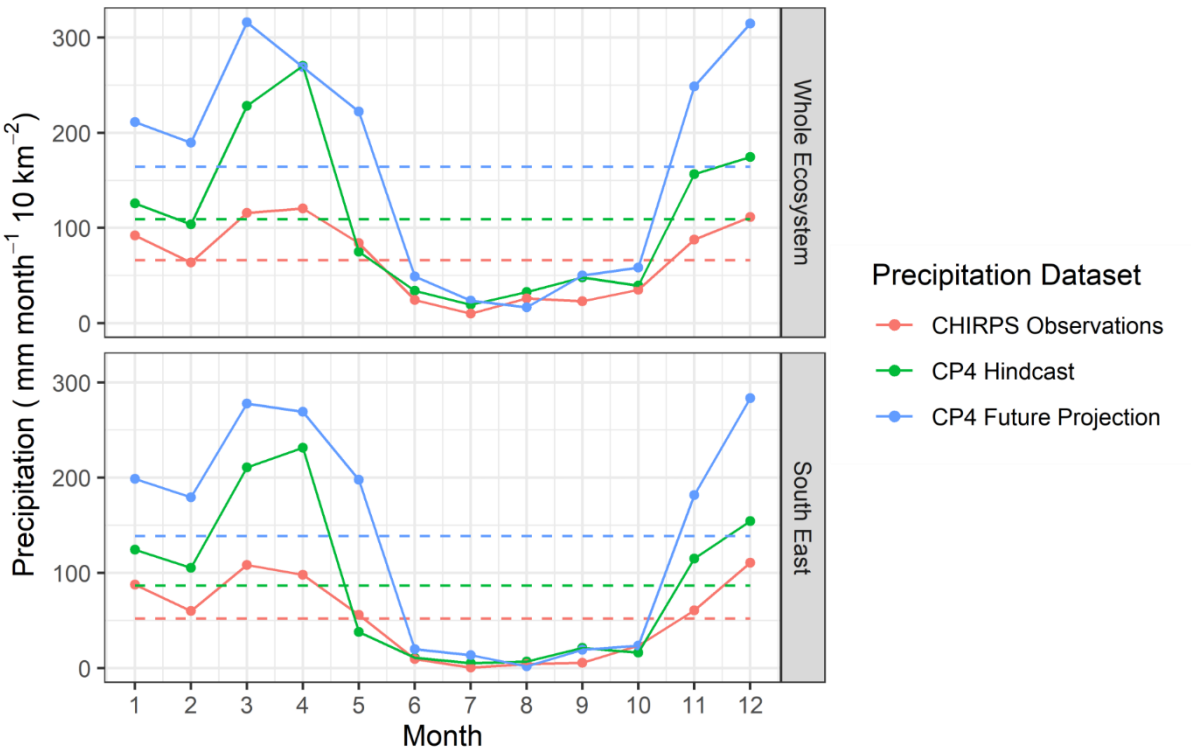

Figure 4.1: Observed and modelled mean annual cycles over the Serengeti-Mara ecosystem (top) and its south-eastern section (bottom). Dashed lines represent mean annual precipitation. Observed data: CHIRPS v2.0 (1997-2006). Modelled data: CP4-Africa hindcast (1997-2006) and future projection (10 years c. 2100). Colour represents precipitation dataset, with red, green and blue representing the CHIRPS, CP4-Africa hindcast and CP4-Africa future projection datasets respectively.

The CP4-Africa hindcast successfully replicated the dry season from June to October and double-peaked wet season from November to May. In both the south-east and SME averages, the dry season monthly hindcast precipitation totals were similar to observed values. Larger monthly totals in the wet season (compared to the observed data) indicate a wet bias, and led to higher annual totals in the hindcast. Peak wet season months were December and April in both the ecosystem average and south-east average. The April peak in the hindcast south-east average contrasts with the observed peak in March.

Compared to the hindcast, monthly precipitation totals in the CP4-Africa future projection increased or remained the same in every month except August. Larger increases occurred in

wet season months than dry season months. The exception was during April, which was unchanged in the SME average and saw a modest increase in the south-east.

4.3.1.2 Annual Precipitation

The SME wildebeest also depend on the spatial distribution of precipitation over the SME. We therefore examined the spatial patterns of past and future annual precipitation in the CP4-Africa model. CHIRPS observations (Figure 4.2a) showed an annual precipitation gradient from the north-west (> 100 mm/month) to the south-east (< 40 mm/month) of the SME. The CP4-Africa hindcast successfully simulated the north-south component of the gradient, with values in the north approximately 3 x higher than the south-east (Figure 4.2b). However hindcast precipitation totals were similar in the west and south-east, showing that the east-west component of the ecosystem's precipitation gradient was not correctly captured. Figure 4.2d shows this is part of a wider pattern. Compared to observed precipitation totals, the hindcast had a wet bias over the majority of the SME and Lake Victoria basin, and a dry bias along Lake Victoria's shoreline and the western tip of the Serengeti National Park. The dry bias was present over the eastern shoreline in every month (not shown).

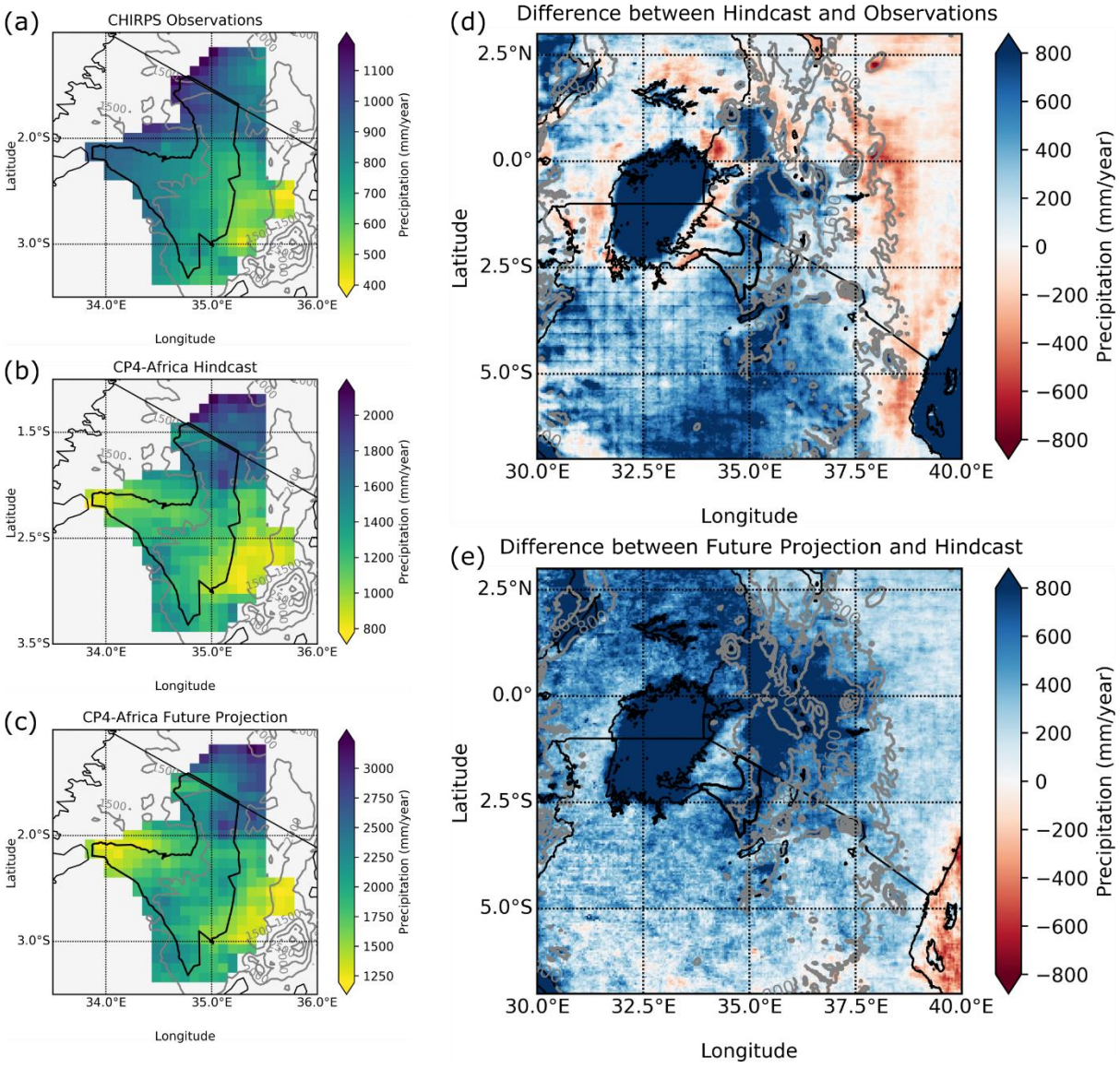

Figure 4.2: Annual precipitation climatologies in mm/year and the differences between them. Climatological annual precipitation over the Serengeti-Mara ecosystem in (a) observed (CHIRPS, 1997-2006), (b) climate model hindcast (CP4-Africa, 1997-2006) and (c) climate model future projection (CP4-Africa, 10 year period circa. 2100) datasets. (d) Differences between mean hindcast and observations over the Lake Victoria basin. (e) Projected changes to mean annual precipitation over the Lake Victoria basin, calculated by subtracting the CP4-Africa model hindcast from the future projection. In panels (a)-(c) precipitation datasets were linearly interpolated to match the 10 km grid size of the SD model, while in panel (d) CHIRPS values were linearly interpolated to match the CP4-Africa grid size and allow comparison between the datasets. Colourbars vary between panels to allow the spatial distribution of precipitation to be clearly displayed.

The spatial distribution of projected future annual precipitation over the SME was similar to the hindcast; a north-south gradient was present, but precipitation totals in the east and west were similar (Figure 4.2c). The future projection also showed increased precipitation totals

across the whole SME and Lake Victoria basin, with particularly high amounts over the Kenya Highlands and Lake Victoria (Figure 4.2e).

4.3.1.3 Past Monthly Wind and Precipitation

Examination of monthly atmospheric conditions may help explain the biases observed in the hindcast model. Figure 4.3 shows that, in both a wet and dry season month, the hindcast simulated lower precipitation on the Lake Victoria shoreline and higher precipitation over the mountains compared to observations. March observations showed easterlies reaching approximately 34.5° E in the north and continuing past 33° E in the south (Figure 4.3a). To the west of these easterlies, precipitation was higher, and winds over land either had a weak westerly component or minimal horizontal motion. In the CP4-Africa hindcast, March precipitation totals were significantly higher compared to the observed data (Figure 4.3c). Westerlies extended further south and east, and precipitation was highest over high ground east of the Serengeti National Park, and lowest over the lake shoreline.

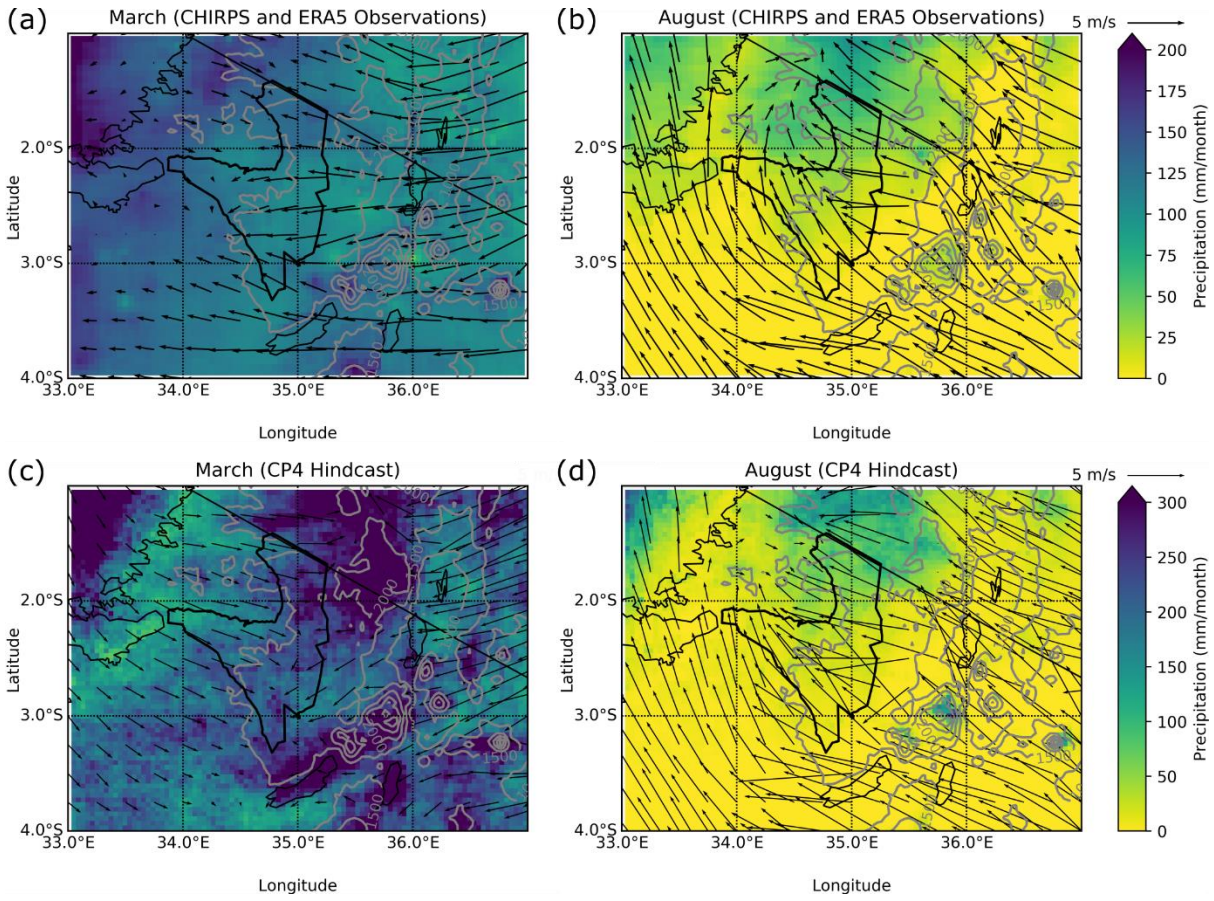

Figure 4.3: Mean monthly precipitation in mm/month and late afternoon 800 hPa wind vectors during March and August. Observed conditions in (a) March and (b) August were calculated from the CHIRPS v2.0 (precipitation, 1997-2006) and ERA5 (winds, 800 hPa, 18:00 EAT, 1997-2006) datasets. Modelled conditions were calculated from the CP4-Africa hindcast dataset (monthly precipitation, monthly 800 hPa winds at 18:00 EAT, 1997-2006). Observed and modelled precipitation have different colour-bar scales to allow the spatial distribution of precipitation to be clearly displayed.

By contrast, August wind and precipitation patterns were similar between the observations (Figure 4.3b) and model hindcast (Figure 4.3d). The main differences between the two datasets were higher absolute totals over the northern highlands and reduced precipitation over the inland waters of Lake Victoria in the hindcast.

4.3.1.4 Future Monthly Wind and Precipitation

We next examined the difference between the CP4-Africa hindcast and future projection in a wet and dry season month, to better understand the projected annual wetting signal. Figure 4.4a shows an increase in precipitation during March over the SME and majority of the northern

and eastern Lake Victoria basin. 700 hPa southerly wind anomalies were present over the whole region.

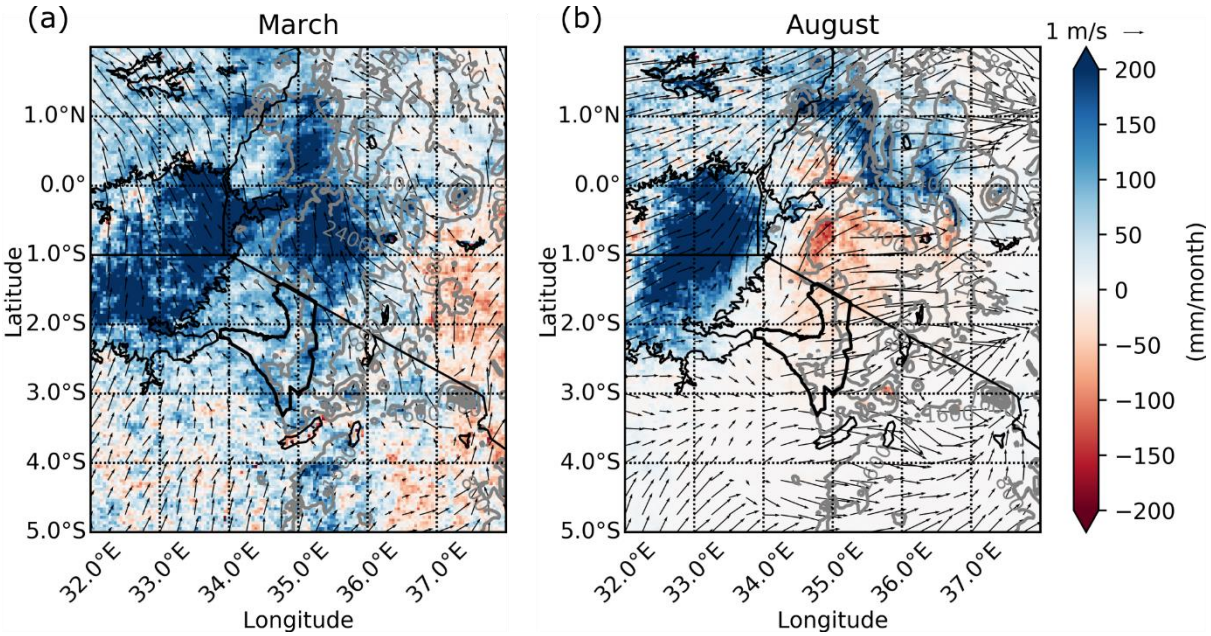

Figure 4.4: Projected future changes to mean monthly precipitation in mm/month and 700 hPa evening (21:00 EAT) wind vectors in (a) March and (b) August. Future changes were calculated by subtracting the mean monthly wind and precipitation values in the CP4-Africa hindcast (1997-2006) from those in the CP4-Africa future projection (10 year period c. 2100).

August precipitation totals increased over the northern Lake Victoria basin, however a drying signal was present over the Kenya Highlands (Figure 4.4b). Mid-tropospheric southerly wind anomalies were also present in August, and appeared to channel moisture from Lake Victoria north and away from the SME and Kenya Highlands.

4.3.2 Wildebeest Response to Precipitation Regimes

4.3.2.1 Model Runs

To assess the potential impact of projected future precipitation change on the SME wildebeest, the SD model was driven with the three precipitation climatologies (Figure 4.5). The SD model runs reached stable equilibrium population sizes after approximately 50 years.

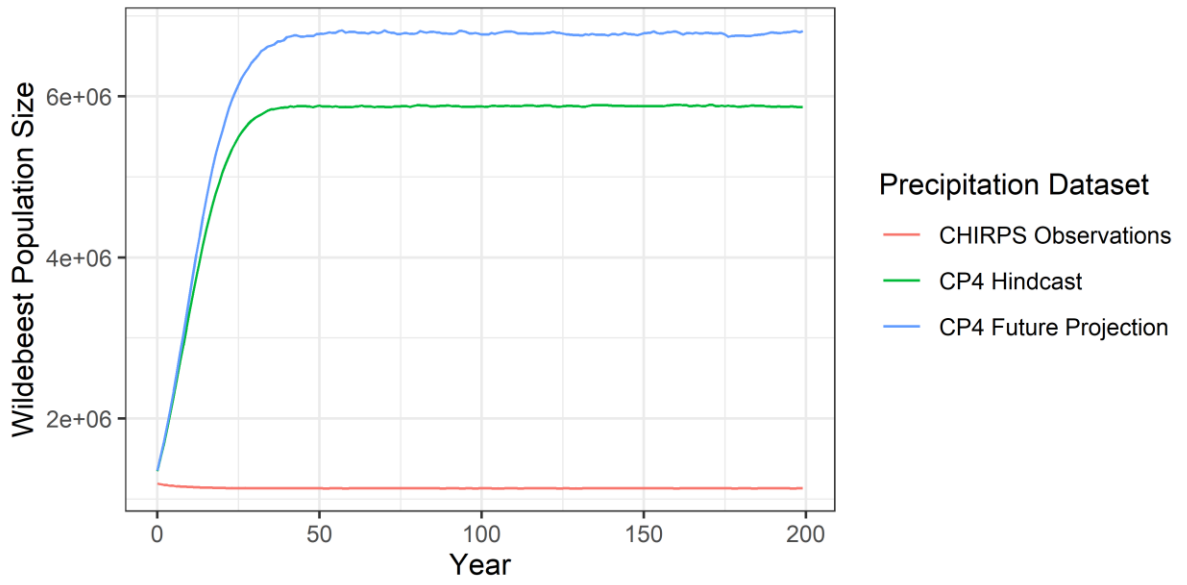

Figure 4.5: Modelled response of wildebeest population to observed past, modelled past, and modelled future mean precipitation conditions. The Savannah Dynamics model was driven with mean monthly precipitation climatologies from 3 datasets: CHIRPS v2.0 (observed precipitation, 1997-2006); CP4-Africa hindcast (modelled precipitation, 1997-2006); and the CP4-Africa future projection (modelled precipitation, 10-year period c. 2100). Colour represents the precipitation dataset used to drive the SD model, with red, green and blue representing the CHIRPS, CP4-Africa hindcast and CP4-Africa future projection datasets respectively.

The population declined from 1.2 million to approximately 1.1 million when driven by observed mean precipitation conditions, but increased to 5.9 million and 6.8 million individuals when driven by the CP4-Africa past and future mean precipitation climatologies respectively. As birth rate is constant in the SD model and death rate is tied to resource availability (*Equation 3*), the large population increases in the SD model runs driven by CP4-Africa precipitation are due to the high rainfall totals generating more resources and therefore sustaining larger wildebeest population sizes compared to the observation-driven runs. The large difference between the model runs driven by observed (CHIRPS) and modelled (CP4-Africa) past precipitation also mean we cannot use the CP4-Africa models to make meaningful predictions about the exact abundance of wildebeest. However, we can still interrogate the SD model

response to find how changes between the rainfall conditions in the climate model hindcast and future projection may affect wildebeest population dynamics.

4.3.2.2 Impact of Spatiotemporal Distribution of Precipitation

To understand the relationship between these modelled population sizes and the spatiotemporal distribution of precipitation conditions which generated them, we first examined the impact of the three rainfall climatologies on wildebeest movement patterns. We found that migration continued to be simulated in each model run (not shown), in a similar manner to Figure 3.3b (representing model runs driven by unaltered nitrogen, tree cover and rainfall maps) in Chapter 3. We next considered the SD model equations (Appendix A). These dictate that the simulated wildebeest respond to annual and daily precipitation totals. In addition, Chapter 3 illustrated that the simulated wildebeest are more sensitive to precipitation totals in the dry season, and over the nutrient-rich, treeless south-east compared to the ecosystem as a whole. Figure 4.6 therefore shows the relationships between wildebeest equilibrium population size, and annual and dry season precipitation, averaged across both the SME and south-east.

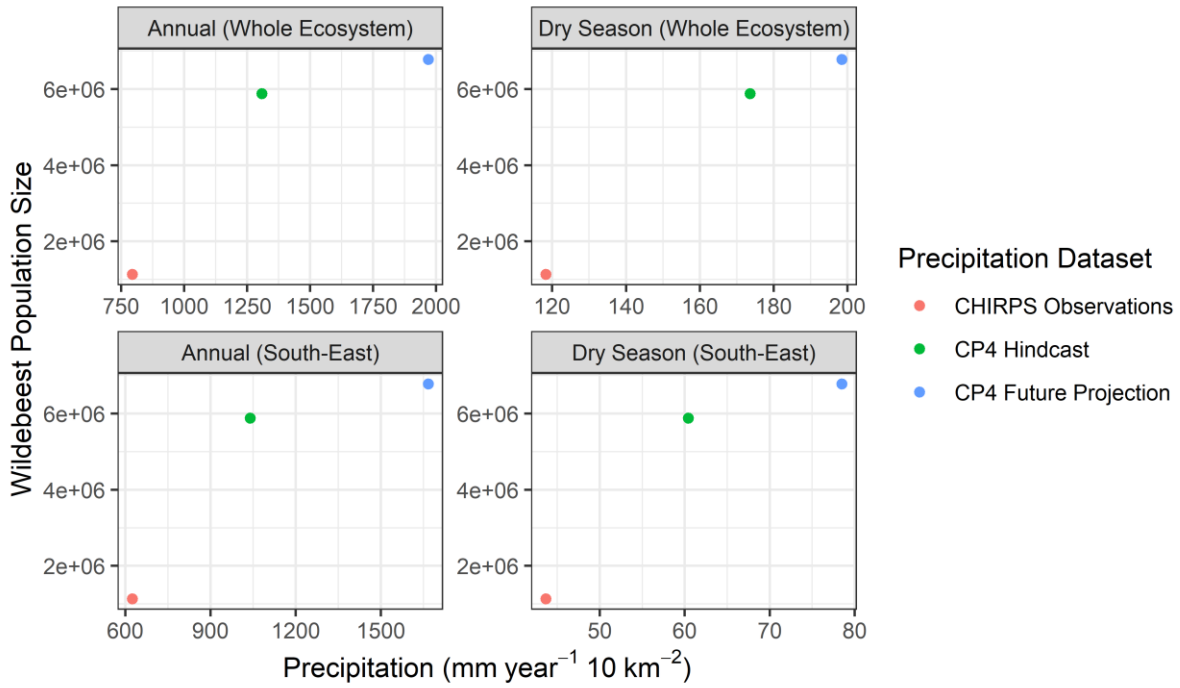

Figure 4.6: Relationships between wildebeest equilibrium population size and seasonal/spatial characteristics of precipitation. Precipitation is spatially averaged over the whole of the SME or just the south-east. Precipitation is temporally summed over either the whole year, or just the dry season months of June to October. X-axis ranges vary between panels due to the differences in the examined precipitation ranges. Colour represents the precipitation dataset used to drive the SD model, with red, green and blue representing the CHIRPS, CP4-Africa hindcast and CP4-Africa future projection datasets respectively.

There is a positive relationship between precipitation and final wildebeest population size, both annually and during the dry season, across the whole ecosystem and in the south-east. This positive relationship also appears to be slightly curved. However this curved shape is less pronounced when dry season precipitation is averaged across the whole ecosystem. This suggests that in this set of simulations, ecosystem-wide dry season precipitation may be the main factor limiting population growth (as a linear relationship between a precipitation metric and wildebeest equilibrium population size would suggest a potential causal relationship). This would make sense for two reasons. First, the ecosystem-wide dry season rainfall totals are similar between all three precipitation datasets, even though the wet season precipitation totals are much higher in the CP4 climate model runs compared to the past observations (Figure 4.1). Second, the projected change in precipitation between the climate model hindcast and forecast

is different in the north and the south; in August, the drying in the north has a greater magnitude than the drying in the south (Figure 4.4). And in July and October, there is drying in a portion of the north while there is no drying in the south (data not shown). This difference between the north and the south could also explain why the relationship between south-eastern dry season rainfall and wildebeest population equilibrium size is less linear, than the one between ecosystem-wide rainfall and wildebeest population size.

4.3.2.3 Population Dynamics

Finally, we wanted to understand how precipitation changes in individual months affected the modelled wildebeest. We therefore examined normalised mean daily population sizes, and mean daily death rates, in the three SD model runs. These daily values were spatially averaged across the SME, and temporally averaged over the final 50 years of the model runs.

Figure 4.7 shows that in all three model runs population sizes increased from November to June and declined from July to September. Daily birth rate is constant in the model (Appendix A), therefore these seasonal population fluctuations were due to low death rates in the wet season and high death rates in the dry season. Precipitation maps were updated monthly within the model, and fluctuations in population size and death rates were associated with these changes.

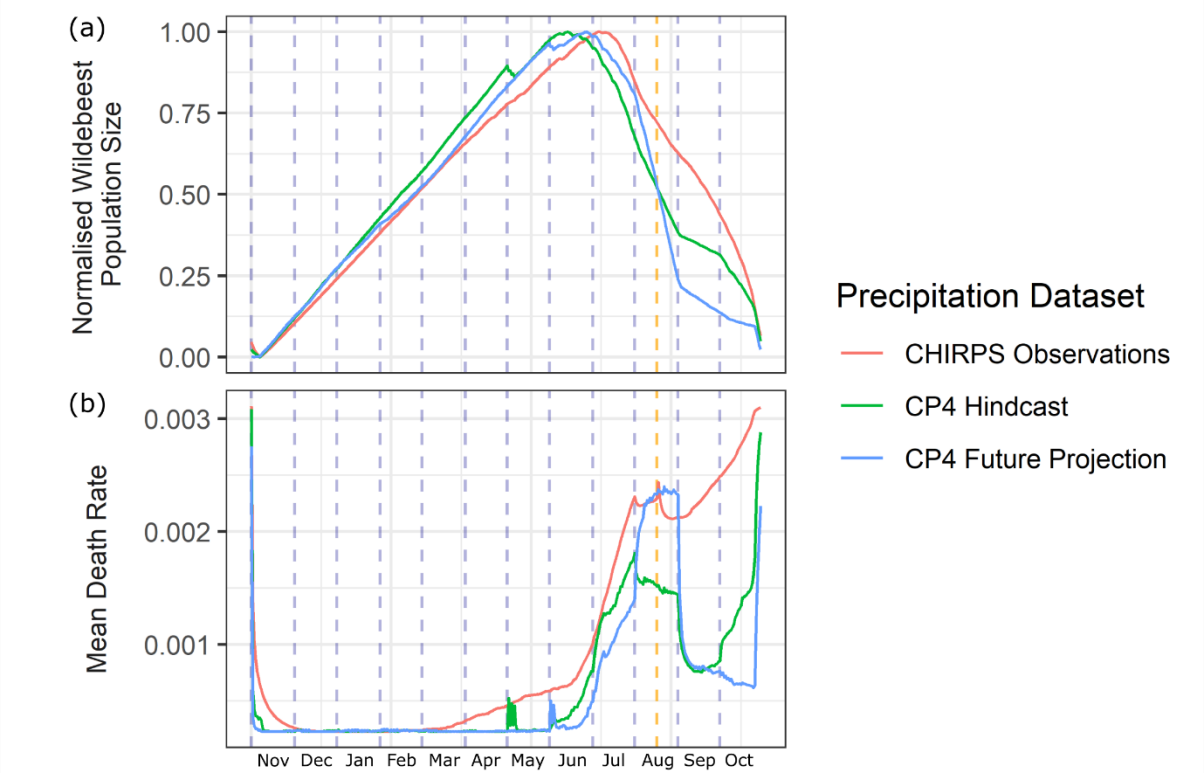

Figure 4.7: Mean daily (a) normalised population size and (b) death rate over the annual cycle. Wildebeest population dynamics in model runs driven by observed, modelled past, and modelled future mean precipitation conditions. Day 0 represents the 1st of November and new months are marked by dashed blue lines. The orange dashed line represents the day fires occur. Colour represents the precipitation dataset used to drive the SD model, with red, green and blue representing the CHIRPS, CP4-Africa hindcast and CP4-Africa future projection datasets respectively.

In all three model runs death rates were high at the start and end of the rainfall year. High death rates at the end of the year were likely due to lack of resources, while those at the beginning of the year were due to the modelled wildebeest being unable to redistribute until day 7 of the new year.

Death rates began to rise at an earlier point in the observed climate driven run compared to the CP4-driven runs, leading to population growth slowing at an earlier point, but being sustained for longer. In the majority of months, death rates were lowest in the model run driven by the CP4-Africa future projection, and highest in the observed climate driven model. This matches the order of the resulting equilibrium population sizes (Figure 4.5).

The exception was in late August, when low ecosystem-wide precipitation totals resulted in the SD model run driven by the future climate projection having a higher death rate than either the observations- or hindcast-driven runs (Figure 4.7). It should be noted that these results are for the final 50 years of the model runs; once the population has already reached an equilibrium. During the first 50 years of the model runs the death rates would be different, and they would be changing year on year.

4.4 Discussion

In the previous section we analysed observed and modelled climatological mean precipitation over the Serengeti National Park and Lake Victoria basin. We drove the SD model with these rainfall conditions and interrogated the model dynamics. Our results showed the CP4-Africa climate model hindcast was able to simulate annual cycle of rainfall over the Serengeti and the meridional component of the rainfall gradient over the Serengeti National Park. However wet season totals were too high and the hindcast did not capture the longitudinal component of the rainfall gradient, with too much rainfall occurring over the eastern highlands and too little over the shoreline of Lake Victoria. 800 hPa winds travelled too far inland. Our analysis of the CP4-Africa future projection showed rainfall increases over the Serengeti National Park during all months except August. The spatial distribution of rainfall changes over the Lake Victoria basin in March and August were associated with anomalous southerlies at 700 hPa. SD model runs driven by observed and modelled mean climatological precipitation showed a slight decline in wildebeest population size in the observed precipitation run, and dramatic increases when driven by CP4-Africa model output. Stable population size was higher for the future projection run than the hindcast run. Comparison between final wildebeest population size and key precipitation metrics (identified in Chapter 3) showed the most linear relationship was been dry season rainfall and final wildebeest population size. During the final 50 years of model runs death rates were higher in the dry season than the wet season. Death rates were typically highest in the observed rainfall-driven run, second highest in the hindcast-driven run, and lowest in the future projection driven-run. The exception was in August, when death rates were exceptionally high in the SD model run driven by the future projection. Here we discuss the reliability of the simulated rainfall, and wildebeest response to those conditions, over the Serengeti National Park.

4.4.1 Evaluation of CP4 Hindcast Climate Model

No climate model perfectly simulates the climate system. However, future projections are generally held to be more reliable when a model simulation of the historical climate system has low bias and the model simulates the observed dynamics responsible for the climate features. Given the large positive precipitation bias in CP4_Africa over East Africa, a feature common to most climate models, we evaluated the representation of SME rainfall and lower tropospheric wind patterns in the CP4-Africa hindcast. The hindcast successfully captured the shape of the annual cycle over the SME; a dry season and double-peaked wet season. This was expected, as the majority of climate models are able to accurately represent precipitation annual cycles over Africa (Dunning *et al.*, 2016) even if the absolute precipitation values are different from observed.

The hindcast was also able to accurately simulate dry season precipitation conditions and August lower tropospheric wind patterns over the SME. However, modelled wet season precipitation totals were significantly higher than past observations. In March, particularly high values were simulated over the East Africa Rift Highlands, and low values over the Lake Victoria shoreline. Finney *et al.* (2019) suggested that the wet bias over Lake Victoria in the CP4-Africa hindcast was caused by unrealistically strong night-time wind convergence over the lake, as well as errors in the model's moisture budget due to a lack of local moisture conservation (the model requires precipitation to match evaporation and moisture flux convergence over the whole CP4-Africa domain, but does not require this locally). Our results suggest a similar phenomenon is occurring during the day. Heavy highland precipitation is associated with lower tropospheric wind convergence between continental easterlies and unrealistically strong, and far-reaching, lake breeze westerlies. In addition, Finney *et al.* (2019) found that peak precipitation over the eastern Lake Victoria basin occurred 3 hours too early

in the hindcast compared to observations. The model simulating precipitation totals that are too high in the late afternoon (when lake breeze winds reach furthest inland), and precipitation totals that are too low in the evening (when land-lake winds reverse and the lake convergence front returns to the shoreline) (Woodhams *et al.*, 2019), could explain the spatial distribution of precipitation observed in the hindcast model.

An unrealistically strong daytime land-lake thermal contrast is a possible cause for the abnormally strong lake breeze winds in the hindcast. Lake surface temperatures in the CP4-Africa hindcast are represented as night-time climatological monthly averages (Stratton *et al.*, 2018). However, in reality the lake surface temperatures change over the diurnal cycle by approximately 2 ^{o} C (MacIntyre, 2012; MacIntyre *et al.*, 2014). If this diurnal cycle were represented in the model, the daytime land-lake temperature gradient would presumably be lower, and the lake breeze winds weaker. Further work investigating internal model dynamics would be needed to understand this issue.

Overall the CP4-hindcast is able to successfully capture the annual cycle, a north-south precipitation gradient over the SME, and simulate key mesoscale flows. However, it is necessary to consider the model's unrealistically high precipitation totals, overly strong lake breeze winds, and low precipitation totals over the Lake Victoria's shoreline, when interpreting the CP4-Africa future projection over the SME.

4.4.2 Future Precipitation Changes over the SME

Our results show a projected increase in annual precipitation over the SME and eastern Lake Victoria basin. The unrealistically high hindcast precipitation totals mean the absolute values in the future projection are not credible. However, it is reasonable to consider the sign of the precipitation change, especially given the model's proven ability to capture key regional atmospheric processes.

The local increase in mean annual precipitation matches projected changes over the broader East Africa domain, in both CP4-Africa (Finney *et al.*, 2020) and other climate models (Shongwe *et al.*, 2011; Niang *et al.*, 2014). Finney *et al.* (2020) suggest the projected increase in East African rainfall in the CP4-Africa future projection was due to greater easterly moisture flux from the Indian Ocean, and altered responses to increased low level specific humidity.

Focusing on the spatial distribution of the projected changes in annual rainfall over the Lake Victoria basin, the strongest increases were seen over the highlands to the east of Lake Victoria. Given the importance of the lake breeze in generating precipitation in this region, this increase may be explained by a strengthened lake breeze. Land surface temperatures warming more rapidly than lake surface temperatures would lead to a stronger daytime land-lake temperature gradient (than is currently present) and greater moisture divergence from the lake (Thiery *et al.*, 2016). This is a likely scenario, as the CP4 future model is explicitly designed to ensure that the land warms faster than the lake, as a thermal inertial term is included when calculating the future surface temperatures of inland water bodies (Kendon *et al.*, 2019). However, an increased daytime temperature gradient should also lead to a reduced land-lake thermal contrast at night, weakening the lake breeze and leading to decreased rainfall over the lake, which is not observed in the CP4 future projection. This could be explained by an increase in extreme rainfall events overwhelming the reduction in the intensity of typical precipitation events, as suggested by Thiery *et al.* (2016). However further analysis of changes to the thermal temperature contrast and local wind patterns would be required to ascertain whether changes to the lake breeze are a key causal mechanism for the spatial pattern of the altered regional rainfall.

Temporally, the majority of the increase in annual rainfall occurred in the wet season months of November to May. The strong increases in seasonal precipitation during the short rains (October to December) and the long rains (March to May) are in agreement with many other

climate model projections (Shongwe *et al.*, 2011; Niang *et al.*, 2014). However the distribution of the projected change in long rains, both spatially and temporally, was unexpected. Dunning *et al.* (2018) found that in most CMIP5 models there would be earlier onset and cessation dates for the long rains over East Africa. This would mean that the duration of the long rains would remain the same, and the increase in total seasonal rainfall would occur solely from an increased intensity of precipitation events. Hourly rainfall intensity does increase in the CP4 model (Kendon *et al.*, 2019), so this would account for much of the increased rainfall seen during the long rains. In addition, an earlier onset of the long rains season could also explain the projected increase in March rainfall. However if there was an earlier cessation to the long rains, we would expect to see reduced precipitation during May; instead May received the largest projected increase in monthly rainfall. It was also unexpected to see the projected reduction in rainfall across the highlands and the western half of Lake Victoria during April, as in the present climate this is the wettest month of the year (Yang *et al.*, 2015; Chapter 2). Further analysis of large scale continental winds and moisture fluxes are likely needed to ascertain the reasons behind these projected changes.

Despite the small change in magnitude, the change in precipitation from June to September is also critical to examine, as the Serengeti wildebeest population are limited by dry season precipitation (Mduma *et al.*, 1999; Chapter 3). Although there is a great deal of uncertainty around projections of future precipitation over the western Kenya highlands and Lake Victoria basin (Dosio *et al.*, 2019), many climate models predict a reduction in July-September precipitation totals over East Africa under high warming scenarios (Patricola and Cook, 2011; Dosio *et al.*, 2019). In these climate model outputs, the rainfall reduction is seen across much of East Africa. This contrasts with the CP4 output used in our study, which shows an increase in rainfall across much of Uganda, South Sudan, Ethiopia and western Kenya during July to September (not shown). This discrepancy between the results of the CP4-Africa and other

climate model projections means that this finding should be interpreted with caution, especially as the CP4-Africa model was only run for 10 years (instead of the 30 years typically advised to calculate climatological normal (WMO, 2017)), and therefore the projected changes could be due to natural variability in the climate system. Yet if the changes over the Lake Victoria basin projected by the CP4-Africa were due to natural variability, it would be expected that the spatial distribution of rainfall would match patterns observed in the past. On a large scale, the observed pattern of rainfall change is similar to the one seen when there is a weak Turkana jet, with increased rainfall over the East African highlands and Lake Victoria basin (Vizy and Cook, 2019). However, when the region containing the Serengeti-Mara ecosystem is considered, this explanation becomes less plausible. If the change were due to a climatologically weaker Turkana jet, we would expect to see an increase in rainfall across the whole of the western Kenya highlands and Serengeti region, as well as a pronounced decrease in rainfall to the west of the Lake Victoria basin (Nicholson, 2016a; Vizy and Cook, 2019). Whereas in the future CP4 projection, rainfall increased to the west of the Lake Victoria basin, and decreased over the Serengeti and eastern highlands during August. This drying signal was also present in the highlands just to the north of the Serengeti during July and September. Different parts of the highlands around Lake Victoria are known to respond differently to remote forcing such as the El Niño Southern Oscillation (Indeje *et al.*, 2000) and the Madden Julian Oscillation (Camberlin, 1996), so large scale forcing cannot necessarily be discounted.

However, our results suggest the changes to August precipitation shown in the CP4-Africa future projection may be due to altered mid-tropospheric wind patterns. Southerly wind anomalies were present over much of the Lake Victoria basin and the Kenya Highlands during August, and their flow appeared to channel and concentrate moisture from Lake Victoria northward. Previous work has shown an association between 700 hPa wind direction and the seasonal orientation of the precipitation gradient over the SME, suggesting that these winds

may be affecting the direction of storm propagation (Chapter 2). The southerly anomalies present in March appear to be performing a similar function; bringing moisture and precipitation north to the SME at a time of year when the tropical rainfall belt is below the equator.

The presence of southerly anomalies in both March and August, months in which East Africa usually has northerly and southerly prevailing tropical easterly winds respectively (Yang *et al.*, 2015), shows that these wind anomalies are not due to the meridional components of existing large scale tropical easterlies strengthening. Given their association with altered precipitation patterns in the Lake Victoria basin, the dynamic causes of these regional wind anomalies would be worth further investigation.

4.4.3 Wildebeest Response to Precipitation Changes

Finally we consider how and why the modelled wildebeest responded to these precipitation regimes.

The stable wildebeest population sizes predicted by the SD model are unrealistically high for all three precipitation scenarios. However this was expected, due to unrealistic driving conditions. Our study focuses on the impact of changes to mean precipitation conditions, therefore none of the precipitation scenarios included interannual variability. Lack of variability in resource availability leads to an increase in stable population sizes (Lande *et al.*, 2003; Chapter 3). This is true of wildebeest, as low rainfall totals in wet seasons are known to kill up to 20 % of calves, while droughts lead to fewer births and high adult mortality (Mduma *et al.*, 1999). Therefore removing interannual variability and using mean rainfall excludes conditions which would lead to high mortality, and would lead to a population rise. Our results show this was clearly true for the SD model runs driven by the CP4-Africa rainfall. Yet the SD model run driven by observed past precipitation led to a (slight) decline in wildebeest numbers,

initially suggesting that the removal of interannual variability does not lead to an increase in population size. However, the reduction in population size was likely due to dry conditions present in northern Tanzania from 1998-2005 (Kijazi and Reason, 2009) resulting in the observed 10-year (1997-2006) precipitation mean used in our study being below the average rainfall conditions usually experienced by the ecosystem. Rainfall across the SME from 1997-2006 was 4 % lower than the 30-year period between 1987-2016 (data not shown). Therefore the slight decline in simulated wildebeest population size that occurred when the SD model was driven by mean 1997-2006 rainfall, was similar to that observed in chapter 3 when the SD model was driven by climatological precipitation that had been reduced by 5 %. This highlights a flaw of using climate models with only 10 years of data; the WMO typically recommends 30 years of data to create a climatological average that captures the mean state and interannual variability (WMO, 2017). While interannual variability in precipitation was not the focus of our study, future increases in extreme wet and dry precipitation events are likely over East Africa (Dosio *et al.*, 2019; Kendon *et al.*, 2019). As this could decrease wildebeest survival, it is an area that warrants further study.

In addition, the annual precipitation totals simulated by CP4-Africa are unrealistically high. Within the SD model, the relationship between grass production and precipitation are based on linear models fitted to precipitation data with annual totals between 300 and 1100 mm/year (McNaughton, 1985; Holdo *et al.*, 2009a; Chapter 3). In Chapter 3 we highlighted that this uncapped linear relationship could allow extremely high rainfall totals to simulate unrealistically large wildebeest population sizes; whereas in reality, above a certain precipitation threshold, the relationship between annual rainfall and wildebeest population size would likely plateau. This scenario has occurred in the SD model runs driven by the CP4-Africa hindcast and future projection, which had mean annual ecosystem-wide averages of 1308 mm/year and 1970 mm/year respectively (compared to 794 mm/year recorded by

CHIRPS in 1997-2006). While the exceptionally high annual precipitation totals simulated in the CP4-Africa model runs could potentially support a wildebeest population that is larger than the one present today, the unprecedentedly high precipitation totals mean we cannot confidently predict the size of that population and it is highly unlikely that it would reach 5-7 million individuals.

Although the exact population sizes are not realistic, the qualitative changes to population size and death rate can provide insight into the potential impact of future precipitation changes. The CP4-Africa future climate projection shows an ecosystem-wide increase in mean annual precipitation, and increases in all months except August. These increases would likely have a strongly positive impact on wildebeest survival and population size, as wildebeest are vulnerable to nutritional stress throughout much of the year (Rysava *et al.*, 2016). In addition, during the wet season the herds spend February to May in the south of the ecosystem (Maddock, 1979), and calves are born in synchrony during a 3-week period in February-March on the south-eastern SME plains (Hopcraft *et al.*, 2015). Therefore southern precipitation conditions during February to May strongly impact calf survival (Murray, 1995; Hopcraft *et al.*, 2015). This effect is not captured in the SD model, as this synchronous birth is not represented in the population dynamics of the SD model (which instead has a constant birth rate; *Equation 3*). Chapter 3 highlighted that by having a constant birth rate through the year, the SD the model underestimated the importance of rainfall in the south-east of the ecosystem during February-May to wildebeest recruitment. Therefore the projected increase in mean south-eastern precipitation from February-May (in the CP4-Africa future projection) could potentially be even more important/beneficial to wildebeest population dynamics during these months than predicted by the SD model. However, the spatial distribution of rainfall in this future projection must be interpreted with caution, due to the overrepresentation of wet season lake breeze winds in the CP4-Africa hindcast and the resulting wet bias over the eastern SME.

In addition, the beneficial impact of increased mean precipitation in this area would be undermined if this was due to fewer extreme precipitation events, instead of a consistent increase that occurred every year.

Dry season precipitation (June-October) is the most important factor limiting wildebeest population size (Mduma *et al.*, 1999), and this is reflected in the SD model death rates. Our results suggest that while the population would be negatively affected by the projected future decrease in August precipitation, this would be offset by the benefit of increased precipitation in other months of the year. However, this does not consider the fact that there is already competition between livestock and wildlife within the Mara Reserve (Veldhuis *et al.*, 2019), and a reduction in dry season precipitation to the north may cause increased competition within the protected area, from livestock and wildlife that are unable to find forage. These issues may be exacerbated by the future drying signal over much of the Kenya Highlands present in the CP4-Africa projection in July. To allow conservationists and communities in the Kenya Highlands to prepare for a potential decline in July and August precipitation, we wish to highlight the need for further investigation into the dynamic causes of this drying signal.

4.5 Conclusions

Overall our results illustrate how sensitive the region's precipitation is to changes to Lake Victoria's land-lake breeze winds and their interactions with the East African Rift Highlands. This both confirms the value of using high resolution climate models which can simulate these mesoscale atmospheric processes, and highlights the importance of evaluating these model projections to identify biases before their use in ecological impact studies.

The CP4-Africa hindcast was able to accurately capture the annual cycle of precipitation and the north-south component of the precipitation gradient over the SME. However, annual and wet season precipitation totals over the SME were too high, and totals over the lake shoreline were too low, resulting in the east-west component of the SME precipitation gradient being poorly represented. This is likely related to unrealistically strong lake breeze winds over the region, which potentially cause enhanced convergence over the rift highlands. Therefore the magnitude and spatial distribution of projected future SME precipitation must be interpreted with caution.

Mean monthly precipitation is projected to increase over the SME, except during August. The spatial distribution of projected monthly precipitation changes in the Lake Victoria basin appears related to southerly mid-tropospheric wind anomalies altering the flow of moisture from Lake Victoria and the tropical rainfall belt.

The projected future increases to annual and monthly mean SME precipitation totals were beneficial to the modelled wildebeest population, resulting in lower death rates and a 15 % rise in stable population equilibrium size compared to CP4-Africa hindcast-driven SD model runs. These increases offset the negative impact of a decline in August precipitation. However, the SD model does not account for potential disruptions caused by competition with livestock and

wildlife from outside the protected areas affected by precipitation declines in dry season months.

Overall, these results suggest that high scenario warming may produce mean precipitation conditions over the SME that are beneficial to the wildebeest. However, these results only represent output from one climate model and do not account for changes to interannual variability.

Chapter 5. Conclusions

The purpose of this thesis was to understand how climate change may affect precipitation patterns over the SME, and its potential impact on the migratory wildebeest.

A modelling approach was taken that combined an ecological model of wildebeest movement and population dynamics with outputs from a climate model. The ethos of this thesis is that a deep understanding of both the ecological and climate models used in ecological impact studies is necessary to be able to confidently interpret the outcomes. To this end the models were critically assessed to ensure their assumptions, limitations, and thus their capacity to simulate the impact of future change over the SME, were fully understood.

The body of the thesis addressed this by: quantifying key atmospheric conditions over the SME (paper 1); investigating the response of modelled wildebeest to a spectrum of novel precipitation conditions (paper 2); evaluating the representation of atmospheric conditions in a high resolution climate model hindcast; examining projected future precipitation and wind patterns over the SME; and modelling the impact of the future projection on the SME wildebeest (paper 3).

The concluding part of this thesis summarises the key findings and limitations of each paper, as well as potential future research directions. The thesis aims and the extent to which they were met are discussed, as well as their contribution to the larger goal of the thesis. Finally, the novel contributions of this thesis to scientific knowledge are summarised.

5.1 Summary of Key Findings

5.1.1 The Characteristics and Drivers of Climatological Precipitation over the Serengeti Region in East Africa.

The first paper characterised the precipitation patterns over the SME and their key atmospheric drivers. Precipitation over the SME and surrounding region was strikingly heterogeneous on annual, monthly and hourly timescales. Differences were observed across the region in peak precipitation months, symmetry between precipitation peaks, and dry season precipitation totals, leading to distinctly different annual cycles. Over the SME, the precipitation gradient across the ecosystem changed orientation on a monthly basis. A difference in time of peak annual precipitation ran through the middle of the Serengeti National Park.

Analysis of mid- and lower-tropospheric wind patterns indicated that precipitation distribution was largely determined by interactions between the topography, large-scale easterlies, and mesoscale lake breeze westerlies. Large-scale easterlies brought moisture from the Indian Ocean, were associated with the movement of the tropical rainfall belt, and therefore controlled the structure of the annual cycle. The rift topography generated topographic precipitation on windward slopes, rain shadows on leeward sides and generated anabatic/katabatic flows. Daytime thermal contrasts between Lake Victoria and the surrounding land resulted in diverging lower tropospheric lake breeze winds, which ascended when they met the large-scale easterlies, resulting in daytime lake circulation cells. The mean position of the afternoon wind convergence line was always over a part of the SME, but the exact position altered seasonally. In the dry season the convergence line occurred in the north over the Mara Highlands. By contrast, the afternoon wind convergence line ran down the middle of the SME in the wet season. Mean hourly precipitation patterns in March were shown to be widespread and light at 12:00, increased to the west of the convergence line and decreased to its east at 15:00, then

receded westward towards Lake Victoria by 18:00. The association between the orientation of the precipitation gradient over the SME and the direction of mid-tropospheric easterlies suggested that storms formed at the wind convergence line were blown in the direction of mid-tropospheric winds.

5.1.2 Modelling Wildebeest Movement and Population Dynamics in the Face of Environmental Change.

The second paper interrogated the SD model to provide a better understanding of its strengths, weaknesses, and key sensitivities to driving precipitation conditions. The simulation of movement was found to continue until all environmental gradients were removed. The modelled population size was most vulnerable to reduced dry season precipitation, in combination with an increase in tree canopy cover. The precipitation conditions to which wildebeest population size was most sensitive were annual precipitation, dry season precipitation, and precipitation over the south-east of the SME.

The model lacked sensitivity to altered precipitation in November, which may result in underestimation of the impact of prolonged drought. In addition, the constant birth rate within the model meant it may underestimate the effect of reduced precipitation on calf survival in February-May. While wildebeest population size has not historically been regulated by calf survival, a change to the mean precipitation state during these months could plausibly have an impact. The linear equations governing grass growth in response to precipitation do not saturate. Hence, unrealistically high population sizes would be generated if the SD model was to be driven by exceptionally high precipitation totals. Despite these limitations, the majority of the modelled wildebeest's responses to altered environmental conditions were plausible, suggesting it is a useful tool for exploring the impact of environmental change on the SME wildebeest.

5.1.3 Modelling the Impact of Future Changes to Mean Precipitation on the Survival Rates of the Serengeti-Mara Wildebeest

The final paper investigated the ability of the CP4-Africa hindcast to represent the mean climate of the SME, examined the projected future changes to regional precipitation and wind patterns, and modelled the impact of these changes on the wildebeest.

The CP4-Africa hindcast captured the annual cycle, but an annual wet bias was present over the SME, largely due to unrealistically high totals simulated from November through April and wet biases over the East African Rift Valley highlands. The model successfully simulated the meridional precipitation gradient over the SME; however the zonal component was not correctly captured, due to a dry bias over Lake Victoria's shoreline. March afternoon lake breeze winds were too strong over the SME, extended too far inland, and persisted too high in the atmosphere compared to reanalysis data. The maximum reach of the lake breeze winds was associated with anomalously wet conditions over the highlands to the east of the SME, suggesting a causal relationship.

The CP4-Africa future projection showed an annual increase in precipitation across the SME and Lake Victoria basin. Over the SME, a net increase occurred in every month except August. The August drying signal was present across the Kenya Highlands and the SME; it was also present in July over the Kenya Highlands, but not the SME. The projected increase and decrease in precipitation over the SME in March and August respectively were associated with southerly wind anomalies over the Lake Victoria basin.

The largest wildebeest population size (approximately 6.8 million individuals) resulted from driving the SD model with the CP4-Africa future climate projection. The highest death rates were found in the SD model run driven by observed precipitation, except during the second half of August, when the highest death rates were present in the SD model run driven by the

CP4-Africa future projection. The results suggest that climate change may lead to a mean state that benefits the SME wildebeest, although the effects of changes to interspecific competition and interannual variability could counteract the favourable future mean state.

5.2 Limitations

5.2.1 The Characteristics and Drivers of Climatological Precipitation over the Serengeti Region in East Africa.

The study did not intend to investigate the various wind conditions present when precipitation occurred in different parts of the SME. However, this resulted in uncertainty about how precipitation was generated in certain areas. For example, a March precipitation peak is present in the south, both to the east and west of the mean wind convergence line. This suggested that lake breeze winds played a part in generating precipitation in this region, and that these winds may extend past their mean position into the far south-east. However this cannot be verified without analysis of variability in the position of the lake breeze front, and/or the wind conditions present during wet and dry periods of the south-east of the SME.

In addition, the sole use of satellite data was sub-optimal for a region with such complex spatial precipitation patterns, as satellites are known to have greater biases over topographically complex regions (Dinku *et al.*, 2007; Haile *et al.*, 2013; Derin and Yilmaz, 2014). This issue was partially mediated by using multiple satellite datasets (too allow comparison and highlight potential errors), examining climatological means instead of daily data, and using the CHIRPS dataset where possible. Calculating climatological means reduces the risk of using inaccurate data, as they average out (normally distributed) errors that may occur on individual days (although not systemic biases, or non-normally distributed errors in the dataset). Furthermore, the CHIRPS dataset was used when analysing monthly totals, as it includes measurements from an extensive network of rain gauges across the African continent, including multiple gauges

within the SME. However, hourly precipitation from the TRMM dataset was also examined. Biases are more likely in this dataset, because fewer rain gauges are available across East Africa to calibrate satellite measurements on this temporal scale. Therefore caution must be exercised when interpreting these values, and it would be useful to be able to evaluate the performance of the hourly satellite measurements over the SME with local ground-based measurements.

5.2.2 Modelling Wildebeest Movement and Population Dynamics in the Face of Environmental Change.

A potential limitation of this study was its decision to drive the model with repeated identical environmental conditions, instead of an ensemble of varied conditions with a specific mean (i.e. allowing interannual variation around a specific mean). This was an explicit part of the study design, as the repeated conditions approach allowed the impact of changes to the mean state to be distinguished from the impact of altered variability. In addition, it is much more difficult to precisely test the impact of small changes to spatiotemporal rainfall conditions when using an ensemble of varied conditions around a specific mean. Nevertheless, using an ensemble approach would have resulted in more realistic population sizes, so the study likely would have benefitted from additional work to test whether ensemble runs around specific mean rainfall conditions had qualitatively similar results to those obtained by running repeated rainfall conditions.

Similarly, removing the spatial gradients during the temporal sensitivity analysis was a simple way to allow the model's response to be solely due to changes in monthly precipitation totals. Yet by removing the spatial gradients, the simulation of the migration ceased.

Ideally, the SD model runs would have also incorporated an internal dynamic feedback between wildebeest population size and tree growth. This was not included as the equations were not coded into the version of the model that was used in this study, despite the fact they

are present in another version of the model by Holdo *et al.*, (2009a). This decision was made based on accessibility to the code from the different versions of the model. However, it would have been beneficial to have a dynamic cap on the large number of wildebeest produced. Therefore future work using the SD model for climate change impact studies should ideally use a version of the model that incorporates changes in tree density and recruitment.

Finally, when assessing the plausibility of the model responses, the paper compared the results to examples from the literature to determine whether the responses matched what had been previously described. A more thorough approach would have been to compare the model's response of observed wildebeest population fluctuations to past precipitation conditions. This could have been achieved by analysing annual wildebeest census data, and comparing the precipitation conditions of the previous year with the resulting population size change from one year to the next. Unfortunately much of the available wildebeest count census data (not included in this thesis) contains gaps between years, resulting in too little data for this analysis to be carried out, meaning that the findings from this chapter are not validated against observed data.

5.2.3 Modelling the Impact of Future Changes to Mean Precipitation on the Survival Rates of the Serengeti-Mara Wildebeest

This paper modelled the impact of future changes to mean SME precipitation on wildebeest population size. Output was used from a single climate model which was known to perform well over the Lake Victoria basin, rather than a spectrum of different climate models that would not necessarily have the capacity to simulate key local processes. There were two reasons for this choice. First, CP4-Africa is the only convection-permitting climate model that has been run over the whole African continent, thus there were no similar models to compare it to. Second, focusing on a single model allowed deeper interrogation of the local precipitation

patterns and lower to mid-tropospheric winds within the model. Unfortunately, the lack of comparison between a spectrum of climate models means it was not possible to analyse the impact of large-scale model biases on local results.

In addition, the CP4-Africa climate model was run for only 10 years. The WMO recommend the use of 30 years of data to create a climatological mean to allow sufficient representation of interannual variability. The use of only 10 years risks the projected increase being due to natural wet phases within the climate system rather than climatological change. However, the extent of the precipitation increase over the SME (approximately 50 %), and the agreement with other climate model projections (the majority of which also show a projected increase over East Africa), mitigates this risk.

The CP4-Africa model was also only run for one Representative Concentration Pathway (RCP8.5), and therefore solely represents a high warming scenario.

Limitations related to smaller-scale processes within the CP4-Africa model include the lack of a dynamic lake component, and the inability of the model to simulate shallow convection or small storms. CP4-Africa is not unusual in this respect, as it is rare for these features to be included in climate models. However, given their importance to atmospheric processes over the SME, there is a possibility that precipitation is sub-optimally simulated because these elements are absent.

With regards to the SD model, limitations that emerged from paper 2 include an uncapped relationship between precipitation and grass growth, and a constant birth rate that does not represent the reality of synchronous wildebeest births in February-March. When driven by the unrealistically high CP4-Africa precipitation totals, the SD model generated an implausibly large wildebeest population. This was caused by the relationship between grass growth and precipitation being unable to saturate. The constant birth rate meant the SD model may be

under-sensitive to a decrease in February-May precipitation, when the wildebeest are born and suckle. This situation did not arise in the future scenario used in the paper, as precipitation in the CP4-Africa future projection increased during these months over the south-east where the wildebeest would be grazing at this time of year. However, increased rainfall in this area could have other knock on effects, such as altering the vegetative species composition or altering the soil chemistry and nutrient content (ecological feedbacks that the SD model is not able to simulate).

Finally, the SD model is unable to capture sub-monthly changes to precipitation. As this study examined changes to mean precipitation rather than variability, changes to daily precipitation would likely have been averaged out over the 10 year period. However, it is an issue for consideration if the SD model were used to study the impact of altered precipitation variability.

5.3 Future Avenues of Research

5.3.1 The Characteristics and Drivers of Climatological Precipitation over the Serengeti Region in East Africa.

The work in Paper 1 provides a foundation for future work investigating wet and dry conditions over the SME, and the atmospheric processes responsible for these states. Separately analysing the mean atmospheric conditions from composites of wet and dry periods, is a typical approach for this type of investigation. This is usually carried out as a composite of wet/dry days or months. However, there are strong diurnal and seasonal cycles of wind over the SME, as well as the effects of competing mesoscale features. Therefore this work should ideally examine separate composites for each part of the SME on daily and hourly timescales. Separate composites should be examined for different parts of the SME, as they likely have different processes generating rainfall in different regions (conditions that cause rainfall in the northwest

of the ecosystem are not necessarily the same as those causing rainfall in the south-east). These composites should only include days in which rainfall occurred (e.g. if examining rainfall in the south-east during July, the majority of days will not receive rainfall and thus should be excluded from the analysis). The time of day should also be considered as there are strong changes in wind patterns on hourly timescales in this region, and identifying the atmospheric conditions present prior to, and during, rainfall events would assist in understanding how they were generated.

Composites for each region identified by the cluster analysis, for each month and hour of the afternoon, would reveal the mean wind patterns present during wet and dry days in that portion of the wider Serengeti domain. This investigation could then be expanded to examine how large scale forcing that is known to affect precipitation over the wider East African domain, such as the Indian Ocean dipole, El Nino Southern Oscillation and Quasibiennial Oscillation, interacted with the mesoscale features that determine precipitation over the SME.

Finally the SME receive substantial rainfall in months that are classified as “dry seasons” in equatorial East Africa. Further research should be carried out into the conditions generating rainfall in the Lake Victoria basin and equatorial East Africa during June-September and January-February, as many ecosystems and communities depend on rain that occurs in these months.

5.3.2 Modelling Wildebeest Movement and Population Dynamics in the Face of Environmental Change.

This study carried out an in depth analysis of how the SD model would respond to being driven by a spectrum of rainfall conditions. This provides guidance for future researchers interested in using the SD model for climate change impact assessment studies. However it has also

provided an opportunity to discuss potential changes that could be made to the SD model to improve its suitability for studying the potential impacts of future climate change.

Further research using the existing SD model

This study examined the impact of altered mean state precipitation, but future research could expand this work by modelling the impact of altered interannual precipitation variability on wildebeest population size.

Potential amendments to SD model code

Relatively minor amendments to the model code could change the range of questions that could be asked with this model. For example the SD model has discrepancies in the time steps of different processes (e.g. rainfall is input monthly, while vegetation dynamics are updated daily). The code could be amended to allow more processes to be updated with daily time steps. This could be valuable for analysing the impact of changes to daily rainfall.

In addition, calculation of the length of the growing season is based on annual rainfall occurring over a rainfall year, beginning on the 1st of November. If daily rainfall was input into the model, it would be a relatively small change to the code to allow the start of the growing season to begin on the day that rainfall over a certain threshold was recorded, rather than this automatically occurring on November the 1st. This may allow the impact of prolonged droughts to be better represented in the model. However further research would need to be carried out to determine whether these changes resulted in model errors, or simulated unrealistic conditions.

Comparison to other versions of the SD model

The version of the SD model used in this study did not include the impacts of multiple herbivore species interactions, changes to tree recruitment, or the impact of human activities such as

farming and poaching. However these have already been simulated in amended versions of the SD model (Holdo *et al.*, 2009a, 2010). Therefore researchers wishing to carry out climate change impact studies with the SD model should aim to choose a version of the model that best matches their research question. In addition, ideally analyses similar to those performed in Chapter 3 would be carried out on the other versions of the SD model. These would allow a comparison with the work carried out in this thesis, and would also illustrate the long-term impact of including and excluding individual ecosystem processes in the model.

Further development of the SD model

There are also a number of processes that have not been represented in any versions of the SD model, but could potentially be developed.

Local population dynamics in the SD model were based on work by Pascual *et al.* (1997), who found that multiple population models fitted wildebeest census data equally well (including age-structured models) and therefore suggested the use of the simplest unstructured model (Holdo *et al.*, 2009a). This approach successfully simulates the stable state population dynamics based on past conditions. However representing recruitment as constant risks underestimating the impact of changes to rainfall on calf mortality. While representing the population as unstructured means the lagged impacts of altered recruitment are not captured. Therefore amending the SD model to contain age-structured population dynamics (potentially based on the equations in Pascual *et al.* (1997)), and including synchronised birth pulses rather than a constant birth rate, could improve the SD model's suitability for use in climate change impact studies.

Future climate model projections suggest that East Africa may receive higher annual rainfall totals, more intense daily rainfall, and longer dry periods between rainfall events (Dosio *et al.*, 2019; Kendon *et al.*, 2019). However the SD model equations do not necessarily allow grass

and nutrient dynamics to respond in an accurate way to these changes. Plant nutrient concentrations are represented as a static layer within the model. However, plant nutrient content is known to change based on many factors, including species community composition, fire, water availability, evapotranspiration and soil nutrient concentrations (Anderson *et al.*, 2008). Many of these factors could be affected by climate change. For example, increased rainfall may cause soil leaching and reduce the fertility of the soils (Schlesinger and Bernhardt, 2013). Wetter conditions may also prevent the formation of caliche and make conditions preferable tree rooting (Sinclair *et al.*, 2008). Incorporating these dynamics into the model would be a complex task, but if they could be included they would be a valuable tool to examine the long-term dynamic changes that may occur due to climate change. Grass productivity equations were based on work by (McNaughton, 1985), which studied the relationship between grass production and rainfall. However these linear models were fitted based on annual rainfall totals between 300 and 1100 mm/year. Presumably after a certain threshold this relationship would saturate, but this is not currently represented in the model. Therefore further research into grass productivity and soil responses to more intense, variable daily rainfall, and higher annual totals, would be valuable to improve the SD model, and gain a better understanding of how the SME may be impacted by climate change.

In addition, factors that are known to have smaller impacts on wildebeest mortality (such as mass drownings (Subalusky *et al.*, 2017) or predation (Sinclair, 2003)) could potentially be developed if they were relevant to a specific research question. However, as they do not currently have a strong impact on wildebeest population size these amendments would not be likely to benefit overall model performance.

Development of new models

Finally the SD model does not represent wildebeest as individuals, so important interactions related to wildebeest navigation and behaviour are not represented. While this may be of less importance for climate change impact assessments, the development of separate, agent-based models that can incorporate factors such as memory and social interactions could help us gain a better understanding of wildebeest movement decisions, and could be a valuable area of future research (Tang and Bennett, 2010; DeAngelis and Diaz, 2019).

5.3.3 Modelling the Impact of Future Changes to Mean Precipitation on the Survival Rates of the Serengeti-Mara Wildebeest

Accurate representation of the lake breeze winds is important for modelling storm generation over the Kenya Highlands and Lake Victoria. Therefore the discrepancy between the strength of observed lake breeze wind patterns and those in the CP4-Africa hindcast is concerning. Research into the potential cause of these overly strong simulated lake breeze winds would benefit local stakeholders wishing to interpret the CP4-Africa future climate projection over this region.

In the future projection, a drying signal over the Kenya highlands was present during July and August, and was associated with southerly anomalies at 700 hPa. Further research into the dynamical causes of this drying signal would be beneficial as dry season precipitation is important to wildlife and livestock in this area.

Analysing output from climate models other than CP4-Africa, would provide information about the range of future rainfall changes that have been projected over the SME. Similarly, process-based evaluation of other high resolution regional climate models, could help identify which atmospheric processes within the models were responsible for the projected rainfall changes, and these results could be compared to the findings of this thesis. For example, models that are able to correctly capture the spatial extent of the lake breeze winds in their hindcasts,

would arguably provide more accurate projections of the future spatial distribution of rainfall over the SME.

Output from multiple climate models could also be used to drive the SD model, to examine how the ecosystem may respond to a range of projected future rainfall regimes. However, the findings of this thesis show how uncertainty and errors within both climate models and the SD model can lead to unrealistic conditions being simulated (e.g. the unrealistically high rainfall totals generated by the CP4-Africa model combined with a lack of saturation in the rainfall-grass relationship in the SD model, led to unrealistically high numbers of wildebeest being simulated). This means results from the SD model driven by different climate model output may be difficult to compare, and should likely be limited to interpreting whether future simulated rainfall conditions are favourable or unfavourable to wildebeest survival (although certain improvements to the SD model suggested in the previous section could also reduce issues related to the accumulation of error).

Finally, while interannual variability cannot be investigated in the 10 year CP4-Africa model run, longer climate model runs could be used to investigate the impact of altered projected interannual variability on the SME wildebeest.

5.4 The Unique Climatic Conditions of the Serengeti-Mara Ecosystem

This study has illustrated some of the climatic features that make the SME unique. Ecosystems that support seasonal mass migrations of large herbivores contain seasonal changes to the spatial distribution of resource availability and/or risk (Fryxell and Sinclair, 1988). The SME is not uncommon in this respect. However, there are certain features of the SME's climate that are unusual compared to the rest of the world.

The SME is situated in a unique location; a savannah-grassland ecosystem, positioned between a large lake and a mountain chain, at a latitude that is very close to the equator. The size of the lake and the height of the mountains are key reasons for the strength of the mesoscale circulations that generate storms in the eastern Lake Victoria basin (Anyah *et al.*, 2006). Therefore, if the lake were smaller or the mountains lower, the circulations may not be strong enough to generate the rainfall totals observed over the Kenya Highlands and the northern SME.

In addition, equatorial savannah and grassland ecosystems are very rare; tropical forests are much more common at the equator (Hutley and Setterfield, 2008). The presence of savannahs at the equator in East Africa are likely facilitated by its anomalously dry climate in comparison to other areas at this latitude (Aleman and Staver, 2018). The reasons for this anomalously dry climate are summarised in Section 1.5.1.1. The latitudinal position of Lake Victoria and the SME may be an important reason the ecosystem is able to sustain such a large population of migratory ungulates. The SME is arguably affected by all four wet seasons that occur over East Africa: the short rains (October-December), the austral summer rainfall season (December-February), the long rains (March-May), and the boreal summer rainfall season (June-September). The whole ecosystem is affected by the long and short rains, similar to the rest of equatorial East Africa. The south of the ecosystem receives higher rainfall totals than the north during January and February and only the north of the ecosystem receives rainfall during June-September.

The work carried out in this thesis showed that the changing gradient of rainfall across the SME is partly due to the direction of the meridional component of mid-tropospheric easterlies (winds at approximately 700 hPa), affecting the propagation direction of storms generated by lake breeze winds from Lake Victoria. However, when considering the rainfall patterns across the whole of East Africa, it's clear that the June-September and January-February rainfall over the

SME are not isolated occurrences of rainfall surrounded by regions that are completely dry. Instead, this rainfall is occurring close to the edges of the wet seasons present over much of the north of the continent in boreal summer, and the south of the continent in austral summer.

Due to its position on the periphery of the austral and boreal summer wet seasons, limited work has been carried out investigating the atmospheric conditions that cause rainfall in equatorial East Africa during the "dry seasons" (an exception is work by Vizy and Cook (2019)). This is despite the fact that many communities and ecosystems depend on dry season rainfall, and it should therefore be prioritised as an area of future research. Considering the spatial distribution of continental rainfall, it is likely that the SME receives higher "dry season" rainfall totals due to its position at the edge of the boreal and austral summer rainfall seasons (as stated by Norton-Griffiths *et al.* (1975)), than it would if rainfall were being generated by mesoscale lake- and orographic-induced circulations alone. However, it is not possible to state this is the case until further research is carried out into the atmospheric processes generating rainfall in equatorial East Africa and the Lake Victoria basin during "dry season" months.

Overall, the SME's location at the spatial limits of the boreal and austral summer rainfall seasons, means that the wildebeest can access rainfall associated with four distinct rainfall seasons (and the grass that rainfall generates) by travelling around the ecosystem. This is a distinct advantage for SME herbivores, when considering that in other parts of the continent animals would have to travel tens of thousands of kilometres to experience these four rainfall seasons. The wildebeest of the SME reside in an area influenced by four rainfall seasons, the second largest freshwater lake in the world, the topography of East African Rift Valley, and the large-scale conditions that facilitate the anomalously dry climate of East Africa. When considering all of these factors, it is clear that the climate in this area, and the ecosystem that it supports, is truly unique.

5.5 Fulfilment of Goal and Aims

The aims of the thesis were set out in sections 1.5 and 1.6 of the introduction. This section evaluates the extent to which they were fulfilled.

Aim 1: Quantify mean climatological precipitation patterns over the SME.

Climatological mean annual, monthly and hourly precipitation patterns were mapped over the SME in the 1st paper of the thesis. Annual and monthly precipitation were examined because the SD model is driven by monthly precipitation sums, and the model equations respond to annual precipitation totals.

Hourly precipitation was examined as it became clear through the course of the study that wind and precipitation patterns over the SME changed dramatically over the diurnal cycle. Therefore monthly and annual spatial patterns could only be explained if the atmospheric dynamics were analysed on an hourly timescale.

Consequently this aim was met and it also provided information that was required in later stages of the thesis.

Aim 2: Identify the key atmospheric processes generating precipitation over the SME.

The annual cycle of precipitation and the seasonally changing precipitation gradient across the SME, are factors of crucial importance to the wildebeest migration. Therefore the fulfilment of this aim focused on identifying the atmospheric processes dictating these patterns. Mid-tropospheric winds were analysed because they are associated with the movement of the tropical rainfall belt, which governs the annual precipitation cycle over East Africa. Hourly lower tropospheric winds were examined to capture local mesoscale flows such as the lake breeze winds, which reverse over the diurnal cycle.

These were found to play a crucial role in the temporal and spatial distribution of monthly precipitation over the SME. Therefore aim 2 was met, and contributed to the wider goal of the thesis by providing an explanation of the atmospheric dynamics responsible for a key driver of the wildebeest migration.

Aim 3: Identify the spatial and temporal precipitation patterns over the SME to which the wildebeest in the SD model are most sensitive.

Paper 2 analysed the impact of altered environmental conditions on simulated wildebeest population size and movement patterns. Analysing wildebeest population size allowed a central concern of the thesis to be investigated i.e. whether climate change could negatively impact wildebeest survival. The precipitation conditions to which wildebeest population size were most sensitive were annual precipitation, dry season precipitation, and precipitation over the south-east of the SME. Movement patterns were investigated due to interest in whether altered precipitation patterns could halt the migration of the SME wildebeest. The cessation of simulated migration was found to be impossible unless additional environmental gradients were removed. This meant the third paper of the thesis focused purely on wildebeest population size.

Aim 4: Assess the plausibility of the SD model response to novel precipitation conditions.

The response of the model to novel environmental conditions was compared to the literature, and the plausibility of the model's response was discussed. As stated in section 5.2.2, it would have been preferable to compare the model results to observed conditions, but gaps in annual census counts meant that this option was not available. Therefore, it can be argued that aim 4 was met to the best standard available.

Overall the work to achieve aims 3 and 4 provided a framework that allows the response of the SD model to novel precipitation patterns to be easily interpreted. It also highlighted key areas

where the model response may differ from reality. This framework was used in the final paper and proved to be a useful tool.

Aim 5: Evaluate the ability of the CP4-Africa climate model to represent climatological mean precipitation over the SME.

The CP4-Africa model was evaluated in paper 3 by comparing modelled mean annual and monthly precipitation to satellite observations, and mean hourly lower tropospheric wind patterns to reanalysis data.

Monthly and annual precipitation totals were assessed as they were used to drive the SD model. Hourly lower tropospheric winds were analysed because these were identified as being crucial to generating precipitation over the SME in paper 1.

This knowledge was used to interpret the CP4-Africa future projection, and reflect on whether it was appropriate for use in an ecological impact study. Therefore aim 5 was met and helped form a foundation for the last two aims of the thesis.

Aim 6: Investigate how climate change may alter future mean precipitation patterns over the SME

Aim 6 was initially addressed by subtracting the annual and monthly precipitation and wind vector values of the hindcast from the forecast. The results showed a projected increase in precipitation in the majority of months over the SME with the exception of August. The spatial patterns of precipitation change over the wider Lake Victoria basin and Kenya Highlands shaped the decision to examine wind patterns at 700 hPa. Changes to lower tropospheric lake breeze winds would be expected to present as a band around the lake itself, whereas the drying signal in August occurred across the whole Kenya Highlands. This suggested the change may be due to changes to wind patterns higher up in the atmosphere. The resulting southerly anomalies showed a pattern that suggested the movement of storms or moisture to a more

northward position. Overall the analysis showed how precipitation conditions over the Lake Victoria basin and SME may change in individual months, and also provided a possible explanation for the spatial distribution of these changes. Therefore the work met aim 6, and it also highlighted a potential future research direction for those interested in altered precipitation over the Lake Victoria basin.

Aim 7: Model the wildebeest response to projected future changes in mean climatological rainfall.

To achieve the final aim, the SD model was driven with mean observed precipitation, mean hindcast precipitation, and mean future precipitation. The model output showed an increase in wildebeest population size as a response to higher precipitation totals in all months except August. Therefore aim 7 was met through a set of relatively simple model runs. Nonetheless, the interpretation of the results drew on all aspects of the thesis.

Goal: Understand how climate change may alter mean precipitation patterns over the SME and thus impact the migratory wildebeest

The results of the 3rd paper showed that, according to the CP4-Africa model, future net mean precipitation over the SME will increase in every month except August, and benefit the migratory SME wildebeest. These results show how the climate of the SME may change and affect the migratory wildebeest. Nevertheless, it is the work of the thesis as a whole that has provided a deeper level of insight as to *why* this may happen.

A greater understanding of the past climate system, and the effect of changes to mean precipitation on the wildebeest, was developed in the first two papers of the thesis. This allowed the climate model hindcast to be evaluated on its ability to simulate the climatic conditions of most importance to wildebeest ecology, which provided answers as to why the model may not be able to simulate certain precipitation features over the SME. The CP4-Africa precipitation

output showed how precipitation may change in the future. However, knowledge of the importance of 700 hPa wind patterns to the direction of local storm propagation, guided an investigation into whether changes at this pressure level may be affecting the distribution of future precipitation patterns. This found an association between a stronger southerly component in future 700 hPa winds and the distribution of the projected future precipitation changes around the Lake Victoria basin. The output from the SD model showed how the population size may respond to the future precipitation conditions, but the knowledge of how the population responds to different spatiotemporal distributions of driving precipitation provided greater insight into why the population responded the way it did.

Overall, the third paper provided the results showing how climate change may alter mean precipitation conditions over the SME and impact the migratory wildebeest. However, the thesis as a whole has provided a deeper understanding of these changes, and thus achieved the goal of the study.

5.6 Contribution to Knowledge

The most recent published description of the SME climate was written in 1975 (Norton-Griffiths *et al.*, 1975). To respond to this gap in the literature the first paper set out to provide an updated description of climatological mean precipitation and its atmospheric drivers over the SME, using datasets with higher resolution and greater spatial and temporal coverage than was previously available. Consequently, this thesis has provided the first study of annual and monthly mean precipitation conditions over the SME that meet the WMO's recommendation of 30 years of data, as well as the first analysis of hourly wind and precipitation patterns over this area. The analysis identified interactions between the local topography, large-scale easterlies and lake breeze westerlies as the key atmospheric processes governing the distribution of precipitation over the SME. These features had previously been suggested as

important to the local precipitation patterns, but this work is the first to map the spatial extent of their relative influences. A key finding was that lake breeze winds from Lake Victoria were shown to have an important role over a much larger portion of the ecosystem than previously reported. This provided a new explanation for spatial differences in long rains peak precipitation month observed across the ecosystem. In addition, knowledge of the extent of Lake Victoria's influence is crucially important for understanding how climate change may affect this region in the future, as areas influenced by Lake Victoria are likely to be impacted in a different way to those that receive moisture solely from the Indian Ocean. Finally, this paper suggested an updated explanation for the changing seasonal orientation of the precipitation gradient across the SME. Previous work had identified the passage of the tropical rainfall belt, lake breeze winds in the north, and the rain shadow in the east as important contributors to this process (Norton-Griffiths *et al.*, 1975). However, this thesis showed that a lower tropospheric wind convergence line is typically present over the SME, which contrasts with the direction of mid-tropospheric easterly winds, suggesting that storms are generated at the wind convergence line and blown in the direction of those mid-tropospheric easterlies. The thesis therefore provides a potential explanation for the distribution of precipitation over the SME in every month, while previous studies did not provide an explanation for the orientation of the precipitation gradient in months, such as January.

The incorporation of key ecological dynamics within the SD model, and its past use in examining the impact of altered precipitation on the SME wildebeest, meant that the SD model was potentially a powerful tool for use in ecological climate change impact studies. However, no previous work had been carried out examining the response of the model to precipitation conditions outside of those recorded from 1960-2006 (Holdo *et al.*, 2010). The second paper therefore aimed to assess the response of the SD model to novel precipitation regimes, and thus examine its suitability for use in climate change impact studies.

The second paper found that modelled wildebeest population size was most sensitive to changes in annual precipitation, dry season precipitation, and precipitation over the south-east. These findings were the result of sensitivity and elasticity analyses, work that had not previously been carried out on this model. The results also provided a new framework which can allow the wildebeest population size, which results from the SD model being driven by novel precipitation patterns, to be interpreted as a response to the above key precipitation regimes. The work also highlighted key areas to check where the model response risks differing from reality.

In addition to filling the above gaps in the literature, the study found that, as long as the annual cycle of precipitation was present, altered spatial distributions of precipitation were not able to stop the modelled SME wildebeest from migrating. Simulated migration only ceased if all environmental gradients were removed. This is the first study that has simulated the impact of altered spatial distribution of precipitation across the SME ecosystem on the movement patterns of the migratory wildebeest. The outcome highlighted the fact that current future projections of rainfall change over East Africa are unlikely to eliminate the nutritional and precipitation gradients across the ecosystem (which are the drivers of the migration), but increased rainfall totals could weaken them. Higher rainfall totals in the south-east could potentially increase soil leaching, which in turn could alter the nutritional and vegetative gradients across the SME (dynamics that the model was not able to capture).

The third paper aimed to evaluate the ability of a climate model to simulate mean precipitation over the SME, examine projected future changes to the regional precipitation, and model the impact of that change on the SME wildebeest. The evaluation of the CP4-Africa hindcast over the SME was novel in its approach for two reasons. First, it is unusual for climate models to be evaluated based on their capacity to simulate ecologically relevant climatic variables and the atmospheric processes responsible for generating them. Second, this work is currently the only

analysis of monthly CP4-Africa data over the Eastern Lake Victoria basin. The work identified an association between abnormally strong lake breeze winds and a dry bias over the shoreline of Lake Victoria and the west of the SME, which had not previously been described in the literature. It also suggested that stronger lake breeze winds may lead to stronger convergence over the rift highlands, and lead to anomalously high precipitation totals over these areas, thus explaining the inability of the CP4-Africa model to capture the zonal component of the precipitation gradient over the SME. This has not previously been suggested, but builds on previous work that found abnormally strong night-time convergence within the CP4-Africa hindcast was responsible for anomalously high precipitation totals over Lake Victoria (Finney *et al.*, 2019).

The examination of the CP4-Africa projected future precipitation and wind patterns provided the first description of future climate model output over the SME. The results showed that mean climatological precipitation is projected to increase over the SME in the future. The thesis identified a potential relationship between southerly anomalies in CP4 future projection and altered precipitation conditions over the eastern Lake Victoria basin and SME. The impact of mid-tropospheric southerly anomalies over the Lake Victoria basin have not previously been described in the literature, in either reanalysis or modelled atmospheric data. As these wind anomalies appear over much of the Lake Victoria basin, and appear to be associated with altered future precipitation patterns, they are of importance to both the people and wildlife of this region.

The final part of the third paper modelled the impact of the altered precipitation on the population size of the SME wildebeest. This analysis was the first study to examine the potential impact of climate change on the SME wildebeest using climate model output data. The results showed that the increased net precipitation across the ecosystem in every month except August generated a mean state that would be beneficial for the migratory wildebeest of

the SME. This is an important finding for those working to protect the SME and its iconic wildlife.

The final paper, and the thesis as a whole, provided a novel example of an ecological impact study that also interrogated the atmospheric dynamics of the driving climate model. It is rare for ecological impact studies to do this, but is arguably a valuable type of interdisciplinary research that allows scientists in both fields to better understand how future climate change may affect ecological processes.

Overall the thesis has integrated climate science and ecology to a much closer degree than is typically carried out. This illustrates the fascinating science that can result from interdisciplinary studies, and provides a case study for future researchers wishing to model the ecological impact of climate change.

References

Aleman, J. C. and Staver, A. C. (2018) 'Spatial patterns in the global distributions of savanna and forest', *Global Ecology and Biogeography*, 27(7), pp. 792–803. doi: 10.1111/geb.12739.

Anderson, G. D. and Talbot, L. M. (1965) 'Soil Factors Affecting the Distribution of the Grassland Types and their Utilization by Wild Animals on the Serengeti Plains, Tanganyika', *The Journal of Ecology*, 53(1), p. 33. doi: 10.2307/2257564.

Anderson, T. M., Bukombe, J. and Metzger, K. L. (2015) 'Spatial and Temporal Drivers of Plant Structure and Diversity in Serengeti Savannas', in Sinclair, A. R. E., Metzger, K. L., Mduma, S. A. R., and Fryxell, J. M. (eds) *Serengeti IV: Sustaining Biodiversity in a Coupled Human-Natural System*. Chicago and London: The University of Chicago Press, pp. 105–124.

Anderson, T. M., Dempewolf, J., Metzger, K. L., Reed, D. N. and Serneels, S. (2008) 'Generation and Maintenance of Heterogeneity in the Serengeti Ecosystem', in Sinclair, A. R. E., Packer, C., Mduma, S. A. R., and Fryxell, J. M. (eds) *Serengeti III: Human Impacts on Ecosystem Dynamics*. Chicago and London, pp. 135–182.

Anderson, T. M., Griffith, D. M., Grace, J. B., Lind, E. M., Adler, P. B., Biederman, L. A., Blumenthal, D. M., Daleo, P., Firn, J., Hagenah, N., Harpole, W. S., MacDougall, A. S., McCulley, R. L., Prober, S. M., Risch, A. C., Sankaran, M., Schütz, M., Seabloom, E. W., Stevens, C. J., Sullivan, L. L., Wragg, P. D. and Borer, E. T. (2018) 'Herbivory and eutrophication mediate grassland plant nutrient responses across a global climatic gradient', *Ecology*, 99(4), pp. 822–831. doi: 10.1002/ecy.2175.

Anderson, T. M., Hopcraft, J. G. C., Eby, S., Ritchie, M., Grace, J. B. and Olff, H. (2010) 'Landscape-scale analyses suggest both nutrient and antipredator advantages to Serengeti herbivore hotspots', *Ecology*, 91(5), pp. 1519–1529. doi: 10.1890/09-0739.1.

Anderson, T. M., Ritchie, M. E., Mayemba, E., Eby, S., Grace, J. B. and McNaughton, S. J. (2007) 'Forage Nutritive Quality in the Serengeti Ecosystem: The Roles of Fire and Herbivory', *The American Naturalist*, 170(3), pp. 343–357. doi: 10.1086/520120.

Anderson, T. M., Schütz, M. and Risch, A. C. (2014) 'Endozoochorous seed dispersal and germination strategies of Serengeti plants', *Journal of Vegetation Science*. Edited by H. H. Bruun, 25(3), pp. 636–647. doi: 10.1111/jvs.12110.

Angerer, J. P., Fox, W. E. and Wolfe, J. E. (2016) 'Land Degradation in Rangeland Ecosystems', in *Biological and Environmental Hazards, Risks, and Disasters*. Elsevier, pp. 277–311. doi: 10.1016/B978-0-12-394847-2.00017-6.

Anyah, R. O., Semazzi, F. H. M. and Xie, L. (2006) 'Simulated Physical Mechanisms Associated with Climate Variability over Lake Victoria Basin in East Africa', *Monthly Weather Review*, 134(12), pp. 3588–3609. doi: 10.1175/MWR3266.1.

Archibald, S. and Bond, W. J. (2004) 'Grazer movements: spatial and temporal responses to burning in a tall-grass African savanna', *International Journal of Wildland Fire*, 13(3), p. 377. doi: 10.1071/WF03070.

Baker, D. J., Hartley, A. J., Pearce-Higgins, J. W., Jones, R. G. and Willis, S. G. (2017) 'Neglected issues in using weather and climate information in ecology and biogeography', *Diversity and Distributions*. Edited by J. Serra-Diaz. doi: 10.1111/ddi.12527.

Barnes, B. V., Zak, D. R., Denton, S. R. and Spurr, S. H. (1998) 'Landscape Ecosystems at Multiple Spatial Scales', in *Forest ecology*. 4th edn. New York: John Wiley & Sons, pp. 21–40.

Barrett, T. and Rossiter, P. B. (1999) 'Rinderpest: The Disease and Its Impact on Humans and Animals', in *Advances in virus research*, pp. 89–110. doi: 10.1016/S0065-3527(08)60344-9.

Beale, C. M., Courtney Mustaphi, C. J., Morrison, T. A., Archibald, S., Anderson, T. M., Dobson, A. P., Donaldson, J. E., Hempson, G. P., Probert, J. and Parr, C. L. (2018) 'Pyrodiversity interacts with rainfall to increase bird and mammal richness in African savannas', *Ecology Letters*. Edited by M. Mayfield, 21(4), pp. 557–567. doi: 10.1111/ele.12921.

Beaumont, L. J., Hughes, L. and Pitman, A. J. (2008) 'Why is the choice of future climate scenarios for species distribution modelling important?', *Ecology Letters*, 11(11), pp. 1135–1146. doi: 10.1111/j.1461-0248.2008.01231.x.

Belsky, A. J. (1984) 'Role of small browsing mammals in preventing woodland regeneration in the Serengeti National Park, Tanzania', *African Journal of Ecology*, 22(4), pp. 271–279. doi: 10.1111/j.1365-2028.1984.tb00701.x.

Belsky, A. J. (1992) 'Effects of Grazing , Competition , Disturbance and Fire on Species Composition and Diversity in Grassland Communities Stable', *Journal of Vegetation Science*, 3(2), pp. 187–200.

Belsky, A. J. (1994) 'Influences of Trees on Savanna Productivity: Tests of Shade, Nutrients, and Tree-Grass Competition', *Ecology*, 75(4), pp. 922–932. doi: 10.2307/1939416.

Belsky, A. J., Amundson, R. G., Duxbury, J. M., Riha, S. J., Ali, A. R. and Mwonga, S. M. (1989) 'The Effects of Trees on Their Physical, Chemical and Biological Environments in a Semi-Arid Savanna in Kenya', *The Journal of Applied Ecology*, 26(3), p. 1005. doi: 10.2307/2403708.

Benton, T. G. and Grant, A. (1999) 'Elasticity analysis as an important tool in evolutionary and population ecology', *Trends in Ecology and Evolution*, 14(12), pp. 467–471. doi: 10.1016/S0169-5347(99)01724-3.

Bignell, D. E. and Eggleton, P. (2000) 'Termites in Ecosystems', in *Termites: Evolution, Sociality, Symbioses, Ecology*. Dordrecht: Springer Netherlands, pp. 363–387. doi: 10.1007/978-94-017-3223-9_17.

Bolger, D. T., Newmark, W. D., Morrison, T. A. and Doak, D. F. (2008) 'The need for integrative approaches to understand and conserve migratory ungulates', *Ecology Letters*, 11(1), pp. 070926060247001-??? doi: 10.1111/j.1461-0248.2007.01109.x.

Camberlin, P. (1996) 'Intraseasonal variations of June-September rainfall and upper-air circulation over Kenya', *Theoretical and Applied Climatology*, 54(3–4), pp. 107–115. doi: 10.1007/BF00865153.

Camberlin, P. (2018) 'Climate of Eastern Africa', in *Oxford Research Encyclopedia of Climate Science*. Oxford University Press, pp. 1–52. doi: 10.1093/acrefore/9780190228620.013.512.

Camberlin, P., Boyard-Micheau, Joseph, Philippon, N., Baron, C., Leclerc, C. and Mwongera, C. (2014) 'Climatic gradients along the windward slopes of Mount Kenya and their implication for crop risks. Part 1: Climate variability', *International Journal of Climatology*, 34, pp. 2136–2152. doi: 10.1002/joc.3427.

Camberlin, P., Gitau, W., Planchon, O., Dubreuil, V., Funatsu, B. M. and Philippon, N. (2018) 'Major role of water bodies on diurnal precipitation regimes in Eastern Africa', *International Journal of Climatology*, 38(2), pp. 613–629. doi: 10.1002/joc.5197.

Codron, D., Lee-Thorp, J. A., Sponheimer, M. and Codron, J. (2009) 'Stable carbon isotope reconstruction of ungulate diet changes through the seasonal cycle', *South African Journal of Wildlife Research*, 37(2), pp. 117–125. doi: 10.3957/0379-4369-37.2.117.

Coleman, J. and Law, K. (2015) 'Meteorology', in *Reference Module in Earth Systems and Environmental Sciences*. Elsevier, pp. 1–7. doi: 10.1016/B978-0-12-409548-9.09492-6.

Collins, M., Knutti, R., Arblaster, J., Dufresne, J.-L., Fichefet, T., Friedlingstein, P., Gao, X., Gutowski, W. J., Johns, T., Krinner, G., Shongwe, M., Tebaldi, C., Weaver, A. J. and Wehner, M. (2013) 'Long-term Climate Change: Projections, Commitments and Irreversibility', in Stocker, T. F., Qin, D., Plattner, G.-K., Tignor, M., Allen, S. K., Boschung, J., Nauels, A., Zia, Y., Bex, V., and Midgley, P. M. (eds) *Climate Change 2013: The Physical Science Basis. Contribution of Working Group I to the Fifth Assessment Report of the Intergovernmental Panel on Climate Change*. Cambridge, United Kingdom and New York, NY, USA: Cambridge University Press, pp. 1029–1136. doi: 10.1017/CBO9781107415324.024.

Copernicus Climate Change Service (C3S) (2017) *ERA5: Fifth generation of ECMWF atmospheric reanalyses of the global climate, Copernicus climate Change Service Climate Data store (CDS)*. Available at: https://cds.climate.copernicus.eu/cdsapp#!/home (Accessed: 1 July 2020).

Copernicus Climate Change Service (C3S) (2019) *ERA5 monthly averaged data on single levels from 1979 to present*. doi: 10.24381/cds.f17050d7.

Coulson, T., Catchpole, E. A., Albon, S. D., Morgan, B. J. T., Pemberton, J. M., Clutton-Brock, T. H., Crawley, M. J. and Grenfell, B. T. (2001) 'Age, sex, density, winter weather, and population crashes in Soay sheep', *Science*, 292(5521), pp. 1528–1531.

Cubasch, U., Wuebbles, D., Chen, D., Facchini, M. C., Frame, D., Mahowald, N. and Winther, J.-G. (2013) 'Introduction in Climate Change 2013', *Intergovernmental Panel on Climate Change 2013: The Physical Science Basis. Contribution of Working Group I to the Fifth Assessment Report of the Intergovernmental Panel on Climate Change*, pp. 119–158. doi: 10.1017/CBO9781107415324.007.

Curtin, N. A., Bartlam-Brooks, H. L. A., Hubel, T. Y., Lowe, J. C., Gardner-Medwin, A. R., Bennitt, E., Amos, S. J., Lorenc, M., West, T. G. and Wilson, A. M. (2018) 'Remarkable

muscles, remarkable locomotion in desert-dwelling wildebeest', *Nature*. Springer US, 563(7731), pp. 393–396. doi: 10.1038/s41586-018-0602-4.

Davies, T. D., Vincent, C. E. and Beresford, A. K. C. (1985) 'July-August Rainfall in West-Central Kenya', *Journal of Climatology*, 5, pp. 17–33.

Dawson, J. B. (2008) 'Chapter 7 The Neogene-Recent volcanic rocks', *Geological Society, London, Memoirs*, 33(1), pp. 39–77. doi: 10.1144/M33.7.

DeAngelis, D. L. and Diaz, S. G. (2019) 'Decision-Making in Agent-Based Modeling: A Current Review and Future Prospectus', *Frontiers in Ecology and Evolution*, 6(JAN), pp. 1–15. doi: 10.3389/fevo.2018.00237.

Dee, D. P., Uppala, S. M., Simmons, A. J., Berrisford, P., Poli, P., Kobayashi, S., Andrae, U., Balmaseda, M. A., Balsamo, G., Bauer, P., Bechtold, P., Beljaars, A. C. M., van de Berg, L., Bidlot, J., Bormann, N., Delsol, C., Dragani, R., Fuentes, M., Geer, A. J., Haimberger, L., Healy, S. B., Hersbach, H., Hólm, E. V., Isaksen, L., Kållberg, P., Köhler, M., Matricardi, M., McNally, A. P., Monge-Sanz, B. M., Morcrette, J.-J., Park, B.-K., Peubey, C., de Rosnay, P., Tavolato, C., Thépaut, J.-N. and Vitart, F. (2011) 'The ERA-Interim reanalysis: configuration and performance of the data assimilation system', *Quarterly Journal of the Royal Meteorological Society*, 137(656), pp. 553–597. doi: 10.1002/qj.828.

Delcourt, H. R. and Delcourt, P. A. (1988) 'Quaternary landscape ecology: Relevant scales in space and time', *Landscape Ecology*, 2(1), pp. 23–44. doi: 10.1007/BF00138906.

Derin, Y. and Yilmaz, K. K. (2014) 'Evaluation of Multiple Satellite-Based Precipitation Products over Complex Topography', *Journal of Hydrometeorology*, 15(4), pp. 1498–1516. doi: 10.1175/JHM-D-13-0191.1.

Dezfuli, A. K. (2011) 'Spatio-temporal variability of seasonal rainfall in western equatorial

Africa', *Theoretical and Applied Climatology*, 104(1–2), pp. 57–69. doi: 10.1007/s00704-010-0321-8.

Dinku, T., Ceccato, P., Grover-Kopec, E., Lemma, M., Connor, S. J. and Ropelewski, C. F. (2007) 'Validation of satellite rainfall products over East Africa's complex topography', *International Journal of Remote Sensing*, 28(7), pp. 1503–1526. doi: 10.1080/01431160600954688.

Dinku, T., Funk, C., Peterson, P., Maidment, R., Tadesse, T., Gadain, H. and Ceccato, P. (2018) 'Validation of the CHIRPS satellite rainfall estimates over eastern Africa', *Quarterly Journal of the Royal Meteorological Society*, 144(S1), pp. 292–312. doi: 10.1002/qj.3244.

Dobson, A. (1995) 'The Ecology and Epidemiology of Rinderpest Virus in Serengeti and Ngorongoro Conservation Area', in Sinclair, A. R. E. and Arcese, P. (eds) *Serengeti II: Dynamics, Management, and Conservation of an Ecosystem*. Chicago and London: The University of Chicago Press, pp. 485–505.

Dobson, A. P., Borner, M., Sinclair, A. R. E., Hudson, P. J., Anderson, T. M., Bigurube, G., Davenport, T. B. B., Deutsch, J., Durant, S. M., Estes, R. D., Estes, A. B., Fryxell, J., Foley, C., Gadd, M. E., Haydon, D., Holdo, R., Holt, R. D., Homewood, K., Hopcraft, J. G. C., Hilborn, R., Jambiya, G. L. K., Laurenson, M. K., Melamari, L., Morindat, A. O., Ogutu, J. O., Schaller, G. and Wolanski, E. (2010) 'Road will ruin Serengeti', *Nature*, 467(7313), pp. 272–273. doi: 10.1038/467272a.

Dosio, A., Jones, R. G., Jack, C., Lennard, C., Nikulin, G. and Hewitson, B. (2019) 'What can we know about future precipitation in Africa? Robustness, significance and added value of projections from a large ensemble of regional climate models', *Climate Dynamics*. Springer Berlin Heidelberg, 53(9–10), pp. 5833–5858. doi: 10.1007/s00382-019-04900-3.

Duane, W. J., Pepin, N. C., Losleben, M. L. and Hardy, D. R. (2008) 'General Characteristics

of Temperature and Humidity Variability on Kilimanjaro, Tanzania', *Arctic, Antarctic, and Alpine Research*, 40(2), pp. 323–334. doi: 10.1657/1523-0430(06-127)[DUANE]2.0.CO;2.

Dublin, H. T. (1995) 'Vegetation Dynamics in the Serengeti-Mara Ecosystem: The Role of Elephants, Fire, and Other Factors', in Sinclair, A. R. E. and Arcese, P. (eds) *Serengeti II: Dynamics, Management, and Conservation of an Ecosystem*. Chicago and London: The University of Chicago Press, pp. 71–90.

Dublin, H. T., Sinclair, A. R. E. and McGlade, J. (1990) 'Elephants and Fire as Causes of Multiple Stable States in the Serengeti-Mara Woodlands', *The Journal of Animal Ecology*, 59(3), p. 1147. doi: 10.2307/5037.

Dunning, C. M., Black, E. and Allan, R. P. (2018) 'Later Wet Seasons with More Intense Rainfall over Africa under Future Climate Change', *Journal of Climate*, 31(23), pp. 9719–9738. doi: 10.1175/JCLI-D-18-0102.1.

Dunning, C. M., Black, E. C. L. and Allan, R. P. (2016) 'The onset and cessation of seasonal rainfall over Africa', *Journal of Geophysical Research: Atmospheres*, 121(19), pp. 11405–11424. doi: 10.1002/2016JD025428.

Eby, S., Dempewolf, J., Holdo, R. M. and Metzger, K. L. (2015) 'Fire in the Serengeti Ecosystem: History, Drivers, and Consequences', in Sinclair, A. R. E., Metzger, K. L., Mduma, S. A. R., and Fryxell, J. M. (eds) *Serengeti IV: Sustaining Biodiversity in a Coupled Human-Natural System*. Chicago and London: The University of Chicago Press, pp. 73–104.

Encyclopaedia Britannica (no date) *East African Rift System*. Available at: https://www.britannica.com/place/East-African-Rift-System#/media/1/176462/1182 (Accessed: 7 April 2020).

Endris, H. S., Lennard, C., Hewitson, B., Dosio, A., Nikulin, G. and Artan, G. A. (2019) 'Future

changes in rainfall associated with ENSO, IOD and changes in the mean state over Eastern Africa', *Climate Dynamics*. Springer Berlin Heidelberg, 52(3–4), pp. 2029–2053. doi: 10.1007/s00382-018-4239-7.

Estes, R. D. (2014) *The Gnu's World: Serengeti Wildebeest Ecology and Life History*. Berkeley and Los Angeles, California: University of California Press.

European Network for Earth System Modelling (no date) *CMIP5 Models and Grid Resolution*. Available at: https://verc.enes.org/data/enes-model-data/cmip5/resolution (Accessed: 11 April 2020).

Evans, J. P. (2011) 'CORDEX – An international climate downscaling initiative', *19th International Congress on Modelling and Simulation*, (December), pp. 12–16. Available at: http://mssanz.org.au/modsim2011.

February, E. C., Higgins, S. I., Bond, W. J. and Swemmer, L. (2013) 'Influence of competition and rainfall manipulation on the growth responses of savanna trees and grasses', *Ecology*, 94(5), pp. 1155–1164. doi: 10.1890/12-0540.1.

Findlater, J. (1971) *Mean Monthly Airflow At Low Levels*, *Geophysical Memoirs No. 115*. London: Her Majesty's Stationery Office.

Finney, D. L., Marsham, J. H., Jackson, L. S., Kendon, E. J., Rowell, D. P., Boorman, P. M., Keane, R. J., Stratton, R. A. and Senior, C. A. (2019) 'Implications of Improved Representation of Convection for the East Africa Water Budget Using a Convection-Permitting Model', *Journal of Climate*, 32(7), pp. 2109–2129. doi: 10.1175/JCLI-D-18-0387.1.

Finney, D. L., Marsham, J. H., Rowell, D. P., Kendon, E. J., Tucker, S. O., Stratton, R. A. and Jackson, L. S. (2020) 'Effects of Explicit Convection on Future Projections of Mesoscale Circulations, Rainfall, and Rainfall Extremes over Eastern Africa', *Journal of Climate*, 33(7),

pp. 2701–2718. doi: 10.1175/JCLI-D-19-0328.1.

Flato, G., Marotzke, J., Abiodun, B., Braconnot, P., Chou, S. C., Collins, W., Coz, P., Driouech, F., Gleckler, P., Guilyardi, E., Jakob, C., Kattsov, V., Reason, C. and Rummukainen, M. (2013) 'Evaluation of Climate Models', in Stocker, T. F., Qin, D., Plattner, G.-K., Tignor, M., Allen, S. K., Boschung, J., Nauels, A., Xia, Y., Bex, V., and Midgley, P. M. (eds) *Climate Change 2013: The Physical Science Basis. Contribution of Working Group I to the Fifth Assessment Report of the Intergovernmental Panel on Climate Change*. Cambridge, United Kingdom and New York, NY, USA: Cambridge University Press, pp. 741–866.

Fraedrich, K. (1972) 'A simple climatological model of the dynamics and energetics of the nocturnal circulation at Lake Victoria', *Quarterly Journal of the Royal Meteorological Society*, 98, pp. 322–335.

Frank, D. A., McNaughton, S. J. and Tracy, B. F. (1998) 'The Ecology of the Earth's Grazing Ecosystems', *BioScience*, 48(7), pp. 513–521. doi: 10.2307/1313313.

Freymann, B. P., Buitenwerf, R., Desouza, O. and Olff, H. (2008) 'The importance of termites (Isoptera) for the recycling of herbivore dung in tropical ecosystems: a review', *European Journal of Entomology*, 105(2), pp. 165–173. doi: 10.14411/eje.2008.025.

Freymann, B. P., de Visser, S. N., Mayemba, E. P. and Olff, H. (2007) 'Termites of the Genus Odontotermes are Optionally Keratophagous', *Ecotropia*, 13(2), pp. 143–147.

Fryxell, J. M. (1995) 'Aggregation and migration by grazing ungulates in relation to resources and predators', in Sinclair, A. R. E. and Arcese, P. . (eds) *Serengeti II: Dynamics, management, and conservation of an ecosystem*. Chicago and London: University of Chicago Press, pp. 257–273.

Fryxell, J. M., Greever, J. and Sinclair, A. R. E. (1988) 'Why are Migratory Ungulates So

Abundant?', *The American Naturalist*, 131(6), pp. 781–798.

Fryxell, J. M., Metzger, K. L., Packer, C., Sinclair, A. R. E. and Mduma, S. A. R. (2015) 'Climate-Induced Effects on the Serengeti Mammalian Food Web', in Sinclair, A. R. E., Metzger, K. L., Mduma, S. A. R., and Fryxell, J. M. (eds) *Serengeti IV: Sustaining Biodiversity in a Coupled Human-Natural System*. Chicago and London: University of Chicago Press.

Fryxell, J. M. and Sinclair, A. R. E. (1988) 'Causes and consequences of migration by large herbivores', *Trends in Ecology & Evolution*, 3(9), pp. 237–241. doi: 10.1016/0169-5347(88)90166-8.

Funk, C. C., Peterson, P. J., Landsfeld, M. F., Pedreros, D. H., Verdin, J. P., Rowland, J. D., Romero, B. E., Husak, G. J., Michaelsen, J. C. and Verdin, A. P. (2014) *A Quasi-Global Precipitation Time Series for Drought Monitoring, U.S. Geological Survey Data Series 832*. Available at: https://dx.doi.org/10.3133/ds832.

Funk, C., Hoell, A., Shukla, S., Husak, G. and Michaelsen, J. (2016) 'The East African Monsoon System: Seasonal Climatologies and Recent Variations', in *Springer Climate*, pp. 163–185. doi: 10.1007/978-3-319-21650-8_8.

Funk, C., Peterson, P., Landsfeld, M., Pedreros, D., Verdin, J., Shukla, S., Husak, G., Rowland, J., Harrison, L., Hoell, A. and Michaelsen, J. (2015) 'The climate hazards infrared precipitation with stations—a new environmental record for monitoring extremes', *Scientific Data*, 2(1), p. 150066. doi: 10.1038/sdata.2015.66.

Gagnon, M. and Chew, A. E. (2000) 'Dietary Preferences in Extant African Bovidae', *Journal of Mammalogy*, 81(2), pp. 490–511.

Geerts, B. and Dejene, T. (2005) 'Regional and Diurnal Variability of the Vertical Structure of Precipitation Systems in Africa Based on Spaceborne Radar Data', *Journal of Climate*, 18(7),

pp. 893–916. doi: 10.1175/JCLI-3316.1.

Gereta, E., Mwangomo, E. and Wolanski, E. (2009) ‘Ecohydrology as a tool for the survival of the threatened Serengeti ecosystem’, *Ecohydrology & Hydrobiology*. Elsevier, 9(1), pp. 115–124. doi: 10.2478/v10104-009-0035-7.

Gesch, D. B., Verdin, K. L. and Greenlee, S. K. (1999) ‘New land surface digital elevation model covers the Earth’, *Eos, Transactions American Geophysical Union*, 80(6), p. 69. doi: 10.1029/99EO00050.

Gong, X. and Richman, M. B. (1995) ‘On the Application of Cluster Analysis to Growing Season Precipitation Data in North America East of the Rockies’, *Journal of Climate*, 8(4), pp. 897–931. doi: 10.1175/1520-0442(1995)008<0897:OTAOCA>2.0.CO;2.

Gregory, P. J. and Nortcliff, S. (eds) (2013) *Soil Conditions and Plant Growth*. Oxford: Blackwell Publishing Ltd. doi: 10.1002/9781118337295.

Griffith, D. M., Anderson, T. M. and Hamilton, E. W. (2017) ‘Ungulate grazing drives higher ramet turnover in sodium-adapted Serengeti grasses’, *Journal of Vegetation Science*. Edited by D. Ward, 28(4), pp. 815–823. doi: 10.1111/jvs.12526.

Haile, A. T., Habib, E., Elsaadani, M. and Rientjes, T. (2013) ‘Inter-comparison of satellite rainfall products for representing rainfall diurnal cycle over the Nile basin’, *International Journal of Applied Earth Observation and Geoinformation*. Elsevier B.V., 21(1), pp. 230–240. doi: 10.1016/j.jag.2012.08.012.

Hamilton, E. W. and Frank, D. A. (2001) ‘Can Plants Stimulate Soil Microbes and Their Own Nutrient Supply? Evidence from a Grazing Tolerant Grass’, *Ecology*, 82(9), p. 2397. doi: 10.2307/2679923.

Harris, G., Thirgood, S., Hopcraft, J., Cromsight, J. and Berger, J. (2009) ‘Global decline in

aggregated migrations of large terrestrial mammals', *Endangered Species Research*, 7(1), pp. 55–76. doi: 10.3354/esr00173.

Herlocker, D. J. (1976) *Structure, Composition and Environment of Some Woodland Vegetation Types of the Serengeti National Park, Tanzania*. Texas A&M University. Available at: http://scholar.google.com/scholar?hl=en&btnG=Search&q=intitle:Xerox+University+Microfilms+300#5.

Hersbach, H., Bell, B., Berrisford, P., Hirahara, S., Horányi, A., Muñoz-Sabater, J., Nicolas, J., Peubey, C., Radu, R., Schepers, D., Simmons, A., Soci, C., Abdalla, S., Abellan, X., Balsamo, G., Bechtold, P., Biavati, G., Bidlot, J., Bonavita, M., Chiara, G., Dahlgren, P., Dee, D., Diamantakis, M., Dragani, R., Flemming, J., Forbes, R., Fuentes, M., Geer, A., Haimberger, L., Healy, S., Hogan, R. J., Hólm, E., Janisková, M., Keeley, S., Laloyaux, P., Lopez, P., Lupu, C., Radnoti, G., Rosnay, P., Rozum, I., Vamborg, F., Villaume, S. and Thépaut, J. (2020) 'The ERA5 global reanalysis', *Quarterly Journal of the Royal Meteorological Society*, 146(730), pp. 1999–2049. doi: 10.1002/qj.3803.

Higgins, S. I., Bond, W. J. and Trollope, W. S. W. (2000) 'Fire, resprouting and variability: a recipe for grass-tree coexistence in savanna', *Journal of Ecology*, 88(2), pp. 213–229. doi: 10.1046/j.1365-2745.2000.00435.x.

Hoell, A., Hoerling, M., Eischeid, J., Quan, X.-W. and Liebmann, B. (2017) 'Reconciling Theories for Human and Natural Attribution of Recent East Africa Drying', *Journal of Climate*, 30(6), pp. 1939–1957. doi: 10.1175/JCLI-D-16-0558.1.

Holdo, R. M., Fryxell, J. M., Sinclair, A. R. E., Dobson, A. and Holt, R. D. (2011a) 'Predicted Impact of Barriers to Migration on the Serengeti Wildebeest Population', *PLoS ONE*, 6(1), p. e16370. doi: 10.1371/journal.pone.0016370.

Holdo, R. M., Galvin, K. A., Knapp, E., Polasky, S., Hlborn, R. and Holt, R. D. (2010) 'Responses to alternative rainfall regimes and antipoaching in a migratory system', *Ecological Applications*, 20(2), pp. 381–397.

Holdo, R. M., Holt, R. D., Coughenour, M. B. and Ritchie, M. E. (2007) 'Plant productivity and soil nitrogen as a function of grazing, migration and fire in an African savanna', *Journal of Ecology*, 95(1), pp. 115–128. doi: 10.1111/j.1365-2745.2006.01192.x.

Holdo, R. M., Holt, R. D. and Fryxell, J. M. (2009a) 'Grazers, browsers, and fire influence the extent and spatial pattern of tree cover in the Serengeti', *Ecological Applications*, 19(1), pp. 95–109. doi: 10.1890/07-1954.1.

Holdo, R. M., Holt, R. D. and Fryxell, J. M. (2009b) 'Opposing Rainfall and Plant Nutritional Gradients Best Explain the Wildebeest Migration in the Serengeti', *The American Naturalist*, 173(4), pp. 431–445. doi: 10.1086/597229.

Holdo, R. M., Holt, R. D., Sinclair, A. R. E., Godley, B. J. and Thirgood, S. (2011b) 'Migration impacts on communities and ecosystems: empirical evidence and theoretical insights', in Milner-Gulland, E. J., Sinclair, A. R. E., and Fryxell, J. M. (eds) *Animal migration: A synthesis*. Oxford and New York: Oxford University Press, pp. 131–143.

Holdo, R. M., Onderdonk, D. A., Barr, A. G., Mwita, M. and Anderson, T. M. (2020) 'Spatial transitions in tree cover are associated with soil hydrology, but not with grass biomass, fire frequency, or herbivore biomass in Serengeti savannahs', *Journal of Ecology*. Edited by I. Oliveras, 108(2), pp. 586–597. doi: 10.1111/1365-2745.13303.

Holt, J. A. and Lepage, M. (2000) 'Termites and Soil Properties', in *Termites: Evolution, Sociality, Symbioses, Ecology*. Dordrecht: Springer Netherlands, pp. 389–407. doi: 10.1007/978-94-017-3223-9_18.

Hook, S., Wildson, R. C., MacCallum, S. N. and Merchant, C. (2012) '[Global Climate] Lake surface temperature [in "State of the Climate in 2011"]', *Bulletin of the American Meteorological Society*, 93(7), pp. S18–S19.

Hopcraft, J. G. C., Anderson, T. M., Pérez-vila, S., Mayemba, E. and Olff, H. (2012) 'Body size and the division of niche space: food and predation differentially shape the distribution of Serengeti grazers', *Journal of Animal Ecology*, 81(1), pp. 201–213.

Hopcraft, J. G. C., Holdo, R. M., Mwangomo, E., Mduma, S. A. R., Thirgood, S. J., Borner, M., Fryxell, J. M., Olff, H. and Sinclair, A. R. E. (2015) 'Why Are Wildebeest the Most Abundant Herbivore in the Serengeti Ecosystem?', in Sinclair, A. R. E., Metzger, K. L., Mduma, S. A. R., and Fryxell, J. M. (eds) *Serengeti IV: Sustaining Biodiversity in a Coupled Human-Natural System*. Chicago and London: The University of Chicago Press, pp. 125–174.

Hopcraft, J. G. C., Sinclair, A. R. E. and Packer, C. (2005) 'Planning for Success: Serengeti Lions Seek Prey Accessibility Rather than Abundance', *Journal of Animal Ecology*, 74(3), pp. 559–566. doi: 10.1111/j.1365-2656.2005.00955.x.

Houze, R. A. (2012) 'Orographic effects on precipitating clouds', *Reviews of Geophysics*, 50(1), p. RG1001. doi: 10.1029/2011RG000365.

Huffman, G. J., Bolvin, D. T., Nelkin, E. J., Wolff, D. B., Adler, R. F., Gu, G., Hong, Y., Bowman, K. P. and Stocker, E. F. (2007) 'The TRMM Multisatellite Precipitation Analysis (TMPA): Quasi-Global, Multiyear, Combined-Sensor Precipitation Estimates at Fine Scales', *Journal of Hydrometeorology*, 8(1), pp. 38–55. doi: 10.1175/JHM560.1.

Hutley, L. B. and Setterfield, S. A. (2008) 'Savanna', in *Encyclopedia of Ecology*. Elsevier, pp. 3143–3154. doi: 10.1016/B978-008045405-4.00358-X.

Indeje, M., Semazzi, F. H. M. and Ogallo, L. J. (2000) 'ENSO signals in East African rainfall

seasons', *International Journal of Climatology*, 20(1), pp. 19–46. doi: 10.1002/(SICI)1097-0088(200001)20:1<19::AID-JOC449>3.0.CO;2-0.

International Federation of Red Cross and Red Crescent Societies (2014) *World Disasters Report 2014: Focus on culture and risk, World Disasters Report*. Geneva.

Järemo, J., Nilsson, P., Tuomi, J. and Jaremo, J. (1996) 'Plant Compensatory Growth: Herbivory or Competition?', *Oikos*, 77(2), p. 238. doi: 10.2307/3546062.

Jouquet, P., Mamou, L., Lepage, M. and Velde, B. (2002) 'Effect of termites on clay minerals in tropical soils: fungus-growing termites as weathering agents', *European Journal of Soil Science*, 53(4), pp. 521–528. doi: 10.1046/j.1365-2389.2002.00492.x.

Kendon, E. J., Stratton, R. A., Tucker, S., Marsham, J. H., Berthou, S., Rowell, D. P. and Senior, C. A. (2019) 'Enhanced future changes in wet and dry extremes over Africa at convection-permitting scale', *Nature Communications*. Springer US, 10(1), p. 1794. doi: 10.1038/s41467-019-09776-9.

Kenya Wildlife Service (no date) *Protected area coverage per country/territory by UN Environment Regions: Kenya, Protected Planet*. UNEP-WCMC & IUCN. Available at: https://www.protectedplanet.net/country/KEN (Accessed: 26 August 2020).

Kija, H. K., Ogutu, J. O., Mangewa, L. J., Bukombe, J., Verones, F., Graae, B. J., Kideghesho, J. R., Said, M. Y. and Nzunda, E. F. (2020) 'Land Use and Land Cover Change Within and Around the Greater Serengeti Ecosystem , Tanzania', *American Journal of Remote Sensing*, 8(1), pp. 1–19. doi: 10.11648/j.ajrs.20200801.11.

Kijazi, A. and Reason, C. (2009) 'Analysis of the 1998 to 2005 drought over the northeastern highlands of Tanzania', *Climate Research*, 38(3), pp. 209–223. doi: 10.3354/cr00784.

Kimaro, H. S., Asenga, A. M., Munishi, L. and Treydte, A. C. (2019) 'Woody Encroachment

Extent and Its Associated Impacts on Plant and Herbivore Species Occurrence in Maswa Game Reserve, Tanzania', *Environment and Natural Resources Research*, 9(3), p. 63. doi: 10.5539/enrr.v9n3p63.

Kirtman, B., Power, S. B., Adedoyin, J. A., Boer, G. J., Bojariu, R., Camilloni, I., Doblas-Reyes, F. J., Fiore, A. M., Kimoto, M., Meehl, G. a., Prather, M., Sarr, A., Schär, C., Sutton, R., Oldenborgh, G. J. Van, Vecchi, G. and Wang, H. J. (2013) 'Near-term Climate Change: Projections and Predictability', in Stocker, T. F., Qin, D., Plattner, G.-K., Tignor, M., Allen, S. K., Boschung, J., Nauels, A., Zia, Y., Bex, V., and Midgley, P. M. (eds) *Climate Change 2013: The Physical Science Basis. Contribution of Working Group I to the Fifth Assessment Report of the Intergovernmental Panel on Climate Change*. Cambridge, United Kingdom and New York, NY, USA: Cambridge University Press, pp. 953–1028. doi: 10.1017/CBO9781107415324.023.

Kizza, M., Rodhe, A., Xu, C.-Y., Ntale, H. K. and Halldin, S. (2009) 'Temporal rainfall variability in the Lake Victoria Basin in East Africa during the twentieth century', *Theoretical and Applied Climatology*, 98(1–2), pp. 119–135. doi: 10.1007/s00704-008-0093-6.

Kreulen, D. (1975) 'Wildebeest habitat selection on the Serengeti plains, Tanzania, in relation to calcium and lactation: a preliminary report', *East Africa Wildlife Journal*, 13, pp. 297–304.

Lande, R., Engen, S. and Saether, B.-E. (2003) *Stochastic Population Dynamics in Ecology and Conservation*. Oxford University Press. doi: 10.1093/acprof:oso/9780198525257.001.0001.

Lewontin, R. C. and Cohen, D. (1969) 'On Population Growth in a Randomly Varying Environment', *Proceedings of the National Academy of Sciences*, 62(4), pp. 1056–1060. doi: 10.1073/pnas.62.4.1056.

Ludwig, F., Kroon, H., Prins, H. H. T. and Berendse, F. (2001) 'Effects of nutrients and shade

on tree-grass interactions in an East African savanna', *Journal of Vegetation Science*, 12(4), pp. 579–588. doi: 10.2307/3237009.

MacCallum, S. N. and Merchant, C. J. (2012) 'Surface water temperature observations of large lakes by optimal estimation', *Canadian Journal of Remote Sensing*, 38(1), pp. 25–45. doi: 10.5589/m12-010.

MacIntyre, S. (2012) 'Climatic Variability, Mixing Dynamics, and Ecological Consequences in the African Great Lakes', in *Climatic Change and Global Warming of Inland Waters*. Chichester, UK: John Wiley & Sons, Ltd, pp. 311–336. doi: 10.1002/9781118470596.ch18.

MacIntyre, S., Romero, J. R., Silsbe, G. M. and Emery, B. M. (2014) 'Stratification and horizontal exchange in Lake Victoria, East Africa', *Limnology and Oceanography*, 59(6), pp. 1805–1838. doi: 10.4319/lo.2014.59.6.1805.

Maddock, L. (1979) 'The "Migration" and Grazing Succession', in Sinclair, A. R. E. and Norton-Griffiths, M. (eds) *Serengeti: Dynamics of an Ecosystem*. Chicago and London: University of Chicago Press, pp. 104–129.

May, R. M., Arms, S. C., Marsh, P., Bruning, E., Leeman, J. R. and Goebbert, Kevin Thielen, Jonathan E. and Bruick, Z. S. (2020) 'MetPy: A Python Package for Meteorological Data.' Boulder, Colorado: Unidata. doi: 10.5065/D6WW7G29.

McCarthy, T. S., Ellery, W. N. and Bloem, A. (1998) 'Some observations on the geomorphological impact of hippopotamus (Hippopotamus amphibius L.) in the Okavango Delta, Botswana', *African Journal of Ecology*, 36(1), pp. 44–56. doi: 10.1046/j.1365-2028.1998.89-89089.x.

McKenzie, P. F., Duveneck, M. J., Morreale, L. L. and Thompson, J. R. (2019) 'Local and global parameter sensitivity within an ecophysiologically based forest landscape model',

Environmental Modelling & Software. Elsevier, 117(March), pp. 1–13. doi: 10.1016/j.envsoft.2019.03.002.

McNaughton, S. J. (1976) 'Serengeti Migratory Wildebeest: Facilitation of Energy Flow by Grazing', *Science*, 191(4222), pp. 92–94.

McNaughton, S. J. (1979) 'Grazing as an Optimization Process: Grass-Ungulate Relationships in the Serengeti', *The American Naturalist*, 113(5), pp. 691–703.

McNaughton, S. J. (1983) 'Serengeti Grassland Ecology: The Role of Composite Environmental Factors and Contingency in Community Organization', *Ecological Monographs*, 53(3), pp. 291–320. doi: 10.2307/1942533.

McNaughton, S. J. (1984) 'Grazing Lawns : Animals in Herds , Plant Form , and Coevolution', *The American Naturalist*, 124(6), pp. 863–886.

McNaughton, S. J. (1985) 'Ecology of a Grazing Ecosystem: The Serengeti', *Ecological Monographs*, 55(3), pp. 259–294.

McNaughton, S. J. (1990) 'Mineral nutrition and seasonal movements of African migratory ungulates', *Nature*, 345(6276), pp. 613–615. doi: 10.1038/345613a0.

McNaughton, S. J. (1994) 'Biodiversity and Function of Grazing Ecosystems', in *Biodiversity and Ecosystem Function*. Berlin, Heidelberg: Springer Berlin Heidelberg, pp. 361–383. doi: 10.1007/978-3-642-58001-7_17.

McNaughton, S. J., Banyikwa, F. F. and McNaughton, M. M. (1997) 'Promotion of the Cycling of Diet-Enhancing Nutrients by African Grazers', *Science*, 278(5344), pp. 1798–1800. doi: 10.1126/science.278.5344.1798.

Mduma, S. A. R., Sinclair, A. R. E. and Hilborn, R. (1999) 'Food Regulates the Serengeti Wildebeest: A 40-Year Record', *Journal of Animal Ecology*, 68(6), pp. 1101–1122.

Metzger, K. L., Sinclair, A. R. E., Macfarlane, S., Coughenour, M. and Ding, J. (2015) 'Scales of Change in the Greater Serengeti Ecosystem', in Sinclair, A. R. E., Metzger, K. L., Mduma, S. A. R., and Fryxell, J. M. (eds) *Serengeti IV: Sustaining Biodiversity in a Coupled Human-Natural System*. Chicago and London: The University of Chicago Press, pp. 33–72.

Milchunas, D. G., Sala, O. E. and Lauenroth, W. K. (1988) 'A Generalized Model of the Effects of Grazing by Large Herbivores on Grassland Community Structure', *The American Naturalist*, 132(1), pp. 87–106.

Morens, D. M., Holmes, E. C., Davis, A. S. and Taubenberger, J. K. (2011) 'Global Rinderpest Eradication: Lessons Learned and Why Humans Should Celebrate Too', *The Journal of Infectious Diseases*, 204(4), pp. 502–505. doi: 10.1093/infdis/jir327.

Morrison, T. A., Holdo, R. M. and Anderson, T. M. (2016) 'Elephant damage, not fire or rainfall, explains mortality of overstorey trees in Serengeti', *Journal of Ecology*. Edited by F. Gilliam, 104(2), pp. 409–418. doi: 10.1111/1365-2745.12517.

Morrison, T. A., Holdo, R. M., Rugemalila, D. M., Nzunda, M. and Anderson, T. M. (2019) 'Grass competition overwhelms effects of herbivores and precipitation on early tree establishment in Serengeti', *Journal of Ecology*. Edited by M. Sankaran, 107(1), pp. 216–228. doi: 10.1111/1365-2745.13010.

Munishi, L. P. (2018) *Tree Species Occurrence Data of Accacia Commiphora Woodland of Tanzania., Version 1.2.* Sokoine University of Agriculture, Department of Ecosystems and Conservation. Available at: https://doi.org/10.15468/mi3taw (Accessed: 31 August 2020).

Murray, M. G. (1995) 'Specific nutrient requirements and migration of wildebeest', in Sinclair, A. R. E. and Arcese, P. (eds) *Serengeti II: dynamics, management, and conservation of an ecosystem*. Chicago: University of Chicago Press, pp. 231–256.

Mwangi, H. M., Julich, S., Patil, S. D., McDonald, M. A. and Feger, K.-H. (2016) 'Relative contribution of land use change and climate variability on discharge of upper Mara River, Kenya', *Journal of Hydrology: Regional Studies*. Elsevier B.V., 5, pp. 244–260. doi: 10.1016/j.ejrh.2015.12.059.

Niang, I., Ruppel, O. C., Abdrabo, M. A., Essel, A., Lennard, C., Padgham, J. and Urquhart, P. (2014) 'Africa', in Barros, V. R., Field, C. B., Dokken, D. J., Mastrandrea, M. D., Mach, K. J., Bilir, T. E., Chatterjee, M., Ebi, K. L., Estrada, Y. O., Genova, R. C., Girma, B., Kissel, E. S., Levy, A. N., MacCracken, S., Mastrandrea, P. R., and White, L. L. (eds) *Climate Change 2014: Impacts, Adaptation, and Vulnerability. Part B: Regional Aspects. Contribution of Working Group II to the Fifth Assessment Report of the Intergovernmental Panel of Climate Change*. Cambridge, United Kingdom and New York, NY, USA: Cambridge University Press, pp. 1199–1265.

Nicholson, S. (2016a) 'The Turkana low-level jet: mean climatology and association with regional aridity', *International Journal of Climatology*, 36(6), pp. 2598–2614. doi: 10.1002/joc.4515.

Nicholson, S. E. (1996) 'A Review of Climate Dynamics and Climate Variability in Eastern Africa', in Johnson, T. C. and Odada, E. O. (eds) *The Limnology, Climatology and Paleoclimatology of the East African Lakes*. Amsterdam: Gordon and Breach Science Publishers, pp. 25–56.

Nicholson, S. E. (2016b) 'An analysis of recent rainfall conditions in eastern Africa', *International Journal of Climatology*, 36(1), pp. 526–532. doi: 10.1002/joc.4358.

Nicholson, S. E. (2017) 'Climate and climatic variability of rainfall over eastern Africa', *Reviews of Geophysics*, 55(3), pp. 590–635. doi: 10.1002/2016RG000544.

Nicholson, S. E. (2018) 'The ITCZ and the Seasonal Cycle over Equatorial Africa', *Bulletin of*

the American Meteorological Society, 99(2), pp. 337–348. doi: 10.1175/BAMS-D-16-0287.1.

Norton-Griffiths, M. (1979) 'The Influence of Grazing, Browsing, and Fire on the Vegetation Dynamics of the Serengeti', in Sinclair, A. R. E. and Norton-Griffiths, M. (eds) *Serengeti: Dynamics of an Ecosystem*. Chicago and London: The University of Chicago Press, pp. 310–352.

Norton-Griffiths, M., Herlocker, D. and Pennycuick, L. (1975) 'The patterns of rainfall in the Serengeti Ecosystem, Tanzania', *African Journal of Ecology*, 13(3–4), pp. 347–374. doi: 10.1111/j.1365-2028.1975.tb00144.x.

Oettli, P. and Camberlin, P. (2005) 'Influence of topography on monthly rainfall distribution over East Africa', *Climate Research*, 28(3), pp. 199–212. doi: 10.3354/cr028199.

Ogutu, J. O., Piepho, H.-P., Dublin, H. T., Bhola, N. and Reid, R. S. (2008a) 'El Niño-Southern Oscillation, rainfall, temperature and Normalized Difference Vegetation Index fluctuations in the Mara-Serengeti ecosystem', *African Journal of Ecology*, 46(2), pp. 132–143. doi: 10.1111/j.1365-2028.2007.00821.x.

Ogutu, J. O., Piepho, H. P., Dublin, H. T., Bhola, N. and Reid, R. S. (2008b) 'Rainfall influences on ungulate population abundance in the Mara-Serengeti ecosystem', *Journal of Animal Ecology*, 77(4), pp. 814–829. doi: 10.1111/j.1365-2656.2008.01392.x.

Ogutu, J. O., Piepho, H. P., Dublin, H. T., Bhola, N. and Reid, R. S. (2010) 'Rainfall extremes explain interannual shifts in timing and synchrony of calving in topi and warthog', *Population Ecology*, 52(1), pp. 89–102. doi: 10.1007/s10144-009-0163-3.

Okeyo, A. E. (1986) 'The Impact of Lake Victoria on the Convective Activities over the Kenya Highlands', *Journal of the Meteorological Society of Japan. Ser. II*. J. Meteorol. Soc. Jpn., 65, 689–695, 64A, pp. 689–695. doi: 10.2151/jmsj1965.64A.0_689.

Olff, H. and Hopcraft, J. G. C. (2008) ‘The Resource Basis of Human-Wildlife Interaction’, in Sinclair, A. R. E., Packer, C., Mduma, S. A. R., and Fryxell, J. M. (eds) *Serengeti III: Human Impacts on Ecosystem Dynamics*. Chicago and London: The University of Chicago Press, pp. 95–134.

Olff, H. and Ritchie, M. E. (1998) ‘Effects of herbivores on grassland plant diversity’, *Trends in Ecology & Evolution*, 13(7), pp. 261–265. doi: 10.1016/S0169-5347(98)01364-0.

Ongoma, V., Chen, H. and Gao, C. (2018) ‘Projected changes in mean rainfall and temperature over East Africa based on CMIP5 models’, *International Journal of Climatology*, 38(3), pp. 1375–1392. doi: 10.1002/joc.5252.

Owen-Smith, N., Mason, D. R. and Ogutu, J. O. (2005) ‘Correlates of Survival Rates for 10 African Ungulate Populations: Density, Rainfall and Predation’, *Journal of Animal Ecology*, 74(4), pp. 774–788. doi: 10.1111/j.1365-2656.2005.00974.x.

Owen-Smith, N. and Ogutu, J. O. (2013) ‘Changing Rainfall and obstructed Movements: Impact on African Ungulates’, in Brodie, J. F., Post, E., and Doak, D. F. (eds) *Wildlife Conservation in a Changing Climate*. Chicago and London: University of Chicago Press, pp. 153–178.

Packer, C., Hilborn, R., Mosser, A., Kissui, B., Borner, M., Hopcraft, G., Wilmshurst, J., Mduma, S. and Sinclair, A. R. E. (2005) ‘Ecological Change, Group Territoriality, and Population Dynamics in Serengeti Lions’, *Science*, 307(5708), pp. 390–393. Available at: http://science.sciencemag.org/content/307/5708/390.abstract.

Pankhurst, R. (1966) ‘The Great Ethiopian Famine of 1888–1892: A New Assessment’, *Journal of the History of Medicine and Allied Sciences*, XXI(2), pp. 95–124. doi: 10.1093/jhmas/XXI.2.95.

Pascual, M. A., Kareiva, P. and Hilborn, R. (1997) 'The Influence of Model Structure on Conclusions about the Viability and Harvesting of Serengeti Wildebeest', *Conservation Biology*, 11(4), pp. 966–976.

Patricola, C. M. and Cook, K. H. (2011) 'Sub-Saharan Northern African climate at the end of the twenty-first century: forcing factors and climate change processes', *Climate Dynamics*, 37(5–6), pp. 1165–1188. doi: 10.1007/s00382-010-0907-y.

Pellew, R. A. P. (1983) 'The impacts of elephant, giraffe and fire upon the Acacia tortilis woodlands of the Serengeti', *African Journal of Ecology*, 21(1), pp. 41–74. doi: 10.1111/j.1365-2028.1983.tb00311.x.

Pennycuick, L. (1975) 'Movements of the migratory wildebeest population in the Serengeti area between 1960 and 1973', *African Journal of Ecology*, 13(1), pp. 65–87. doi: 10.1111/j.1365-2028.1975.tb00124.x.

Peters, C. R., Blumenschine, R. J., Hay, R. L., Livingstone, D. A., Marean, C. W., Harrison, T., Armour-Chelu, M., Andrews, P., Bernor, R. L., Boneefille, R. and Werdelin, L. (2008) 'Paleoecology of the Serengeti-Mara Ecosystem', in Sinclair, A. R. E., Packer, C., Mduma, S. A. R., and Fryxell, J. M. (eds) *Serengeti III: Human Impacts on Ecosystem Dynamics*. Chicago and London: The University of Chicago Press.

Pielke, R. A., Bluestein, H. B., Enfield, D. B., Wells, N. C., Cenedese, C., Davies, R., Waggoner, P. E., Gentilli, J., Lamb, H. H., Smith, P. J., Arnfield, A. J., Mason, B. J., Krishnamurti, T. N., Hayden, B. P. and Loewe, F. P. (2020) *Climate*, *Encyclopædia Britannica*. Available at: https://www.britannica.com/science/climate-meteorology (Accessed: 24 August 2020).

Platts, P. J., Omeny, P. A. and Marchant, R. (2015) 'AFRICLIM: high-resolution climate projections for ecological applications in Africa', *African Journal of Ecology*, 53(1), pp. 103–203

108. doi: 10.1111/aje.12180.

Prein, A. F., Langhans, W., Fosser, G., Ferrone, A., Ban, N., Goergen, K., Keller, M., Tölle, M., Gutjahr, O., Feser, F., Brisson, E., Kollet, S., Schmidli, J., Lipzig, N. P. M. and Leung, R. (2015) 'A review on regional convection-permitting climate modeling: Demonstrations, prospects, and challenges', *Reviews of Geophysics*, 53(2), pp. 323–361. doi: 10.1002/2014RG000475.

Probert, J. R., Parr, C. L., Holdo, R. M., Anderson, T. M., Archibald, S., Courtney Mustaphi, C. J., Dobson, A. P., Donaldson, J. E., Hopcraft, G. C., Hempson, G. P., Morrison, T. A. and Beale, C. M. (2019) 'Anthropogenic modifications to fire regimes in the wider Serengeti-Mara ecosystem', *Global Change Biology*, 25(10), pp. 3406–3423. doi: 10.1111/gcb.14711.

R Core Team (2019) 'R: A language and environment for statistical computing'. Vienna, Austria: R Foundation for Statistical Computing. Available at: https://www.r-project.org/.

Randall, D. A., Wood, R. A., Bony, S., Colman, R., Fichefet, T., Fyfe, J., Kattsov, V., Pitman, A., Shukla, J., Srinivasan, J., Stouffer, R. J., Sumi, A. and Taylor, K. E. (2007) 'Climate Models and Their Evaluation', in Solomon, S., Qin, D., Manning, M., Chen, Z., Marquis, M., Averyt, K. B., Tignor, M., and Miller, H. L. (eds) *Climate Change 2007: The Physical Science Basis. Contribution of Working Group I to the Fourth Assessment Report of the Intergovernmental Panel on Climate Change*. Cambridge, United Kingdom and New York, NY, USA: Cambridge University Press, pp. 589–662. doi: 10.1016/j.cub.2007.06.045.

Reed, D. N., Anderson, T. M., Dempewolf, J., Metzger, K., Serneels, S. and Bowman, J. (2009) 'The Spatial Distribution of Vegetation Types in the Serengeti Ecosystem: The Influence of Rainfall and Topographic Relief on Vegetation Patch Characteristics', *Journal of Biogeography*, 36(4), pp. 770–782. doi: 10. 11 1 1/j. 1365-269.

Rentsch, D. and Packer, C. (2015) 'The effect of bushmeat consumption on migratory wildlife

in the Serengeti ecosystem, Tanzania', *Oryx*, 49(2), pp. 287–294. doi: 10.1017/S0030605313001038.

Reynolds, R. W., Smith, T. M., Liu, C., Chelton, D. B., Casey, K. S. and Schlax, M. G. (2007) 'Daily High-Resolution-Blended Analyses for Sea Surface Temperature', *Journal of Climate*, 20(22), pp. 5473–5496. doi: 10.1175/2007JCLI1824.1.

Riginos, C. (2009) 'Grass competition suppresses savanna tree growth across multiple demographic stages', *Ecology*, 90(2), pp. 335–340. doi: 10.1890/08-0462.1.

Ritchie, M. E. (2008) 'Global Environmental Changes and Their Impact on the Serengeti', in Sinclair, A. R. E., Packer, C., Mduma, S. A. R., and Fryxell, J. M. (eds) *Serengeti III: Human Impacts on Ecosystem Dynamics*. University of Chicago Press, pp. 209–240. doi: 10.7208/chicago/9780226760353.001.0001.

Robinson, B. G. and Merrill, E. H. (2013) 'Foraging-vigilance trade-offs in a partially migratory population: comparing migrants and residents on a sympatric range', *Animal Behaviour*. Elsevier Ltd, 85(4), pp. 849–856. doi: 10.1016/j.anbehav.2013.02.004.

Robinson, R., Crick, H., Learmonth, J., Maclean, I., Thomas, C., Bairlein, F., Forchhammer, M., Francis, C., Gill, J., Godley, B., Harwood, J., Hays, G., Huntley, B., Hutson, A., Pierce, G., Rehfisch, M., Sims, D., Santos, B., Sparks, T., Stroud, D. and Visser, M. (2009) 'Travelling through a warming world: climate change and migratory species', *Endangered Species Research*, 7(2), pp. 87–99. doi: 10.3354/esr00095.

Rowell, D. P., Booth, B. B. B., Nicholson, S. E. and Good, P. (2015) 'Reconciling Past and Future Rainfall Trends over East Africa', *Journal of Climate*, 28, pp. 9768–9788. doi: 10.1175/JCLI-D-15-0140.1.

Rowell, D. P. and Chadwick, R. (2018) 'Causes of the uncertainty in projections of tropical

terrestrial rainfall change: East Africa', *Journal of Climate*, 31(15), pp. 5977–5995. doi: 10.1175/JCLI-D-17-0830.1.

Rugemalila, D. M., Anderson, T. M. and Holdo, R. M. (2016) 'Precipitation and elephants, not fire, shape tree community composition in Serengeti National Park, Tanzania', *Biotropica*, 48(4), pp. 476–482. doi: 10.1111/btp.12311.

Rugemalila, D. M., Cory, S. T., Smith, W. K. and Anderson, T. M. (2020) 'The role of microsite sunlight environment on growth, architecture, and resource allocation in dominant Acacia tree seedlings, in Serengeti, East Africa', *Plant Ecology*. Springer Netherlands, 5. doi: 10.1007/s11258-020-01074-5.

Rysava, K., Mcgill, R. A. R., Matthiopoulos, J. and Hopcraft, J. G. C. (2016) 'Re-constructing nutritional history of Serengeti wildebeest from stable isotopes in tail hair : seasonal starvation patterns in an obligate grazer', *Rapid Communications in Mass Spectrometry*, 30, pp. 1461–1468. doi: 10.1002/rcm.7572.

Sankaran, M., Hanan, N. P., Scholes, R. J., Ratnam, J., Augustine, D. J., Cade, B. S., Gignoux, J., Higgins, S. I., Le Roux, X., Ludwig, F., Ardo, J., Banyikwa, F., Bronn, A., Bucini, G., Caylor, K. K., Coughenour, M. B., Diouf, A., Ekaya, W., Feral, C. J., February, E. C., Frost, P. G. H., Hiernaux, P., Hrabar, H., Metzger, K. L., Prins, H. H. T., Ringrose, S., Sea, W., Tews, J., Worden, J. and Zambatis, N. (2005) 'Determinants of woody cover in African savannas', *Nature*, 438(7069), pp. 846–849. doi: 10.1038/nature04070.

Schlesinger, W. H. and Bernhardt, E. S. (eds) (2013) 'The Lithosphere', in *Biogeochemistry: An Analysis of Global Change*. 3rd edn. Oxford: Elsevier Science & Technology, pp. 93–134.

Schneider, D. C. (2001) 'The rise of the concept of scale in ecology', *BioScience*, 51(7), pp. 545–553. doi: https://doi.org/10.1641/0006-3568(2001)051[0545:TROTCO]2.0.CO;2.

Scholes, J. R., Betts, R., Bunn, S., Leadley, P., Nepstad, D., Overpeck, J. T. and Taboada, M. A. (2014) 'Terrestrial and inland water systems', in Field, C. B., Barros, V. R., Dokken, D. J., Mach, K. J., Mastrandrea, M. D., Bilir, T. E., Chatterjee, M., Ebi, K. L., Estrada, Y. O., Genova, R. C., Girma, B., Kissel, E. S., Levy, A. N., MacCracken, S., Mastrandrea, P. R., and White, L. L. (eds) *Climate Change 2014: Impacts, Adaptation, and Vulnerability. Part A: Global and Sectoral Aspects. Contribution of Working Group II to the Fifth Assessment Report of the Intergovernmental Panel on Climate Change*. Cambridge and New York: Cambridge University Press, pp. 271–359.

Scholes, R. J. and Archer, S. R. (1997) 'Tree-Grass Interactions in Savannas', *Annual Review of Ecology and Systematics*, 28(1), pp. 517–544. Available at: http://doi.wiley.com/10.2307/3235707.

Scoon, R. N. (2018) *Geology of National Parks of Central/Southern Kenya and Northern Tanzania, Geology of National Parks of Central/Southern Kenya and Northern Tanzania*. Cham: Springer International Publishing. doi: 10.1007/978-3-319-73785-0.

Selebatso, M., Fynn, R. and Maude, G. (2017) 'Adaptive activity patterns of a blue wildebeest population to environmental variability in fragmented, semi-arid Kalahari, Botswana', *Journal of Arid Environments*. Elsevier Ltd, 136, pp. 15–18. doi: 10.1016/j.jaridenv.2016.10.001.

Shongwe, M. E., van Oldenborgh, G. J., van den Hurk, B. and van Aalst, M. (2011) 'Projected Changes in Mean and Extreme Precipitation in Africa under Global Warming. Part II: East Africa', *Journal of Climate*, 24(14), pp. 3718–3733. doi: 10.1175/2010JCLI2883.1.

Shrestha, A. K., van Wieren, S. E., van Langevelde, F., Fuller, A., Hetem, R. S., Meyer, L., de Bie, S. and Prins, H. H. T. (2014) 'Larger antelopes are sensitive to heat stress throughout all seasons but smaller antelopes only during summer in an African semi-arid environment', *INTERNATIONAL JOURNAL OF BIOMETEOROLOGY*, 58(1), pp. 41–49. doi:

10.1007/s00484-012-0622-y.

Sinclair, A. R. E. (1979a) ‘Dynamics of the Serengeti Ecosystem’, in Sinclair, A. R. E. and Norton-Griffiths, M. (eds) *Serengeti: Dynamics of an Ecosystem*. Chicago and London: The University of Chicago Press, pp. 1–30.

Sinclair, A. R. E. (1979b) ‘The Eruption of the Ruminants’, in Sinclair, A. R. E. and Norton-Griffiths, M. (eds) *Serengeti: Dynamics of an Ecosystem*. Chicago and London: University of Chicago Press, pp. 83–103.

Sinclair, A. R. E. (1979c) ‘The Serengeti Environment’, in Sinclair, A. R. E. and Norton-Griffiths, M. (eds) *Serengeti: Dynamics of an Ecosystem*. Chicago: University of Chicago Press, pp. 31–45.

Sinclair, A. R. E. (1995) ‘Serengeti Past and Present’, in Sinclair, A. R. E. and Arcese, P. (eds) *Serengeti II: Dynamics, Management, and Conservation of an Ecosystem*. Chicago and London: The University of Chicago Press, pp. 3–30.

Sinclair, A. R. E. (2003) ‘Mammal Population Regulation, Keystone Processes and Ecosystem Dynamics’, *Philosophical Transactions: Biological Sciences*, 358(1438), pp. 1729–1740. doi: 10.1098/rstb.2003.1359.

Sinclair, A. R. E., Dobson, A., Mduma, S. A. R. and Metzger, K. L. (2015a) ‘Shaping the Serengeti Ecosystem’, in Sinclair, A. R. E., Metzger, K. L., Mduma, S. A. R., and Fryxell, J. M. (eds) *Serengeti IV: Sustaining Biodiversity in a Coupled Human-Natural System*. Chicago and London, pp. 11–32.

Sinclair, A. R. E., Dobson, A., Metzger, K. L., Fryxell, J. M. and Mduma, S. A. R. (2015b) ‘The Future of Conservation: Lessons from the Serengeti’, in Sinclair, A. R. E., Metzger, K. L., Mduma, S. A. R., and Fryxell, J. M. (eds) *Serengeti IV: Sustaining Biodiversity in a Coupled*

Human-Natural System. Chicago and London, pp. 797–811.

Sinclair, A. R. E., Hopcraft, J. G. C., Olff, H., Mduma, S. A. R., Galvin, K. A. and Sharam, G. J. (2008) 'Historical and Future Changes to the Serengeti Ecosystem', in Sinclair, A. R. E., Packer, C., Mduma, S. A. R., and Fryxell, J. M. (eds) *Serengeti III*. University of Chicago Press, pp. 7–46. doi: 10.7208/chicago/9780226760353.003.0002.

Sinclair, A. R. E., Mduma, S. A. R., Hopcraft, J. G. C., Fryxell, J. M., Hilborn, R. and Thirgood, S. J. (2007) 'Long-Term Ecosystem Dynamics in the Serengeti: Lessons for Conservation', *Conservation Biology*, 21(3), pp. 580–590. doi: 10.1111/j.1523-1739.2007.00699.x.

Sinclair, S. J., White, M. D. and Newell, G. R. (2010) 'How Useful Are Species Distribution Models for Managing Biodiversity under Future Climates?', *Ecology and Society*, 15(1), p. art8. doi: 10.5751/ES-03089-150108.

Smith, J. M. B. (2020) *Grassland*, *Encyclopedia Britannica*. Available at: https://www.britannica.com/science/grassland (Accessed: 12 April 2020).

Smith, P. (2014) 'Do grasslands act as a perpetual sink for carbon?', *Global Change Biology*, 20(9), pp. 2708–2711. doi: 10.1111/gcb.12561.

Staver, A. C., Archibald, S. and Levin, S. A. (2011) 'The global extent and determinants of savanna and forest as alternative biome states', *Science*, 334(6053), pp. 230–232. doi: 10.1126/science.1210465.

Stratton, R. A., Senior, C. A., Vosper, S. B., Folwell, S. S., Boutle, I. A., Earnshaw, P. D., Kendon, E., Lock, A. P., Malcolm, A., Manners, J., Morcrette, C. J., Short, C., Stirling, A. J., Taylor, C. M., Tucker, S., Webster, S. and Wilkinson, J. M. (2018) 'A Pan-African Convection-Permitting Regional Climate Simulation with the Met Office Unified Model: CP4-Africa', *Journal of Climate*, 31(9), pp. 3485–3508. doi: 10.1175/JCLI-D-17-0503.1.

Strauch, A. M. (2013) ‘The role of water quality in large mammal migratory behaviour in the Serengeti’, *Ecohydrology*, 6(3), pp. 343–354. doi: 10.1002/eco.1279.

Stronach, N. R. H. and McNaughton, S. J. (1989) ‘Grassland Fire Dynamics in the Serengeti Ecosystem, and a Potential Method of Retrospectively Estimating Fire Energy’, *The Journal of Applied Ecology*, 26(3), p. 1025. doi: 10.2307/2403709.

Subalusky, A. L., Dutton, C. L., Rosi, E. J. and Post, D. M. (2017) ‘Annual mass drownings of the Serengeti wildebeest migration influence nutrient cycling and storage in the Mara River’, 114(29), pp. 7647–7652. doi: 10.1073/pnas.1614778114.

Talbot, L. M. and Talbot, M. H. (1963) ‘The Wildebeest in Western Masailand, East Africa’, *Wildlife Monographs*. Cambridge: Cambridge University Press, 12, pp. 3–88.

Tang, W. and Bennett, D. A. (2010) ‘Agent-based Modeling of Animal Movement: A Review’, *Geography Compass*, 4(7), pp. 682–700. doi: 10.1111/j.1749-8198.2010.00337.x.

Tanzanian National Parks (no date) *Protected area coverage per country/territory by UN Environment Regions: United Republic of Tanzania*, *Protected Planet*. UNEP-WCMC & IUCN. Available at: https://www.protectedplanet.net/country/TZA (Accessed: 26 August 2020).

Tarnavsky, E., Grimes, D., Maidment, R., Black, E., Allan, R. P., Stringer, M., Chadwick, R. and Kayitakire, F. (2014) ‘Extension of the TAMSAT Satellite-Based Rainfall Monitoring over Africa and from 1983 to Present’, *Journal of Applied Meteorology and Climatology*, 53(12), pp. 2805–2822. doi: 10.1175/JAMC-D-14-0016.1.

Thiery, W., Davin, E. L., Seneviratne, S. I., Bedka, K., Lhermitte, S. and van Lipzig, N. P. M. (2016) ‘Hazardous thunderstorm intensification over Lake Victoria’, *Nature Communications*. Nature Publishing Group, 7, p. 12786. doi: 10.1038/ncomms12786.

Thirgood, S., Mosser, A., Tham, S., Hopcraft, G., Mwangomo, E., Mlengeya, T., Kilewo, M., Fryxell, J., Sinclair, A. R. E. and Borner, M. (2004) 'Can parks protect migratory ungulates? The case of the Serengeti wildebeest', *Animal Conservation*. Blackwell Publishing Ltd, 7(2), pp. 113–120. doi: 10.1017/S1367943004001404.

Torney, C. J., Hopcraft, J. G. C., Morrison, T. A., Couzin, I. D., Levin, S. A., Hopcraft, G. C. and Torney, C. J. (2018) 'From single steps to mass migration : the problem of scale in the movement ecology of the Serengeti wildebeest'.

Traniello, J. F. A. and Leuthold, R. H. (2000) 'Behavior and Ecology of Foraging in Termites', in *Termites: Evolution, Sociality, Symbioses, Ecology*. Dordrecht: Springer Netherlands, pp. 141–168. doi: 10.1007/978-94-017-3223-9_7.

Le Treut, H., Somerville, R., Cubasch, U., Ding, Y., Mauritzen, C., Mokssit, A., Peterson, T. and Prather, M. (2007) 'Historical Overview of Climate Change Science', in Solomon, S., Qin, D., Manning, M., Chen, Z., Marquis, M., Averyt, K. B., Tignor, M., and Miller, H. L. (eds) *Climate Change 2007: The Physical Science Basis. Contribution of Working Group I to the Fourth Assessment Report of the Intergovernmental Panel on Climate Change*. Cambridge, United Kingdom and New York, NY, USA. doi: 10.1016/j.soilbio.2010.04.001.

Tucker, M. A., Böhning-Gaese, K., Fagan, W. F., Fryxell, J. M., Van Moorter, B., Alberts, S. C., Ali, A. H., Allen, A. M., Attias, N., Avgar, T., Bartlam-Brooks, H., Bayarbaatar, B., Belant, J. L., Bertassoni, A., Beyer, D., Bidner, L., van Beest, F. M., Blake, S., Blaum, N., Bracis, C., Brown, D., de Bruyn, P. J. N., Cagnacci, F., Calabrese, J. M., Camilo-Alves, C., Chamaillé-Jammes, S., Chiaradia, A., Davidson, S. C., Dennis, T., DeStefano, S., Diefenbach, D., Douglas-Hamilton, I., Fennessy, J., Fichtel, C., Fiedler, W., Fischer, C., Fischhoff, I., Fleming, C. H., Ford, A. T., Fritz, S. A., Gehr, B., Goheen, J. R., Gurarie, E., Hebblewhite, M., Heurich, M., Hewison, A. J. M., Hof, C., Hurme, E., Isbell, L. A., Janssen, R., Jeltsch, F., Kaczensky,

P., Kane, A., Kappeler, P. M., Kauffman, M., Kays, R., Kimuyu, D., Koch, F., Kranstauber, B., LaPoint, S., Leimgruber, P., Linnell, J. D. C., López-López, P., Markham, A. C., Mattisson, J., Medici, E. P., Mellone, U., Merrill, E., de Miranda Mourão, G., Morato, R. G., Morellet, N., Morrison, T. A., Díaz-Muñoz, S. L., Mysterud, A., Nandintsetseg, D., Nathan, R., Niamir, A., Odden, J., O'Hara, R. B., Oliveira-Santos, L. G. R., Olson, K. A., Patterson, B. D., Cunha de Paula, R., Pedrotti, L., Reineking, B., Rimmler, M., Rogers, T. L., Rolandsen, C. M., Rosenberry, C. S., Rubenstein, D. I., Safi, K., Saïd, S., Sapir, N., Sawyer, H., Schmidt, N. M., Selva, N., Sergiel, A., Shiilegdamba, E., Silva, J. P., Singh, N., Solberg, E. J., Spiegel, O., Strand, O., Sundaresan, S., Ullmann, W., Voigt, U., Wall, J., Wattles, D., Wikelski, M., Wilmers, C. C., Wilson, J. W., Wittemyer, G., Zięba, F., Zwijacz-Kozica, T. and Mueller, T. (2018) 'Moving in the Anthropocene: Global reductions in terrestrial mammalian movements', *Science*, 359(6374), pp. 466–469. doi: 10.1126/science.aam9712.

Turkington, R., Sharam, G. and Sinclair, A. R. E. (2015) 'Biodiversity and the Dynamics of Riverine Forests in Serengeti', in Sinclair, A. R. E., Metzger, K. L., Mduma, S. A. R., and Fryxell, J. M. (eds) *Serengeti IV: Sustaining Biodiversity in a Coupled Human-Natural System*. Chicago and London: The University of Chicago Press, pp. 235–264.

Unal, Y., Kindap, T. and Karaca, M. (2003) 'Redefining the climate zones of Turkey using cluster analysis', *International Journal of Climatology*, 23(9), pp. 1045–1055. doi: 10.1002/joc.910.

University of Reading (no date) *Lake Surface Water Temperature*. Available at: http://www.laketemp.net/home/ (Accessed: 10 August 2020).

Vanderkelen, I., van Lipzig, N. P. M. and Thiery, W. (2018) 'Modelling the water balance of Lake Victoria (East Africa) – Part 2: Future projections', *Hydrology and Earth System Sciences*, 22(10), pp. 5527–5549. doi: 10.5194/hess-22-5527-2018.

Veldhuis, M. P., Hofmeester, T. R., Balme, G., Druce, D. J., Pitman, R. T. and Cromsigt, J. P. G. M. (2020) 'Predation risk constrains herbivores' adaptive capacity to warming', *Nature Ecology & Evolution*. Springer US, 4(8), pp. 1069–1074. doi: 10.1038/s41559-020-1218-2.

Veldhuis, M. P., Ritchie, M. E., Ogutu, J. O., Morrison, T. A., Beale, C. M., Estes, A. B., Mwakilema, W., Ojwang, G. O., Parr, C. L., Probert, J., Wargute, P. W., Hopcraft, J. G. C. and Olff, H. (2019) 'Cross-boundary human impacts compromise the Serengeti-Mara ecosystem', *Science*, 363(April), pp. 1424–1428. doi: 10.1126/science.aav0564.

Venter, Z. S., Cramer, M. D. and Hawkins, H. J. (2018) 'Drivers of woody plant encroachment over Africa', *Nature Communications*. Springer US, 9(1), pp. 1–7. doi: 10.1038/s41467-018-04616-8.

Verschuren, D., Laird, K. R. and Cumming, B. F. (2000) 'Rainfall and drought in equatorial east Africa during the past 1,100 years', *Nature*, 403, pp. 410–414.

de Visser, S. N., Freymann, B. P., Foster, R. F., Nkwabi, A. K., Metzger, K. L., Harvey, A. W. and Sinclair, A. R. E. (2015) 'Invertebrates of the Serengeti: Disturbance Effects on Arthropod Diversity and Abundance', in Sinclair, A. R. E., Metzger, K. L., Mduma, S. A. R., and Fryxell, J. M. (eds) *Serengeti IV: Sustaining Biodiversity in a Coupled Human-Natural System*. Chicago and London: The University of Chicago Press, pp. 265–300.

de Visser, S. N., Freymann, B. P. and Schnyder, H. (2008) 'Trophic interactions among invertebrates in termitaria in the African savanna: a stable isotope approach', *Ecological Entomology*, 33(6), pp. 758–764. doi: 10.1111/j.1365-2311.2008.01029.x.

Vizy, E. K. and Cook, K. H. (2019) 'Observed relationship between the Turkana low-level jet and boreal summer convection', *Climate Dynamics*. Springer Berlin Heidelberg, 53(7–8), pp. 4037–4058. doi: 10.1007/s00382-019-04769-2.

Wainwright, C. M., Marsham, J. H., Keane, R. J., Rowell, D. P., Finney, D. L., Black, E. and Allan, R. P. (2019) '"Eastern African Paradox" rainfall decline due to shorter not less intense Long Rains', *npj Climate and Atmospheric Science*. Springer US, 2(1), p. 34. doi: 10.1038/s41612-019-0091-7.

Walters, D., Baran, A. J., Boutle, I., Brooks, M., Earnshaw, P., Edwards, J., Furtado, K., Hill, P., Lock, A., Manners, J., Morcrette, C., Mulcahy, J., Sanchez, C., Smith, C., Stratton, R., Tennant, W., Tomassini, L., Van Weverberg, K., Vosper, S., Willett, M., Browse, J., Bushell, A., Carslaw, K., Dalvi, M., Essery, R., Gedney, N., Hardiman, S., Johnson, B., Johnson, C., Jones, A., Jones, C., Mann, G., Milton, S., Rumbold, H., Sellar, A., Ujiie, M., Whitall, M., Williams, K. and Zerroukat, M. (2019) 'The Met Office Unified Model Global Atmosphere 7.0/7.1 and JULES Global Land 7.0 configurations', *Geoscientific Model Development*, 12(5), pp. 1909–1963. doi: 10.5194/gmd-12-1909-2019.

Ward, J. H. (1963) 'Hierarchical Grouping to Optimize an Objective Function', *Journal of the American Statistical Association*, 58(301), pp. 236–244. doi: 10.2307/2282967.

Weltzin, J. F. and Coughenour, M. B. (1990) 'Savanna tree influence on understory vegetation and soil nutrients in northwestern Kenya', *Journal of Vegetation Science*, 1(3), pp. 325–334. doi: 10.2307/3235707.

Wickham, H. (2016) *ggplot2: Elegant Graphics for Data Analysis*. Springer-Verlag New York.

Wilcove, D. S. and Wikelski, M. (2008) 'Going, Going, Gone: Is Animal Migration Disappearing', *PLoS Biology*, 6(7), p. e188. doi: 10.1371/journal.pbio.0060188.

Wilks, D. S. (2011) 'Cluster Analysis', in *International Geophysics*, pp. 603–616. doi: 10.1016/B978-0-12-385022-5.00015-4.

Williams, E., Elia Ntandu, J., Ficinski, P. and Vorontsova, M. (2016) 'Checklist of Serengeti

Ecosystem Grasses', *Biodiversity Data Journal*, 4(1), p. e8286. doi: 10.3897/BDJ.4.e8286.

WMO (2017) *WMO Guidelines on the Calculation of Climate Normals*. Available at: https://library.wmo.int/doc_num.php?explnum_id=4166.

Woodhams, B. J., Birch, C. E., Marsham, J. H., Lane, T. P., Bain, C. L. and Webster, S. (2019) 'Identifying Key Controls on Storm Formation over the Lake Victoria Basin', *Monthly Weather Review*, 147(9), pp. 3365–3390. doi: 10.1175/MWR-D-19-0069.1.

World Bank (no date) *Data for Kenya and Tanzania: GDP, World Development Indicators: The World Bank Group*. Available at: https://data.worldbank.org/?locations=KE-TZ (Accessed: 3 April 2020).

Xu, X., Medvigy, D. and Rodriguez-Iturbe, I. (2015) 'Relation between rainfall intensity and savanna tree abundance explained by water use strategies', *Proceedings of the National Academy of Sciences*, 112(42), pp. 12992–12996. doi: 10.1073/pnas.1517382112.

Yang, W., Seager, R., Cane, M. A. and Lyon, B. (2015) 'The Annual Cycle of East African Precipitation', *American Meteorological Society*, 28, pp. 2385–2404. doi: 10.1175/JCLI-D-14-00484.1.

Appendix A. The Migration, Movement and Grass Dynamics Equations of the Savannah Dynamics Model

Document structure:

A1. Model Description

A2. Model terms

A3. Grass dynamics

A3.1 Rainfall and Grass growth rate (r_{max})

A3.2 Grass carrying capacity (K_G)

A3.3 Grass proportion (g) and tree canopy cover (T)

A3.4 Intake of green grass (I_G) and dry grass (I_D)

A4. Resource availability

A5. Wildebeest movement dynamics

A5.1 Emigration (Θ_{ij})

A5.2 Immigration (Ω_{ij})

A5.3 Change in wildebeest density ΔW_{ij}

A6. Wildebeest population dynamics

A7. References

A1. Model description

The Savannah Dynamics (SD) model is a discrete-time, spatially explicit model. It simulates grass dynamics, as well as wildebeest movement and population dynamics. The model is implemented across a lattice with a 10 km grid spacing, which represents the Serengeti-Mara ecosystem (Figure A-1). The boundaries of the ecosystem were defined by the "recce" dataset, a series of monthly aerial surveys of wildebeest distribution, which was used to validate the SD model's movement patterns (Holdo et al. 2009b).

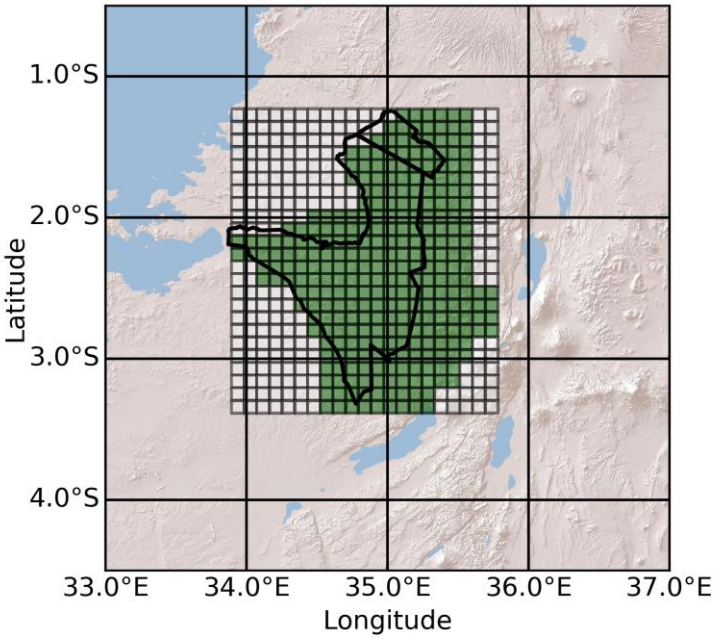

Figure A-1: Map of the Serengeti-Mara Ecosystem and spatial extent of the savannah dynamics model. The boundaries of the Serengeti National Park and Mara Reserve are outlined in black. The green grid cells show the area used in the SD model (each grid cell is 10 km x 10 km).

The grass and modelled wildebeest population dynamics are updated daily, while the wildebeest move at weekly time steps. Movement occurs across the landscape, and their movements and local population growth are determined by resource availability.

This document summarises the key model equations, however this information is taken from more detailed descriptions in Holdo et al. (2009a) and Holdo et al. (2009b).

A2. Model terms

The individual terms are defined below in alphabetical order. If the term is a constant, the value is also shown.

Variable	Value	Unit	Description
α_W	10.5	kg day $^{-1}$	Maximum wildebeest cropping rate
a_w	0.24	ha g^{-1} m^2	Conversion of food intake to energy for wildebeest

β_W	9.9	g m^{-2}	Grass biomass at which wildebeest intake is 50 % of maximum
b_w	0.00049	day^{-1}	Wildebeest birth rate
δ_D	0.0012	day^{-1}	Decay rate for D
δ_G	0.061	day^{-1}	Decay rate for G
D		g m^{-1}	Dry grass
DVI_D	4.4	kg day^{-1}	Wildebeest maximum voluntary intake of D
DVI_G	5.4	kg day^{-1}	Wildebeest maximum voluntary intake of G
f	0.42		Fraction of decaying G moving into compartment D
G		g m^{-1}	Green grass
g			Proportion of each cell occupied by grass versus trees, rocks, bare ground, etc.
Θ		ha^{-1}	Wildebeest emigration
I_D		kg day^{-1}	Per capita intake of D
I_G		kg day^{-1}	Per capita intake of G
K_G		g m^{-1}	Grass carrying capacity
μ_0	141	g m^{-1}	Rainfall effect on grass carrying capacity (intercept)
μ_1	0.264	g m^{-1} mm^{-1}	Rainfall effect on grass carrying capacity (slope)
m_w	0.0032	day^{-1}	Maximum wildebeest mortality rate
N		%	Plant nitrogen concentration
ρ	0.5		Shading effect of D on production of G
q	3.15		Fitted exponent parameter
R_{ann}		mm	Annual rainfall
R_{day}		mm	Daily rainfall
r_{max}			Grass growth rate
σ	46	g m^{-1}	Parameter to shift incremental grass growth curve towards origin
T		%	Percentage tree canopy cover
t		day	Day of the year (0 = November 1st)
t_{grow}		day	Length of growing season
W		ha^{-1}	Wildebeest density
Z			Resource availability

Ψ	0.0167	mm^{-1}	Rainfall effect on maximum grass growth
ω	1.39		Parameter controlling the strength of the competitive effect of tree canopy
Ω		ha^{-1}	Wildebeest immigration

The variables that are not given values in this table are calculated in the model, or defined on a cell by cell basis, informed by observed data.

A3. Grass dynamics

There are 2 key equations governing the within cell dynamics of green (G) and dry (D) grass.

$$\Delta G = r_{max}(G+\sigma)\left(1-\frac{G+\rho}{K_G}\right)-\delta_G G-\frac{I_G W}{g}$$

$$\Delta D = \delta_G f G-\delta_D D-\frac{I_D W}{g}$$

G = Green grass (g m^{-1})

D = Dry grass (g m^{-1})

r_{max} = Grass growth rate

σ = 46 = Parameter to shift incremenetal grass growth curve towards origin (g m^{-1})

ρ = 0.5 = Shading effect of D on production of G

K_G = Grass carrying capacity (g m^{-1})

δ_G = 0.061 = Decay rate for G (day^{-1})

δ_D = 0.0012 = Decay rate for D (day^{-1})

I_G = Per capita intake of G (kg day^{-1})

I_D = Per capita intake of D (kg day^{-1})

W = Wildebeest density (ha^{-1})

g = Proportion of each cell occupied by grass versus trees, rocks, bare ground, etc

f = 0.42 = Fraction of decaying G moving into compartment D

These equations can be summarised as:

$$Change\ in\ G\ =\ +\ Green\ grass\ growth\ -\ Green\ grass\ decay$$
$$-\ Wildebeest\ consumption\ of\ green\ grass$$

$$Change\ in\ D\ =\ +\ Dry\ grass\ standing\ biomass\ -\ Dry\ grass\ decay$$
$$-\ Wildebeest\ consumption\ of\ dry\ grass$$

The dry grass standing biomass is calculated based on the assumption that a fraction f of decaying green grass remains as dry standing biomass, whereas the rest is removed as litter.

A3.1 Rainfall and Grass growth rate (r_{max})

Grass growth in the model is dependent on rainfall. Annual rainfall (R_{ann}) and monthly rainfall are calculated from rainfall data layers that are input to the model. Daily rainfall (R_{day}) is calculated by dividing the monthly rainfall totals by 30, and other terms such as grass growth rate (r_{max}) are derived from these values.

$$r_{max} = \begin{cases} \Psi R_{day} & if\ t < t_{grow} \\ 0 & otherwise \end{cases}$$

r_{max} = Grass growth rate

Ψ = 0.0167 = Rainfall effect on maximum grass growth (mm^{-1})

R_{day} = daily rainfall (mm)

t = day

t_{grow} = length of the growing season (days)

The length of the growing season (t_{grow}) is proportional to total annual rainfall (R_{ann}), and can be calculated using the following formula:

$$t_{grow} = 60 + \frac{300e^{R_{ann}/100}}{e^{R_{ann}/100} + 518}$$

t_{grow} = length of the growing season (days)

R_{ann} = Annual rainfall (mm)

A3.2 Grass carrying capacity (K_G)

Grass carrying capacity (K_G) is also related to annual rainfall, although this relationship is described with a linear equation:

$$K_G = \mu_0 + \mu_1 R_{ann}$$

K_G = Grass carrying capacity (g m^{-1})

μ_0 = 141 = Rainfall effect on grass carrying capacity (intercept) (g m^{-1})

μ_1 = 0.264 = Rainfall effect on grass carrying capacity (slope) (g m^{-1} mm^{-1})

A3.3 Grass proportion (g) and tree canopy cover (T)

Grass biomass tends to decline as a function of woody cover in savannah ecosystems. Therefore a term was included to recognise that only a certain proportion of a cell is able to be occupied by grass, as opposed to tree cover.

$$g = e^{-\omega T}$$

g = Proportion of each cell occupied by grass versus trees

ω = 1.39 = parameter controlling the strength of the competitive effect of tree canopy

T = tree canopy cover (%)

A3.4 Intake of green grass (I_G) and dry grass (I_D)

The possible intake of green grass by wildebeest within a cell (I_G) is governed by either the wildebeest maximum voluntary intake of food (DVI_G), or the food available, whichever is smaller.

$$I_G = min\left(DVI_G, \frac{\alpha_W G}{\beta_W + G + D}\right)$$

A similar equation describes the intake of dry grass (I_D).

$$I_D = min\left(DVI_D, \frac{\alpha_W D}{\beta_W + G + D}\right)$$

I_G = per capita intake of G (kg day^{-1})

I_D = per capita intake of D (kg day^{-1})

DVI_G = 5.4 = Wildebeest maximum voluntary intake of G (kg day^{-1})

DVI_D = 4.4 = Wildebeest maximum voluntary intake of D (kg day^{-1})

α_W = 10.5 g ha m^{-2} day^{-1} = Maximum wildebeest cropping rate

β_W = 9.9 g m^{-2} = Biomass at which wildebeest intake is 50 % of maximum

G = Green grass (g m^{-1})

D = Dry grass (g m^{-1})

A4. Resource availability

The resource richness of a cell (Z) is determined both by the amount of grass available, and the quality of that grass. Therefore, the nitrogen concentration of the grass in each cell is included.

$$Z = gI_G N^q$$

Z = Resource availability

g = Proportion of each cell that is occupied by grass versus trees, rocks, bare ground, etc

I_G = per capita intake of G (kg day^{-1})

N = Plant Nitrogen Content (%)

q = 3.15 = Fitted exponent parameter

A5. Wildebeest movement dynamics

In this model, the virtual wildebeest move across the ecosystem toward the areas with the highest resources. Two key equations dictate whether they migrate, and if they do, to which part of the landscape they migrate. These equations are calculated in each individual grid cell.

A5.1 Emigration

Emigration from a cell is calculated by comparing the resources available in the current cell to the resources available in the surrounding neighbourhood. In the version of the model used in this study, the "neighbourhood" is defined as the whole ecosystem.

$$\Theta_{ij} = \frac{E(Z_r)^{\phi}}{(Z_{ij})^{\phi} + E(Z_r)^{\phi}} W_{ij}$$

Θ_{ij} = wildebeest emigration from cell ij

Z_{ij} = value of resource variable Z within a given cell ij

Z_r = mean value of Z, evaluated within a surrounding neighbourhood of cell ij

$E(Z_r)$ = expected value of Z_r across the neighborhood

ϕ = controls the shape of the migration function

W_{ij} = wildebeest density in cell ij

A5.2 Immigration

Immigration can only occur from one cell (ab) into another (ij) if the destination cell has greater resources. The resources in this potential destination cell (Z_{ij}) are then compared to resources available in other potential destination cells $(\sum Z_n)$. The fraction of wildebeest emigrating from cell ab that immigrate into cell ij, depends on cell ij's resource richness relative to other potential destination cells in the neighbourhood.

Provided $Z_{ij} \geq Z_{ab}$

$$\Omega_{ab->ij} = \frac{Z_{ij}}{\sum Z_n} \Theta_{ab}$$

ab = location of a given cell surrounding cell ij, from which immigration can occur into cell ij.

$\Omega_{ab->ij}$ = immigration into cell ij due to emigration from cell ab

Z_{ij} = value of resource variable Z within a given cell ij

cd = location of a given cell surrounding cell ab, from which wildebeest in cell ab can emigrate

$\sum Z_n$ = sum of Z over all cells for which $Z_{cd} \geq Z_{ab}$ (including the value in cell ab)

Θ_{ab} = total emigration from cell ab

The total amount of immigration that occurs into a cell (Ω_{ij}), is the sum of the immigration that occurs from all the less resource rich cells in the neighbourhood.

$$\Omega_{ij} = \sum \Omega_{ab->ij}$$

Ω_{ij} = total wildebeest immigration into cell ij

$\Omega_{ab->ij}$ = immigration into cell ij due to emigration from individual cell ab

It may appear that there is a discrepancy between the immigration and emigration equations, as the emigration equation is multiplied by W_{ij}, and thus represents *total* emigration, while the immigration equation is not multiplied by wildebeest density, so appears to only be a probability. However, as wildebeest density is incorporated into the emigration calculation, and emigration (Θ) is included in the immigration (Ω) calculation, the immigration equation does represent total immigration.

A5.3 Change in wildebeest density ΔW_{ij}

The movement of wildebeest across the ecosystem is a result of the weekly emigration and immigration of the wildebeest to the areas of highest resource availability. In an individual cell, the change in wildebeest density is lowered by emigration to cells with higher resources (Θ_{ij}) and increased by immigration from cells with lower resources (Ω_{ij}).

$$\Delta W_{ij} = -\Theta_{ij} + \Omega_{ij}$$

W_{ij} = wildebeest density in cell ij

Θ_{ij} = wildebeest emigration from cell ij

Ω_{ij} = wildebeest immigration into cell ij

A6. Wildebeest population dynamics

Finally, the wildebeest population dynamics are updated daily in every cell. The change in wildebeest population size (ΔW) is proportional to a constant birth rate (b_w) and a maximum death rate (m_w) which is modulated by resource availability (Z).

$$\Delta W_{ij} = [b_w - m_w e^{-a_w Z_{ij}}]W_{ij} - \Theta_{ij} + \Omega_{ij}$$

W_{ij} = wildebeest density in cell ij

b_w = 0.00049 = Wildebeest birth rate

m_w = 0.0032 = Maximum wildebeest mortality rate

a_w = 0.24 = Conversion of food intake to energy for wildebeest

Z_{ij} = value of resources in cell ij

Θ_{ij} = wildebeest emigration from cell ij

Ω_{ij} = wildebeest immigration into cell ij

The model is unstructured, has a constant recruitment rate, and a density dependent mortality rate. This was based on research by Pascual et al. (1997), who found no additional benefit to using a more complex model. Holdo et al (2009a) obtained estimates for b_w, m_w, and a_w by fitting the model to historical wildebeest census data, driven with rainfall data between 1960-2001.

A full explanation of the construction of this equation can be found in Appendix A of Holdo et al (2009a) (Ecological Archives A019-005-A1).

A7. References

Holdo, R. M., Holt, R. D. and Fryxell, J. M. (2009a). 'Grazers, browsers, and fire influence the extent and spatial pattern of tree cover in the Serengeti', Ecological Applications, 19(1), pp. 95–109. doi: 10.1890/07-1954.1.

Holdo, R. M., Holt, R. D. and Fryxell, J. M. (2009b). 'Opposing Rainfall and Plant Nutritional Gradients Best Explain the Wildebeest Migration in the Serengeti', *The American Naturalist*, 173(4), pp. 431–445. doi: 10.1086/597229.

Pascual, M. A., Kareiva, P. and Hilborn, R. (1997) 'The influence of model structure on conclusions about the viability and harvesting of Serengeti wildebeest', *Conservation Biology*, 11(4), pp. 966-976.

Appendix B. Cluster Analysis

Cluster analysis was carried out using the Ward error sum of squares hierarchical clustering method (Ward, 1963; Murtagh and Legendre, 2014). We chose the number of clusters used in our study based on the Euclidean distance between different steps of the clustering algorithm.

At the beginning of the analysis, each object (annual cycles in our case) is assigned its own cluster, then the algorithm iteratively links the most similar clusters together. This process is repeated until all clusters are linked together, and the Euclidean distances between the clusters is shown for each step.

B1. TRMM Cluster Analysis

Cluster analysis of TRMM climatological annual cycles (1998-2014) displayed as (a) a cluster dendogram, and (b)-(c) Euclidean distance between clusters vs. agglomeration step. Different scales are shown in (b) and (c) to better illustrate the step changes in final stages of the clustering algorithm. The dendrogram shows the order in which the observations (annual cycles at individual locations) were clustered together. The Euclidean distance at which the clustering occurred depended on the similarity between the two clusters being joined.

The results of clustering the climatological annual cycles in the TRMM dataset are shown in Figure B-1. The largest differences between clusters, were between 1 to 2, and 2 to 3 clusters. The third largest step change was between 4 and 5 clusters.

(a)

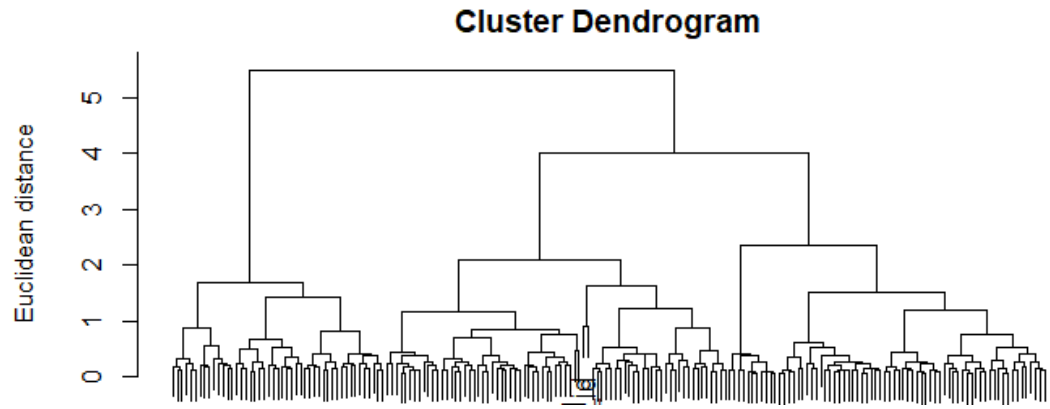

(b) (c)

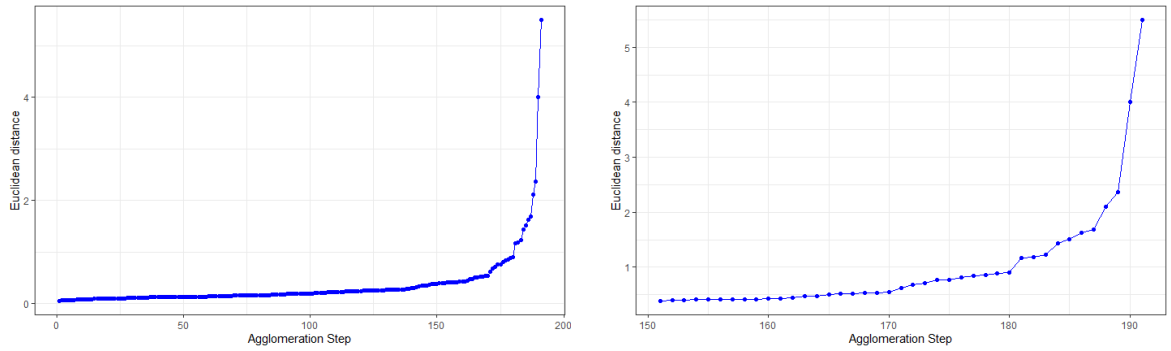

Figure B-1: Cluster analysis of TRMM climatological annual cycles (1998-2014) displayed as (a) a cluster dendogram, and (b)-(c) Euclidean distance between clusters vs. agglomeration step. Different scales are shown in (b) and (c) to better illustrate the step changes in final stages of the clustering algorithm. The dendrogram shows the order in which the observations (annual cycles at individual locations) were clustered together. The Euclidean distance at which the clustering occurred depended on the similarity between the two clusters being joined.

B2. CHIRPS Cluster Analysis

Figure B-2 shows the results of clustering the CHIRPS data. The largest step change in Euclidean distance was between having 2 clusters and 1 cluster. The second largest step change was between having 4 and 3 clusters.

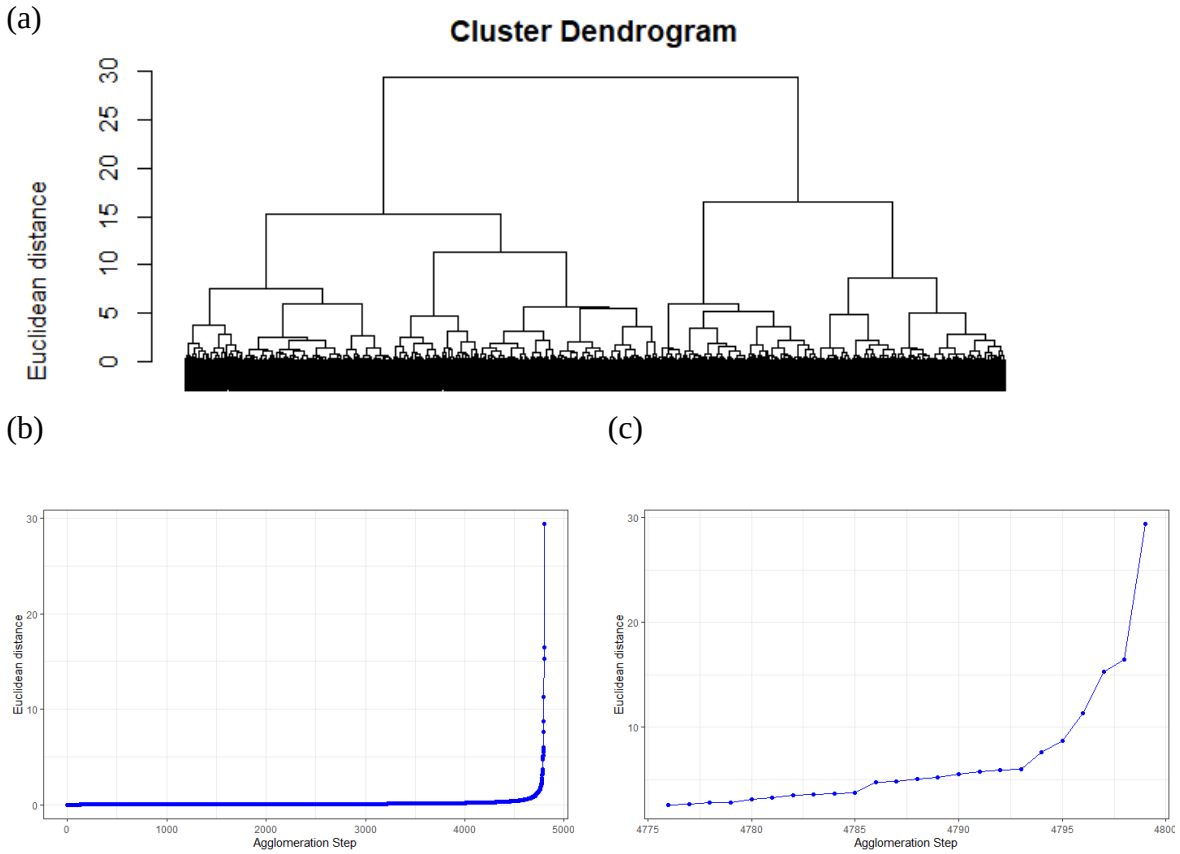

Figure B-2: Cluster analysis of CHIRPS climatological annual cycles (1987-2016) displayed as (a) a cluster dendogram, and (b)-(c) Euclidean distance between clusters vs. agglomeration step. Different scales are shown in (b) and (c) to better illustrate the step changes in final stages of the clustering algorithm. The dendrogram shows the order in which the observations (annual cycles at individual locations) were clustered together. The Euclidean distance at which the clustering occurred depended on the similarity between the two clusters being joined.

In both datasets, a large step change was present between 1 and 2 clusters, showing that there was a strong difference between these two sets of annual cycles. However, we were interested in further spatial differentiation of the region, so we therefore looked for the distinctions between higher numbers of clusters. In the CHIRPS and gauge dataset, there was a large step change between 3 and 4 clusters, suggesting that there was a strong distinction between the 4 clusters. In the TRMM dataset there were strong step changes in Euclidean distance between 2-3 clusters, and 4-5 clusters. As we were aiming to spatially differentiate the region, we chose to investigate 5 clusters in the TRMM dataset, and 4 clusters in the CHIRPS datasets.

B3. References

Murtagh, F. and Legendre, P. (2014) ‘Ward’s Hierarchical Agglomerative Clustering Method: Which Algorithms Implement Ward’s Criterion?’, *Journal of Classification,* 31(3), pp. 274-295. doi: 10.1007/s00357-014-9161-z.

Ward, J. H. (1963) ‘Hierarchical Grouping to Optimize an Objective Function’, *Journal of the American Statistical Association*, 58(301), pp. 236-244. doi: 10.2307/2282967.